

**REMARKS**

Applicant confirms election of the single species Gadolinium ( $Gd^{3+}$ ) with traverse. Applicant, however, respectfully requests reconsideration of the election requirement. The claims as amended herein are directed to methods of treating glaucoma by administering at least one compound that blocks stretch-activated channels of eye retinal ganglion cells and compositions and devices comprising at least one compound that blocks stretch-activated channels of eye retinal ganglion cells, which may be useful in such methods. The specification provides a number of examples of compounds that may have this activity. These compounds are related by a generic function. Applicants submit that a reasonable number of species are presented in claims 11 and 14 and reserve the right to request reconsideration and rejoinder of the remaining species in accordance with 37 C.F.R. § 1.141.

**A. Informalities**

The Office Action of April 19, 2004 indicated that the references cited in the Invention Disclosure Statement filed October 18, 2002, which were made of record in the parent application, were not present in the parent file. Applicant submits herewith as Attachment A copies of the references that were not readily retrievable by the Examiner (C1-C7). Applicant request that the Examiner acknowledge that she reviewed the documents by initialing the Form 1449 provided with the Invention Disclosure Statement of October 18, 2002. If the Examiner would like a new form to initial, the undersigned Applicant's representative will gladly provide one to the Examiner.

In the Response to the Restriction Requirement of August 28, 2003, Applicant canceled claims 1, 2, 4-9. Under current PTO procedure, the non-elected claims should have been considered withdrawn. Applicant re-introduces the non-elected claims as new claims 15-22. New claims 15-16 correspond to non-elected claims 1 and 2, respectively. New claims 17-22 correspond to non-elected claims 4-9, respectively. Because the new claims are directed to non-elected subject matter, they are also listed as withdrawn.

Claim 3 has been amended to supply the missing term. Support for this amendment can be found throughout the specification, e.g., at least at page 4, lines 11-16, and page 9, lines 1-9.

Claims 11 and 14 are amended herein to correct a typographical error. The amended claims recite the correct spelling of "colchicine."

Claim 12 is amended herein such that it is directed to an eye drop solution for the treatment of glaucoma having a concentration of at least one compound which blocks stretch activated channels of eye retinal ganglion cells sufficient to protect the cells from apoptotic cell death when administered to such cells. Support for the amendment can be found throughout the specification, e.g., at least at page 8, lines 14 30.

Claims 13 is amended to a Jepson-type claim directed to a device for administering solution to the eye, wherein the improvement comprises the eye drop solution of claim 12. Support for this amendment can be found throughout the specification, e.g., at least at page 8, line 14, to page 9, line 15.

Claim 14 as amended herein to correctly recite "eye drop solution of claim 12" rather than "method of claim 12."

#### **B. Outstanding Rejections**

Claims 3, and 10-14 stand rejected under an alleged judicially created doctrine as being drawn to an improper Markush group.

Claims 3 and 10-14 stand rejected under 35 U.S.C. § 112, first paragraph, as allegedly lacking written description.

Claims 3 and 10-14 also stand rejected under 35 U.S.C. § 112, first paragraph, as allegedly lacking enablement.

Claim 12 stands rejected under 35 U.S.C. § 102(b) as allegedly anticipated by Calabrese et al.

#### **C. Patentability Arguments**

##### **1. The improper Markush group rejection should be withdrawn**

Claims 3, and 10-14 stand rejected under an alleged judicially created doctrine as being drawn to an improper Markush group. The rejection, however, fails to provide the judicial basis for the rejection. Without the judicial basis for the rejection, Applicant is unable to address the issue. Applicant respectfully requests clarification of the rejection.

The members of the Markush group share the common utility of blocking stretch activated channels of eye retinal ganglion cells. In regards to the present invention, they are functionally equivalent. The Examiner argues that the members of the Markush group are patentably distinct from each other. The fact that members of a genus may be patentably distinct does not render the genus improper. As stated in MPEP § 806.04(d):

For the purpose of obtaining claims to more than one species in the same case, the generic claim cannot include limitations not present in each of the added species claims. Otherwise stated, the claims to the species which can be included in a case in addition to a single species must contain all the limitations of the generic claim.

The Markush group to compounds, which block stretch-activated channels in eye retinal ganglion cells, sets forth species having common utility and such individual species claims contained therein contain all the limitations of the generic claim. To limit the claim to the single elected species would be improper. Applicant respectfully requests withdrawal of the rejection of claims 3 and 10-14 under an alleged judicially created doctrine as being drawn to an improper Markush group.

2. The written description rejection under 35 U.S.C. § 112, first paragraph should be withdrawn

Claims 3 and 10-14 stand rejected for allegedly lacking written description as to the phrase, "other pressure sensitive mechanisms of retinal ganglion cells." Applicant respectfully traverses the rejection. In order to expedite prosecution of the claims, however, Applicant has amended the claims herein to remove the phrase, rendering the rejection moot. Applicant reserves the right to pursue the subject matter of the prior claims in future prosecution. The rejection of claims 3 and 10-14 under 35 U.S.C. § 112, first paragraph should be withdrawn.

3. The enablement rejection under 35 U.S.C. § 112, first paragraph, should be withdrawn

Claims 3 and 10-14 stand rejected under 35 U.S.C. § 112, first paragraph, as allegedly not enabled by the specification. Specifically, the rejection states, "[t]he specification provides neither support for administration of Gadolinium for treatment of glaucoma nor

support for compositions comprising Gadolinium as an eye drop or systemic preparation. Applicant respectfully disagrees.

At pages 8-10 of the specification there is included a description of how to make formulations containing any of the stretch-activated channel blocking agents. This description encompasses lists of suitable carriers, buffers, diluents, stabilisers and the like. Furthermore, there is a description as to the amount of any particular compound necessary to protect neural tissue from pressure-induced apoptotic cell death, which includes reference to the various factors that should be taken into account, including the location of the tissue and the severity of the condition being treated.

The skilled person, whom the Examiner has conceded would be a skilled ophthalmologist with a Ph.D. or M.D., would possess a high degree of knowledge regarding the formulation of compounds and compositions for topical administration to the eye, or for systemic administration for ocular conditions. This skilled person would be further guided by the description in the present application, and be readily able to formulate the compounds and compositions for the treatment of glaucoma as therapeutically appropriate vehicles. While it is conceded that a small degree of testing would be required in order to establish that these therapeutic vehicles were of the appropriate dosage and formulation, this would not fall within the scope of experimentation set out by In re Wands, 8 USPQ2d 1400. Indeed, the testing that would be necessary to be performed by the skilled person would merely represent routine trial and experimentation, and would not involve any undue physical or mental effort.

The potency of many of the compounds recited in the claims (*i.e.*, as stretch-activated channel blockers), is already known. Furthermore, this potency value may be readily calculated. Indeed, it is a matter of routine to measure the potency of any particular compound, for example, a stretch-activated receptor blocker, using a simple, *in vitro*, dose-response type experiment, e.g., the apoptotic assay described on page 7, line 20-27. Furthermore, topical absorption across ocular membranes is known for many of the compounds, and can be readily tested by routine experimentation using organ-bath type experiments. Such simple experiments would permit the skilled person to approximate the amount of the compound or composition of interest that would be necessary to be provided as a topical eye drop.



Furthermore, the systemic bioavailability and inter-compartmental distribution of the compounds of the claims are known, such that the skilled person, when wanting to formulate a systemic delivery vehicle, could readily calculate the amount of compound necessary for such administration, so that a therapeutically efficacious dose can be delivered to the eye via systemic administration. Bioavailability and biodistribution studies are also a matter of routine experimentation in the field of ophthalmology and compound formulation. Such experiments involve administration of set dosages of a compound of interest to a laboratory mammal, the animal then being sacrificed and the amount of the compound of interest and/or its metabolites being assessed in tissues of interest.

Accordingly, using such routine experimentation the amount of the stretch-activated channel blocking compound, or composition, suitable for systemic administration, could be readily determined. Again, this routine experimentation cannot be said to constitute undue experimentation for the skilled person. Applicant respectfully requests withdrawal of the rejection of claims 3 and 10-14 under 35 U.S.C. § 112, first paragraph, for lack of enablement.

4. The rejection under 35 U.S.C. § 102(b) should be withdrawn

Claim 12 stands rejected under 35 U.S.C. § 102(b) as allegedly anticipated by Calabrese *et al.* In order for a claim to be anticipated, a single item of prior art must disclose *each* element of the claim. See *Hybritech Inc. v. Monoclonal Antibodies, Inc.*, 231 U.S.P.Q.2d 81, 90 (Fed. Cir. 1986). Applicant has amended claim 12 to specifically clarify that the the subject matter being claimed is an eye drop solution, and the claim expressly recites that the solution contains at least one compound which blocks stretch activated channels of eye retinal ganglion cells. Calabrese *et al.* cannot serve as a legitimate anticipatory reference for the subject matter being claimed in claim 12 because this reference fails to teach an eye drop solution for the treatment of glaucoma. One skilled in the art would not recognize that the solutions used in the *in vitro* experiments disclosed in Calabrese *et al.* could or should be formulated as eye drops for the treatment of glaucoma. Applicants respectfully request that 35 U.S.C. §102(b) rejection based on Calabrese *et al.* be withdrawn in view of the amendment to claim 12 and the comments provided above.

In view of the above amendment, applicant believes the pending application is in condition for allowance.

Dated: October 19, 2004

Respectfully submitted,

By 

Thomas J. Wrona, Ph.D.

Registration No.: 44,410

MARSHALL, GERSTEIN & BORUN LLP

233 S. Wacker Drive, Suite 6300

Sears Tower

Chicago, Illinois 60606-6357

(312) 474-6300

Attorney for Applicant

Application No.: 10/084,604

Docket No.: 29264/38278

ATTACHMENT A



# Pressure Related Apoptosis in Neuronal Cell Lines

Ashish Agar,<sup>1,2</sup> Sonia S. Yip,<sup>1</sup> Mark A. Hill,<sup>1\*</sup> and Minas T. Coroneo<sup>2</sup>

<sup>1</sup>Cell Biology Lab, School of Anatomy, University of New South Wales, Sydney, Australia

<sup>2</sup>Department of Ophthalmology, Prince of Wales Hospital, University of New South Wales, Sydney, Australia

Pressure is a crucial component of the cellular environment, and can lead to pathology if it varies beyond its normal range. The increased intra-ocular pressures in acute glaucoma are associated with the loss of neurons by apoptosis. Little is known regarding the interaction between pressure and apoptosis at the level of the cell. The model developed in this study examines the effects of elevated ambient hydrostatic pressure directly upon cultured neuronal lines. Conditions were selected to be within physiological limits: 100 mmHg over and above atmospheric pressure for a period of 2 hr, as seen clinically in acute glaucoma. This system can be used to investigate pressure relatively independently of other variables. Neuronal cell line cultures (B35 and PC12) were subjected to pressure conditions in specially designed pressure chambers. Controls were treated identically, except for the application of pressure, and positive controls were treated with a known apoptotic stimulus. Apoptosis was detected by cell morphology changes and by 2 specific apoptotic markers: TUNEL (Terminal transferase dUTP Nick-End Labeling) and Annexin V. These fluorescent markers were detected and quantified by automated Laser Scanning Cytometry. All techniques showed that increased pressure was associated with a greater level of apoptosis compared to equivalent controls. Our results suggest that pressure alone may act as a stimulus for apoptosis in neuronal cell cultures. This raises the possibility of a more direct relationship at the cellular level between pressure and neuronal loss. *J. Neurosci. Res.* 60:495–503, 2000.

© 2000 Wiley-Liss, Inc.

**Key words:** hydrostatic pressure; pressure chamber; glaucoma; neuronal culture; apoptosis; laser scanning cytometer

Pressure is a fundamental physical quantity, being a determinant of both the integrity and function of cells including neurons. Disorders of this relationship, such as when pressures vary beyond physiological limits, can thus lead to disease states. In the ocular disease glaucoma, for example, the most frequent and important association is that of raised intraocular pressure (IOP), either acute or chronic (Armaly et al., 1980). This disease is characterized by the progressive loss of Retinal Ganglion Cells (RGCs).

Induced increases in IOP in animal models have been shown to result in the loss of RGCs, confirming the relationship seen in clinical glaucoma (Nickells, 1996). These studies have revealed the major mode of RGC loss to be via apoptosis, the genetically programmed form of cell death. Recently this has also been validated in human glaucoma (Kerrigan et al., 1997). The molecular events that result in apoptosis can be initiated by a variety of stimuli (Nickells, 1996).

This mechanism, whereby an increase in IOP triggers events that damage and then destroy RGCs, remains to be fully explained. Theories of glaucoma pathogenesis include mechanodistortion of the optic nerve at its exit from the eyeball affecting RGC transport mechanisms, and compression of optic nerve head microvasculature compromising neuronal circulation (reviewed by Quigley, 1995). It has been reported that inhibition of retrograde axonal flow can only partly explain RGC loss post axotomy (Fagioli et al., 1997). There is evidence from other studies that RGC loss may be mediated independently of these mechanisms (Radus 1981; Johansson 1983, 1988). Therefore, in addition to the known components of glaucoma pathology, pressure may also have some direct effect on RGC apoptosis.

Of the few published studies that have applied increased physiological levels of hydrostatic pressure alone to cells in vitro, none have used neurons. In-vitro cultures of other cell types have been placed in pressure chambers (Kosnosky et al., 1995), and neurons have been subjected to pressure conditions in vivo in animal models (Weber et al., 1998). Apoptosis has been induced in cultured neuroblastoma cells, but in response to mechanical shear (Edwards et al., 1998). A large range of sometimes non-physiological pressures have been applied to cell cultures. Human lymphoblasts have been subjected to pressures ≈7000 mmHg, far in excess of those seen in disease states

Abbreviations: GI, green integral; GMP, green max pixel; IOP, intra ocular pressure; LSC, laser scanning cytometer; PI, propidium iodide; RGC, retinal ganglion cell; TUNEL, terminal transferase dUTP nick-end labeling.

Contract grant sponsor: Allergan Australia.

\*Correspondence to: Dr. M.A. Hill, Cell Biology Lab, School of Anatomy, University of New South Wales, Sydney NSW 2052, Australia. E-mail: m.hill@unsw.edu.au

Received 4 October 1999; Revised 1 February 2000; Accepted 2 February 2000

Agar et al.

adding glaucoma (Takano, et al., 1997). Significantly, experiment has demonstrated that pressure can be an independent stimulus for inducing apoptosis.

This current study investigates the effect of elevated hydrostatic pressure *in vitro* on neuronal cell lines. The experimental parameters were selected to simulate the *in vivo* clinical scenario of acute glaucoma. Our initial approach, presented here, investigated a single pressure duration and duration at physiological levels, relevant to intraocular pressures seen in this disease. Cultures of neuronal cell lines were exposed to an increased ambient hydrostatic pressure of 100 mmHg for 2 hr. The cells were then assessed for apoptosis morphologically and by means of specific fluorescent markers of apoptosis.

## MATERIALS AND METHODS

### Cell Culture

Cell cultures were generated using the neuroblastoma cell B35, derived from the rat central nervous system (Schubert 1994). Cells were grown in Dulbecco's modified Eagle medium (DMEM, Gibco) supplemented with 10% heat inactivated fetal serum (Gibco) and 1% penicillin/streptomycin.

As B35 cells are not post-mitotic and continue to proliferate, we have also used a second neuronal cell line PC12 (Schubert and Tischler, 1976). These cells were differentiated in order to produce neurons that had exited the cell cycle (Michel 1995). Undifferentiated PC12 cultures were maintained in DMEM with 5% fetal calf serum and 10% heat inactivated horse serum (Gibco). PC12 cultures were cultured in DMEM with 10% heat inactivated horse serum supplemented with 1 mM butyryl cAMP (Sigma) and 50 ng/mL NGF (kindly provided Prof. I. Hendry) for 3 days to induce differentiation.

Neurons were plated (10,000/cm<sup>2</sup>) onto poly-L-lysine coated glass coverslips in 24-well culture dishes. Neuronal cultures were grown in 250  $\mu$ L of growth media per well, and incubated at 37°C in 5% CO<sub>2</sub> and air.

### Pressure System

Specialised pressure chambers were designed based upon a simple model described previously for use with cell cultures (Majno et al., 1994; Kosnosky et al., 1995; Mattana et al., 1996). Briefly, a Perspex and glass chamber was constructed with a gas inlet and flow valves incorporated for connection to a pressure regulator (BOC Gases). The chamber could be pressurized with a 5% CO<sub>2</sub> and air gas mix to a constant hydrostatic pressure ranging from 0–200 mmHg. Pressure levels were monitored continuously by mercury column barometer, with atmospheric pressure (760 mmHg) calibrated to 0 mmHg. Compression and decompression to 100 mmHg (over and above atmospheric pressure) was attained over 30 sec. The apparatus was equilibrated and maintained within an electronically controlled CO<sub>2</sub> incubator at 37°C (Nuair NU4500E).

The possibility that increased hydrostatic pressure could affect gas exchange was assessed. Culture growth medium was sampled in pressure and control cultures before and immediately after the 2 hr pressurization, and at subsequent timepoints. Measurements for pH, pCO<sub>2</sub> and pO<sub>2</sub> analysis were done by stat analyzer (Radiometer ABL 725).

### Experimental Protocol

Experimental neuronal culture dishes were placed within the pressure chamber and the gas mix was then pressurized to subject the cells to conditions of 100 mmHg for 2 hr, simulating conditions analogous to acute glaucoma. After this period of pressure elevation cultures were restored to atmospheric pressure and the culture dishes removed from the chamber and incubated for a further 24 hr. Control neuronal culture dishes were treated identically, being placed within the pressure chamber but without the application of pressure. At serial timepoints of 2, 6 and 20 or 24 hr after initiation of pressure, duplicate coverslips were removed for analysis. These were fixed for DNA fragmentation assays and morphological examination, or stained live for the Annexin V assay before fixation. Cell fixation used in all experiments was 4% w/v paraformaldehyde in phosphate buffered saline pH 7.5 for 10 min.

A maximum apoptosis control for the B35 cell line was established in each experiment by treatment with ethanol (Fig. 1A), a known stimulator of apoptosis (De et al., 1994; Oberdoerster et al., 1998; Mizushima et al., 1999). This enabled validation in each experiment of the various apoptosis detection methods. Initial studies using a range of culture timepoints established maximal inducible apoptosis with 5% ethanol treatment after 2 hr (data not shown). These cultures were used in both apoptosis marker assays (TUNEL and Annexin V) as a positive 'maximum cell death' control for each experiment. Ethanol treatment of differentiated PC12 neurons led to excessive cell loss by detachment. In PC12 experiments a fixed control culture was treated with DNase (Promega) for 25 min at room temperature to elicit maximal TUNEL signal. Using this data results were normalized to the cell line's maximal apoptosis control within each experiment, allowing comparison between the experiments.

### Apoptosis Detection

Morphologically apoptosis is characterized by progressive condensation of the cytoplasm and nucleus, followed by fragmentation and phagocytosis by other cells (Majno and Joris, 1995). In neurons there is also seen a withdrawal of cell processes and a "blebbing" or "budding" of the cell membrane. Neurons were examined by phase contrast microscopy for these features of apoptosis and to allow identification of necrotic cells.

TUNEL is a well-established assay for the detection of apoptosis. Endonuclease activation in the nucleus cleaves DNA into segments that can be labeled by terminal transferase dUTP nick-end labeling (Ben-Sasson et al., 1995). After fixation adherent cells on the coverslips were assayed for TUNEL using direct binding fluorescein-conjugated dUTP (green fluorochrome), with propidium iodide (PI) providing the red counterstain, as described by the *in situ* detection kit (Promega). Mounted coverslips were then analyzed by fluorescent microscopy and laser scanning cytometry.

To complement the detection of later nuclear changes associated with apoptosis measured by TUNEL, a relatively early marker of apoptosis was also studied. Annexin V detects one of the earliest molecular events in apoptosis, the translocation of phosphatidyl-serine to the outer leaflet of the cell membrane (van Engeland et al., 1996). The staining procedure was carried out on live cells using a direct binding Annexin V-FITC conjugate, ac-

cordi  
Coul  
distir  
lyzed  
or w

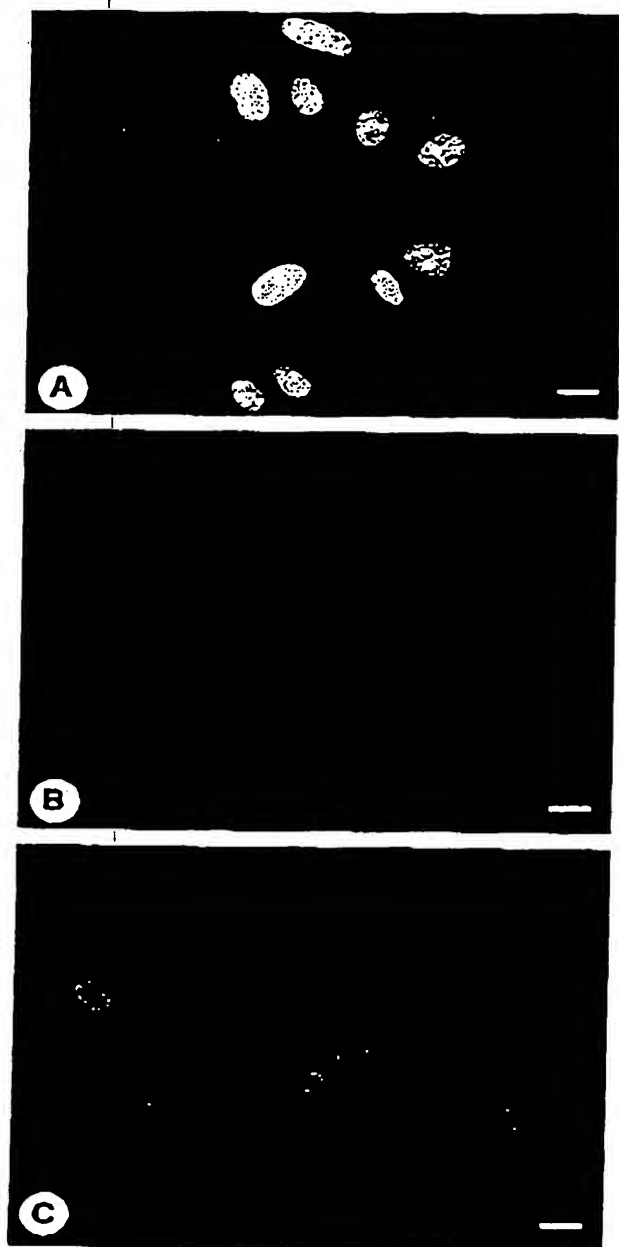
Ana

pus  
1.61  
ptos

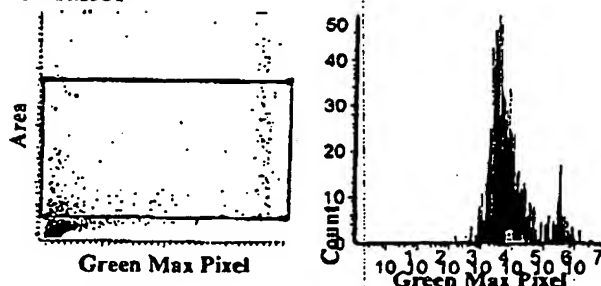
according to the protocol supplied with the detection kit (Zymed). Counterstaining live cells with PI enables necrotic cells to be distinguished by the dye exclusion principle. Cells were then analyzed by fluorescent microscopy and laser scanning cytometry, with or without fixation and mounting of the coverslip.

#### Analysis

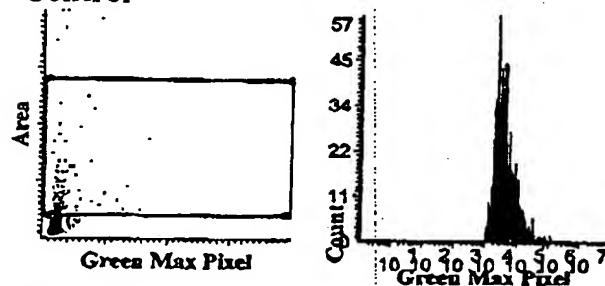
Morphological assessment was carried out using an Olympus IX-70 phase contrast microscope with NIH Image (version 1.61) software. Visualization of Annexin V and TUNEL apoptosis markers was performed with a confocal Laser Scanning



#### Ethanol



#### Control



#### Pressure

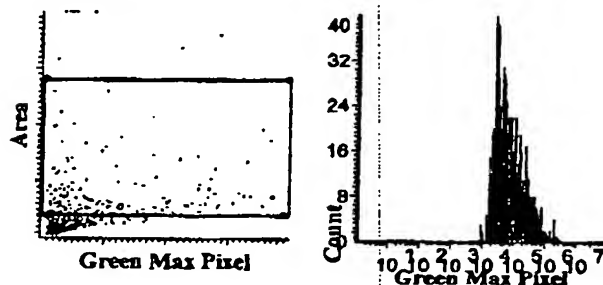


Figure 2. (Legend on following page.)

Fig. 1. (A) Ethanol (positive control) neurons. Immunofluorescent images of cultured B35 neurons treated with 5% ethanol for 2 hr, a known stimulus of apoptosis. Cells stained with TUNEL assay for DNA fragmentation (green). Counterstain with propidium iodide (red). Ethanol treatment gave maximal fluorochrome signal strength, with intense green and red signals appearing as yellow. Neurons show high level of apoptosis, with strongly positive nuclei for TUNEL marker, and chromatin condensation also evident in some nuclei. Remainder of cells in late stage apoptosis show morphological features of shrunken cell body, loss of processes and membrane blebs. Scale bar = 10  $\mu$ m. (B) Control neurons. B35 neural cell line maintained in pressure chamber apparatus for 2 hr but not subject to increased pressure conditions. TUNEL assay and propidium iodide staining. Neurons show generally normal morphology and little or no nuclear staining for DNA fragmentation. Note centrally located cell showing weakly TUNEL positive nucleus. (C) Neurons subject to pressure conditions. B35 neural cell line after 2 hr of elevated ambient hydrostatic pressure (first timepoint). Cells assayed with TUNEL (green) and counterstained with propidium iodide (red). Neurons show increased level of DNA fragmentation and some chromatin condensation as detected by fluorescent label compared to controls (B).

Microscope (Olympus GB200). Quantitative determination of these fluorochromes, as well as concurrent morphological inspection, was made possible using the relatively new technique of laser scanning cytometry (laser scanning cytometer, or LSC, Compucyte, USA) that allows automated analysis of adherent fluorescently labeled cells. Recently the LSC has been demonstrated to be an accurate tool for the detection of apoptosis using both markers employed in this study (Schutte et al., 1998; Darzynkiewicz et al., 1998).

Fluorescein isothiocyanate or FITC is the hapten label in both Annexin and TUNEL assays. The LSC Argon laser was set to 488 nm and appropriate sensors selected for the FITC fluorochrome, to detect and measure this green fluorescent marker, (note red PI intensity not measured). FITC label intensity is measured and cell values determined for two parameters. Green max pixel (GMP) or fluorescence peak reflects the highest value within a cell. Hyperchromicity of DNA in condensed chromatin of apoptotic cells can be recognized by high GMP values with the nuclear TUNEL assay. Membrane bound Annexin V label also gives high readings for apoptotic cells, as other cells do not stain or do so at a significantly lower intensity. The sum of the signal value for all pixels over threshold for a scanned cell is given as the green integral (GI). This measure of total fluorescence is similarly indicative of the degree of labeling (Darzynkiewicz et al., 1998). The spatial X-Y coordinates of each scanned cell are recorded, so an individual neuron can be relocated after initial LSC measurement for visual microscopy. As the resolution of the LSC image is limited, these features are visualized at greater detail via a co-mounted fluorescent microscope. The position is recorded and the image then captured digitally using the confocal laser scanning microscope. The LSC determines the size of all scanned objects by the number of pixels over threshold, or the 'fluorescent area.' Visual inspection of cells during scanning allowed exclusion of debris and cell clumps on the basis of size. Appropriate area limits were then set to select or gate the target group of single cells, seen within the colored rectangular region in the data scattergrams (Fig. 2).

A total of seven experiments were undertaken with the B35 cells and 3 with the PC12 cell line. Neurons on the coverslips were scanned in each of four equal sized quadrants. At each timepoint in each experiment 4 sets of LSC measurements were made, one per quadrant. Data were collected for both GMP and GI parameters as well as fluorescent area for each cell. Absolute measured values were

TABLE 1. Measurement of pH, pCO<sub>2</sub> and pO<sub>2</sub> Initially and Following 2 hr With or Without Pressure Application

Treatment	Control	Control	Pressure
Time (hr)	0	2	2
pH	7.63 ± 0.02	7.67 ± 0.04	7.66 ± 0.04
pCO <sub>2</sub> (mmHg)	27.8 ± 0.4	26.1 ± 1.0	25.6 ± 0.4
pO <sub>2</sub> (mmHg)	164 ± 1.4	168.5 ± 2.8	168.5 ± 3.8

Statistical analysis (Student's paired *t*-test) of these results showed no significant variation in the readings of pH, pCO<sub>2</sub> or pO<sub>2</sub> following the experimental procedure (2 hr values) for control or pressure groups, compared to initial or 'atmospheric' measurements ( $P > 0.1$  to  $P > 0.5$ ,  $n = 6$ ). Further, after the experimental conditions of 100 mmHg for 2 hr, the results show no significant difference in pCO<sub>2</sub>, pO<sub>2</sub> or pH between the pressure and control neuronal cultures ( $P > 0.5$ ,  $n = 6$ ).

recorded by the LSC and data analyzed as the average for the gated single cell population. Normalized data of pooled results were generated by comparison of individual absolute measurements with the averaged positive control (maximal apoptosis) value for that experiment. Data could thus be expressed as a ratio of the positive control. The quantitative data are presented as the mean ± standard error (SE). Analysis of variance was determined using Student's paired *t*-test.

## RESULTS

### Pressure System

Conditions of raised pressure of 100 mmHg were attained for 2 hr with a variance of ±2 mmHg on continuous monitoring. Taking into account the 0.25 ml of culture media per well, experimental pressure conditions were thus maintained with a variability of approximately ±2.25 mmHg, or ±2.25%, for the duration of the experiment. Stat gas analysis was undertaken on samples of well culture media before the experimental procedure ('atmospheric' or 0 hr), immediately after pressure conditions of 100 mmHg for 2 hr (Table 1) and at later timepoints (data not shown). Analyses for the later timepoints were similar to the initial 0 hr findings, with control and pressure groups not differing significantly. Statistical analysis (Student's paired *t*-test) of pressure and control values for pH, pCO<sub>2</sub> or pO<sub>2</sub> before (0 hr) and after 2 hr showed no significant differences ( $P > 0.1$  to  $P > 0.5$  respectively,  $n = 6$ ). Furthermore, after the experimental conditions of 100 mmHg for 2 hr, the results showed no significant difference in pCO<sub>2</sub>, pO<sub>2</sub> or pH between the pressure and control neuronal cultures ( $P > 0.5$ ,  $n = 6$ ).

### Morphological Apoptosis Detection

Apoptosis was confirmed by phase contrast microscopy and fluorescent microscopy (Fig. 1). These findings were applicable to both B35 and PC12 neuronal cell lines, with few subjective differences. Morphological analysis revealed several characteristics of apoptosis including: shrunken cell size, plasma membrane blebbing, loss of processes, and nuclear condensation. This combination of advanced apoptosis features was most pronounced in the positive ethanol-treated neurons (Fig. 1A). A greater range

Fig. 2. (Figure appears on preceding page.) Typical quantitative TUNEL data from LSC analysis of B35 cultures after ethanol, control or pressure treatment. Single scan for green dUTP-FITC fluorochrome, shown as displayed by LSC software. Scattergrams (left column) show green max pixel (peak TUNEL label intensity of cell) plotted against area (fluorescent area of scanned cell). Boxed area in graph includes only single cells (red), and excludes cell clumps and debris (black). Scattergram data reflected in adjacent histogram (right column; note arbitrary 'Count' scale is set by LSC software). Colors correspond to scattergram with red region lying within selected box. High apoptosis in ethanol treated culture shown by high fluorescent signal (red peak shifted right). Corresponding scattergram also shows strongly fluorescent cells at right within boxed region. This pattern is seen in pressure treated cells but not control cells.

of apoptotic morphological features was seen in the control (Fig. 1B) and pressure cells (Fig. 1C), with affected neurons displaying some but not all of these features. Therefore, using this criteria alone, it would be difficult to quantify apoptosis in these cultures. Qualitatively, there were fewer cells showing apoptotic morphological features in control than pressure conditions.

Staining of live cells with Annexin V and PI counterstain confirmed necrosis as not being significant in the studied populations by PI dye exclusion. Morphological examination of randomly selected fields looked for necrotic features such as: swelling of both soma and nucleus, plasma membrane rupture, vacuolation or karyolysis. These were uncommon in all experimental groups. Neurons in various stages of apoptosis showed features including loss of processes, shrunken cell body, membrane blebbing and condensed nuclei.

Confocal fluorescent microscopy allowed concomitant examination of both morphology and fluorochrome molecular marker. This generally confirmed the association of visual features of apoptosis with positive labeling (Fig. 1) in individual cells. In a large population of cells staining variability may be a factor, as would the presence of a range of apoptotic stages.

### Quantitative Apoptosis Detection

Quantitative analysis by LSC revealed detectable differences in fluorescent label intensity among the experimental cell groups (Fig. 2). The ethanol treated positive controls recorded significantly higher values across all experiments. This was true for both parameters GMP and GI. Positively staining cells as determined by the LSC were also examined for morphology. Visualization confirmed the presence of characteristics of apoptosis such as condensed cells, nuclei and process retraction, as well as the high FITC-marker staining in these cells. The technique was therefore able to identify and distinguish cells positive for the apoptosis markers.

Data for all groups is the mean measurement value for the scanned population of single cells. GI data for TUNEL staining on a single B35 run are presented normalized against the ethanol treated positive control (Fig. 3). This illustrates the relative staining intensity of the respective neuronal cell groups. Neurons subjected to conditions of 100 mmHg pressure for 2 hr had higher levels of apoptotic marker compared to negative control neurons. This was significant at the 2 hr timepoint ( $P < 0.005$ ,  $n = 4$ ). B35 data was pooled for all TUNEL experiments and normalized as previously described (Fig. 4). Neurons subjected to pressure conditions showed increased apoptotic marker intensity compared to controls. This result was significant at the 2 hr timepoint for both parameters GMP ( $P < 0.05$ ,  $n = 24$ ) and especially GI ( $P = 0.005$ ,  $n = 24$ ). Later timepoints showed a similar trend but with greater variability, such that no significant differences were found at 6 hr or 20 hr. Quantitative data for a single B35 run using Annexin V showed experimental neurons subjected to pressure conditions had greater values for Annexin V staining compared with negative controls (Fig. 5). By contrast with the TUNEL data, this effect was interestingly more marked with time (20 hr,  $P < 0.05$ ,  $n = 4$ ). The

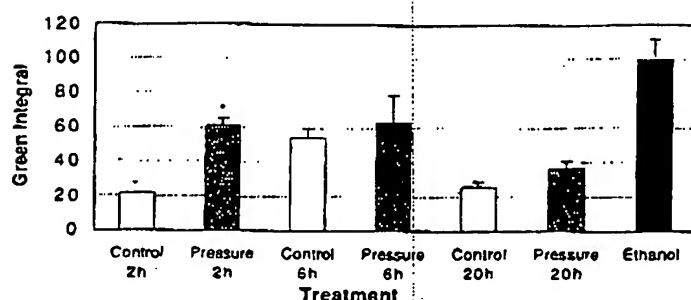


Fig. 3. LSC data for TUNEL apoptosis marker over time for B35 neurons after control, pressure and ethanol (positive control) treatment. Green integral LSC fluorescent values from single experimental run normalized to average positive control for that run (5% ethanol treatment for 2 hr to generate maximum detected apoptosis). Greater TUNEL labeling of neurons subjected to pressure conditions in comparison to control neurons significant at 2 hr ( $P < 0.005$ ,  $n = 4$ ). Control bars =  $\pm 1$  SE. Note that pressure measurements are always higher than the controls at the equivalent time period, though there are variations of these values with time after treatment.

intensity levels were also increased at the later timepoints, for both pressure and negative control neurons. Positive control data was similarly greater than in other groups.

PC12 differentiated neurons had increased cell surface areas, compared with rounded undifferentiated PC12 cells, and expressed neurites. Results for differentiated PC12 neurons show a similar pattern of increased apoptosis after elevated pressure. Figure 6 shows GI TUNEL data for a single PC12 run normalized against the maximal apoptosis control of DNase treatment. Apoptosis marker intensities for neurons subjected to pressure conditions were higher than comparable controls at all timepoints, with significance at 24 hr ( $P < 0.05$ ,  $n = 4$ ). Pooled TUNEL data for all PC12 experiments was also normalized to positive DNase control (Fig. 7). In these post-mitotic neurons the effect was statistically significant at 24 hr. GI and GMP data showed greater levels of apoptosis marker intensity for pressure treated neurons compared to controls (significance  $P < 0.05$ ,  $n = 11$ ).

### DISCUSSION

This study subjected neuronal cell lines to raised pressures and durations similar to those found in acute glaucoma, and found an increase in neuronal apoptosis under these conditions. This effect was noted in both proliferative B35 cells and in differentiated post-mitotic PC12 neurons. Apoptosis was confirmed qualitatively by cell morphology analysis and quantitatively by two separate specific markers of apoptosis. Laser scanning cytometry also allowed quantitative analysis of the fluorescent labels. These results support earlier findings using this experimental model and bioassay (Agar et al., 1999).

Increased ambient hydrostatic pressure of a defined incubation gas mix (5%  $\text{CO}_2$  and air) on a liquid phase culture media could alter partial pressures of the vital gases  $\text{O}_2$  and  $\text{CO}_2$ , and through dissolved  $\text{CO}_2$  on pH, poten-



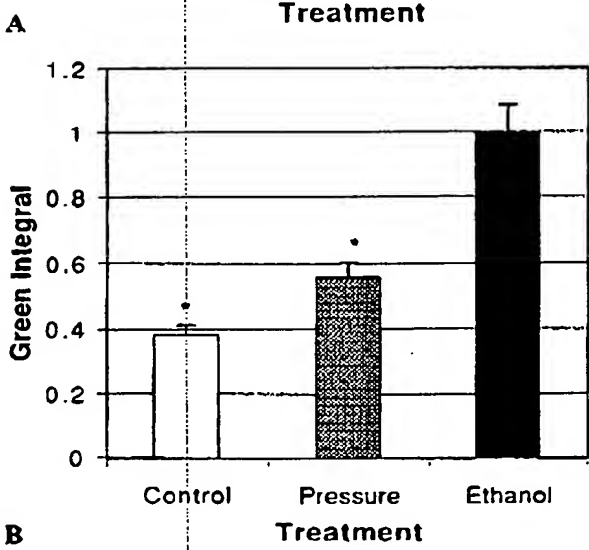
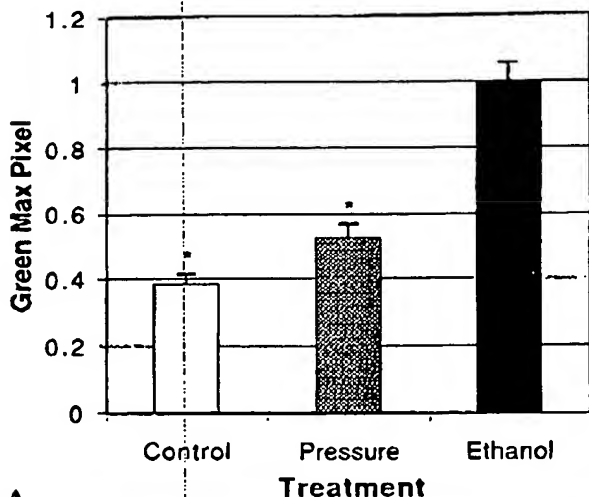


Fig. 4. Apoptosis in B35 neurons after 2 hr as measured by TUNEL using the LSC. An increase in apoptosis in neuronal cultures subjected to elevated pressure relative to control neurons is shown for both measures of quantitative fluorescence green integral (A) and green max pixel (B). Data is the mean of 7 separate experiments, normalized to average value for positive (ethanol) control. Significance of differences for green integral:  $P = 0.005$  and green max pixel:  $P < 0.05$ , ( $n = 24$ , scale bars =  $\pm 1$  SE).

ially affecting neuronal viability. Our experiments showed no significant difference in pH or the vital gases in cultures subjected to pressure compared to controls. It therefore seems that the experimental protocol did not significantly alter gas relationships of the neuronal cultures. With other parameters constant, this suggests any effects noted in cultured neurons were attributable primarily to the altered pressure conditions. Our findings agree with studies using similar pressure chamber designs with other cell types showing a negligible impact on gas relationships of culture media (Sumpio et al., 1994; Kosnosky et al.,

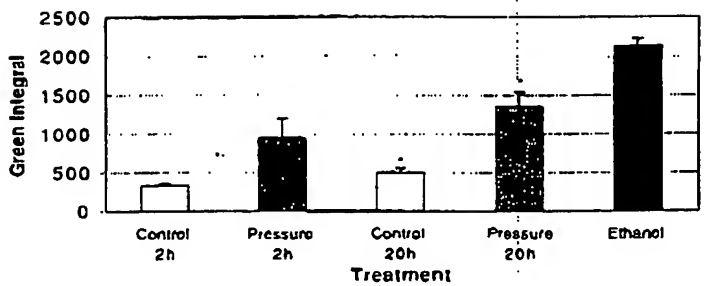


Fig. 5. Annexin V apoptosis assay of B35 neuronal cultures over time after ethanol, pressure and control treatments. Findings for single experimental run show increased apoptosis for both early (2 hr) and late (20 hr) timepoints in neurons subjected to pressure conditions compared to controls. Positive control for maximal apoptosis induction for experiment was 5% ethanol treatment for 2 hr. Differences significant at 20 hr ( $P < 0.05$ , Scale bars =  $\pm 1$  SE). Quantitative LSC data displayed for green integral (averaged label fluorescence for cell) absolute values for single experiment of 4 measurements.

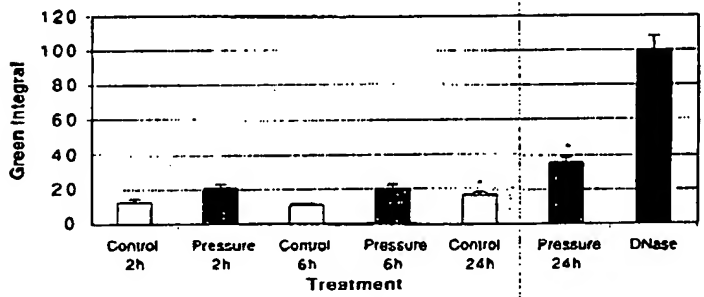


Fig. 6. Apoptosis in differentiated PC12 neurons after control, pressure and DNase treatment. LSC TUNEL data for single experimental run normalized to average positive control for that run (DNase treatment for 25 min to generate maximum detected apoptosis); Greater apoptosis marker labeling of neurons subjected to pressure conditions in comparison to control neurons significant at 24 hr ( $P < 0.05$ ,  $n = 4$ , Scale bars =  $\pm 1$  SE). TUNEL values for pressure treated neurons are always higher than equivalent controls, with the difference increasingly apparent with time after treatment.

1995; Mattana and Singhal 1995; Qian et al., 1999). Relatively small variations of pH,  $pCO_2$  and  $IO_2$  have been noted but were not considered to have affected viability in endothelial cells (Sumpio et al., 1994). Other studies on mesangial cells found small but statistically significant changes in  $pCO_2$  and pH, but none in  $pO_2$ . A series of experiments were then run with culture media adjusted to various pH levels to assess the impact of this effect on cell viability, with no significant effect found (Mattana and Singhal, 1995).

Our assay techniques using morphology and apoptotic markers all indicated that cell death after experimental pressure conditions occurred by apoptosis. Apoptosis is an active and physiological mode of cell death characterized by a series of morphological and molecular events, that can be detected by a variety of techniques. It is increasingly

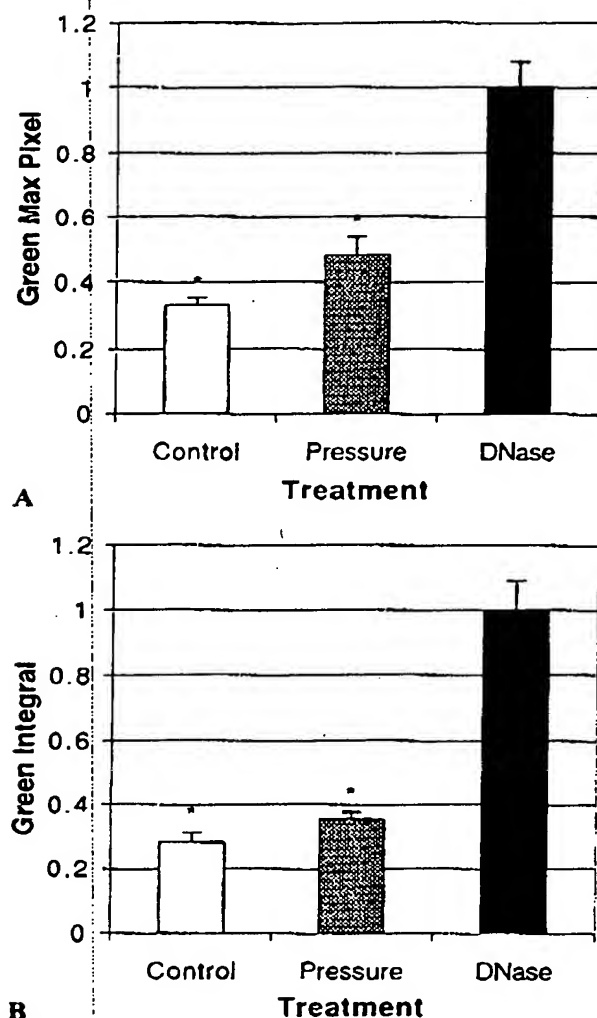


Fig. 7. Increased apoptosis in differentiated PC12 neurons 24 hr after treatment with elevated pressure, compared to controls. Quantitative analysis of TUNEL as measured by LSC. Both measures of fluorescence, green integral (A) and green max pixel (B), show significance differences  $P < 0.05$ , ( $n = 11$ , Scale bars =  $\pm 1$  SE). Data is the mean of 3 separate experiments, normalized to average value for positive (DNase) control.

apparent that no single method can be reliably used to identify apoptosis. Rather, the use of more than one technique, ideally based on different detection principles, is likely to distinguish apoptotic cells (Darzynkiewicz et al., 1998). The approach used in this study combines morphology, molecular markers of nuclear fragmentation (TUNEL) and membrane alterations (Annexin V) to optimize apoptosis detection. Several factors may confound the observations made in this study. Cells could be at different stages of apoptosis and may not exhibit all the features (morphological or molecular) of this process. TUNEL may also stain necrotic cells, though relatively

infrequently. Annexin V in conjunction with PI can distinguish the two modes of cell death in live cells more accurately, but this is less reliable in the late stages of apoptosis. The combination here of multiple techniques should enhance the sensitivity of apoptosis detection and also improve its accuracy.

This study also establishes the Laser Scanning Cytometer as an efficient bioassay tool for apoptosis in neurons. The LSCs automation minimizes potential observer influence on data collection and analysis; data can be normalized between separate pressure runs using a positive control; and storing of vectored data in relation to each scanned cell allows results to be confirmed by visual, and hence morphological, analysis. Results for positive control cells subjected to a known stimulus show much greater labeling for TUNEL (ethanol and DNase stimuli) and Annexin V (ethanol). Combined with morphological findings, they suggest the experimental protocol was able to detect apoptotic neurons. We detected a background level of apoptosis occurring in control B35 and PC12 neurons. It would be expected that this would apply to all experimental groups equally, as the cells used are from the same populations and identical.

Data for B35 cultures showed increased TUNEL labeling was statistically significant at the 2 hr timepoint, i.e., after application of pressure conditions. Later results were more varied and not conclusive after further statistical analysis. In view of a consistently significant difference for the initial timepoint alone, the neuronal effect may be temporally related to application of pressure if this is a factor in triggering apoptosis. Any effect then, if present, would be expected to be maximal closer to the time of the stimulus relative to a more remote period. Our early work with the Annexin V assay confirms similar results to the TUNEL data with greater apoptosis in pressure treated cells compared to controls. Differentiated PC12 neurons subject to pressure treatment were also found to have increased apoptosis labeling compared to controls, significant 24 hr after the initiation of pressure treatment. Differentiated PC12 neurons have been previously shown to undergo apoptosis upon withdrawal of growth factors (Michel et al., 1995; Oberdoerster et al., 1998, 1999). In our current study all PC12 cells were maintained in growth factors at all times.

Interestingly the B35 neurons seem to have an early pressure induced apoptosis response whereas the PC12 neurons respond later. At this point we suggest there may be two possibilities to help explain this difference in timecourse. The variation could be due to the cell type, or more likely may relate to the proliferative state of B35 cells versus the post-mitotic PC12 cells. The B35 cells in this study were not cell cycle synchronized, and therefore at all stages of the cell cycle, that may help explain the variable results at later timepoints. Perhaps the pressure conditions in this current study selectively affected a specific phase of the cell cycle early, with the remaining population less susceptible thereafter. Studies on lymphoblast cultures have reported pressure induced apoptosis and necrosis to be accelerated in the S phase of the cell

cycle (Takano et al., 1997). PC12 cells, on the other hand, were induced to differentiate to a post-mitotic state. Having exited the cell cycle they may demonstrate a differing response to the extracellular stimulus of elevated pressure. Post-mitotic PC12 neurons behave differently with other apoptotic stimuli, even when compared to their undifferentiated state. Other studies have shown undifferentiated (proliferative) cells to be more sensitive to an apoptotic stimulus, as we found for the B35 cells, than post-mitotic neurons (Oberdoerster et al., 1999). Our finding of significant apoptosis induction in differentiated PC12 neurons at the later timepoint (24 hr) is also the same as found in this other study using the same cells (Oberdoerster et al., 1999).

Apoptotic stimuli are varied and include internal and external activators, trophic factor deprivation and cellular damage. Physical stimuli can also induce apoptosis. Irradiation with UV light, for example, mediates apoptotic nuclear strand cleavage (Buja et al., 1993). We know little, however, about pressure acts as an apoptotic stimulus. In vivo research into heart failure has found pressure overload to induce apoptosis in animals (Teiger et al., 1996) and humans (Olivetti et al., 1996). A study into neural cell cultures and physical stressors in relation to glaucoma found mechanical shear to induce apoptosis (Edwards et al., 1998). In comparison, extremely high hydrostatic pressure (non-physiological) can induce apoptosis and necrosis in human lymphoblasts (Takano et al., 1997). Our current study indicates physiological changes in hydrostatic pressure may also stimulate neural apoptosis. We believe this is the first study of the effect on neurons of clinically relevant raised hydrostatic pressures alone, and to demonstrate apoptosis related to these pressure conditions. In addition to the broad range of known triggers for apoptosis, we suggest pressure may also be included as potential activators of apoptotic pathways.

The mechanisms that may mediate such a stimulus remain unclear. The cell cycle stage may be relevant, as suggested by our data and alluded to by other studies (Takano et al., 1997; Oberdoerster et al., 1999). Apoptosis in the neuronal study involving mechanical shear was associated with an increase in NO production and G protein activation (Edwards et al., 1998). Cellular responses to pressure other than apoptosis also provide clues to potential mechanisms. Cell cultures subject to similar pressure models to that used in this study reveal enhanced cell proliferation and modification of protein expression (Mattana and Singhal, 1995). This suggests cytoskeletal proteins may be subject to modulation by ambient pressure, consistent with tension-rigidity models of cell structure where such proteins contribute to and may therefore mediate physical force transfers (Wang et al., 1993). Such a concept is supported by findings of morphological responses to pressure (Sumpio et al., 1994). If neuronal compression is significant in our work, it is unclear whether the stimulus is related to compression or decompression or the static period of elevated pressure. Further, we do not know how the rates and durations of these changes affect the neuronal response. This first study using our model dealt with a specific set of experimental variables, and has found an effect related to these pressure conditions. Subsequent work will

allow evaluation of the basic parameters involved in pressure induced apoptosis, such as the rate of change and response threshold of the pressure stimulus.

Apoptosis may be stimulated by a sensitivity of the cell membrane to pressure changes. How pressure alterations are detected, let alone the mechanism of conversion of this into intercellular responses, is yet to be resolved. Hydrostatic pressure has been shown to influence transmembrane ion fluxes (Goldinger et al., 1980) and membrane receptor and protein activity, including the crucial Na-K-ATPase pump (Somero 1991). Pressure has been found to decrease spinal cord transmitter release (Gilman et al., 1987) and affect  $Ca^{2+}$  currents in chromaffin cells (Heinemann et al., 1987). Neuronal electrophysiological activity can also vary with pressure. Depression of near threshold orthodromic responses has been postulated to be due to a direct effect of high pressures on the conductance of specific  $K^{+}$  channels (Southan and Wann, 1996).

The possibility that pressure may be related to apoptosis is an interesting concept. At the cellular level there could be a greater sensitivity to this physical variable than previously thought. Because there seem to be a variety of cellular processes already shown to be modulated by pressure, it is not unreasonable to also consider apoptosis as an endpoint. This is of relevance in a disease such as glaucoma where neuronal apoptosis is somehow associated with an environment of altered pressure conditions. In addition to the known macroscopic anatomical and circulatory pathophysiology of glaucoma, this concept suggests retinal ganglion cells may be susceptible to elevated pressure at the cellular level. A neuronal response may be mediated by a more direct exposure to elevated pressure. Indeed large neurons, in the retina (RGC), cerebellum (Purkinje), and spinal cord (motor neurons) all seem to respond differently (usually more sensitive) to physiological stressors compared with smaller neurons.

We have shown a pressure stimulus to have an effect on apoptosis in more than one cell line, and in proliferating as well as post-mitotic neurons. The differentiated PC12 neurons have exited the cell cycle, as is the case in vivo for retinal neurons, including RGCs. Future work on the response of primary cultures to pressure would help broaden the relevance to disease processes. The potential activation of an apoptotic pathway also requires exploration to understand the conversion of this physical stimulus to a biological outcome. Both molecular and genetic processes, such as signal transduction and analysis of protein and mRNA or DNA expression, can be studied using this bioassay.

This study is the first to demonstrate in a biological assay system that physiologically relevant levels of pressure may have an impact on neuronal survival. This also suggests that conditions of elevated hydrostatic pressure, such as those found in acute glaucoma, may stimulate apoptosis. We would also suggest the possibility that raised hydrostatic pressures associated with other neural diseases, or after trauma, could induce neuronal apoptosis. The specific mechanism of pressure activation of this apoptotic pathway is not known at present. This system now allows

us to further investigate a number of other variables including different neurons and the basic parameters of the pressure stimulus. We can also study pharmacological and genetic factors that may support neuronal survival after these pressure conditions.

# ACKNOWLEDGMENTS

The authors wish to thank Dr. Stephanie Watson (Dept. Ophthalmology, Prince of Wales Hospital) for invaluable guidance in developing this model system; Prof. R. Frost (Dept. Mechanical Engineering, University of New South Wales) for assistance in designing the pressure chambers; Prof. M. Perry and Amanda Marsh (Dept. Physiology, University of New South Wales) for help in assessing our system; Ms. Moya Seeto (Cell Biology Lab) for extensive technical assistance; and Mr. Rob Wadley (Cellular Analysis Facility, University of New South Wales) for generous support with the Laser Scanning Cytometer. This study was supported in part by a discretionary general grant from Allergan Australia.

# REFERENCES

- Agar A, Hill M, Coroneo MT. 1999. Pressure induced apoptosis in neurons [ARVO Abstract]. Invest Ophthalmol Vis Sci 40:S265.
- Armaly MF, Krueger DE, Maunier L, Becker B, Hetherington J, Jr., Kolker AE, Levene RZ, Maunier AE, Pollack IP, Shaffer RN. 1980. Biostatistical analysis of the collaborative glaucoma study. I. Summary report of the risk factors for glaucomatous visual-field defects. Arch Ophthalmol 98:2163-2171.
- Ben-Sasson SA, Sherman Y, Gavrieli Y. 1995. Identification of dying cells—in situ staining Methods Cell Biol 46:29-39.
- DuJa LM, Eigenbrodt ML, Eigenbrodt EH. 1993. Apoptosis and necrosis. Basic types and mechanisms of cell death. Arch Pathol Lab Med 117: 1208-1214.
- Darzynkiewicz Z, Bedner E, Traganos F, Murakami T. 1998. Critical aspects in the analysis of apoptosis and necrosis. Hum Cell 11:3-12.
- De A, Boyadjieva NI, Pastorci M, Reddy BV, Sarkar DK. 1994. Cyclic AMP and ethanol interact to control apoptosis and differentiation in hypothalamic beta-endorphin neurons. J Biol Chem 269:26697-26705.
- Edwards ME, Chiou GCY, Good TA. 1998. Biomechanical force mediated G-protein activation and RGC apoptosis [ARVO Abstract]. Invest Ophthalmol Vis Sci 39:S916.
- Fagioli M, Galeo M, Strettoi E, Maffei L. 1997. Axonal transport blockade in the neonatal rat optic nerve induces limited retinal ganglion cell death. J Neurosci 17:7045-7052.
- Gilman SC, Colton JS, Durka AJ. 1987. Effect of pressure on the release of radioactive glycine and gamma-aminobutyric acid from spinal cord synaptosomes. J Neurochem 49:1571-1578.
- Golding JM, Kang BS, Choo YE, Paganelli CV, Hong SK. 1980. Effect of hydrostatic pressure on ion transport and metabolism in human erythrocytes. J Appl Physiol 49:224-231.
- Greene LA, Tischler AS. 1976. Establishment of a noradrenergic clonal line of rat adrenal pheochromocytoma cells which respond to nerve growth factor. Proc Natl Acad Sci USA 73:2424-2428.
- Heinemann SH, Conti F, Stuhmer W, Neher E. 1987. Effects of hydrostatic pressure on membrane processes. Sodium channels, calcium channels, and exocytosis. J Gen Physiol 90:765-778.
- Johansson JO. 1983. Inhibition of retrograde axoplasmic transport in rat optic nerve by increased IOP in vitro. Invest Ophthalmol Vis Sci 24: 1552-1558.
- Johansson JO. 1988. Inhibition and recovery of retrograde axoplasmic transport in rat optic nerve during and after elevated IOP in vivo. Exp Eye Res 46:223-227.
- Kerrigan LA, Zack DJ, Quigley HA, Smith SD, Pease ME. 1997. TUNEL-positive ganglion cells in human primary open-angle glaucoma. Arch Ophthalmol 115:1031-1035.
- Kosnosky W, Tripathi BJ, Tripathi RC. 1995. An in vitro system for studying pressure effects on growth, morphology and biochemical aspects of trabecular meshwork cells. Invest Ophthalmol Vis Sci 36:8731.
- Majno G, Joris I. 1995. Apoptosis, oncosis, and necrosis. An overview of cell death. Am J Pathol 146:3-15.
- Mattana J, Sankaran RT, Singhal PC. 1996. Increased applied pressure enhances the uptake of IgG complexes by macrophages. Pathobiology 64:40-45.
- Mattana J, Singhal PC. 1995. Applied pressure modulates mesangial cell proliferation and matrix synthesis. Am J Hypertens 8:1112-1120.
- Michel PP, Vyas S, Agid Y. 1995. Synergistic differentiation by chronic exposure to cyclic AMP and nerve growth factor renders rat pheochromocytoma PC12 cells totally dependent upon trophic support for survival. Eur J Neurosci 7:251-260.
- Mizushima T, Tsunumi S, Rokutan K, Tsuchiya T. 1999. Suppression of ethanol-induced apoptotic DNA fragmentation by geranylgeranylacetone in cultured guinea pig gastric mucosal cells. Dig Dis Sci 44:510-514.
- Nickells RW. 1996. Retinal ganglion cell death in glaucoma: the how, the why, and the maybe. J Glaucoma 5:345-356.
- Oberdorster J, Kamei AR, Rabin RA. 1998. Differential effect of ethanol on PC12 cell death. J Pharmacol Exp Ther 287:359-365.
- Oberdorster J, Rabin RA. 1999. NGF-differentiated and undifferentiated PC12 cells vary in induction of apoptosis by ethanol. Life Sci 64:PL267-272.
- Olivetti G, Quaini F, Sala R, Lagrasta C, Corradi D, Bonacina E, Gambert SR, Cigola E, Anversa P. 1996. Acute myocardial infarction in humans is associated with activation of programmed myocyte cell death in the surviving portion of the heart. J Mol Cell Cardiol 28:2005-2016.
- Qian Y, Tripathi BJ, Tripathi RC. 1999. Short-term elevation of hydrostatic pressure reduces TGF-beta 2 secretion and has no effect on the level of fibronectin in trabecular cells [ARVO Abstract]. Invest Ophthalmol Vis Sci 40:S668.
- Quigley HA. 1995. Ganglion cell death in glaucoma: pathology recapitulates ontogeny. Aust N Z J Ophthalmol. 23:85-91.
- Radius RL. 1981. Rapid axonal transport in primate optic nerve. Arch Ophthalmol 99:650-654.
- Schubert D. 1974. Induced differentiation of clonal rat nerve and glial cells. Neurobiology 4:376-387.
- Schutte B, Nuydens R, Geerts H, Ramaekers F. 1998. Annexin V binding assay as a tool to measure apoptosis in differentiated neuronal cells. J Neurosci Methods 86:63-69.
- Somero GN. 1991. Hydrostatic pressure and adaptation to the deep sea. New York: Wiley-Liss 167-204.
- Southan AP, Wann KT. 1996. Effects of high helium pressure on intracellular and field potential responses in the CA1 region of the in vitro rat hippocampus. Eur J Neurosci 8:2571-2581.
- Sumpio BE, Widmann MD, Ricotta J, Awolesi MA, Warase M. 1994. Increased ambient pressure stimulates proliferation and morphologic changes in cultured endothelial cells. J Cell Physiol 158:133-139.
- Takano KJ, Takano T, Yamanouchi Y, Satou T. 1997. Pressure-induced apoptosis in human lymphoblasts. Exp Cell Res 235:155-160.
- Teiger E, Than VD, Richard L, Wisniewsky C, Tea BS, Gaboury L, Tremblay J, Schwartz K, Hamer P. 1996. Apoptosis in pressure overload-induced heart hypertrophy in the rat. J Clin Invest 97:2891-2897.
- van Engeland M, Ramaekers FC, Schutte B, Reutelingsperger CP. 1996. A novel assay to measure loss of plasma membrane asymmetry during apoptosis of adherent cells in culture. Cytometry 24:131-139.
- Wang N, Butler JP, Ingber DE. 1993. Mechanotransduction across the cell surface and through the cytoskeleton. Science 260:1124-1127.
- Weber AJ, Kaufman PL, Hubbard WC. 1998. Morphology of single ganglion cells in the glaucomatous primate retina. Invest Ophthalmol Vis Sci. 39:2304-2320.

# The Pharmacology of Mechanogated Membrane Ion Channels

OWEN P. HAMILL AND DON W. MCBRIDE, JR.

*Department of Physiology and Biophysics, The University of Texas Medical Branch, Galveston, Texas*

I. Introduction .....	231
II. Classifications of mechanogated channels .....	232
A. Open channel properties .....	232
B. Gating properties .....	232
C. Molecular mechanisms .....	233
III. Mechanogated channel drugs .....	233
A. Blockers .....	233
1. Amiloride and analogs .....	234
2. Aminoglycoside antibiotics .....	236
3. Gadolinium .....	237
4. Other blockers .....	240
5. Blocker sensitivity of mechanosensitive processes .....	245
B. Activators .....	246
1. Amphipathic molecules .....	246
2. Fatty acids and lipids (amphiphilic molecules) .....	247
3. Other activators .....	247
IV. Summary and conclusions .....	248
V. Acknowledgments .....	248
VI. References .....	248

## I. Introduction

More than 30 years ago, A.S. Paintal (1964) reviewed in this Journal the pharmacology of vertebrate mechanoreceptors. His review summarized drug effects on a variety of specialized mechanosensory receptors, including cutaneous, muscle and visceral receptors. His main conclusion was that the drugs then known to inhibit or stimulate mechanosensation did not act on mechanotransduction itself but rather on ancillary processes such as the action potential or muscular/vascular tone. He further concluded that mechanotransduction usually has a low susceptibility to chemical influence. In subsequent years, voltage clamp studies confirmed that specific drugs reviewed by Paintal such as local anesthetics and veratrum alkaloids were indeed potent blockers and activators, respectively, of the voltage-gated  $\text{Na}^+$  channel (Hille, 1992). Since Paintal's review, a vast number of new drugs and toxins have been discovered that selectively act on various voltage- and ligand-gated channels (Hille, 1992). This wealth of new drugs has provided

a means of classifying, purifying and studying the function of many of these channels. Unfortunately, the large majority of these drugs has not been systematically studied for possible effects on mechanotransduction. This may be partially because of the practical problem of direct recording from specialized sensory mechanotransducers. However, it is also clear that the discovery of drugs that act on mechanosensors, such as those mediating various cardiovascular reflexes or specific forms of visceral pain, would have profound clinical significance.

Over the last 10 years, there has been a resurgence of interest in mechanotransduction because of a number of technical and conceptual advances. In particular, patch clamp recording, with its inherent ability to mechanically stimulate a membrane patch while simultaneously measuring the current response (Hamill et al., 1981), has revealed the existence of a class of mechanogated (MG) membrane ion channels. This class appears distinct from voltage- and ligand-gated channels (Sachs, 1988), although recent studies indicate that mechanical stimulation can also modulate voltage- and ligand-gated channels (see Section II, B). For practical reasons related to the inaccessibility of tissue embedded or fine ciliated endings of specialized mechanoreceptors, these

Address for correspondence: Dr. Owen P. Hamill, Department of Physiology/Biophysics, The University of Texas, Medical Branch, Galveston, TX 77555-0641.

MG channels have been studied mainly in nonsensory cell types and have been shown to be expressed in cell types representative of all five living kingdoms (Martinac, 1992). MG channels form a complex class, displaying different mechanosensitivities, gating dynamics and modalities, and open channel properties (Howard et al., 1988; Sachs, 1988; Morris, 1990; French, 1992; Petrov and Usherwood, 1994; Sackin, 1995; Hamill and McBride, 1995a). Presumably, the different properties reflect different roles played by MG channels in the various cell types. Although the role of MG channels in mechanosensory cells is obvious, they have also been implicated in such basic functions as cell volume regulation (Hamill, 1983a; Christensen, 1987; Sackin, 1989) and development (Medina and Bregestovski, 1988; however, see Wilkinson et al., 1996a, b). Nevertheless, their exact role(s) in many nonsensory cells remains unknown (Morris, 1992). For this reason, high specificity inhibitors or stimulators of MG channels would be extremely useful for implicating them in specific cellular processes. Furthermore, the existence of high affinity ligands that could label specific MG channels would facilitate protein purification procedures (Sukharev et al., 1993). Although no "ideal" high specificity/affinity drug for MG channels has yet been found, recent studies have begun to reveal a number of agents that do affect different MG channel activities. The purpose of this review is to discuss this emerging pharmacology.

## II. Classifications of MG Channels

To better appreciate the possible mechanisms and sites of drug action on MG channels, the various classifications and mechanisms of MG channel activation will be summarized. In general, membrane ion channels tend to be classified in terms of either their open channel properties and/or their gating properties. These two properties can be considered independent in the sense that knowledge of one does not determine the other.

### A. Open Channel Properties

MG channels, like voltage-gated and ligand-gated channels, display a variety of open channel properties with different ion selectivities (e.g., cation, anion,  $K^+$  and nonselective) and single channel conductances (~20 to 2000 pS). However, in general, the ion selectivity and conductance of biological channels are not mechanosensitive (but see Opsahl and Webb, 1994). Although some cells express only one type of MG channel, there are also cells that express as many as five types, which can be distinguished by their open channel properties (Berrier

et al., 1992; Ruknudin et al., 1993). Presumably, such differences reflect variations in the pore structure (i.e., binding sites and geometry) of the channels. In terms of drugs that act by binding to specific pore lining residues, it is conceivable that channels that share open channel properties (e.g.,  $K^+$  or cation selectivity) might be susceptible to pore occlusion or open channel block by the same drug or class of drugs.

### B. Gating Properties

In terms of gating, MG channels have tended to be divided into two broad groups, namely stretch-activated (SA) and stretch-inactivated (SI), depending upon whether they are opened or closed by mechanical stimulation, respectively (Guharay and Sachs, 1984; Morris and Sigurdson, 1989). However, this basic distinction may be complicated by dynamic or nonstationary kinetic properties of the SA channel. For example, certain SA channels show rapid and complete adaptation in response to sustained stimulation (i.e., appear to inactivate) (Hamill and McBride, 1992). Furthermore, SA channel activity can shift irreversibly from an adapting to nonadapting mode during the course of patch clamp recording (Hamill and McBride, 1992). Another possible complication concerns the SI channel terminology and relates to a recent demonstration that specific MG channels can respond differentially, depending on the direction of patch curvature. For example, in rat aortic endothelial cells, suction applied to the patch decreases channel activity, whereas applied pressure increases channel activity (Marchenko and Sage, 1996). Whether this phenomenon is specific to the MG channel of this cell type or a general property of the so-called SI channel remains to be determined.

Another aspect of MG channel gating relates to their sensitivity to the magnitude of mechanical stimulation (see Hamill and McBride, 1994a). Some MG channels are so sensitive that they can be gated by random fluctuations in thermal noise (Denk and Webb, 1989) or sub-Angstrom displacements (Brownell and Farley, 1979), whereas other MG channels are relatively insensitive and require stimulation that often causes membrane patch (Vandorpe et al., 1994) or cell rupture (Morris and Horn, 1991). However, the large majority of MG channels appear to be activated by modest stimuli, above the thermal noise level yet well below the level that causes membrane damage (Hamill and McBride, 1994a). Apart from the magnitude or quantitative aspects of the mechanical stimulus, there are also qualitative aspects concerning its form. For example, cell stretch and compression, osmotic swelling, fluid shear stress, and suction or pressure applied to the membrane patch are all forms of mechanical stimulation, yet each may be expected to perturb, at the molecular level, the membrane in different manners. Indeed, specific membrane channels have been found that selectively respond to one but not another form of mechanical stimulation

Abbreviations: MG, mechanogated; SA, stretch-activated; SI, stretch-inactivated; MS, mechanosensitive;  $IP_3$ , inositol trisphosphate;  $IC_{50}$ , concentration that inhibits 50%; *E. coli*, *Escherichia coli*; TTX, tetrodotoxin; TEA, tetraethylammonium;  $K_d$ , dissociation constant; TC, tubocurarine; RGDS, Arg-Gly-Asp-Ser; GS, *Grammostola spatulata*; RVD, regulatory volume decrease; I-NMBA, 6-iodide-2-methoxy-5-nitrobenzamil.



(Olesen et al., 1988; Burton and Hutter, 1990; Sasaki et al., 1992). On the other hand, there are channels that respond to multiple forms of mechanical stimulation (Christensen, 1987; Uhl et al., 1988; Sackin, 1989; Olet and Bourque, 1993). In this review, attention is focused almost exclusively on MG channels gated by suction/pressure applied to the membrane patch. In most cases, pressure and suction are equally effective in activating the MG channel (Sachs, 1988; Morris, 1990; McBride and Hamill, 1992), which is consistent with the channel responding to membrane tension rather than pressure itself. However, as stated above, some MG channels may be sensitive to the direction of membrane curvature (Bowman et al., 1992; Bowman and Lohr, 1996; Marchenko and Sage, 1996). Presumably, these different MG channel gating sensitivities depend upon specific extracellular/membrane/cytoskeleton interactions.

Finally, some MG channels, rather than being exclusively gated by membrane stretch, are also gated by nonmechanical stimulation such as ligands (Kirber et al., 1992; Vandoorpe and Morris, 1992; Van Wagoner, 1993; Paoletti and Ascher, 1994; Vandoorpe et al., 1994) and/or membrane voltage (Hisada et al., 1991; Kirber et al., 1992; Chang and Loretz, 1992; Davidson, 1993; Langton, 1993; Ben-Tabou et al., 1994; Hamill and McBride, 1996a). In specific cases, membrane stretch may only modulate activity rather than directly gate the channel (Kirber et al., 1992; Paoletti and Ascher, 1994). Such polymodal activation of a membrane ion channel complicates, from a biophysical viewpoint, the characterization and classification of the channel but nevertheless may be critical in its role(s) under different physiological and/or pathological conditions. Clearly, recognition of the normal gating behavior of a channel is essential for proper interpretation of drug effects on that channel.

### C. Molecular Mechanisms

Mechanisms of mechanosensitivity can be classified into either direct or indirect, according to the way mechanical energy is coupled to the gating mechanism of the channel. In the direct mechanism, mechanical energy is directly coupled to the MG channel protein without the intervention of biochemical reactions, although energy may be focused onto the channel via cytoskeletal and/or extracellular elements. In the indirect mechanism, there are intervening biochemical steps between the initial mechanical event and channel gating such as a membrane bound mechanosensitive (MS) enzyme, which regulates a second-messenger and, in turn, influences sensitive channels. For instance, activation of a mechanosensitive phospholipase C (Brophy et al., 1993) would elevate inositol trisphosphate ( $IP_3$ ), in turn releasing  $Ca^{2+}$  from  $IP_3$ -sensitive internal  $Ca^{2+}$  stores (Boitano et al., 1994) and, in this way, stimulating  $Ca^{2+}$ -sensitive channels in the plasma and possibly organelle membranes. In this example, both  $Ca^{2+}$ -release and  $Ca^{2+}$ -activated channels contribute to the MS response

without themselves being directly MS. One criterion for distinguishing between direct and indirect mechanisms involves measuring the latency of channel turn-on after a step change in stimulation (Corey and Hudspeth, 1979; Ordway et al., 1991; McBride and Hamill, 1993). Another criterion is to compare mechanosensitivities in cell-attached and cell-free patches to determine the role, if any, of cytoplasmic second-messengers. Unfortunately, for many channels that display mechanosensitivity, this most basic distinction between direct and indirect mechanisms of activation has not always been made.

Both direct and indirect mechanisms may be subdivided into intrinsic or extrinsic mechanisms according to bilayer versus cytoskeletal (or extracellular) involvement in the gating mechanism. In the intrinsic mechanism, mechanosensitivity is dependent upon interactions exclusively within the membrane bilayer (Martinac et al., 1990; Sukharev et al., 1993; Opsahl and Webb, 1994). For example, intrinsic mechanisms may involve tension-dependent protein subunit recruitment or realignment within the bilayer (Opsahl and Webb, 1994; Hamill and McBride, 1994a). In the extrinsic mechanism, mechanical stimulation is applied to the channel or membrane enzyme via cytoskeletal or extracellular elements (Guharay and Sachs, 1984; Howard et al., 1988; Hamill and McBride, 1992). In this mechanism, mechanosensitivity might be lost if mechanical coupling between the channel and cytoskeletal/extracellular elements is disrupted without rupturing the patch itself (Assad et al., 1991; Hamill and McBride, 1992). In fact, such disruption can arise during the course of routine patch recordings and can result in modified MG channel properties (Hamill and McBride, 1992).

In considering the site of action of a drug, the type of mechanism underlying mechanosensitivity may be critical. For example, in the indirect mechanism, a drug could block mechanosensitivity by acting along the biochemical pathway with or without a direct action on the channel or MS enzyme. Similarly, with the extrinsic mechanism, a drug could be active because of its action on the cytoskeleton or extracellular matrix without having any direct effect on the channel itself.

## III. MG Channel Drugs

The drugs that affect MG channel activity will be considered under two general categories involving either channel block or channel activation. Within these two classes, further distinctions may be made depending upon, for example, the drug's exact mechanism of action (e.g., open versus closed channel block) or its likely site of action (e.g., protein, bilayer or cytoskeleton).

### A. Blockers

Of the various chemicals and drugs that block MG channels, three groups have received the most attention. These include amiloride and its analogs, aminoglycoside

antibiotics and the lanthanides, in particular, gadolinium. In addition to these three groups, other less well characterized blocking agents will also be considered.

**1. Amiloride and analogs.** Amiloride is discussed first because it has been the most rigorously studied and is the only drug that has been quantitatively modeled in terms of its blocking mechanism (Lane et al., 1991; Ruesch et al., 1994). Amiloride is a member of a group of over 1000 structurally related compounds known as pyrazinecarboxyamides (Kleyman and Cragoe, 1988, 1990). Amiloride and many of its analogs are potent diuretics that act by blocking, in nanomolar to micromolar concentrations, the epithelial  $\text{Na}^+$  channel (Benos, 1982). Although the native epithelial  $\text{Na}^+$  channel has not been directly demonstrated to be mechanosensitive, recent cloning studies of the rat epithelial  $\text{Na}^+$  channel indicate that the three subunits ( $\alpha\beta\gamma$ ) that compose it show strong sequence homology to *Caenorhabditis elegans* genes, cloned from touch-insensitive mutants and believed to encode MG channel proteins (Canessa et al., 1993, 1994; Driscoll and Chalfie, 1991; Huang and Chalfie, 1994; Hong and Driscoll, 1994). Furthermore, a recent report indicates that the  $\alpha$ -subunit of the bovine renal epithelial  $\text{Na}^+$  channel may form a stretch-sensitive  $\text{Na}^+$  channel when reconstituted into painted lipid bilayers in which tension was altered hydrostatically (Awayada et al., 1995). However, this result must be considered tentative, because with painted lipid bilayers, the membrane tension is not simply a function of the hydrostatic pressure gradient (e.g., see Fettiplace et al., 1971; Fettiplace personal communication). In fact, membrane tension will be determined by the equilibrium distribution of lipids between the bilayer itself and the surrounding meniscus. On this basis, the result should be confirmed under conditions in which membrane tension can be better controlled (e.g., by using the patch clamp tip-dip method (Opsahl and Webb, 1994)). Perhaps it is even more relevant to determine whether the heterologous ( $\alpha\beta\gamma$ ) or native  $\text{Na}^+$  channel displays mechanosensitivity. Unfortunately, two recent studies attempting to directly address this important issue have not resolved it. In one case, the inability to obtain consistent results regarding the stretch sensitivity or insensitivity of the epithelial  $\text{Na}^+$  channel in cells of the rat cortical collecting tubule precluded a resolution (Palmer and Frindt, 1996). In the other case, the lack of controls with regard to both the magnitude and form (i.e., compression versus stretch) of the mechanical stimulation casts doubt on the reported stretch sensitivity of the  $\text{Na}^+$  currents measured in human  $\beta$  lymphocytes (Achard et al., 1996).

The original indication that amiloride might act on MG channels arose from observations that amiloride blocked mechanosensitivity in both the lateral line organ of *Necturus* and the skin of *Xenopus* (Jorgensen, 1985). Subsequently, amiloride was shown to directly block MG currents in dissociated audiovestibular hair

cells of the chick (Jorgensen and Ohmori, 1988) and mouse (Ruesch et al., 1994) inner ear. The first study of amiloride block at the single MG channel level was carried out on the SA cation channel of *Xenopus* oocytes (Lane et al., 1991, 1992, 1993; Hamill et al., 1992). This SA channel shows basic similarities to the hair cell channel in terms of its cation selectivity (i.e., conducts  $\text{Na}^+$ ,  $\text{K}^+$  and  $\text{Ca}^{2+}$ ) conductance ( $\sim 50$  pS) and rapid activation and adaptation kinetics (Howard et al., 1988; Taglietti and Toselli 1988; Yang and Sachs, 1989; Hamill and McBride, 1992, 1994b). Furthermore, external amiloride causes a similar voltage-dependent block of both the hair cell and oocyte MG channels. In both cases, inward current recorded at negative potential is reduced, but outward current recorded at positive potentials is almost unaffected (Jorgensen and Ohmori, 1988; Lane et al., 1991).

**a. MECHANISM OF AMILORIDE BLOCK.** At the single channel level, amiloride block involves brief interruptions in the inward current events that increase in frequency with amiloride concentration but decrease with depolarization (Lane et al., 1991). Because the interruptions are too brief to resolve fully, they result in an apparent reduction in single channel current amplitude with associated increased open channel noise. This type of voltage-dependent "flickery" block is often taken to reflect open channel or pore block with intermediate kinetics (e.g., see Hamill, 1983b). According to this model, amiloride, which is positively charged at physiological pH, would be driven by negative potentials into the open channel, where it would occlude or "plug" the channel. Positive potentials would reverse this block by driving the impermeant blocker back out of the channel. Modifications of the simple plug model include the partial and permeant block models (see Lane et al., 1991).

Although the various plug models are intuitively attractive, a number of observations argue against their relevance to amiloride block in both the oocyte and hair cell (Lane et al., 1991; Ruesch et al., 1994). In the first place, the channel conductance in amiloride reaches a voltage-independent value at hyperpolarized potentials. Second, the concentration dependence of amiloride block yields a Hill coefficient of 2, which indicates two amiloride molecules are required to block the channel; this seems unlikely within a single file permeation pathway. Third, amiloride block does not depend on current flux through the MG channel, thus ruling out a mechanism by which permeating ions are able to knock amiloride off the channel.

In contrast to plug models, a "conformational" model can explain both the voltage and concentration dependence of external amiloride block (Lane et al., 1991; Ruesch et al., 1994). This model assumes that the open channel can exist in one of two different voltage-dependent conformations. The open channel conformation favored at negative potentials reveals two amiloride binding sites, whereas the open conformation favored at



positive potentials is such that these sites are inaccessible to amiloride. Thus, at positive potentials, amiloride has no effect, whereas at negative potentials, amiloride binds to the exposed sites in a cooperative, voltage-independent manner to block the channel. Furthermore, at least in the hair cell, relaxation measurements directly demonstrate that amiloride analogs block the open rather than closed channel conformation at negative potentials. Although most attention has focused on external block, in the oocyte, internally applied amiloride produces a low potency voltage-independent block that was not observed in the hair cell.

**b. IONIC EFFECTS ON AMILORIDE BLOCK.** External amiloride is 10 times less effective in blocking the oocyte channel (concentration that inhibits 50% ( $IC_{50}$ ) = 500  $\mu$ M) compared with the hair cell channel ( $IC_{50}$  = 50  $\mu$ M). This difference in potency was shown not to be caused by the different ionic recording conditions used in the two preparations (Lane et al., 1993). To be specific, in the original oocyte study, amiloride block was measured in the absence of external  $Ca^{2+}$  as well as other divalent cations and in the presence of high (100 mM) external  $K^+$  and low (5 mM) external  $Na^+$ . In contrast, hair cell measurements were made in the presence of divalent cations (2 mM) with high external  $Na^+$  and low  $K^+$  (Jorgensen and Ohmori, 1988; Ruesch et al., 1994). Furthermore, it has been suggested that amiloride block requires the presence of external  $Ca^{2+}$  (Cuthbert and Wong, 1972; but see Desmedt et al., 1991) and is influenced by changes in external  $Na^+$  concentration (Benos, 1982). However, direct experiments with the oocyte indicate that inclusion of 2 mM  $Ca^{2+}$  in fact reduced (by a factor of 2) rather than increased amiloride potency. On the other hand, substitution of external  $Na^+$  with  $K^+$

had no effect (Lane et al., 1993). The potency reduction by  $Ca^{2+}$  was shown to occur without altering the voltage dependence of block and could be modeled by a screening of surface negative charges (Lane et al., 1993). If  $Ca^{2+}$  has a similar effect in the hair cells, then amiloride may be even more potent in situ (i.e.,  $IC_{50}$  < 50  $\mu$ M) because  $Ca^{2+}$  concentration in the normal endolymph is only ~50  $\mu$ M (Crawford et al., 1991).

**c. STRUCTURE-ACTIVITY STUDIES.** The difference in amiloride potency for MG channels in hair cells compared with oocytes presumably reflects real differences in the binding affinities for sites on the two channels. Although these difference may indicate structural differences in the sites, "potency-sequence-fingerprinting" indicates that the binding sites may be structurally related. For example, examination of the order of blocking potency of a series of amiloride analogs indicates both channels display identical potency sequences (Lane et al., 1992; Ruesch et al., 1994). In contrast, other transport pathways that are blocked by amiloride analogs, including the epithelial  $Na^+$  channel, show different analog potency sequences (table 1). Therefore sequence fingerprinting with amiloride analogs can compensate for amiloride's low specificity. For example, table 1 indicates that amiloride and only one appropriate analog need be tested to implicate MG channels over other suspected transporters in a specific cellular function.

Examination of the structure-activity relation in table 1 indicates that analog potency in both the oocyte and hair cell can be increased by adding hydrophobic side chains to the amiloride core structure (Lane et al., 1992; Ruesch et al., 1994). However, the hair cell studies indicate a limit where potency decreases when the bulkiness of the side chains becomes too great. This may

TABLE 1  
Amiloride analog<sup>a</sup> potency ( $IC_{50}$  amiloride/ $IC_{50}$  analog) of MG channels and other transport pathways.

	Amiloride ( $IC_{50}$ $\mu$ M)	DMA	Phenamil	PBDCB	Benzamil	HMA	I-NMBA	Ref.
MG channel mouse hair cell (cation)	1 (53)	1.3	4.4	5	9.6	12.3	29	Ruesch et al., 1994
MG channel frog oocyte (cation)	1 (500)	1.4	—	—	5.3	14.7 [BrHMA]	—	Lane et al., 1992
Epithelial $Na^+$ channel (high affinity)	1 (0.34)	0.04	17	—	9	0.04	7	Kleyman and Cragoe, 1988
Epithelial $Na^+$ channel (low affinity)	1 (10)	2.2	2.9	—	3.8	—	—	Kleyman and Cragoe, 1988
$Ca^{2+}$ channel L-type	1 (100)	3	—	400	4	—	26	Garcia et al., 1990
$Na^+$ - $Ca^{2+}$ exchanger	1 (1100)	2	5.5	300	11	11	28	Kleyman and Cragoe, 1988
$Na^+$ - $H^+$ exchanger	1 (84)	20	0.01	—	0.08	524	—	Kleyman and Cragoe, 1988
MG channel snail ( $K^+$ )	1 (2000)	—	—	—	—	—	—	Small and Morris, 1995
$Ca^{2+}$ channel T-type	1 (30)	—	—	—	—	—	—	Tang et al., 1988
Voltage-gated $Na^+$ channel	1 (600)	—	—	—	37	—	—	Velly et al., 1988
Voltage-gated $K^+$ channel (delayed rect.)	1 (5)	—	—	—	—	—	—	Bielefeld et al., 1986
Nicotinic AChR cation channel	1 (100)	—	—	—	—	—	—	Kleyman and Cragoe, 1990

<sup>a</sup> Dimethylamiloride (DMA), hexamethyleneamiloride (HMA), 6-iodide-2-methoxy-5-nitrobenzamil (I-NMBA), bromohexamethyleneamiloride (BrHMA), 5-(N-propyl-N-butyl)-dichlorobenzamil (PBDCB).

indicate the amiloride binding sites are located within sterically restricted hydrophobic pockets. The most potent amiloride analog that has been found to date is 6-iodide-2-methoxy-5-nitrobenzamil (I-NMBA), which blocks the hair cell MG channel with an  $IC_{50}$  of  $\sim 2 \mu M$ . However, this drug may be even more potent when measured in the absence of external divalent cations (see Section III.A.1.b).

d. SUMMARY. Although amiloride has not proven a highly potent/specific MG channel blocker, it has provided valuable information regarding one type of MG channel. First, amiloride sensitivity of the MG cation channel provided the initial clue that this channel may somehow be related to the amiloride-sensitive epithelial  $Na^+$  channel. This idea has subsequently been reinforced by (a) apparent immunological cross-reactivity between the epithelial  $Na^+$  channel and the hair cell MG channel for an antibody raised against the former (Hackney et al., 1992) and (b) sequence homology between the epithelial  $Na^+$  channel and putative MG channel proteins (Canessa et al., 1994). Second, detailed analysis of amiloride block indicates multiple, voltage-sensitive open channel conformations of the MG cation channel. This feature must be incorporated into any gating model of the channel. Third, potency sequence fingerprinting using amiloride analogs provides a way of identifying MG channel involvement in specific cellular processes. Finally, because all amiloride analogs so far tested have proven more potent than amiloride, future screening of the  $\sim 1000$  available analogs may reveal even more potent/specific MG channel blockers.

2. *Aminoglycoside antibiotics.* Antibiotics of the aminoglycoside family (e.g., gentamicin, neomycin and streptomycin) also block MG cation channels in hair cells (Kroese et al., 1989) and skeletal muscle (Sokabe et al., 1993). However, compared with amiloride, less detailed information exists on their mechanism of action, ionic interactions and structure-activity requirements. Aminoglycosides consist of two or more amino sugars in glycosidic linkage to a hexose nucleus, and most have several positive charges because each sugar may have up to two positively charged amino residues (Daniels, 1978). In contrast to amiloride analogs, aminoglycosides are quite soluble ( $> 500 mM$ ) in aqueous solution, which from a practical standpoint, makes them more convenient for experimental use (e.g., see Jaramillo and Hudspeth, 1991). In terms of MG channel block, most attention has focused on actions on hair cells because chronic exposure to aminoglycosides causes hair cell death, resulting in clinically significant and irreversible hearing impairment (Rybak, 1986). Although the exact mechanism of antibiotic ototoxicity is unknown, one possibility is an action involving the MG channel (Denk et al., 1992).

The first acute studies of aminoglycoside action were on the hair cells of the amphibian lateral line organ, where gentamicin was shown to cause a reversible, dose-dependent block of microphonic potentials and afferent

fiber activity (Kroese and Van den Bercken, 1980, 1982). Subsequently, voltage-clamp studies of frog vestibular hair cells indicated a rapid ( $< 100 \mu sec$ ), voltage-dependent block of the MG currents by gentamicin and a number of other aminoglycoside antibiotics (Kroese et al., 1989; and see table 2). Comparison of tables 1 and 2 indicates the potency of aminoglycosides and amiloride analogs are comparable. In addition, block by both classes of drugs is decreased by both depolarization or external  $Ca^{2+}$  (Kroese et al., 1989; Lane et al., 1993). However, despite these similarities, the two drugs most likely involve different blocking mechanisms (Kroese et al., 1989). To begin with, the concentration dependence of aminoglycoside block indicates a Hill coefficient of 1, rather than the coefficient of 2 seen for amiloride. Second, with aminoglycosides, MG conductance and currents approach zero with hyperpolarization (e.g., see Kimitsuki and Ohmori, 1993) instead of approaching a nonzero value, as seen with amiloride. Taken together, these observations are consistent with the idea that aminoglycosides block the open channel according to a simple plug model (see Section III.A.1.a). The voltage dependence of the block indicates that external aminoglycosides binding site senses 20 to 40% of the membrane field (Kroese et al., 1989). In addition to blocking hair cell MG channels, aminoglycosides may also have direct effects on the adaptation mechanism that changes the channel's mechanosensitivity in response to steady state stimulation (Kimitsuki and Ohmori, 1993). A molecular mechanism has been put forward to explain adaptation in the hair cell (Howard et al., 1988; Hudspeth and Gillespie, 1994), and the availability of drugs that affect adaptation should prove useful in analyzing such mechanisms. Another practical use of aminoglycosides has been focal application of gentamicin to localize the MG channels on the tips of the hair cell cilia (Jaramillo and Hudspeth, 1991).

Aminoglycosides also block two different types of SA cation channels in chick skeletal muscle, namely a 60 pS voltage-independent channel and a 190 pS voltage-dependent channel. These two SA channels can further be distinguished pharmacologically by their sequence-potency-fingerprint using various aminoglycosides (Sokabe et al., 1993; and see table 2). Aminoglycosides also block a variety of other MS processes (see Section III.A.5), including the slow adapting activity of cat cutaneous mechanoreceptors (Baumann et al., 1988), hair cell activity in squid statocysts (Williamson, 1990), mechanically induced nematocyte discharge in hydrozoans (Gitter et al., 1993) and stretch-induced increase in intracellular  $Ca^{2+}$  in guinea pig ventricular myocytes (Gannier et al., 1994). Although the aminoglycoside sensitivity of these processes points to an underlying MG channel mechanism, a complication in interpretation exists because aminoglycosides, like amiloride analogs, lack specificity and have been shown to also block voltage-gated  $Ca^{2+}$  channels (Nakagawa et al., 1992),  $Ca^{2+}$ -

## PHARMACOLOGY OF MECHANOGATED MEMBRANE ION CHANNELS

237

TABLE 2  
Aminoglycoside antibiotic block of MG and other channels

	Aminoglycoside	IC <sub>50</sub> ( $\mu$ M)	Reference
MG channels			
Frog hair cell cation:	verdamycin	2.0	Kroese et al., 1988
	gentamicin C2	2.5	
	gentamicin C1	5.5	
	sisomicin	6.0	
	gentamicin	7.6	
	dihydrostreptomycin	8.0	
	netilmicin	25.0	
	streptomycin	25.0	
	amikacin	95.0	
Chick skeletal muscle SA cation: 60 pS	neomycin	2.4	Sokabe et al., 1993
	streptomycin	20.7	
	ribostamycin	32.4	
	dibekacin	47.5	
190 pS	kanamycin	54.7	Sokabe et al., 1993
	neomycin	2.4	
	dibekacin	17.5	
	kanamycin	22.1	
	streptomycin	25.4	
	ribostamycin	55.9	
Other channels			
Voltage-gated Ca <sup>2+</sup> (N-type) frog nerve terminals:	neomycin	<50	Redman and Silinsky, 1994
	streptomycin	~50	
	gentamicin	>50	
Voltage-gated Ca <sup>2+</sup> (L-type) guinea pig outer hair cells:	neomycin	300	Nakagawa et al., 1992
	gentamicin	1000	
	kanamycin	~1000	
	streptomycin	1000	
Ca <sup>2+</sup> -activated K <sup>+</sup> channel rat brain:	neomycin	195	Nomura et al., 1990
	dibekacin	600	
	ribostamycin	2390	
	kanamycin	2830	
ATP-activated K <sup>+</sup> current Guinea pig outer hair cells:	neomycin	90	Lin et al., 1993

activated K<sup>+</sup> channels (Nomura et al., 1991) and adenosine triphosphate-sensitive channels (Lin et al., 1993) as well as increasing desensitization of acetylcholine receptor channels (Okamoto et al., 1991).

**3. Gadolinium.** Gadolinium (Gd<sup>3+</sup>) is the most commonly used blocker of MG channels and is often used as a pharmacological tool for testing the putative role of MG channels in various MG processes. It is a member of the lanthanide series, which is composed of the 15 elements, inclusively, between lanthanum (La, atomic number 57, ionic radius 1.061 Å) and lutetium (Lu, atomic number 71, ionic radius 0.85 Å), with Gd in the middle (atomic number 64, ionic radius 0.938 Å). All the lanthanides are trivalent ions in aqueous solution and have proven useful in biochemical studies because of their remarkable similarity to Ca<sup>2+</sup> in terms of size (ionic radius 0.99 Å), bonding, coordination geometry and donor atom preference (Moeller, 1973; Evans, 1990).

Millet and Pickard were the first to focus attention on Gd<sup>3+</sup> as a possible MG channel blocker when they reported that Gd<sup>3+</sup> (10 to 250  $\mu$ M) blocked both thigmotropism and geotropism in plants, whereas similar concentrations of La<sup>3+</sup> were without effect (Millet and Pickard, 1988). They hypothesized that Gd<sup>3+</sup> blocked these mechanosensitive processes by specifically inhibiting Ca<sup>2+</sup>-permeable MG channels (see also Edwards and Pickard, 1987). Subsequent patch clamp studies confirmed that Gd<sup>3+</sup> did indeed block single MG channel currents in not only plant cells (Alexandre and Lassalles, 1991; Ding and Pickard, 1993a; Garrill et al., 1993) but also in fungi (Zhou et al., 1991), bacteria (Berrier et al., 1992; Martinac, 1992; Cui et al., 1995; Hase et al., 1995) and a variety of animal cells (see table 3). In particular, Yang and Sachs (1989) showed that 10  $\mu$ M Gd<sup>3+</sup> in solutions perfused onto outside-out patches of *Xenopus* oocytes completely and reversibly blocked MG cation channel activity. In contrast, in the same

study, much higher concentrations (i.e.,  $> 10 \times$ ) of either  $\text{La}^{3+}$  or  $\text{Lu}^{3+}$  were required to cause MG channel block.

Generally,  $\text{Gd}^{3+}$  blocks MG channels in the concentration range of 1 to 100  $\mu\text{M}$ , independently of either their single channel conductance or ion selectivity of the MG channel (table 3). However, there are exceptions. For instance, in one study of *Escherichia coli* (*E. coli*),  $\text{Gd}^{3+}$  in lower concentrations (20  $\mu\text{M}$ ) was shown to increase the activity of a 350 pS and a 1100 pS channel but inhibit their activity in higher concentrations ( $> 20 \mu\text{M}$ ) (Cui et al., 1995). Similar concentration-dependent excitatory and inhibitory effects were reported for MG cation channel activity in onion protoplasts by Ding and Pickard (1993a). However, as noted by these authors (Ding and Pickard, 1993a), these mixed  $\text{Gd}^{3+}$  effects seen at low concentrations (0.1 to 2  $\mu\text{M}$ ) are highly variable. In another *E. coli* study, 100  $\mu\text{M}$   $\text{Gd}^{3+}$  was shown

to block larger conductance (300 to 2300 pS) MG channels without affecting lower conductance (100 to 220 pS) MG channels (Berrier et al., 1992). Other exceptions include the relatively low potency ( $\sim 1 \text{ mM}$ ) block of an SA  $\text{K}^+$  channel in human myelinated nerve (Quasthoff, 1994) and a cation MG channel in one strain of yeast (c.f., Zhou and Kung, 1992; Zhou et al., 1991) and its apparent ineffectiveness in blocking SA cation channels in atrial heart muscle (Kim, 1993) as well as SA  $\text{K}^+$  channels in astrocytes (Yang and Sachs, 1989), lymphocytes (Schlichter and Sakellaropoulos, 1994) and molluscan neurons (Small and Morris, 1995). However, in some studies, the presence of anions such as bicarbonate and phosphate or the  $\text{Ca}^{2+}$  chelator, ethylene glycol-bis-N,N'-tetraacetic acid (EGTA), may contribute to the observed low potencies. These chemicals interact with or chelate  $\text{Gd}^{3+}$  and therefore change its effective concentration (Boland et al., 1991).

TABLE 3  
Gadolinium block of MG and other channels

Species cell type	Ion selectivity	Channel conduct. (pS)	Blocking concent. ( $\mu\text{M}$ )	Reference(s)
<b>MG channels</b>				
<i>E. coli</i>	nonselective	300-2300	100	Berrier et al., 1992
<i>E. coli</i>	nonselective	350 and 1100	100	Cui et al., 1995
<i>Saccharomyces</i> (yeast)	nonselective	40	10	Gustin et al., 1988
<i>Schizosacchar</i> (yeast)	cation	180	1000	Zhou and Kung, 1992
<i>Uromyces</i> (fungi)	cation	600	50	Zhou et al., 1991
Hyphae (fungi)	cation	—	100	Garrill et al., 1993
Red beet vacuole	cation	70	10	Alexandre and Lasalles, 1991
Onion protoplast	cation	35	10	Ding and Pickard, 1993
<i>Necturus</i> kidney	cation	18	20	Filipovic and Sackin, 1991
<i>Xenopus</i> oocyte	cation	50	10	Yang and Sachs, 1989
<i>Xenopus</i> kidney	cation	70	10	Kawahara and Matsuzaki, 1993
Bone cell line	cation	40	20	Duncan et al., 1992
Guinea pig bladder	cation	80	20	Wellner and Isenberg, 1993; 1995
Mouse skeletal muscle	cation	20-50	$>10$	Franco and Lansman, 1990
Mouse skeletal muscle	cation (SI)	20-50	$>10$	Franco et al., 1991
Rat hepatoma cells	cation	40	50	Bear and Li, 1991
Rat supraoptic neurons	cation	$\sim 30$	100	Oliet and Bourque, 1994
Mouse BC3H1 muscle	cation	30	100	Hamill and McBride, 1993
Rat cardiocytes	cation	42	1	Sandoshima et al., 1992
Chick cardiocytes	cation	25 and 50	20	Ruknudin et al., 1993
Chick cardiocytes	$\text{K}^+$	100 and 200	20	Ruknudin et al., 1993
Human demyelinated axon	$\text{K}^+$	52	1000	Quasthoff, 1994
<i>E. coli</i>	anion	100-250	No effect 100	Berrier et al., 1992
Rat astrocyte	$\text{K}^+$	70	No effect 10	Yang and Sachs, 1989
Mouse Ehrlich ascites	cation	15-40	No effect 20	Christensen and Hoffmann, 1992
Rat atrial cells	cation	20	No effect 100*	Kim, 1993
Rat atrial cells	$\text{K}^+$	50-100	No effect 100	Kim et al., 1995
Snail ( <i>Lymnaea</i> ) neur.	$\text{K}^+$	44	No effect 100*	Small and Morris, 1995
<b>OTHER CHANNELS</b>				
Species, cell type	Channel type		[ $\mu\text{M}$ ]	Reference
Guinea pig ventricul. myocytes	$\text{Ca}^{2+}$ (L-type)		10	Lacampagne et al., 1994
Rat pituitary	$\text{Ca}^{2+}$ (L-type)		$<0.2$	Biagi and Enyeart, 1990
Rat pituitary	$\text{Ca}^{2+}$ (T-type)		2.5	Biagi and Enyeart, 1990
<i>Xenopus</i> myelinated nerve	$\text{K}^+$ (delayed rec.)		100	Elinder and Arhem, 1994
<i>Xenopus</i> myelinated nerve	$\text{Na}^+$ (voltage-gated)		100	Elinder and Arhem, 1994
<i>E. coli</i>	Colicin A, N		30,100	Bonhivers et al., 1995
<i>Bryonia dioica</i> (plant)	$\text{Ca}^{2+}$ -release channel ER membrane		10	Kluesener et al., 1995

\* EGTA present with  $\text{Gd}^{3+}$ .

All channels are SA unless indicated SI.

a. MECHANISM OF  $Gd^{3+}$  ACTION. To date, no detailed mechanism for  $Gd^{3+}$  block of any MG channel has been determined. One reason for this, at least for SA channels, may be that  $Gd^{3+}$  action is complex and most likely has multiple mechanisms and sites of action depending upon its concentration. In addition to any specific interactions with membrane channel proteins,  $Gd^{3+}$ , as well as other lanthanides, has been shown to exhibit strong interactions with lipid bilayers. For example, lanthanides bind strongly to both charged and neutral bilayers (Lehrmann and Seelig, 1994). Furthermore, differential scanning calorimetric and freeze-fracture studies have shown that lanthanides are capable of increasing phase transition temperatures, decreasing membrane fluidity and promoting phase separations or domains and membrane dipole potentials (Li et al., 1994; Yu et al., 1996). Such effects may alter MG channel activity by changing the physical environment of the membrane channel protein (Yu et al., 1996). In relation to these ideas, temperature studies of MG channel activity in plant cells indicate a membrane phase transition that affects MG channel activity (Ding and Pickard, 1993b).

The most detailed analysis of  $Gd^{3+}$  block has been carried out on the *Xenopus* oocyte SA cation channel (Yang and Sachs, 1989). The properties of the various  $Gd^{3+}$  effects on this channel and the extremely narrow concentration range (5 to 10  $\mu M$ ) over which they occur seem to rule out a simple open channel block mechanism. Instead, Yang and Sachs (1989) proposed a combination of three different mechanisms that are evident at different  $Gd^{3+}$  concentrations. First, at low concentrations (1 to 5  $\mu M$ ), the  $Gd^{3+}$  reduced single channel current amplitude, seen as an almost parallel shift of the single channel current-voltage curve along the voltage axis, was proposed to be caused by  $Gd^{3+}$  screening of negative surface charges in or near the vestibule of the channel. Second, also at low concentrations, the observed voltage-independent reduction in open channel lifetime was proposed to be caused by  $Gd^{3+}$  interacting with an external allosteric site (i.e., outside the membrane field) that caused transition of the channel to a short-lived closed state. Finally, at 10  $\mu M$  but not 5  $\mu M$ , channel activity completely disappeared. This last effect was believed to occur because of a  $Gd^{3+}$ -induced, highly cooperative transition of the channel to a long-lived closed state. Such highly cooperative behavior would be consistent with  $Gd^{3+}$ -induced shifts in phase transitions or promotion of phase domains in the lipid bilayer, as discussed above.

Although most  $Gd^{3+}$  studies have been on SA channels, there is at least one detailed report describing  $Gd^{3+}$  block of the so-called SI cation channel in mouse (*mdx*) muscle (Franco et al., 1991). This study found, as with the SA cation channel, that  $Gd^{3+}$  block can occur with no shift in the mechanosensitivity (i.e., the pressure-response relation) of the channel (Franco et al.,

1991; Yang and Sachs, 1989). Nevertheless, comparison of the voltage- and concentration-dependent properties of  $Gd^{3+}$  block of SI and SA channels indicates notable differences. In particular, the block of the SI channel involves brief, yet resolvable, channel closures with no change in single channel current amplitude. Furthermore, the voltage and concentration dependence of the open-close transitions indicates a blocking mechanism consistent with  $Gd^{3+}$  being an open pore, permeant blocker. To be specific, although the blocking rate (i.e.,  $Gd^{3+}$  entry into the channel) is diffusion-limited and displays no voltage dependence, the rate of unblocking increases with hyperpolarization, presumably as  $Gd^{3+}$  is driven through the channel.

The differences in  $Gd^{3+}$  block of SI and SA cation channels may reflect real differences in the nature of  $Gd^{3+}$  interactions with the two channels. However, strict comparison between the two studies is complicated because of the different ionic conditions. In the SI case,  $Gd^{3+}$  block was measured in the presence of divalent cations (2 mM  $Ca^{2+}$  and 1 mM  $Mg^{2+}$ ) but in their absence in the SA case. This difference undoubtedly contributes to the different blocking effects because  $Ca^{2+}$  also permeates and blocks both channel types (Taglietti and Toselli, 1988; Yang and Sachs, 1989; Franco et al., 1991; Lane et al., 1993). Clearly, more detailed experiments on  $Gd^{3+}$  action under similar recording conditions would be helpful. Furthermore, a more systematic study of the blocking effect of the other 15 lanthanides of SA and SI channels may provide a means of dissecting or distinguishing different mechanisms and sites of action. For example, one possible physical basis for  $Gd^{3+}$ 's higher potency compared with other lanthanides is the "gadolinium break," a term that refers to the drastic change in the stability of organic ion complexes that occurs around the middle of the lanthanide series (Nieboer, 1975). On the other hand, it is interesting that in one systematic study of lanthanides,  $Tm^{3+}$ ,  $Er^{3+}$ ,  $Dy^{3+}$ ,  $Tb^{3+}$ ,  $Eu^{3+}$  were found to be as equally potent as  $Gd^{3+}$  in blocking the touch-induced action potential of the plant *Chara* (Staves and Wayne, 1993).

b.  $Gd^{3+}$  BLOCK OF NON-MG CHANNELS. Although  $Gd^{3+}$  was initially thought to be selective for MG channels, it has subsequently been shown to be a particularly potent blocker of voltage-gated L-type  $Ca^{2+}$  channels (complete block with 0.2  $\mu M$ ) as well as T- and N-type  $Ca^{2+}$  channels (Biagi and Enyeart, 1990; Boland et al., 1991; Docherty, 1988; Song et al., 1992; Lacampagne et al., 1994; Romano-Silva et al., 1994). Furthermore, it also blocks, although less potently ( $\sim 100 \mu M$ ), voltage-gated  $Na^{+}$  channels and  $K^{+}$  channels as well as voltage-independent leak channels in myelinated nerves (Elinder and Arhem, 1994a). A multisite mechanism of block similar to that of Yang and Sachs has been proposed for  $Gd^{3+}$  block of voltage-gated  $Na^{+}$  and  $K^{+}$  channels (Elinder and Arhem, 1994b). On the other hand, a de-



tailed analysis of the block of L-type  $\text{Ca}^{2+}$  channels by  $\text{Gd}^{3+}$  and other lanthanides indicates a mechanism similar to that used to explain  $\text{Gd}^{3+}$  block of the SI channel (Lansman, 1990).

c. SUMMARY.  $\text{Gd}^{3+}$  is a potent blocker of a wide variety of MG channels and, as predicted by Millet and Pickard, has proven to be the inhibitor of choice for testing the putative role of MG channels in MG processes, not only in plants, but in a wide range of animal cells (see table 4). Its action, at least on the SA cation channel, is complex, and more detailed studies taking advantage of the other lanthanides and their known physical chemistry should be helpful in distinguishing different mechanisms and sites (i.e., lipid or protein) of action.

4. Other blockers. In this section, we list a number of less characterized blockers of MG channels. Some of the drugs listed are better known as blockers of other voltage- and transmitter-gated channels.

a.  $\text{Na}^+$  CHANNEL BLOCKERS. Tetrodotoxin (TTX) is best known for its ability to block the voltage-gated  $\text{Na}^+$  channel. However, whereas some studies of the Pacinian corpuscle indicate that TTX only blocks the action potential, other studies indicate it may also reduce the mechanoreceptor potential (see Bell et al., 1994). It remains unresolved whether this reduction occurs because of direct block of MG channels or block of voltage-gated channels that may contribute to the receptor potential. At least in chick cardiomyocytes, TTX does block a 25-pS SA cation channel without affecting four other classes of SA channels also expressed in the myocyte (Ruknudin et al., 1993). Whereas TTX has no effect on the microphonic potential recorded from goldfish saccula, procaine, another  $\text{Na}^+$  channel blocker, produces a partial (35%) reduction at a concentration of  $2 \times 10^{-3}$  g/ml (Matsuura et al., 1971). In a quite different preparation, the ciliated protozoan, 1 mM procaine blocks the mechanoreceptor  $\text{K}^+$  current (Deitmer, 1992). However, further down the evolutionary scale, 0.5 mM procaine activates the anion MG channel in *E. coli* (see Section III, B.1, and table 5). Given these divergent effects, it would seem worthwhile to screen procaine action on other MG channels.

b.  $\text{Ca}^{2+}$  CHANNEL BLOCKERS. As indicated above, amiloride, aminoglycosides and  $\text{Gd}^{3+}$  all block  $\text{Ca}^{2+}$  channels as well as MG channels. This complicates functional studies, because reports indicate that the L-type  $\text{Ca}^{2+}$  channel may be mechanosensitive as well as voltage-sensitive (Langton, 1993; Ben-Tabou et al., 1994). One strategy to discriminate its role has been to test more specific  $\text{Ca}^{2+}$  channel blockers such as dihydropyridines (see Naruse and Sokabe, 1993). However, some caution is required with this approach because such  $\text{Ca}^{2+}$  channel blockers also affect MG channel activities, including diltiazem, which blocks the 25-pS SA, TTX-sensitive cation channel in chick cardiomyocytes (Ruknudin et al., 1993). Other known  $\text{Ca}^{2+}$  blockers, including  $\text{Co}^{2+}$ ,  $\text{La}^{3+}$ , heptanol and octanol, block mechanotransduction in hair cells (Ohmori, 1985).

c.  $\text{K}^+$  CHANNEL BLOCKERS. To date, blocker pharmacology has been mostly focused on the SA cation-selective channel, and the major blockers of this channel have also been shown to act on  $\text{Na}^+$  and  $\text{Ca}^{2+}$  channels. By analogy, one might expect that SA  $\text{K}^+$  channels would be sensitive to the various toxins and drugs that act selectively on  $\text{K}^+$  channels. Indeed, a number of  $\text{K}^+$  channel blockers do act on SA  $\text{K}^+$  channels but appear to be ineffective against the SA cation channels (Morris, 1990). However, in general, these blockers are of relatively low potency and overall low specificity for  $\text{K}^+$  channels. For example, the SA  $\text{K}^+$  channel in frog renal proximal tubule can be blocked by external  $\text{Ba}^{2+}$  (5 mM) (Filipovic and Sackin, 1991; Cemerikic and Sackin, 1993), whereas the SA  $\text{K}^+$  channel in molluscan neurons is blocked by external tetraethylammonium (TEA) ( $K_d$  of 10 mM) and quinidine ( $K_d = 0.8$  mM) but unaffected by either of these internally. Also ineffective on the latter channel when applied externally are  $\text{Ba}^{2+}$  (50 mM), apamin (1  $\mu\text{M}$ ) and 4-aminopyridine (10 mM) (Small and Morris, 1995). In contrast,  $\text{Ba}^{2+}$  (2 mM) blocks the SA  $\text{K}^+$  channels in rat brain neurons, but external TEA, 4-aminopyridine or quinidine apparently does not (Kim et al., 1995). On the other hand, in the ciliated protozoan, *Stylonychia*, external 4-aminopyridine (0.5 mM) and TEA (1 mM) but not  $\text{Cs}^+$  block the MG  $\text{K}^+$  current (Deitmer, 1992). Neither external TEA (1 mM) nor 4-aminopyridine (1 mM) blocks the MG cation channel in crayfish stretch receptor (Erxleben, 1989).

d. CALCIUM IONS.  $\text{Ca}^{2+}$  has been shown to block MG cation channels in *Xenopus* oocytes (Taglietti and Toselli, 1988; Yang and Sachs, 1989; Lane et al., 1993) and vertebrate hair cells (Crawford et al., 1991). Detailed analysis of this  $\text{Ca}^{2+}$  block by Taglietti and Toselli (1988) indicates a permeant ion block mechanism in which  $\text{Ca}^{2+}$ , like  $\text{Na}^+$  and  $\text{K}^+$ , enters and binds to the channel but displays a much smaller  $K_d$  (50  $\mu\text{M}$ ) and much longer occupancy time (400 nsec) compared with  $\text{Na}^+$  (2 mM and 20 nsec) or  $\text{K}^+$  (3.2 mM and 12 nsec). The higher affinity for  $\text{Ca}^{2+}$  results in greater channel occupancy so that inward flow of  $\text{Na}^+$  and  $\text{K}^+$  is competitively inhibited.

e. PROTONS. The open probability of SA cation channels is reduced to near zero when external pH is reduced from 7.2 to 4.5 in onion cell epidermis (Ding et al., 1993) and from 7.2 to 5.8 in *E. coli* (Cui et al., 1995). In *E. coli*, acidic pH was also shown to reduce the sensitivity of the MG channel (i.e., shifted the pressure-response curve to the right). The mechanism of the acid effects on MG channel gating remains unknown but may be due to protonation of amino groups or a proton-induced conformation change (Cui et al., 1995). In the case of plants, the pH effect has been proposed to underlie the inhibitory effect of acid soil syndrome on plant root tip growth (Ding et al., 1993). In contrast to the strong inhibitory effects of acid pH, alkaline pH up to 8.6 has only a slight inhibitory affect on the *E. coli* channels (Cui et al., 1995).

## PHARMACOLOGY OF MECHANOGATED MEMBRANE ION CHANNELS

241

TABLE 4  
Processes tested for MG channel drug sensitivity

Process/ Stimulation used	Cell type	Gd <sup>3+</sup>	Amilor.	Amino- glycoside	Conc. tested $\mu$ M except when in ( )	Reference
<b>Stimulated increase in internal Ca<sup>2+</sup></b>						
Touch	Cultured chick heart	Y			20	Sigurdson et al., 1992
Touch	Rabbit airway epithelial	Y			50-100	Boitano et al., 1994
Touch	Rabbit osteoclasts	N			200	Xia and Ferrier, 1995
Cell-stretch	Pig vascular smooth muscle	Y			10	Davis et al., 1992
Cell-stretch	Guinea pig ventricular myocyt.			Y	40	Gannier et al., 1994
Substrate-stretch	Human umbilical endothelial	Y			10	Naruse and Sokabe, 1993
Substrate-stretch	Pulmonary arterial smooth musc.	Y			10	Bialecki et al., 1992
Substrate-stretch	Rat lung cell	Y			10	Liu et al., 1994
Osmotic swelling	Guinea pig outer hair cells	Y			50	Harada et al., 1993
Osmotic swelling	Human dystrophic myotubes	Y			50	Pressmar et al., 1994
Osmotic swelling	Human fibroblasts	Y			50	Bibby and McCulloch, 1994
Osmotic swelling	Human T lymphocytes	Y			200	Schlichter and Sakellaropoulos, 1994
Osmotic swelling	Rat renal collecting duct cells	N			40	Mooren and Kinne, 1994
Fluid shear stress	Bovine aortic endothelial cells	Y			10	Oliver and Chase, 1992
<b>Volume regulatory events</b>						
Volume regulatory decrease in response to osmotic swelling	Human blood lymphocytes	Y			1	Deutsch and Lee, 1988
	Mouse neuroblastoma cells	Y			10	Lippmann et al., 1995
	Guinea pig cochlear hair cells	Y			10	Crist et al., 1993
	Frog kidney proximal cells	Y			10	Robson and Hunter, 1994
	Mouse Ehrlich ascite cells	Y			10	Christensen and Hoffmann, 1992
	Human fibroblasts	Y			50	Bibby and McCulloch, 1994
	Human astrocytoma cells	Y			100	Medrano and Gruenstein, 1993
	Human leukemic cells lines	N			10-100	Gallin et al., 1994
<b>Hypoosmotic-induced</b>						
Cation current	Rat osteosarcoma cell	Y			10	Duncan et al., 1992
Cation current	Frog kidney proximal cells	Y			10	Robson and Hunter, 1994
K <sub>Ca</sub> <sup>+</sup> current	Guinea pig outer hair cell	Y			50	Harada et al., 1993
Cl <sub>Ca</sub> <sup>-</sup> current	Rat lacrimal acinar cells	Y			20	Kotera and Brown, 1993
Cl <sup>-</sup> current	<i>Xenopus</i> oocytes	Y			>250	Ackerman et al., 1994
Osmolyte efflux	<i>E. coli</i>	Y			1000	Berrier et al., 1992
<b>Hyperosmotic-induced</b>						
Cation current	Human airway epithelial cells	Y			10	Chan and Nelson, 1992
Cl <sup>-</sup> currents	Rat osteoblastic cells	N			100	Chesnoy-Marchais and Fritsch, 1994
<b>Growth/development/metabolism</b>						
Oocyte maturation	<i>Xenopus</i> oocytes	N	N	N	(1,2,1)	Wilkinson et al., 1996a,b
Fertilization	<i>Xenopus</i> oocytes	N	N	N	(1,2,1)	Wilkinson et al., 1996a,b
Embryogenesis	<i>Xenopus</i> oocytes	N	N	N	(1,2,1)	Wilkinson et al., 1996a,b
Sperm motility	<i>Xenopus</i> sperm	N	N	N	(1,2,1)	Wilkinson et al., 1996a,b
Embryogenesis	<i>Xenopus</i> and ascidian oocytes	N			100	Steffensen et al., 1991
<b>Stretch-induced</b>						
Myoblast fusion	Chick skeletal muscle	Y			10	Shin et al., 1996
Cell alignment	Cultured endothelial cells	Y			10	Naruse et al., 1993
Cell proliferation	Rat lung cells	Y			10	Liu et al., 1994
DNA synthesis	Rat lung cells	Y			10	Liu et al., 1994
Phospholipase C	Rabbit aortic smooth musc.	N			100	Matsumoto et al., 1995

TABLE 4 continued

Process Stimulation used	Cell type	Gd <sup>3+</sup>	Amilor.	Amino- glycoside	Conc. tested $\mu$ M except when in ( )	Reference(s)
Actin polymerization	Human fibroblasts	N			10	Pender and McCulloch, 1991
Hypertrophy	Rat cardiac myocytes	N			50	Sadoshima and Izumo, 1993
Genes activation	Rat cardiac myocytes	N			10	Sadoshima et al., 1992
Strain-activated Depolarization	Rat osteosarcoma cells	Y			10	Duncan and Hruska, 1994
<b>Specialized mechanosensory receptors</b>						
Pressure-induced						
Baroreceptor discharge	Rat arterial	N			400	Andresen and Yang, 1992
Baroreceptor discharge	Rabbit carotid	Y			10	Hajduczuk et al., 1994
Stretch-induced						
Depolarization	Frog muscle spindles	Y	Y		(1 mM, 1 mM)	Ito et al., 1990
Depolarization	Crayfish stretch receptor	Y			400	Swerup et al., 1991
Touch-induced						
Calcium increase	Rat nodose sensory neurons	Y			10	Sharma et al., 1995
Depolarization	Cat cutaneous mechanoreceptors			Y	(i.v. 2.5 mg/min)	Baumann et al., 1988
Depolarization	Squid statocyst			Y	(10 mM)	Williamson, 1990
Cation inward current	Rat nodose sensory neurons	Y			20	Cunningham et al., 1995
Cation inward current	Rat supraortic neurons	Y			100	Oliet and Bourque, 1994
Voltage-induced						
Hair cell motion	Guinea pig outer hair cells	Y			500	Santos-Sacchi, 1991
<b>Muscle</b>						
Stretch-induced						
Force development	Guinea pig papillary muscle	Y			10	Lab et al., 1994
Contracture	Rat uterine smooth muscle	Y	N		100, 3000	Kasai et al., 1995
Arrhythmias	Canine ventricular muscle	Y			10	Hansen et al., 1990
Depolarization	Canine ventricular muscle	Y			10	Stacy et al., 1992
Depolarization	Guinea pig urinary bladder myocytes	Y			40	Wellner and Isenberg, 1994
Peptide secretion	Rat atrial myocytes	Y			5-80	Laine et al., 1994
Transmitter release	Frog neuromuscular junction	N			100	Chen and Grinnell, 1995
<b>Plants and some lower invertebrates</b>						
Touch-induced action potential	<i>Chara corallina</i>	Y			0.0001	Staves and Wayne, 1993
Touch-induced tendril coiling	<i>Byronia dioica</i>	Y			10,000	Kluesener et al., 1995
Ca <sup>2+</sup> efflux from ER vesicles	<i>Byronia dioica</i>	Y			20	
Gravity-induced						
Thigmotropism	<i>Zea mays</i>	Y			10	Millet and Pickard, 1988
Orthogeotropism	<i>Zea mays</i>	Y			250	Millet and Pickard, 1988
Tip growth	<i>Saprolegnia ferax</i> (Fungi)	Y			100	Garrill et al., 1993
Rise in [Ca <sup>2+</sup> ] <sub>i</sub>	Fungi growing tip	Y			100	Garrill et al., 1993
Wind-induced						
Rise in [Ca <sup>2+</sup> ] <sub>i</sub>	<i>Nicotiana glauca</i>	N			(10 mM)	Knight et al., 1992
Touch-induced						
Nematocyte discharge	<i>Hydra vulgaris</i>			Y	50	Gitter et al., 1993
Nematocyte discharge	Cnidaria (Coelenterates)	Y			1	Salleo et al., 1994a,b

However, for the SA cation channel in chick skeletal muscle, raising pH from 7.4 to 10 significantly increases the channel's stretch sensitivity as well as its voltage sensitivity without affecting single channel conductance (Guharay and Sachs, 1985). These last effects were proposed to occur because a titratable site, possibly involving a lysine group of an N-terminal amino acid, may be

responsible for controlling voltage and stretch sensitivity (Guharay and Sachs, 1985).

f. ALUMINUM IONS. Aluminum ions (Al<sup>3+</sup>) (10 to 100  $\mu$ M) also inhibit the SA Ca<sup>2+</sup> channel in the plasma membrane of onion cells. This inhibition might also contribute to acid soil syndrome because low pH elevates free Al<sup>3+</sup> in the soil (Ding et al., 1993).



g. **TUBOCURARINE.** (+)-Tubocurarine (TC) and other bisquarternary amines (gallamine, decamethonium and succylcholine) selectively depress (TC:  $IC_{50} = 19 \mu M$ ) the mechanoreceptor current of the ciliate protozoan *Stentor coeruleus* without affecting the resting potential and the action potential (Wood, 1985). The mechanoreceptor current, in the absence of TC, is increased by depolarization (i.e., MG channel open probability increases with depolarization), whereas TC block is relieved by depolarization. To explain these observations, Wood (1985) proposed that the MG channel can exist in two voltage-dependent closed conformations (R and U) and one open conformation. One of the closed conformations (R), predominates at depolarized potentials and can be mechanically activated to open. The other closed conformation (U), predominates at hyperpolarized potentials and cannot be opened by mechanical stimulation. TC blocks the channel by selectively binding to the U form and thus prevents the channel from being mechanically activated. This model is similar to the conformation model proposed for amiloride block of the MG channel in *Xenopus* oocytes (Lane et al., 1991), except the oocyte model proposes two open conformations. In both cases, drug binding occurs to the conformation that predominates at hyperpolarized potentials.

h. **HALOTHANE AND OTHER INHALATION ANESTHETICS.** Halothane reduces the mechanoreceptor potential of crustacean stretch receptors: TTX was present to block  $Na^+$  channels. The mechanism of this block may involve effects on cable properties because neither the time course nor amplitude of the mechanoreceptor current appeared to be altered (see fig. 8 in Swerup and Rydqvist, 1985). In a whole lung preparation halothane, enflurane and isoflurane were shown to raise the pressure threshold for recruitment of slowly adapting stretch receptors in the tracheobronchial system and inhibit pulmonary irritant receptors (Nishino et al., 1994). Again, in this situation, the exact mechanism of drug action remains unknown.

i. **QUININE.** Quinine, a cinchona alkaloid used for the treatment of malaria, is known to induce a reversible hearing loss in mammals in millimolar concentrations (see references cited in Matsuura et al., 1971). Quinine causes an irreversible suppression of microphonic potentials recorded from fish saccular hair cells (Matsuura et al., 1971) and an apparent increase in stiffness of the hair bundle of the fish lateral line organ (Van Netten et al., 1994). These results are similar to the effects of aminoglycosides on hair cells and may indicate a direct blockage of the MG channel by quinine.

j. **FATTY ACIDS.** A group of positively charged (medium to long chain) fatty acid analogs (table 5) has been shown to suppress a SA  $K^+$  channel in toad gastric smooth muscle (Petrou et al., 1994). In contrast, negatively charged (medium to long chain) fatty acids activate the same channel and will be considered in more detail in the next section (Petrou et al., 1994). Short chain fatty

acids, whether positively or negatively charged, have no effect on the channel activity (Petrou et al., 1994). In addition to the fatty acids, the naturally occurring positively charged amino alcohol, sphingosine, also suppresses channel activity. These positively charged compounds do not appear to act as open channel blockers because they do not reduce either channel open time or single channel conductance (Petrou et al., 1994). Instead, their inhibitory actions has been proposed to arise through an allosteric mechanism (Petrou et al., 1994).

k. **INTEGRIN-BLOCKING PEPTIDES AND ANTIBODIES.** A specific model of mechanotransduction proposes that mechanical energy distorting the extracellular matrix is focused through to the cytoskeleton via integrins that span the plasma membrane (Wang et al., 1993; Ingber, 1993). In this model, one would expect that agents, such as blocking peptides or antibodies, that inhibit integrin binding to extracellular matrix proteins would reduce or block mechanosensitivity. Two studies, although not directly on MG channels, lend support to this idea. In one study (Wayne et al., 1992), it has been demonstrated that the integrin blocking peptide Arg-Gly-Asp-Ser (RGDS) inhibits both the gravitational and hydrostatic pressure-induced polarity of cytoplasmic streaming in the plant *Chara*. Both processes have been proposed to be mediated by MG channels. In another study (Chen and Grinnell, 1995), it has been demonstrated that the integrin-blocking peptide RGD, as well as integrin antibodies, suppress stretch-induced release of transmitter from frog nerve terminals. Stretch-induced release still occurs in the absence of external  $Ca^{2+}$ , is not blocked by  $100 \mu M$   $Gd^{3+}$  and may involve either MG release of internal  $Ca^{2+}$  or shift in  $Ca^{2+}$  sensitivity of the release process. Unfortunately, for patch clamp studies, a practical problem in testing integrin function using blocking peptides is that the extracellular matrix must typically be removed before the plasma membrane can be patch clamped.

l. **CISPLATIN.** Cisplatin is the major antineoplastic agent used to treat solid tumors such as ovarian, testicular and bladder cancers (Rosenberg, 1985; Seymour, 1993). Unfortunately, cisplatin has a number of dose-limiting side effects that include ototoxicity with consequent hearing loss (see McAlpine and Johnstone, 1990) and distal sensory neuropathy, indicated by early decreased vibratory sensibility (Thompson et al., 1985). Based on acute studies on guinea pig cochlear microphonic potentials, it has been proposed that cisplatin acts by blocking the MG channel in hair cells in a manner analogous to aminoglycoside antibiotics (McAlpine and Johnstone, 1990). However, voltage clamp studies of hair cells have not been carried out to confirm this action. In our own studies to test this proposed action, we have found that, at up to  $100 \mu M$ , neither cisplatin nor transplatin blocks the MG cation channel in *Xenopus* oocytes (L. Hu, D.W.M and O.P.H, unpublished observations).

TABLE 5  
Amphipathic and amphiphilic actions on MG channels

Cell Type	Channel Ion Selectivity Conductance	Compound Tested	Action <sup>a</sup>	Reference
Rat brain neurons	SA K <sup>+</sup> -selective 45, 52, and 143 pS	Arachidonic acid	A	(Kim et al., 1995)
		Linoleic acid	A	
		$\gamma$ -Linolenic acid	A	(Kim et al., 1995)
		Docosahexaenoic acid	A	
		Myristic acid	NE	
		Oleic acid	NE	
		Elaidic acid	NE	
		Palmitic acid	NE	
		Stearic acid	NE	
		Palmitoleic acid	NE	
		Arachidic acid	NE	
		Erucic acid	NE	
		Nervonic acid	NE	
Toad ( <i>Bufo marinus</i> )	SA K <sup>+</sup> selective 50 pS	(Negative compounds)		(Petrout et al., 1994)
		Arachidonic acid	A	
		Myristic acid	A	
		Oleic acid	A	
		Tetradecanesulphonate	A	
		(Positive compounds)		
		Decylamine	I	
		Dodecylamine	I	
		Tetradecylamine	I	
		Oleylamine	I	
		Sphingosine	I	
		(Neutral compounds)		
		Octanol	NE	
Rabbit pulmonary artery smooth muscle	SA K <sub>v</sub> Ca <sub>v</sub> <sup>2+</sup> 270 pS	Arachidonic acid	A	(Kirber et al., 1992)
		Myristic acid	A	
		Linoleic acid	A	
<i>E. coli</i>	SA Anion selective ~700 pS	Chlorpromazine (+ve)	A	(Martinac et al., 1990)
		Procaine (+ve)	A	
		Tetracaine (+ve)	A	
		Trinitrophenol (-ve)	A	
		Lysolcithin (neutral)	A	
Chick skeletal muscle	SA cation 60 pS Voltage-independent	Chlorpromazine	A	(Sokabe et al., 1993)
		Trinitrophenol	A	
Canine ventricular myocytes	Swelling activated Cl <sup>-</sup> conductance	Chlorpromazine	I	(Tseng, 1992)
		Trinitrophenol	A	

<sup>a</sup> A, activate; NE, no effect; I, inhibit.

m. TARANTULA SPIDER (*GRAMMOSTOLA SPATULATA*) VENOM. Preliminary reports indicate that the venom from the tarantula spider (*Grammostola spatulata*) (GS) blocks SA channel currents in *Xenopus* oocytes and chick heart cells (Niggell et al., 1996). GS venom also blocks the hypotonic swelling-induced elevation of intracellular Ca<sup>2+</sup> (sensed with Fura-2) in GH3 cells proposed to be mediated by SA cation channels (Chen et al., 1996). The blocking concentrations of venom used were 1000 to 15,000 times dilutions in saline. Identification of the MG channel active components of the venom has yet to be made. Concerning the venom's specificity for MG channels, it was demonstrated in GH3 cells that the crude venom did not block L-type Ca<sup>2+</sup> channels (Chen et al.,

1996). However, in another study on rat hippocampal neurons, it has been shown that a purified GS venom component (*w*-grammotoxin) does block in the micromolar range N-, P- and Q-type but not L-type Ca<sup>2+</sup> channels (Piser et al., 1995).

n. COLCHICINE AND VINBLASTINE. The antimiotic drugs, colchicine and vinblastine, which act by disrupting microtubules (Borgers et al., 1975), abolish mechanotransduction in the nematode *Caenorhabditis elegans* (Chalfie and Thomson, 1982) and the cricket *Acheta domesticus* (Erler, 1983), respectively. The concentrations and incubation times used were 0.5 to 1 mM for 12 hours for colchicine and 10 mM for up to 21 hours for vinblastine. In each case, the specific microtubule struc-

ture that is disrupted is proposed to be part of a supramolecular complex that underlies touch sensitivity (Thurm et al., 1983; Huang et al., 1995; for review see Hamill and McBride, 1996b). In contrast to the blocking effects of these drugs on lower invertebrates, neither colchicine nor vinblastine reduces MG channel activity in chick skeletal muscle (see Sachs, 1988) or in *Xenopus* oocytes (OPH and DWM unpublished observations). This lack of sensitivity in the oocyte may indicate that other types of non-microtubule cytoskeletal structures can focus mechanical energy onto MG channels (see Sachs, 1988; Hamill and McBride, 1995a).

5. *Blocker sensitivity of mechanosensitive processes.* Table 4 lists the wide variety of mechanosensitive processes that have been tested at the tissue or whole cell level for MG channel blocker sensitivity. Clearly,  $Gd^{3+}$  has proven the most popular agent in such studies. A likely reason for this is that  $Gd^{3+}$  causes a complete and voltage-independent block (i.e., "knock out" effect) of many types of SA channels, often at relatively low concentrations (1 to 20  $\mu M$ ). In contrast, amiloride and aminoglycosides only produce a partial and highly voltage-dependent block, even with relatively high drug concentrations (1 to 2 mM). However, even if  $Gd^{3+}$ 's action is all-or-none, additional control experiments should be carried out before either accepting or rejecting an MG channel role in a specific process. For example, a false positive could arise if the process involved a voltage-gated  $Ca^{2+}$  channel or another process that was  $Gd^{3+}$  blocked. Conversely, a false negative may arise if an underlying MG channel is  $Gd^{3+}$  insensitive (see table 3). Notwithstanding these caveats, the breadth of physiologically important mechanosensitive processes that display, at the tissue and/or whole cell level, the same  $Gd^{3+}$  sensitivity and ionic requirements as single MG channels recorded in the membrane patch is highly impressive. Presumably, it is the functional versatility of MG channels that underlies their ubiquitous expression in cells spanning the full evolutionary spectrum. Other notable highlights, trends and exceptions indicated in table 4 are discussed below (see Section III.A.5.a-f).

a. *MECHANICALLY INDUCED ELEVATION OF INTERNAL  $Ca^{2+}$ .* Internal  $Ca^{2+}$  is well recognized as a second-messenger in a wide range of cellular processes. In table 4, the various forms of mechanical stimulation that cause elevation of  $[Ca^{2+}]_i$  in various cell types are listed. In general,  $[Ca^{2+}]_i$  elevation may come about from one or a combination of the following mechanisms: increased  $Ca^{2+}$  influx from the external solution; decreased  $Ca^{2+}$  efflux from the cell and/or increased  $Ca^{2+}$  mobilization from internal stores. In many of the cases listed in table 4, the MS  $[Ca^{2+}]_i$  increase is blocked by  $Gd^{3+}$ . This is consistent with a  $Ca^{2+}$  influx via  $Gd^{3+}$ -sensitive SA cation channels (Sigurdson et al., 1992; Oliver and Chase, 1992; Naruse and Sokabe, 1993; Harada et al., 1993; Sharma et al., 1995). However, there is also pharmacological evidence for L-type  $Ca^{2+}$  channel involvement (e.g., nifedipine and nimodipine sensitivity) (Mc-

Carty and O'Neil, 1991; Boitano et al., 1994; Mooren and Kinne, 1994, but see Naruse and Sokabe, 1993), which is significant given the recently demonstrated mechanosensitivity of this channel (Ben Tabou et al., 1994; Langton, 1993). In cases in which the mechanically induced increase in  $[Ca^{2+}]_i$  occurs via release from internal stores, external  $Ca^{2+}$  is not necessary (Boitano et al., 1994; Charles et al., 1991; Demer et al., 1993; but see Sigurdson et al., 1992). For example, in airway epithelial cells, internal  $Ca^{2+}$  release is proposed to be mediated by a mechanosensitive phospholipase C that modulates, via  $IP_3$ ,  $Ca^{2+}$  release from internal  $Ca^{2+}$  stores (Boitano et al., 1994). Interestingly,  $Gd^{3+}$  addition, in the absence of external  $Ca^{2+}$ , can cause a larger MS increase in  $[Ca^{2+}]_i$ , presumably because  $Gd^{3+}$  blocks  $Ca^{2+}$  efflux via MG channels in the plasma membrane (Boitano et al., 1994).

b. *VOLUME REGULATORY EVENTS.* Many cell types show a regulatory volume decrease (RVD) when swollen in hypotonic solutions. Table 4 lists examples of RVD that can be blocked by low (10  $\mu M$ )  $Gd^{3+}$ . In general, RVD is mediated by an increase in  $K^+$  and  $Cl^-$  efflux and consequent net water efflux and may involve either  $Ca^{2+}$ -dependent or  $Ca^{2+}$ -independent mechanisms (for critical review see Foskett, 1994). Therefore,  $Gd^{3+}$  could presumably block RVD either by blocking  $Ca^{2+}$  influx into the cell (e.g., via a SA cation channel), thereby indirectly blocking  $K^+_{(Ca)}$  and/or  $Cl^-_{(Ca)}$  channels (table 4) or by directly blocking swelling-activated  $K^+$  and/or  $Cl^-$  channels (Deutsch and Lee, 1988; Berrier et al., 1992; Medrano and Gruenstein, 1993; Ackerman et al., 1994). Many cells also show a regulatory volume increase (RVI) when shrunk in hypertonic solution. RVI may arise through net influx of  $Na^+$  and  $Cl^-$  and consequent net water influx. In this regard,  $Gd^{3+}$  also blocks a cation channel activated by osmotic shrinkage (Chan and Nelson, 1992), although it remains unclear at this stage whether the channel is MG.

c. *GROWTH AND DEVELOPMENTAL EVENTS.* It is plausible that as cells grow in size, develop and divide that mechanical signals play a regulatory role. In this regard, MG channels would seem attractive candidates to sense and transduce tension changes in the cell membrane during cell growth and development. This idea has received some experimental support in the form of  $Gd^{3+}$  sensitivity of stretch-induced endothelial cell alignment, lung cell proliferation and myoblast fusion (see table 4). In the case of *Xenopus* oocytes, which do express a relatively high and uniform density of MG channels, the lack of MG channel blocker sensitivity seems to rule out MG channels playing a critical role in oocyte maturation, fertilization or embryogenesis (see Wilkinson et al., 1996a, b). However, a possible role in oocyte growth and differentiation has not been excluded. The proposal that SA cation channels are involved in stretch-induced cardiac hypertrophy (Bustamante et al., 1991) seems unlikely, given that  $Gd^{3+}$  does not block stretch-induced hypertrophy of rat cardiac myocytes (Sadoshima et al., 1992).

d. **SPECIALIZED MECHANORECEPTORS.** An obvious question concerning the various MG channel blockers is whether they also act on specialized mechanoreceptors such as those studied by Paintal (1964). In the case of arterial baroreceptors, although an initial study indicated little or no  $Gd^{3+}$  sensitivity (Andresen and Yang, 1992), more recent studies indicate that  $10\ \mu M$   $Gd^{3+}$  is sufficient to block baroreceptor discharge in carotid receptors (Hajduczuk et al., 1994) as well as mechanotransduction in the nodose sensory neurons that project to the carotid (Sharma et al., 1995; Cunningham et al., 1995). In the case of central osmoreception, which is important in regulating fluid balance and thirst, it has been demonstrated that  $Gd^{3+}$  blocks ( $IC_{50} = 20\ \mu M$ ) the hypertonically induced MG cation conductance that underlies osmosensitivity in rat brain supraoptic neurons (Oliet and Bourque, 1994, 1996). However, in the most recent study, examination of the single channel data indicates that  $Gd^{3+}$  only partially blocked the channel, even at  $100\ \mu M$ . Unfortunately, a complicating factor in these measurements was the presence of the chelator ethylenediamine-tetraacetic acid ( $1\ mM$ ) in the pipette recording solution. In the case of vertebrate muscle stretch receptors, relatively high ( $\sim 1\ mM$ )  $Gd^{3+}$  or high ( $2\ mM$ ) amiloride concentrations only produce partial block (Ito et al., 1990). Similarly, high ( $400\ \mu M$ )  $Gd^{3+}$  is required to block the crayfish muscle stretch receptor (Swerup et al., 1991). Unfortunately, no reports exist on the  $Gd^{3+}$  sensitivity of specialized cutaneous mechanoreceptors such as the Pacinian corpuscle. Finally, although amiloride and aminoglycosides are well established blockers of mechanotransduction in the vertebrate audiovestibular hair cells, there are no published reports on the  $Gd^{3+}$  sensitivity of mechanotransduction in this preparation, although high  $Gd^{3+}$  concentrations ( $500\ \mu M$ ) have been reported to block voltage-dependent outer hair cell motility (Santos-Sacchi, 1989, 1991; however, see Gale and Ashmore, 1994).

e. **MUSCLE.** MG channel blocker sensitivity supports a role for SA cation channels in stretch-induced contraction in smooth muscle (table 4; see also Kirber et al., 1988) and stretch-induced depolarizations and arrhythmias in ventricular muscle (Hansen et al., 1991; Stacy et al., 1992).

f. **PLANTS.** Perhaps the most notable feature of plant studies is the wide range of  $Gd^{3+}$  concentrations required to block different processes. For example, whereas only  $100$  picomolar  $Gd^{3+}$  is required to block the touch-induced action potential in *Chara*,  $10\ mM$   $Gd^{3+}$  only partially blocks tendril coiling in *Bryonia* (table 4).

## B. Activators

A diverse group of compounds including lipid metabolites, free fatty acids, lipids and amphipathic molecules are able to activate certain MG channels. It is believed that these compounds themselves directly affect channel activity by either interacting with the channel protein or the lipid environment rather than by producing active

metabolites through various enzymatic pathways (e.g., lipoxygenase or cyclo-oxygenase pathways) that then act on the channel (Meves, 1994). A number of possible mechanisms have been proposed: (a) partitioning into the bilayer to alter membrane tension (Martinac et al., 1990; Markin and Martinac, 1991), (b) changing membrane deformation energy (Lundbaek and Andersen, 1994) or (c) interacting with allosteric sites on the channel protein (Petrou et al., 1994; Kirber et al., 1992; Kim et al., 1995).

1. **Amphipathic molecules.** Amphipathic molecules have both hydrophilic and hydrophobic groups and may be either positive, negative or have no net electric charge (e.g., chlorpromazine, trinitrophenol and lysolecithin, respectively). Martinac et al. (1990) demonstrated that amphipathic molecules, when introduced into the external bathing solution, could reversibly increase the open probability of an SA anion channel in *E. coli*. When a particular amphipath, either cationic or anionic, was used alone, the effects were always stimulatory (i.e., open probability increased). However, cationic and anionic amphipaths, used in succession, first stimulated, then neutralized, this stimulatory effect and eventually resulted in a stimulatory effect. The effects were typically slow, sometimes taking up to an hour to increase open probability to unity. Amphipaths appeared to act by shifting the sigmoidal stimulus-response relation to the left so that lower pressures activated the channel without affecting the slope of the Boltzmann (i.e., stimulus-response curve). These effects were interpreted in terms of the bilayer couple hypothesis, in which cationic amphipaths insert into the positive inner monolayer and anionic species partition into the negative outer leaflet of the *E. coli* membrane (Sheetz and Singer, 1974). According to this hypothesis, the introduction of molecules into one leaflet increases the membrane tension in the adjacent leaflet and thereby activates the MG channel. However, it remains unclear why neutral amphipaths have a stimulatory effect unless steric factors also result in unequal partition within the different monolayers (Martinac et al., 1990; Markin and Martinac, 1991). A notable feature of the bilayer couple model is that mechanosensitivity derives entirely from interactions within the bilayer. This basic idea has received strong support, at least for the *E. coli* MG channel, in the form of recent studies showing that mechanosensitivity is retained when the MG channel protein, either purified from membranes or in vitro transcribed from the cloned gene, is reconstituted into artificial lipid bilayers (Sukharev et al., 1993; 1994). It will be interesting to determine whether amphipath sensitivity is retained when channels are reconstituted into bilayers formed from only pure neutral phospholipid.

The bilayer couple model contrasts with models that depend upon cytoskeletal (Guharay and Sachs, 1984) or extracellular protein interactions (Howard et al., 1988; Wang et al., 1993). Although different mechanisms of

mechanosensitivity need not be mutually exclusive, it is interesting that chlorpromazine and trinitrophenol also stimulate SA cation channels in chick skeletal muscle preparation (Sokabe et al., 1993) where the initial cytoskeleton model was developed (Guharay and Sachs, 1984). On the other hand, lipid molecules have been shown to trigger changes in the elasticity of the cytoskeletal network in plant cells (Grabski et al., 1994), raising the possibility that amphiphiles and amphipaths have multiple sites of action capable of influencing MG channel activity.

**2. Fatty acids and lipids (amphiphilic molecules).** Amphiphilic molecules have polar heads attached to a long hydrophobic tail and include such compounds as fatty acids and lipid molecules. Recent studies indicate that fatty acids activate various MG channels independent of fatty acid metabolic pathways (i.e., cyclo-oxygenase or lipoxygenase pathways) (Kiber et al., 1992; Kim, 1992; Petrou et al., 1994; Kim et al., 1995). In particular, Kirber et al. (1992) demonstrated that arachidonic acid increases or modulates the activity of a large conductance, SA  $K^+_{(Ca)}$  channel in rabbit arterial smooth muscle. This effect does not depend on the generation of arachidonic acid metabolites because saturated fatty acids such as myristic and linoelaidic acids, which are not substrates for the enzymes that convert arachidonic acid to active metabolites, also activate the channel. Further evidence of a direct effect was indicated by cell-free patch experiments in which activation by fatty acids was retained in the absence of soluble cytoplasmic enzymes (Kirber et al., 1992). Another SA  $K^+$  channel, in this case in gastric smooth muscle, also displays fatty acid activation (Petrou et al., 1994). However, although negatively charged fatty acids stimulate MG channel activity, positively charged fatty acids inhibit activity (see above in Section III, A.4.j), and neutral analogs are without effect (table 5). This SA  $K^+$  channel seems likely to be indirectly mechanosensitive (see mechanisms above) because stretch activation occurs with latencies of seconds rather than milliseconds (Ordway et al., 1991), persists for seconds after removal of stretch, and activation can be suppressed by perfusion with albumin, which is known to remove fatty acids from membranes (Ordway et al., 1995). These observations have led to the proposal that membrane stretch alters channel activity by generation of fatty acids, possibly via a stretch sensitive membrane phospholipase (Jukka et al., 1995).

In a third cell type, involving neurons from the mesencephalic and hypothalamic regions of the rat brain, there are a number of fatty acid-activated SA  $K^+$  channels that can be distinguished by their open channel properties. In all cases, albumin fails to reduce stretch sensitivity, indicating that stretch and fatty acids may activate this channel by different mechanisms (Kim et al., 1995). A similar conclusion was made for the arachidonic sensitive SA  $K^+$  channel in heart muscle (Kim, 1992). Another difference between SA  $K^+$  channels in

neurons and smooth muscle is that the saturated fatty acids myristic acid and oleic acid, which activate the smooth muscle  $K^+$  channels, have no effect on the neuronal channels. Taken together, the evidence indicates that the SA  $K^+$  channels in muscle and neurons involve direct fatty acid activation of the channel protein itself or an associated regulatory protein on smooth muscle and neurons. The fact that the fatty acid activation profile of  $K^+$  channels in muscle and neurons differs indicates there may be a number of cell type-specific fatty acid binding sites, which may or may not be involved in conferring mechanosensitivity on the channel. Arachidonic acid and other fatty acids, apart from effecting the SA channels described above, also have actions on a wide range of other non-MG channels involving a variety of mechanisms (for review see Meves, 1994).

A number of features distinguish amphipathic from amphiphilic activation. First, the time course of activation differs. Whereas amphipaths activate the channel slowly ( $\sim 1$  hour), fatty acid activation is relatively fast and occurs in seconds. Second, at least for the  $K^+_{(Ca)}$ , fatty acids are not capable of activating the channel in the absence of basal activity (i.e., in zero external  $Ca^{2+}$  or at very negative potentials), indicating a modulatory role rather than primary activation (Kirber et al., 1988). In contrast, amphipaths can activate the *E. coli* MG channel in the absence of mechanical stimulation (Martinac et al., 1990). Third, the dependence of charge polarity of fatty acid effects differs from the polarity-independent stimulatory effect of amphipaths (Martinac et al., 1990). Finally, although the  $K^+_{(Ca)}$  channel is stretch-sensitive, it is not clear to what extent stretch and fatty acids can act independently of one another. For example, it may be stretch sensitivity does not reside in the channel itself but instead resides in a stretch-sensitive phospholipase that generates fatty acids (Brophy et al., 1993; Jukka et al., 1995). In contrast, with the *E. coli* channel, it is quite clear from reconstitution experiments, using the purified channel protein, that mechanosensitivity arises purely from interactions between the protein and its surrounding bilayer environment (Sukharev et al., 1994).

**3. Other activators.** As in the case with blockers, there are a number of chemicals that have been reported to have activating effects on specific MG channels.

**a. ALUMINOFLUORIDE.** In contrast to blocking effects of  $Al^{3+}$  described above, it has been reported that aluminofluoride ( $20 \mu M AlCl_3$  plus  $20 mM KF$ ) activates a SA cation channel in gastric smooth muscle cells (Hisada et al., 1993). However,  $AlF_3$  effects were studied on SA channel activity activated by membrane hyperpolarization rather than by stretch (see Hisada et al., 1991). Interestingly, in contrast to the plant study in which  $Al^{3+}$  was reported to have an inhibitory effect (Ding et al., 1993), application of  $20 \mu M AlCl_3$  had no effect on SA channel activity when applied in the absence of  $F^-$  (Hisada et al., 1993). The mechanism of action of  $AlF_3$



remains unknown but it has been proposed that this activation may play a role in smooth muscle contraction (Hisada et al., 1993).

b. ETHYL-N-PHENYLCARBAMATE. The herbicide, ethyl-N-phenylcarbamate, which is known to interfere with gravitropism in plants, has been shown to gradually stimulate MG channel activity in onion protoplasts over the concentration range of 10 to 1000  $\mu\text{M}$  (Ding and Pickard, 1993a). Although the mechanism of action has not been determined, this compound is known to alter the plant cytoskeleton (Nick et al., 1991).

c. CYTOCHALASINS. A specific theory of SA channel activation is based on cytoskeletal involvement in focusing mechanical energy onto the SA channel. Because several classes of compounds interact with specific cytoskeletal proteins, a reasonable assumption is that at least one or more of these drugs may have effects on channel activities (see Mills and Mandel, 1994). However, as it turns out, the results so far have been either negative or ambiguous. For example, the microtubule disrupting drugs, colchicine and vinblastine, while blocking mechanotransduction in lower invertebrates, have been shown to have no effect on SA channels activity in at least two different vertebrate preparations (see Section III, A.4.n). In the case of cytochalasins, which are known to selectively disrupt actin filaments, the reports on SA channels have been contradictory between laboratories; even conflicting reports have arisen from a single laboratory. The basis of the discrepancies is that some studies report that cytochalasins increase the SA channel's sensitivity to stretch (Guharay and Sachs, 1984; Small and Morris, 1994), whereas others report no effect on stretch sensitivity (Sokabe et al., 1991; O.P.H. and D.W.M., unpublished observations). Despite the apparent failure of pharmacological means to clearly implicate specific cytoskeletal proteins in SA channel function, other studies, using nonpharmacological means, have clearly implicated some form of cytoskeletal involvement (Hamill and McBride, 1995a). These studies involve conditions in which the membrane in the patch is physically decoupled from the underlying cytoskeleton (Hamill and McBride, 1992) or in which cytoskeleton free vesicles of plasma membrane have been studied (Hamill et al., 1995; Zhang et al., 1996). Under both conditions, mechanosensitivity is either lost entirely or significantly reduced.

#### IV. Summary and Conclusions

In this article, the actions, mechanisms and applications of various ions and drugs that interact with MG channels have been discussed. At present, no compound has been found that displays the high specificity and affinity exhibited by tetrodotoxin or  $\alpha$ -bungarotoxin that proved so useful in the functional and structural characterization of the voltage-gated  $\text{Na}^+$  channel and the acetylcholine receptor channel, respectively. Neverthe-

less, three different classes of compounds have been discovered since Paintal's review that clearly block MG channels. These compounds, represented by amiloride, gentamicin and gadolinium, act mainly on the SA cation channel, which appears to be shared by many nonsensory and some mechanosensory cells. Each class of compound can be distinguished by the voltage and concentration dependence of the block and most likely involves different mechanisms of blocking action. In general, the MG channel blocker pharmacology indicates a variety of "receptor sites" on MG channels. The recognition and acceptance of such receptors should provide added impetus for continued screening for more potent drugs, venoms and toxins.

In the case of activators, little is understood of the mechanisms by which the various amphipathic and amphiphilic compounds stimulate MG channels, although different bilayer and protein mechanisms have been evoked. Even less is understood of the role the new class of MG  $\text{K}^+$  channel and their modulation by fatty acids plays in physiological and perhaps pathological processes. However, given that  $\text{K}^+$  channels in general tend to reduce the excitability of nerve and muscle, plausible roles include fatty acid regulation of vascular tone and control of neuronal network excitability. In both cases, more detailed understanding is required regarding the physiological stimuli that modulate these channels through their fatty acid receptors. It may turn out that recognition and/or development of cell-type specific agents that activate such MG channels will possess high therapeutic potential. In any case, the observation that MG channels can be chemically blocked and/or activated by a wide range of compounds requires revision of the long-standing conclusion of Paintal that mechanotransduction is a process that has a low susceptibility to chemical influence.

**Acknowledgements.** Our research is supported by the National Institutes of Health, the National Science Foundation and the Muscular Dystrophy Association.

#### REFERENCES

- ACHARD, J.-M., BUBIEN, J. K., BENOS, D. J., AND WARNOCK, D. G.: Stretch modulates amiloride sensitivity and cation selectivity of sodium channels in human  $\beta$  lymphocytes. *Am. J. Physiol.* 270: C224-C234, 1996.
- ACKERMAN, M. J., WICKMAN, K. D., AND CLAPHAM, D. E.: Hypotonicity activates a native chloride channel in *Xenopus* oocytes. *J. Gen. Physiol.* 103: 153-179, 1994.
- ALEXANDRE, J., AND LASSALLES, J.-P.: Hydrostatic and osmotic pressure activated channel in plant vacuole. *Biophys. J.* 60: 1326-1336, 1991.
- ANDRESEN, M. C., AND YANG, M.: Gadolinium and mechanotransduction in rat aortic baroreceptors. *Am. J. Physiol.* 262: H1415-H1421, 1992.
- ASSAD, J. A., SHEPHERD, G. M. G., AND COREY, D. P.: Tip link integrity and mechanical transduction in vertebrate hair cells. *Neuron* 7: 985-994, 1991.
- AWAYADA, M. S., ISMAILOV, I. I., BERDIEV, B. K., AND BENOS, D. J.: A cloned renal epithelial  $\text{Na}^+$  channel protein displays stretch activation in planar bilayers. *Am. J. Physiol.* 268: C1450-C1459, 1995.
- BAUMANN, K. I., HAMANN, W., AND LEUNG, M. S.: Responsiveness of slowly adapting cutaneous mechanoreceptors after close arterial infusion of neomycin in cats. *Prog. Brain Res.* 74: 43-49, 1988.
- BEAR, C. E., AND LI, C.: Calcium-permeable channels in rat hepatoma cells are activated by extracellular nucleotides. *Am. J. Physiol.* 261: C1018-C1024, 1991.
- BELL, J., BOLANOWSKI, S., AND HOLMES, M. H.: The structure and function of Pacinian corpuscles: a review. *Prog. Neurobiol.* 42: 79-128, 1994.

- RENOS, D. J.: Amiloride: a molecular probe of sodium transport in tissues and cells. *Am. J. Physiol.* 242: C131-C145, 1982.
- BEN-TABOU, S., KELLER, E., AND NUSSINOVITCH, I.: Mechanosensitivity of voltage-gated calcium currents in rat anterior pituitary cells. *J. Physiol.* 476, 1: 29-39, 1994.
- BERRIER, C., COULOMBE, A., SZABO, I., ZORATTI, M., AND GHAZI, A.: Gadolinium ion inhibits loss of metabolites induced by osmotic shock and large stretch activated channels in bacteria. *Eur. J. Biochem.* 206: 559-565, 1992.
- BIAGI, B. A., AND ENYEART, J. J.: Gadolinium blocks low and high threshold calcium currents in pituitary cells. *Am. J. Physiol.* 264: C1037-C1044, 1990.
- BIALECKI, R. A., KULIK, T. J., AND COLLUCI, W. S.: Stretching increases calcium influx and efflux in cultured pulmonary arterial smooth muscle cells. *Am. J. Physiol.* 263: L602-L606, 1992.
- BIBBY, K. J., AND MCCULLOCH, C. A. G.: Regulation of cell volume and  $[Ca^{2+}]$  in attached human fibroblasts responding to anisotonic buffers. *Am. J. Physiol.* 266: C1639-C1649, 1994.
- BIELEFELD, D. R., HADLEY, R. W., VASSILEV, P. M., AND HUME, J. R.: Membrane electrical properties of vesicular Na-Ca exchange inhibitors in single atrial myocytes. *Circ. Res.* 59: 381-389, 1986.
- BOITANO, S., SANDERSON, M. J., AND DIRKSEN, E. R.: A role for  $Ca^{2+}$  conducting ion channels in mechanically induced signal transduction of airway epithelial cells. *J. Cell Sci.* 107: 3037-3044, 1994.
- BOLAND, L. M., BROWN, T. A., AND DINGELDINE, R.: Gadolinium block of calcium channels: influence of bicarbonate. *Brain Res.* 563: 142-150, 1991.
- BONHIVERS, M., GUIHARD, G., PATTUS, F., AND LETELLIER, L.: *In vivo* and *in vitro* studies of the inhibition of the channel activity of colicins by gadolinium. *Eur. J. Biochem.* 229: 155-163, 1995.
- BORCERS, M., AND BRADANDER, M.: Microtubules and Microtubule Inhibitors, 357 pp., North Holland, Amsterdam, 1975.
- BOWMAN, C. L., DING, J.-P., SACHS, F., AND SOKABE, M.: Mechanotransducing ion channels in astrocytes. *Brain Res.* 584: 272-286, 1992.
- BOWMAN, C. L., AND LOHR, J. W.: Curvature-sensitive mechanosensitive ion channels and osmotically-evoked movements of the patch membrane (abstract). *Biophys. J.* 70: A365, 1996.
- BROPHY, C. M., MILLS, I., ROSALES, O., ISALES, C., AND SUMPIO, B. E.: Phospholipase C: a putative mechanotransducer for endothelial cell response to acute hemodynamic changes. *Biochem. Biophys. Res. Comm.* 109: 576-581, 1993.
- BROWNELL, P., AND FARLEY, R. D.: Detection of vibrations in sand by tarsal sense organs of the nocturnal scorpion, *Paruroctonus mesaensis*. *J. Comp. Physiol.* 131: 23-30, 1979.
- BURTON, F. L., AND HUTTER, O. F.: Sensitivity to flow of intrinsic gating in inwardly rectifying potassium channel from mammalian skeletal muscle. *J. Physiol.* 424: 253-261, 1990.
- BUSTAMANTE, J. O., RUKNUDIN, A., AND SACHS, F.: Stretch activated channels in heart cells: relevance to cardiac hypertrophy. *J. Cardiovasc. Pharmacol.* 17(suppl. 2): S110-S113, 1991.
- CANESSA, C. M., HORISBERGER, J.-D., AND ROSSIER, B. C.: Epithelial sodium channel related to proteins involved in neurodegeneration. *Nature (Lond.)* 361: 467-470, 1993.
- CANESSA, C. M., SCHILD, L., BUELL, G., THORENS, B., GAUTSCHI, I., HORISBERGER, J.-D., AND ROSSIER, B. C.: Amiloride-sensitive epithelial  $Na^{+}$  channel is made of three homologous subunits. *Nature (Lond.)* 367: 463-467, 1994.
- CEMERIKIC, D., AND SACKIN, H.: Substrate activation and mechanosensitive whole cell currents in renal proximal tubule. *Am. J. Physiol.* 264: F697-F714, 1993.
- CHALFIE, M., AND THOMSON, J. N.: Structural and functional diversity in the neuronal microtubules of *Caenorhabditis elegans*. *J. Cell Biol.* 93: 15-23, 1982.
- CHAN, H.-C., AND NELSON, D. J.: Chloride-dependent cation conductance activated during cellular shrinkage. *Science (Wash. DC)* 257: 669-671, 1992.
- CHANG, W., AND LORETZ, C. A.: Activation by membrane stretch and depolarization of an epithelial monovalent cation channel from teleost intestine. *J. Exp. Biol.* 169: 87-104, 1992.
- CHARLES, A. C., MERRILL, J. E., DIRKSEN, E. R., AND SANDERSON, M. J.: Intercellular signalling in glial cells: calcium waves and oscillations in response to mechanical stimulation and glutamate. *Neuron* 6: 983-992, 1991.
- CHEN, B.-M., AND GRINNELL, A. D.: Integrins and modulation of transmitter release from motor terminals by stretch. *Science (Wash. DC)* 269: 1578-1580, 1995.
- CHEN, Y., SIMASKO, S. M., NIGGEL, J., SIQRDSON, W. J., AND SACHS, F.:  $Ca^{2+}$  uptake in GH3 cells during hypotonic swelling: evidence for the sensory role of stretch activated ion channels. *Am. J. Physiol.*, in press.
- CHESNOV-MARCHAIS, D., AND FRITSCH, J.: Activation by hyperpolarization and atypical osmosensitivity of a  $Cl^{-}$  current in rat osteoblastic cells. *J. Membr. Biol.* 140: 173-188, 1994.
- CHRISTENSEN, O.: Mediation of cell volume by  $Ca^{2+}$  influx through stretch activated channels. *Nature (Lond.)* 330: 66-68, 1987.
- CHRISTENSEN, O., AND HOFFMANN, E. K.: Cell swelling activates  $K^{+}$  and  $Cl^{-}$  channels as well as nonselective, stretch-activated cation channels in Ehrlich ascites tumor cells. *J. Membr. Biol.* 129: 13-36, 1992.
- COREY, D. P., AND HUDEPETH, A. J.: Response latency of vertebrate hair cells. *Biophys. J.* 26: 499-506, 1979.
- CRAWFORD, A. C., EVANS, M. G., AND FETTLPLACE, R.: The action of calcium on the mechanoelectrical transducer current of turtle hair cells. *J. Physiol.* 434: 369-398, 1991.
- CRIST, J. R., FALLON, M., AND BOBBIN, R. P.: Volume regulation in cochlear outer hair cells. *Hearing Res.* 69: 194-198, 1993.
- CUI, C., SMITH, D. O., AND ADLER, J.: Characterization of mechanosensitive channels in *Escherichia coli* cytoplasmic membrane by whole cell patch clamp recording. *J. Membr. Biol.* 144: 31-42, 1995.
- CUNNINGHAM, J. T., WACHTEL, R. E., AND ABOUD, F. M.: Mechanosensitive currents in putative aortic baroreceptor neurons *in vitro*. *J. Neurophysiol.* 73: 2094-2098, 1995.
- CUTHBERT, A. W., AND WONG, P. Y. D.: The role of calcium ion in the interaction of amiloride with membrane receptors. *Mol. Pharmacol.* 8: 222-229, 1972.
- DANIELS, P. J. L.: Aminoglycosides. In Kirk-Othmer: Encyclopedia of Chemical Technology, ed. by G. J. Bushey, A. Kingsburg, and L. Van Nes, vol. 2, ed. 3, pp. 819-852, John Wiley and Sons, New York, 1978.
- DAVIDSON, R. M.: Membrane stretch activates a high conductance  $K^{+}$  channel in G292 Osteoblastic-like cells. *J. Membr. Biol.* 131: 81-92, 1993.
- DAVIS, M. J., MEININGER, G. A., AND ZAWIEJA, D. C.: Stretch-induced increases in intracellular calcium of isolated vascular smooth muscle cells. *Am. J. Physiol.* 263: H1292-H1299, 1992.
- DEITMER, J. W.: Mechanosensory transduction in ciliates (protozoa). *Adv. Comp. Environ. Physiol.* 10: 30-54, 1992.
- DEMER, L. L., WORTHAM, C. M., DIRKSEN, E. R., AND SANDERSON, M. J.: Mechanical stimulation induces intercellular calcium signalling in bovine aortic endothelial cells. *Am. J. Physiol.* 264: H2094-H2102, 1993.
- DENK, W., KEOLIAN, R. M., AND WEBB, W. W.: Mechanical response of frog saccular hair bundles to the aminoglycoside block of mechanoelectrical transduction. *J. Neurophysiol.* 68: 927-932, 1992.
- DENK, W., AND WEBB, W. W.: Thermal noise-limited transduction observed in mechanosensory receptors of the inner ear. *Phys. Rev. Lett.* 63: 207-210, 1989.
- DESMEDT, L., SIMAELS, J., AND VAN DRIESSE, W.: Amiloride blockage of  $Na^{+}$  channels in amphibian epithelia does not require external  $Ca^{2+}$ . *Pfluegers Arch.* 419: 632-638, 1991.
- DEUTSCH, C., AND LEE, S. C.: Cell volume regulation in lymphocytes. *Renal Physiol. Biochem.* 3-5: 260-276, 1988.
- DING, J. P., BADOT, P. -M., AND PICKARD, B. G.: Aluminum and hydrogen ions inhibit a mechanosensory calcium-selective cation channel. *Aust. J. Plant. Physiol.* 20: 771-778, 1993.
- DING, J. P., AND PICKARD, B. G.: Mechanosensory calcium-sensitive cation channels in epidermal cells. *Plant J.* 3(suppl. 1): 83-110, 1993a.
- DING, J. P., AND PICKARD, B. G.: Modulation of mechanosensitive calcium-selective cation channels by temperature. *Plant J.* 3: 713-720, 1993b.
- DOCHERTY, R. J.: Gadolinium selectively blocks a component of calcium current in rodent neuroblastoma x glioma hybrid (NG108-15) cells. *J. Physiol.* 398: 33-47, 1988.
- DRISCOLL, M., AND CHALFIE, M.: The *mec-4* gene is a member of a family of *Caenorhabditis elegans* genes that can mutate to induce neuronal degeneration. *Nature (Lond.)* 349: 588-593, 1991.
- DUNCAN, R. L., AND HRUSKA, K. A.: Chronic intermittent loading alters mechanosensitive channel characteristics in osteoblast-like cells. *Am. J. Physiol.* 267: F909-F916, 1994.
- DUNCAN, R. L., HRUSKA, K. A., AND MISLER, S.: Parathyroid hormone activation of stretch-activated cation channels in osteosarcoma cells (UMR-106.01). *FEBS Letts.* 307: 219-223, 1992.
- EDWARDS, K. L., AND PICKARD, B. G.: Detection and transduction of physical stimuli in plants. In *The Cell Surface and Signal Transduction*, ed. by E. Wagner, H. Greppin, and B. Millet, pp. 41-66, Springer-Verlag, Heidelberg, Germany, 1987.
- ELINDER, F., AND ARHEM, P.: Effects of gadolinium on ion channels in the myelinated axon of *Xenopus laevis*: four sites of action. *Biophys. J.* 67: 71-83, 1994a.
- ELINDER, F., AND ARHEM, P.: The modulatory site for the action of gadolinium on surface charges and channel gating. *Biophys. J.* 67: 84-90, 1994b.
- ERLER, G.: Reduction of mechanical sensitivity in an insect mechanoreceptor correlated with destruction of its tubular body. *Cell Tissue Res.* 232: 451-461, 1983.
- ERKLEBEN, C.: Stretch-activated current through single ion channels in the abdominal stretch receptor organ of the crayfish. *J. Gen. Physiol.* 94: 1071-1083, 1989.
- EVANS, C. H.: Biochemistry of the Lanthanides, 444 pp., Plenum Press, New York, 1990.
- FETTLPLACE, R., ANDREWS, D. M., AND HAYDON, D. A.: The thickness, composition and structure of some lipid bilayers and natural membranes. *J. Membr. Biol.* 5: 277-296, 1971.
- FILIPOVIC, D., AND SACKIN, H.: A calcium permeable stretch-activated cation channel in renal proximal tubule. *Am. J. Physiol.* 260: F119-F129, 1991.
- FOSKETT, J. K.: The role of calcium in the control of volume regulatory transport pathways. In *Cellular and Molecular Physiology of Cell Volume Regulation*, ed. by K. Strange, pp. 259-277, CRC Press, Boca Raton, FL, 1994.
- FRANCO, A. JR., AND LANSMAN, J. B.: Stretch-sensitive channels in developing muscle cells from a mouse cell line. *J. Physiol.* 427: 361-380, 1990.
- FRANCO, A. JR., WINEGAR, B. D., AND LANSMAN, J. B.: Open channel block by gadolinium ion of the stretch-inactivated ion channel in *mdx* myotubes. *Biophys. J.* 59: 1164-1170, 1991.

- FRENCH, A. S.: Mechanotransduction. *Ann. Rev. Physiol.* 54: 135-152, 1992.
- GALE, J. E., AND ASHMORE, J. F.: An intracellular site for the inhibition of outer hair cell motility by gadolinium (abstract). XXXth Workshop on Inner Ear Biology, P67, 1994.
- GALLIN, E. K., MASON, T. M., AND MORAN, A.: Characterization of regulatory volume decrease in the THP-1 and HL-60 human myelocytic cell lines. *J. Cell. Physiol.* 159: 573-581, 1994.
- GANNIER, F., WHITE, E., LACAMPAGNE, A., GARNIER, D., AND LE GUENNEC, J.-Y.: Streptomycin reverses a large stretch induced increase in  $[Ca^{2+}]$  in isolated guinea pig ventricular myocytes. *Cardiovasc. Res.* 28: 1193-1198, 1994.
- GARCIA, M. L., KING, F., SHEVELL, J. L., SLAUGHTER, R. S., SUAREZ-KURTZ, G., WINQUIST, R. J., AND KACZOROWSKI, G. J.: Amiloride analogs inhibit L-type calcium channels and display calcium entry blocker activity. *J. Biol. Chem.* 265: 3763-3771, 1990.
- GARRILL, A., JACKSON, S. L., LEW, R. R., AND HEATH, I. B.: Ion channel activity and tip growth: tip-localized stretch-activated channels generate an essential  $Ca^{2+}$  gradient in the oomycete *Saprolegnia ferax*. *Eur. J. Cell Biol.* 60: 358-365, 1993.
- GITTER, A. H., OLIVER, D., AND THURM, U.: Streptomycin inhibits nematocyte discharge in *Hydra vulgaris* by blockage of mechanosensitivity. *Naturwissenschaften*. 80: 273-276, 1993.
- GRABSKI, S., XIE, K. G., HOLLAND, J. F., AND SCHINDLER, M.: Lipids trigger changes in the elasticity of the cytoskeleton in plant cells: a cell optical displacement assay for live cell measurements. *J. Cell Biol.* 126: 713-726, 1994.
- GUHARAY, F., AND SACHS, F.: Stretch-activated single ion channel currents in tissue cultured embryonic chick skeletal muscle. *J. Physiol.* 362: 685-701, 1984.
- GUHARAY, F., AND SACHS, F.: Mechanotransducer ion channels in chick skeletal muscle: the effects of extracellular pH. *J. Physiol.* 363: 119-134, 1985.
- GUSTIN, M. C., ZHOU, X.-L., MARTINAC, B., AND KUNG, C. C.: A mechanosensitive ion channel in the yeast plasma membrane. *Science (Wash. DC)* 242: 762-763, 1988.
- HACKNEY, C. M., FURNESS, D. N., BENOS, D. J., WOODLEY, J. F., AND BARRATT, J.: Putative immunolocalization of the mechanoelectrical transduction channels in mammalian cochlear cells. *Proc. R. Soc. London Ser. B* 248: 215-221, 1992.
- HADJUCZOK, G., CHAPLEAU, M. W., FERLIC, R. J., MAO, H. Z., AND ABOUD, F. M.: Gadolinium inhibits mechanoelectrical transduction in rabbit carotid baroreceptors: implications for stretch-activated channels. *J. Clin. Invest.* 94: 2392-2396, 1994.
- HAMILL, O. P.: Potassium and chloride channels in red blood cells. In *Single Channel Recording*, ed. by B. Sakmann and E. Neher, pp. 451-471, Plenum Press, New York, 1983a.
- HAMILL, O. P.: Membrane ion channels. In *Topics in Molecular Pharmacology*, ed. by A. Burgen and A. K. Roberts, vol. 3, pp. 183-205, Elsevier, Holland, 1983b.
- HAMILL, O. P., CHEN, M., ZHANG, Y., AND MCBRIDE, JR., D. W.: A cytoskeleton (CSK) deficient plasma membrane vesicle preparation from *Xenopus* oocytes for studying CSK affects on membrane ion channel gating. *J. Physiol.* 483.P: 162P, 1995.
- HAMILL, O. P., LANE, J. W., AND MCBRIDE, D. W.: Amiloride: a molecular probe for mechanosensitive channels. *Trends Pharmacol. Sci.* 13: 372-376, 1992.
- HAMILL, O. P., MARTY, A., NEHER, E., SAKMANN, B., AND SIOWORTH, F. W.: Improved patch clamp techniques for high current resolution from cells and cell-free membrane patches. *Pfluegers Arch.* 391: 85-100, 1981.
- HAMILL, O. P., AND MCBRIDE, JR., D. W.: Rapid adaptation of the MG channel in *Xenopus* oocytes. *Proc. Natl. Acad. Sci. USA* 89: 7462-7466, 1992.
- HAMILL, O. P., AND MCBRIDE, JR., D. W.: Patch and whole-cell MG currents recorded from BC3H-1 muscle cells (abstract). *Biophys. J.* 64: A93, 1993.
- HAMILL, O. P., AND MCBRIDE, JR., D. W.: The cloning of a mechano-membrane channel. *Trends Neurosci.* 17: 439-443, 1994a.
- HAMILL, O. P., AND MCBRIDE, JR., D. W.: Molecular mechanisms of mechanoreceptor adaptation. *News Physiol. Sci.* 9: 53-59, 1994b.
- HAMILL, O. P., AND MCBRIDE, JR., D. W.: Mechanoreceptive membrane ion channels. *Am. Sci.* 83: 30-37, 1995a.
- HAMILL, O. P., AND MCBRIDE, JR., D. W.: Pressure/patch-clamp methods. In *Patch Clamp Techniques and Protocols*, ed. by A. A. Boulton, G. B. Baher, and W. Walz, pp. 75-87, Humana Press, Totowa, NJ, 1995b.
- HAMILL, O. P., AND MCBRIDE, JR., D. W.: Membrane voltage and tension interactions in the gating of the mechano-gated cation channel in *Xenopus* oocytes (abstract). *Biophys. J.* 70: A348, 1996a.
- HAMILL, O. P., AND MCBRIDE, JR., D. W.: A supramolecular complex underlying touch sensitivity. *Trends Neurosci.* 19: 1-5, 1996b.
- HANSEN, D. E., BORGANELLI, M., STACY, G. P., AND TAYLOR, L. K.: Dose dependent inhibition of stretch-induced arrhythmias by gadolinium in isolated canine ventricles: evidence for a unique mode of antiarrhythmic action. *Circ. Res.* 69: 820-831, 1991.
- HARADA, N., ERNST, A., AND ZENNER, H. P.: Hypoosmotic activation hyperpolarizes outer hair cells of guinea pig cochlea. *Brain Res.* 614: 205-211, 1993.
- HASE, C. C., LE DAIN, A. C., AND MARTINAC, B.: Purification and functional reconstitution of the recombinant large mechanosensitive ion channel (MacL) of *Escherichia coli*. *J. Biol. Chem.* 270: 18329-18334, 1995.
- HILLE, B.: *Ionic Channels of Excitable Membranes*, ed. 2. 607 pp., Sinauer Assoc., Sunderland, MA, 1992.
- HISADA, T., ORDWAY, R. W., KIRBER, M. T., SINGER, J. J., AND WALSH, JR., J. V.: Hyperpolarization-activated cationic channels in smooth muscle cells are stretch sensitive. *Pfluegers Arch.* 417: 493-499, 1991.
- HISADA, T., SINGER, J. J., AND WALSH, JR., J. V.: Aluminumfluoride activates hyperpolarization- and stretch-activated cationic channels in single smooth muscle cells. *Pfluegers Arch.* 422: 397-400, 1993.
- HONG, K., AND DRISCOLL, M.: A transmembrane domain of the putative channel subunit MEC-4 influences mechanotransduction and neurodegeneration in *C. elegans*. *Nature (Lond.)* 387: 470-473, 1994.
- HOWARD, J., ROBERTS, W. M., AND HUDSPETH, A. J.: Mechanoelectrical transduction by hair cells. *Annu. Rev. Biophys. Biophys. Chem.* 17: 99-124, 1988.
- HUANG, M., AND CHALFIE, M.: Gene interactions affecting mechanosensory transduction in *Caenorhabditis elegans*. *Nature (Lond.)* 367: 467-470, 1994.
- HUANG, M., GU, G., FERGUSON, E. L., AND CHALFIE, M.: A stomatin-like protein necessary for mechanosensation in *C. elegans*. *Nature (Lond.)* 378: 292-295, 1995.
- HUDSPETH, A. J., AND GILLESPIE, P. G.: Pulling strings to fine tune transduction: adaptation by hair cells. *Neuron* 12: 1-9, 1994.
- INOBER, D.: Integrins as mechanochemical transducers. *Curr. Opin. Cell Biol.* 3: 841-848, 1991.
- ITO, F., SOKABE, M., NOMURA, K., NARUSE, K., FUJITSUKA, N., AND YOSHIMURA, A.: Effects of ions and drugs on the responses of sensory axon terminals of decapsulated frog muscle spindles. *Neurosci. Res.* 12(suppl.): S15-S26, 1990.
- JARAMILLO, F., AND HUDSPETH, A. J.: Localization of the hair cell's transduction channels at the hair bundle's top by iontophoretic application of a channel blocker. *Neuron* 7: 409-420, 1991.
- JORGENSEN, F. O.: Effects of amiloride on the mechanosensitivity of lateral line organs of *Necturus maculosus* and *Xenopus laevis*. *Acta Physiol. Scand.* 124(suppl. 542): 249, 1985.
- JORGENSEN, F. O., AND OHMORI, H.: Amiloride blocks the mechano-electrical transduction channel of hair cells of the chick. *J. Physiol.* 403: 577-586, 1988.
- JUKKA, Y., LEHTONEN, A., AND KINNUNEN, P. K. J.: Phospholipase  $A_2$  as a mechanosensor. *Biophys. J.* 68: 1888-1894, 1995.
- KASAI, Y., TSUTSUMI, O., TAKTANI, Y., ENDO, M., AND IDNO, M.: Stretch-induced enhancement of contractions in uterine smooth muscle of rats. *J. Physiol.* 486: 373-384, 1995.
- KAWAHARA, K., AND MATSUZAKI, K.: A stretch-activated cation channel in the apical membrane of A6 cells. *Jpn. J. Physiol.* 43: 817-832, 1993.
- KIM, D.: A mechanosensitive  $K^+$  channel in heart cells: activation by arachidonic acid. *J. Gen. Physiol.* 100: 1021-1040, 1992.
- KIM, D.: Novel cation-selective mechanosensitive ion channel in the atrial cell membrane. *Circ. Res.* 72: 225-231, 1993.
- KIM, D., SLADEK, C. D., AGUADO-VELASCO, C., AND MATHIASSEN, J. R.: Arachidonic acid activation of a new family of  $K^+$  channels in cultured rat neuronal cells. *J. Physiol.* 484: 643-660, 1995.
- KIMITSUKI, T., AND OHMORI, H.: Dihydrostreptomycin modifies adaptation and blocks the mechano-electric transducer in chick cochlear hair cells. *Brain Res.* 624: 143-150, 1993.
- KIRBER, M. T., ORDWAY, R. W., CLAPP, L. H., WALSH, JR., J. V., AND SINGER, J. J.: Both membrane stretch and fatty acids directly activate large conductance  $Ca^{2+}$ -activated  $K^+$  channels in vascular smooth muscle cells. *FEBS Lett.* 287: 24-28, 1992.
- KIRBER, M. T., WALSH, JR., J. V., AND SINGER, J. J.: Stretch-activated ion channels in smooth muscle: a mechanism for the initiation of stretch induced contraction. *Pfluegers Arch.* 412: 339-345, 1988.
- KLEYMAN, T. R., AND CRAGOE, E. J.: Amiloride and its analogs in the study of ion transport. *J. Membr. Biol.* 105: 1-21, 1988.
- KLEYMAN, T. R., AND CRAGOE, E. J.: Cation transport probes: the amiloride series. *Methods Enzymol.* 191: 739-754, 1990.
- KLUESNER, B., BOHEIM, G., LIES, H., ENGELBERTH, J., AND WEILNER, E. W.: Gadolinium-sensitive, voltage-dependent calcium release channels in the endoplasmic reticulum of a higher plant: mechanoreceptor. *EMBO J.* 14: 2708-2714, 1996.
- KNIGHT, M. R., SMITH, S. M., AND TREWAVAS, A. T.: Wind induced plant motion immediately increases cytosolic calcium. *Proc. Natl. Acad. Sci. USA* 89: 4967-4971, 1992.
- KOTERA, T., AND BROWN, P. D.: Calcium-dependent chloride current activated by hypoosmotic stress in rat lacrimal acinar cells. *J. Membr. Biol.* 134: 67-74, 1993.
- KROESE, A. B. A., DAS, A., AND HUDSPETH, A. J.: Blockage of the transduction channels of hair cells in the bullfrog's sacculus by aminoglycoside antibiotics. *Hear. Res.* 37: 203-218, 1989.
- KROESE, A. B. A., AND VAN DEN BERCKEN, J.: Dual action of ototoxic antibiotics on sensory hair cells. *Nature (Lond.)* 283: 395-397, 1980.
- KROESE, A. B. A., AND VAN DEN BERCKEN, J.: Effects of ototoxic antibiotics on sensory hair cell functioning. *Hear. Res.* 6: 183-197, 1982.
- LAU, M. J., ZHOU, B. Y., SPENCER, C. I., MORNER, S. M., AND SEED, W. A.: Effects of gadolinium on length-dependent force in guinea-pig papillary muscle. *Exp. Physiol.* 78: 249-255, 1994.
- LACAMPAGNE, A., GANNIER, F., ARGIBAY, J., GARNIER, D., AND LE GUENNEC, J.-L.: The stretch-activated ion channel blocker gadolinium also blocks L-type calcium channels in isolated ventricular myocytes of the guinea pig. *Biochim. Biophys. Acta* 1191: 205-208, 1994.



- LAINE, M., ARIAMAA, O., VUOLTEENAHO, O., RUSKOaho, H., AND WECKSTROM, M.: Block of stretch-activated atrial natriuretic peptide secretion by gadolinium in isolated rat atrium. *J. Physiol.* 480: 553-561, 1994.
- LANE, J. W., MCBRIDE, JR., D. W., AND HAMILL, O. P.: Amiloride block of the mechanosensitive cation channel in *Xenopus* oocytes. *J. Physiol.* 441: 347-366, 1991.
- LANE, J. W., MCBRIDE, JR., D. W., AND HAMILL, O. P.: Structure-activity relations of amiloride and its analogues in blocking the mechanosensitive channel in *Xenopus* oocytes. *Br. J. Pharmacol.* 106: 283-286, 1992.
- LANE, J. W., MCBRIDE, JR., D. W., AND HAMILL, O. P.: Ionic effects of amiloride block of the mechanosensitive channel in *Xenopus* oocytes. *Br. J. Pharmacol.* 108: 116-119, 1993.
- LANGTON, P. D.: Calcium channel currents recorded from isolated myocytes of rat basilar artery are stretch sensitive. *J. Physiol.* 471: 1-11, 1993.
- LANSMAN, J. B.: Blockade of current through single calcium channels by trivalent lanthanide cations: effects of ionic radius on the rates of ion entry and exit. *J. Physiol.* 95: 679-696, 1990.
- LEHRMANN, R., AND SEELIG, J.: Adsorption of  $\text{Ca}^{2+}$  and  $\text{La}^{3+}$  to bilayer membranes: measurement of the adsorption enthalpy and binding constant with titration calorimetry. *Biochim. Biophys. Acta.* 1189: 89-95, 1994.
- LI, X.-M., ZHANG, Y. F., NI, J.-Z., CHEN, J. W., AND HWANG, F.: Effect of lanthanide ions on the phase behavior of dipalmitoylphosphatidylcholine multilamellar liposomes. *J. Inorg. Biochem.* 53: 139-149, 1994.
- LIN, X., HUME, R. I., AND NUTALL, A. L.: Voltage-dependent block of neomycin of the ATP-induced whole cell current of guinea-pig outer hair cells. *J. Neurophysiol.* 70: 1593-1600, 1993.
- LIPPMANN, B. J., YANG, R., BARNETT, D. W., AND MISLER, S.: Pharmacology of volume regulation following hypotonicity-induced cell swelling in clonal N1E115 neuroblastoma cells. *Brain Res.* 688: 29-36, 1996.
- LIU, M., XU, J., TANSWELL, K., AND POST, M.: Inhibition of mechanical strain-induced fetal rat lung cell proliferation by gadolinium, a stretch-activated channel blocker. *J. Cell Physiol.* 161: 501-507, 1994.
- LUNDBAERK, J. A., AND ANDERSEN, O. S.: Lysophospholipids modulate channel function by altering the mechanical properties of lipid bilayers. *J. Gen. Physiol.* 104: 645-673, 1994.
- MARCHENKO, S. M., AND SAGE, S. O.: Mechanosensitive channels from endothelium of excised intact rat aorta (abstract). *Biophys. J.* 70: A365, 1996.
- MARKIN, V. S., AND MARTINAC, B.: Mechanosensitive ion channels as reporters of bilayer expansion: a theoretical model. *Biophys. J.* 60: 1120-1127, 1991.
- MARTINAC, B.: Mechanosensitive ion channels: biophysics and physiology. In *Thermodynamics of Cell Surface Receptors*, ed. by M. B. Jackson, pp. 327-352, CRC Press, Boca Raton, FL, 1992.
- MARTINAC, B., ADLER, J., AND KUNG, C.: Mechanosensitive ion channels of *E. coli* activated by amphipaths. *Nature (Lond.)* 348: 261-263, 1990.
- MATSUMOTO, H., BARON, C. B., AND COBURN, R. F.: Smooth muscle stretch-activated phospholipase C activity. *Am. J. Physiol.* 268: C458-C465, 1995.
- MATSUURA, S., IKEDA, K., AND FURUKAWA, T.: Effects of streptomycin, kanamycin, quinine, and other drugs on the microphonic potentials of the goldfish sacculus. *Jpn. J. Physiol.* 21: 579-590, 1971.
- MCALPINE, D., AND JOHNSTONE, B. M.: The ototoxic mechanism of cisplatin. *Hear. Res.* 47: 191-204, 1990.
- MCBRIDE, JR., D. W., AND HAMILL, O. P.: Pressure clamp: a method for rapid step perturbation of mechanosensitive channels. *Pfluegers Arch.* 421: 606-612, 1992.
- MCBRIDE, JR., D. W., AND HAMILL, O. P.: Pressure-clamp technique for measurement of the relaxation kinetics of mechanosensitive channels. *Trends Neurosci.* 16: 341-345, 1993.
- MCCARTY, N. A., AND O'NEIL, R. G.: Calcium-dependent control of volume regulation in renal proximal tubule cells: II roles of dihydropyridine-sensitive and insensitive  $\text{Ca}^{2+}$  entry pathways. *J. Membr. Biol.* 128: 161-170, 1991.
- MEDINA, I. R., AND BREGESTOVSKI, P. D.: Stretch-activated ion channels modulate the resting potential during early embryogenesis. *Proc. R. Soc. London Ser. B.* 235: 95-102, 1988.
- MEDRANO, S., AND GRUENSTEIN, E.: Mechanisms of regulatory volume decrease in UC-11 MG human astrocytoma cells. *Am. J. Physiol.* 264: C1201-C1209, 1993.
- MEVES, H.: Modulation of ion channels by arachidonic acid. *Prog. Neurobiol.* 43: 175-186, 1994.
- MILLET, B., AND PICKARD, B. G.: Gadolinium ion is the inhibitor suitable for testing the putative role of stretch-activated ion channels in geotropism and thigmotropism (abstract). *Biophys. J.* 63: 155a, 1992.
- MILLS, J. W., AND MANDEL, L. J.: Cytoskeletal regulation of membrane transport events. *FASEB J.* 8: 1161-1165, 1994.
- MOELLER, T.: The lanthanides. In *Comprehensive Inorganic Chemistry*, ed. by A. F. Trotman-Dickenson, pp. 1-101, Pergamon, Oxford, UK, 1973.
- MOOREN, F. C., AND KINNE, R. K. H.: Intracellular calcium in primary cultures of rat renal inner medullary collecting duct cells during variations of extracellular osmolarity. *Pfluegers Arch.* 427: 463-472, 1994.
- MORRIS, C. E.: Mechanosensitive ion channels. *J. Membr. Biol.* 113: 93-107, 1990.
- MORRIS, C. E.: Are stretch-sensitive channels in molluscan cells and elsewhere physiological mechanotransducers? *Experientia.* 48: 852-858, 1992.
- MORRIS, C. E., AND HORN, R.: Failure to elicit neuronal macroscopic mechanosensitive currents anticipated by single channel studies. *Science (Wash. DC)* 251: 1246-1249, 1991.
- MORRIS, C. E., AND SIGURDSON, W. J.: Stretch-inactivated ion channels coexist with stretch-activated ion channels. *Science (Wash. DC)* 243: 807-809, 1989.
- NAKAGAWA, T., KAKAHATA, S., AKAIKE, N., KUIMUNE, S., TAKASAKA, T., AND UEMURA, T.: Effects of  $\text{Ca}^{2+}$  antagonists and aminoglycoside antibiotics on  $\text{Ca}^{2+}$  currents in isolated outer hair cells of guinea pig cochlea. *Brain Res.* 580: 345-347, 1992.
- NARUSE, K., ASANO, H., AND SOKABE, M.: Gadolinium inhibits stretch induced alignment of cultured endothelial cells (abstract). *Biophys. J.* 64: A93, 1993.
- NARUSE, K., AND SOKABE, M.: Involvement of stretch-activated ion channels in  $\text{Ca}^{2+}$  mobilization to mechanical stretch in endothelial cells. *Am. J. Physiol.* 264: C1037-C1044, 1993.
- NICK, P., SCHAEFER, E., HERTEL, R., AND FURUYA, M.: On the putative role of microtubules in gravitropism of maize coleoptiles. *Plant Cell Physiol.* 32: 873-880, 1991.
- NIEBOER, E.: The lanthanide ions as structural probes in biological and model systems. *J. Struct. Bonding.* 22: 1-47, 1975.
- NIGGEL, J., HU, H., SIGURDSON, W., BOWMAN, C., AND SACHS, F.: *Grammostola spatulata* venom blocks mechanical transduction in GH3 neurons, *Xenopus* oocytes and chick heart cells (abstract). *Biophys. J.* 70: A347, 1996.
- NISHINO, T., ANDERSON, J. W., AND SANTAMBROGIO, G.: Response of tracheobronchial receptors to halothane, enflurane, and isoflurane in anesthetized dogs. *Respir. Physiol.* 95: 281-294, 1994.
- NOMURA, K., NARUSE, K., WATANABE, K., AND SOKABE, M.: Aminoglycoside blockage of  $\text{Ca}^{2+}$ -activated  $\text{K}^{+}$  channels from rat brain synaptosomal membranes incorporated into planar bilayers. *J. Membr. Biol.* 115: 241-251, 1991.
- OHMORI, H.: Mechano-electrical transduction currents in isolated vestibular hair cells of the chick. *J. Physiol.* 359: 189-217, 1985.
- OKAMOTO, R., AND SUMIKAWA, K.: Antibiotics cause changes in desensitization of ACh receptors expressed in *Xenopus* oocytes. *Mol. Brain Res.* 9: 165-168, 1991.
- OLESEN, S.-P., CLAPHAM, D. E., AND DAVIES, P. F.: Haemodynamic shear stress activates a  $\text{K}^{+}$  current in vascular endothelial cells. *Nature (Lond.)* 330: 168-170, 1988.
- OLIET, S. H. R., AND BOURQUE, C. W.: Mechanosensitive channels transduce osmosensitivity in supraoptic neurons. *Nature (Lond.)* 364: 341-343, 1993.
- OLIET, S. H. R., AND BOURQUE, C. W.: Gadolinium-induced block of osmosensitivity and mechanosensitive channels in rat supraoptic neurons. *Soc. Neurosci. Abstr.* 20: 1568, 1994.
- OLIET, S. H. R., AND BOURQUE, C. W.: Gadolinium uncouples mechanical detection and osmoreceptor potential in supraoptic neurons. *Neuron.* 16: 175-181, 1996.
- OLIVER, J. A., AND CHASE, JR., H. S.: Changes in luminal flow rate modulate basal and bradykinin-stimulated cell ( $\text{Ca}^{2+}$ ) in aortic endothelium. *J. Cell Physiol.* 151: 37-40, 1992.
- OPSAHL, L., AND WEBB, W. W.: Transduction of membrane tension by the ion channel alamethicin. *Biophys. J.* 68: 71-74, 1994.
- ORDWAY, R. W., PETROU, S., KIRBER, M. T., WALSH, J. V., AND SINGER, J. J.: Two distinct mechanisms of ion channel activation by membrane stretch: evidence that endogenous fatty acids mediate stretch activation of  $\text{K}^{+}$  channels (abstract). *Biophys. J.* 61: A390, 1991.
- ORDWAY, R. W., PETROU, S., KIRBER, M. T., WALSH, JR., J. V., AND SINGER, J. J.: Stretch activation of a toad smooth muscle  $\text{K}^{+}$  channel may be mediated by fatty acids. *J. Physiol.* 484: 3311-3337, 1995.
- PAINTAL, A. S.: Effects of drugs on vertebrate mechanoreceptors. *Pharmacol. Rev.* 16: 341-380, 1964.
- PALMER, L. G., AND FRINDT, G.: Gating of Na channels in the rat cortical collecting tubule: effects of voltage and membrane stretch. *J. Gen. Physiol.* 107: 35-45, 1996.
- PAOLETTI, P., AND AESCHER, P.: Mechanosensitivity of NMDA receptors in cultured mouse central neurons. *Neuron.* 13: 645-655, 1994.
- PENDER, N., AND MCCULLOCH, C. A. G.: Quantitation of actin polymerization in two human fibroblast sub-types responding to mechanical stretching. *J. Cell Sci. (Wash. DC)* 100: 187-193, 1991.
- PETROU, S., ORDWAY, R. W., HAMILTON, J. A., WALSH, JR., J. V., AND SINGER, J. J.: Structural requirements for charged lipid molecules to directly increase or suppress  $\text{K}^{+}$  channels activity in smooth muscle cells. *J. Gen. Physiol.* 103: 471-486, 1994.
- PETROV, A. G., AND USHERWOOD, P. N. R.: Mechanosensitivity of cell membranes: ion channels, lipid matrix and cytoskeleton. *Eur. Biophys. J.* 23: 1-19, 1994.
- PISER, T. M., LAMPE, R. A., KEITH, R. A., AND THAYER, S. A.:  $\omega$ -Grammotoxin SIA blocks multiple, voltage-gated,  $\text{Ca}^{2+}$  channel subtypes in cultured rat hippocampal neurons. *Mol. Pharmacol.* 48: 131-139, 1995.
- PRESSMAR, J., BRUNMEIER, H., SEEWALD, M. J., NAUMANN, T., AND RUEDEL, R.: Intracellular  $\text{Ca}^{2+}$  concentrations are not elevated in resting cultured muscle from Duchenne (DMD) patients and in MDX mouse muscle fibers. *Pfluegers Arch.* 426: 499-505, 1994.
- QUASTHOFF, S.: A mechanosensitive  $\text{K}^{+}$  channel with fast gating kinetics on human axons blocked by gadolinium ions. *Neurosci. Lett.* 169: 39-42, 1994.
- REDMAN, R. S., AND SILINSKY, E. M.: Decrease in calcium currents induced by

- aminoglycoside antibiotics in frog motor nerve endings. *Br. J. Pharmacol.* 113: 375-378, 1994.
- ROBSON, L., AND HUNTER, M.: Volume regulatory responses in frog isolated proximal cells. *Plügers Arch.* 428: 60-68, 1994.
- ROMANO-SILVA, M. A., GOMEZ, M. V., AND BRAMMER, M. J.: The use of gadolinium to investigate the relationship between  $\text{Ca}^{++}$  influx and glutamate release in rat cerebrocortical synaptosomes. *Neurosci. Lett.* 178: 155-158, 1994.
- ROSENBERG, B.: Fundamental studies with cisplatin. *Cancer* 55: 2302-2316, 1985.
- RUESCH, A., KROS, C. J., AND RICHARDSON, G. P.: Block by amiloride and its derivatives of mechano-electrical transduction in outer hair cells of mouse cochlear cultures. *J. Physiol.* 474: 75-86, 1994.
- RUTKUDIN, A., SACHS, F., AND BUSTAMANTE, J. O.: Stretch-activated ion channels in tissue-cultured chick heart. *Am. J. Physiol.* 264: H960-H972, 1993.
- RYBAK, L. P.: Drug ototoxicity. *Annu. Rev. Pharmacol. Toxicol.* 26: 79-99, 1986.
- SACHS, F.: Mechanical transduction in biological systems. *CRC Crit. Rev. Biomed. Eng.* 18: 141-169, 1988.
- SACKIN, H.: A stretch-activated  $\text{K}^+$  channel sensitive to cell volume. *Proc. Natl. Acad. Sci. USA* 86: 1731-1735, 1989.
- SACKIN, H.: Mechanosensitive channels. *Annu. Rev. Physiol.* 57: 333-353, 1995.
- SADOSHIMA, J.-I., AND IZUMO, S.: Mechanotransduction in stretch-induced hypertrophy of cardiac myocytes. *J. Recept. Res.* 13: 777-794, 1993.
- SADOSHIMA, J.-I., TAKAHASHI, T., JAHN, L., AND IZUMO, S.: Roles of mechanosensitive ion channels, cytoskeleton, and contractile activity in stretch-induced immediate-early gene expression and hypertrophy of cardiac myocytes. *Proc. Natl. Acad. Sci. USA* 89: 9905-9909, 1992.
- SALLEO, A., LA SPADA, G., AND BARBERA, R.: Gadolinium is a powerful blocker of the activation of nematocytes of *Palgia notiluca*. *J. Exp. Biol.* 187: 201-206, 1994a.
- SALLEO, A., LA SPADA, G., DRAGO, M., AND CURCIO, G.: Hypoosmotic shock induced discharge of sientia of *Calliactis parasitica* is blocked by gadolinium. *Experientia* 50: 148-152, 1994b.
- SANTOS-SACCHI, J.: Gadolinium ions reversible block voltage dependent movements of isolated outer hair cells. *Soc. Neurosci. Abstr.* 15: 208, 1989.
- SANTOS-SACCHI, J.: Reversible inhibition of voltage-dependent outer hair cell motility and capacitance. *J. Neurosci.* 11: 3096-3110, 1991.
- SASAKI, N., MITSUYU, T., AND NOMA, A.: Effects of mechanical stretch on membrane currents of single ventricular myocytes of guinea pig heart. *Jpn. J. Physiol.* 42: 957-970, 1992.
- SCHLICHTER, L. C., AND SAKELLARPOPOULOS, G.: Intracellular  $\text{Ca}^{++}$  signalling induced by osmotic shock in human T-lymphocytes. *Exp. Cell Res.* 215: 211-222, 1994.
- SEYMOUR, M. T.: The pharmacokinetics and pharmacodynamics of chemotherapeutic agents. In *Emesis in Anticancer Therapy: Mechanisms and Treatment*, ed. by P. L. R. Andrews and G. J. Sanger, pp. 9-44, Chapman and Hall, London, 1993.
- SHARMA, R. V., CHAPLEAU, M. V., HAJDUCZOK, G., WACHTEL, R. E., WAITE, L. J., BHALLA, R. C., AND ABOUD, F. M.: Mechanical stimulation increases intracellular calcium concentration in nodose sensory neurons. *Neuroscience* 66: 433-441, 1995.
- SHEETZ, M. P., AND SINGER, S. J.: Biological membranes as bilayer couples: a molecular mechanism of drug-erythrocyte interactions. *Proc. Natl. Acad. Sci. USA* 71: 4457-4461, 1974.
- SHIN, K. S., PARK, J. Y., HA, D. B., CHUNG, C. H., AND KANG, M.-S.: Involvement of  $\text{K}^+$  channels and stretch-activated channels in calcium influx, triggering membrane fusion of chick embryonic myoblasts. *Develop. Biol.* 175: 14-23, 1996.
- SIGURDSON, W. S., RUTKUDIN, A., AND SACHS, F.: Calcium imaging of mechanically induced fluxes in tissue cultured chick heart: role for stretch-activated ion channels. *Am. J. Physiol.* 262: H1110-H1115, 1992.
- SMALL, D. L., AND MORRIS, C. E.: Delayed activation of single mechanosensitive channels in *Lymanaea neurons*. *Am. J. Physiol.* 267: C598-C606, 1994.
- SMALL, D. L., AND MORRIS, C. E.: Pharmacology of stretch-activated  $\text{K}^+$  channels in *Lymanaea neurons*. *Br. J. Pharmacol.* 114: 180-186, 1993.
- SOKABE, M., HASEGAWA, N., AND YAMAMORI, K.: Blockers and activators for stretch-activated ion channels of chick skeletal muscle. *Ann. N. Y. Acad. Sci.* 707: 417-421, 1993.
- SOKABE, M., SACHS, F., AND JING, Z.: Quantitative video microscopy of patch clamped membranes: stress, strain, capacitance, and stretch activation. *Biophys. J.* 59: 722-728, 1991.
- SONO, J. B., HOOD, J. D., AND DAVIS, M. J.: Gadolinium blocks calcium channels in coronary artery smooth muscle cells (abstract). *Biophys. J.* 61: A515, 1992.
- STACY, JR., G. P., JOBE, R. L., TAYLOR, K., AND HANSEN, D. E.: Stretch-induced depolarization as a trigger of arrhythmias in isolated canine left ventricles. *Am. J. Physiol.* 263: H613-H621, 1992.
- STAVES, M. P., AND WAYNE, R.: The touch-induced action potential in *Chara*: inquiry into the ionic basis and the mechanoreceptor. *Aust. J. Plant. Physiol.* 20: 471-488, 1993.
- STEFFENSEN, I., BATES, W. R., AND MORRIS, C. E.: Embryogenesis in the presence of blockers of mechanosensitive ion channels. *Dev. Growth Differ.* 33: 437-442, 1991.
- SUKHAREV, S. I., BLOUNT, P., MARTINAC, B., BLATTNER, F. R., AND KUNG, C.: A large-conductance mechanosensitive channel in *E. coli* encoded by *mecL* alone. *Nature (Lond.)* 388: 265-268, 1994.
- SUKHAREV, S. I., MARTINAC, B., ARSHAVSKY, V. Y., AND KUNG, C.: Two types of mechanosensitive channels in the *E. coli* cell envelope: solubilization and functional reconstitution. *Biophys. J.* 66: 177-183, 1993.
- SWERUP, C., PURALI, N., AND RYDQVIST, B.: Block of receptor response in the stretch receptor neuron of the crayfish by gadolinium. *Acta Physiol. Scand.* 143: 21-26, 1991.
- SWERUP, C., AND RYDQVIST, B.: Effects of halothane on the transducer and potential activated currents of the crustacean stretch receptor. *Acta Physiol. Scand.* 125: 359-368, 1985.
- TAGLIETTI, V., AND TOSELLI, M.: A study of stretch activated ion channels of frog oocytes: interactions with  $\text{Ca}^{++}$  ions. *J. Physiol.* 407: 311-328, 1988.
- TANG, C.-M., PRESSER, F., AND MORAD, M.: Amiloride selectively blocks the low threshold (T) calcium current. *Science (Wash. DC)* 240: 213-215, 1988.
- THOMPSON, S. W., DAVIS, L. E., KORNFELD, M., HILGERS, R. D., AND STANDERFER, J. C.: Cisplatin neuropathy. *Cancer* 54: 1269-1275, 1985.
- THURM, U., ERLER, G., GOEDDE, J., KASTRUP, H., KEIL, T. H., VOELKER, W., AND VOHWINKEL, B.: Cilia specialized for mechanoreception. *J. Submicrosc. Cytol.* 15: 151-155, 1983.
- TSENG, G.-N.: Cell swelling increases membrane conductance of canine cardiac cells: evidence for a volume-sensitive  $\text{Cl}^-$  channel. *Am. J. Physiol.* 262: C1056-C1068, 1992.
- UBL, J., MURER, H., AND KOLB, H.-A.: Ion channels activated by osmotic or mechanical stress in membranes of opossum kidney cells. *J. Membr. Biol.* 104: 223-232, 1988.
- VANDORPE, D. H., AND MORRIS, C. E.: Stretch activation of the *Aplysia* S-channel. *J. Membr. Biol.* 127: 205-214, 1992.
- VANDORPE, D. H., SMALL, D. L., DABROWSKI, A. R., AND MORRIS, C. E.: FMRFamide and membrane stretch as activators of the *Aplysia* S-channel. *Biophys. J.* 66: 46-58, 1994.
- VAN NETTEN, S. M., KARLSSON, K. K., KHANNA, S. M., AND FLOCK, A.: Effects of quinine on the mechanical frequency response of the cupula in the fish lateral line. *Hear. Res.* 73: 223-230, 1994.
- VAN WAGONER, D. R.: Mechanosensitive gating of atrial ATP-sensitive potassium channels. *Circ. Res.* 72: 973-983, 1993.
- VELLY, J., CRIMA, M., DECKER, N., CRAGOE, JR., E. J., AND SCHWARTZ, J.: Effects of amiloride and its analogues on  $[^3\text{H}]$  batrachotoxin-A 20-a benzoate binding,  $[^3\text{H}]$  tetracaine binding and  $^{22}\text{Na}$  influx. *Euro. J. Pharmacol.* 149: 97-105, 1988.
- WANG, N., BUTLER, J. P., AND INCBER, D. E.: Mechanotransduction across the cell surface and through the cytoskeleton. *Science (Wash. DC)* 260: 1124-1127, 1993.
- WAYNE, R., STAVES, M. P., AND LEOPOLD, A. C.: The contribution of the extracellular matrix to graviscensing in characean cells. *J. Cell Sci.* 101: 611-623, 1992.
- WELLNER, M.-C., AND ISENBERG, G.: Properties of stretch-activated channels in myocytes from the guinea pig urinary bladder. *J. Physiol.* 466: 213-227, 1993.
- WELLNER, M.-C., AND ISENBERG, G.: Stretch effects on whole-cell currents of guinea-pig urinary bladder myocytes. *J. Physiol.* 480: 439-448, 1994.
- WELLNER, M.-C., AND ISENBERG, G.: cAMP accelerates the decay of stretch-activated inward currents in guinea-pig urinary bladder myocytes. *J. Physiol.* 482: 141-156, 1995.
- WILKINSON, N. C., MCBRIDE, JR., D. W., AND HAMILL, O. P.: Testing the putative role of a mechano-gated channel in *Xenopus* oocyte maturation, fertilization and tadpole development (abstract). *Biophys. J.* 70: A349, 1996a.
- WILKINSON, N. C., MCBRIDE, JR., D. W., AND HAMILL, O. P.: On the role of a mechano-gated cation channel in *Xenopus* oocytes. *J. Physiol.* 491P: 101P-102P, 1996b.
- WILLIAMSON, R.: The responses of primary and secondary sensory hair cells in the squid statocyst to mechanical stimulation. *J. Comp. Physiol.* 167: 655-664, 1990.
- WOOD, D. C.: The mechanism of tubocurarine action on mechanoreceptor channels in the protozoan *Stentor coeruleus*. *J. Exp. Biol.* 117: 215-235, 1985.
- XIA, S.-H., AND FERRIER, J.: Calcium signal induced by mechanical perturbation of osteoclasts. *J. Cell Physiol.* 163: 493-501, 1995.
- YANG, X.-C., AND SACHS, F.: Block of stretch-activated ion channels in *Xenopus* oocytes by gadolinium and calcium ions. *Science (Wash. DC)* 243: 1068-1071, 1989.
- YU, A., ERMAKOV, A. Z., AVERBAKH, V. I., LOBYSHEV, V. I., AND SUKHAREV, S. I.: Effects of gadolinium on electrostatic and thermodynamic properties of lipid membranes (abstract). *Biophys. J.* 70: A96, 1996.
- ZHANG, Y., GAO, F., MCBRIDE, D. W., AND HAMILL, O. P.: On the nature of mechano-gated channel activity in cytoskeleton deficient vesicles shed from *Xenopus* oocytes (abstract). *Biophys. J.* 70: A349, 1996.
- ZHOU, X.-L., AND KUNG, C.: A mechanosensitive channel in *Schistosoma* oocytes. *EMBO J.* 11: 2869-2875, 1992.
- ZHOU, X.-L., STUAPP, M. A., HOCH, H. C., AND KUNG, C.: A mechanosensitive channel in whole cells and in membrane patches of the fungus *Uromyces*. *Science (Wash. DC)* 253: 1415-1417, 1991.

## Mechanically Activated Currents in Chick Heart Cells

H. Hu\*, F. Sachs

Biophysical Sciences, 120 Cary Hall, SUNY at Buffalo, Buffalo, NY 14214

Received: 8 April 1996/Revised: 8 August 1996

**Abstract:** As predicted from stretch-induced changes of rate and rhythm in the heart, acutely isolated embryonic chick heart cells exhibit whole-cell mechanosensitive currents. These currents were evoked by pressing on cells with a fire polished micropipette and measured through a perforated patch using a second pipette. The currents were carried by  $\text{Na}^+$  and  $\text{K}^+$  but not  $\text{Cl}^-$ , and were independent of external  $\text{Ca}^{2+}$ . The currents had linear  $I/V$  curves reversing at  $-16$  mV and were completely blocked by  $\text{Gd}^{3+} \geq 30 \mu\text{M}$  and *Grammostola spatulata* venom at a dilution of 1:1000. Approximately 20% of cells showed time dependent inactivation. In contrast to direct mechanical stimulation, hypotonic volume stress produced an increase in conductance for anions rather than cations—the two stimuli are not equivalent. The cells had two types of stretch-activated ion channels (SACs): a 21 pS nonspecific cation-selective reversing at  $-2$  mV and a 90 pS  $\text{K}^+$  selective reversing at  $-70$  mV in normal saline. The activity of SACs was strongly correlated with the presence of whole-cell currents. Both the whole-cell currents and SACs were blocked by  $\text{Gd}^{3+}$  and by *Grammostola spatulata* spider venom. Mechanical stimulation of spontaneously active cells increased the beating rate and this effect was blocked by  $\text{Gd}^{3+}$ . We conclude that physiologically active mechanosensitive currents arise from stretch activated ion channels.

**Key words:** Stretch — Volume — Voltage clamp — Patch clamp — Transduction

## Introduction

Mechanical stimulation has long been known to increase automaticity and alter the action potential in whole hearts

and isolated tissues (Bainbridge, 1915; Rajala, Kalbfleisch & Kaplan, 1976; Lab, 1980). The simplest explanation for these effects would appear to be stretch-activated channels. Such channels have been observed in a variety of isolated cardiac cells including frog (Kohl et al., 1992), chick (Ruknudin, Sachs & Bustamante, 1993), rat (Kim, 1992; Craelius, 1993), rabbit (Hagiwara et al., 1992), guinea-pig (Bustamante Ruknudin & Sachs, 1991), and human (Naruse & Sokabe, 1993). Despite the wide variety of the data on effects of stretch on cardiac tissues, only a single study has been made of the corresponding whole-cell currents (Sasaki, Mitsuiye & Noma, 1992), and because of the difficulty of applying repeatable stimuli, that study provided limited data. Many researchers have used hypotonic swelling or inflation through the recording pipette as alternative "mechanical" stimuli although it is not clear that such stimuli act via a common mechanism (Hagiwara et al., 1992; Van Wagoner, 1993; Kim, 1993; Zhang et al., 1993; Kim & Fu, 1993; Ackerman, Wickman & Clapham, 1994).

Stretching the heart may lead to arrhythmias of clinical significance (Dean & Lab, 1989; Franz et al., 1989; Hansen, Craig & Hondeghem, 1990). Such stretch-induced arrhythmias in dog hearts can be blocked by  $\text{Gd}^{3+}$  (Yang & Sachs, 1989) but not by organic blockers of  $\text{Ca}^{2+}$  channels (Hansen et al., 1991) suggesting that mechanosensitive (MS) ion channels may be involved. In this paper, we demonstrate stable whole-cell currents activated by direct mechanical strain and show that these currents are not the same as those activated by hypotonic swelling. The strain sensitive current is capable of altering the beating rate of the cells and this effect can be accounted for by the presence of two types of stretch-activated channels (SACs) found in the cells. We used chick heart cells—an established preparation whose mechanical sensitivity has been demonstrated by pressure-induced changes in rate, strain-induced  $\text{Ca}^{2+}$  fluxes and the presence of SACs (Rajala et al., 1976; Sigurdson et al., 1992; Ruknudin et al., 1993).

Present address: 844 Ross Building, Johns Hopkins School of Medicine, Baltimore, MD 21205.

Correspondence to: F. Sachs

## Materials and Methods

### CHICK VENTRICULAR CELL PREPARATION

The cell preparation method was modified from Sada et al. (1988). Briefly, hearts of 16–17 day old White Leghorn chick embryos were dissected, ventricles were removed, washed with divalent-ion free saline (D-PBS, GIBCO, Grand Island, NY), minced, then stirred in a 37°C incubator with an enzyme solution containing 0.02% collagenase (Sigma, St. Louis, MO) and 0.2% trypsin (Sigma). The isolation proceeded stepwise. The supernatant obtained by the first stirring of 15 min contained few cells and was discarded. Steps two through four used fresh aliquots of enzyme solution for 5 min, and the supernatants of these steps were saved. The cell suspensions were mixed with minimum essential medium (MEM, GIBCO, supplemented with 10% horse serum, GIBCO, plus 2% chick embryo extract), and gently centrifuged. The cells were gently resuspended, distributed into culture dishes and maintained in a tissue culture incubator at 37°C. We conducted our experiments 1–3 days after cell preparation when the cells had stuck to the coverslip. We used rounded rather than elongated cells because it was simpler to apply the mechanical stimulation. Using a single pipette to press on the top of the cells, we could expect relatively uniform stimulation (*see below*) compared to the same stimulation applied to part of an elongated cell. The cells could be electrically or mechanically stimulated to beat indicating that they were healthy. All experiments were conducted at a room temperature of 22–24°C.

### ELECTROPHYSIOLOGY AND MECHANICAL STIMULATION

We conducted studies using whole-cell, single-channel, and loose-seal recording. Patch-clamp techniques followed standard procedures (Hamill et al., 1981). Micropipettes were made from 100 $\mu$ m capillaries (Drummond Microcaps, Thomas Scientific, Swedesboro, NJ), fire polished, and having a resistance of 2–3 M $\Omega$  when the pipette solution was high K<sup>+</sup> saline and the bath solution was normal saline (*see Solutions below*). Currents and voltages were recorded with a CV-3 headstage (Axon Instruments, Foster City, CA), using an Axopatch-1B patch clamp (Axon), a VR-10 CRC digital data recorder (Instrutech, Elmont, NY) and a VCR (JVC, HR-S7000U, Japan). A 902LPF low-pass filter (Frequency Devices, Haverhill, MA) was applied before data acquisition. Bath solutions with a perfusion rate of 1.5 ml/min and the volume of the chamber was 0.5 ml.

In the whole-cell studies, we used one micropipette for perforated-patch voltage-clamp (Horn & Marty, 1988) and another for mechanical stimulation. These are noted respectively as the recording and stimulating pipettes. The whole-cell configuration was considered as formed (noted time 0 for stability tests) when the series resistance decreased to 15 M $\Omega$  or lower and was stable for at least 2 min. The tip of the stimulation pipette was a few  $\mu$ m in diameter, fire-polished and mounted on a piezoelectric manipulator with the axis of the pipette tip nearly parallel to the stage. We pressed the side of the pipette against the cell using the vertical displacement of the pipette as a measure of the cell strain. Maximal displacements were less than 4  $\mu$ m and were expected to produce mean cortical tensions of <1–3 dyne/cm (*c.f.* Discussion). The manipulator (Burleigh PCS-1000, Fishers, NY) was controlled either manually or by a computer running Labview™. In the latter case we used trapezoidal stimulus pulses to avoid mechanical resonances of the probe and manipulator. Unless otherwise noted, the results below refer to noninactivating currents. Single-channel experiments used standard techniques (Hamill et al., 1981), and only seals with a resistance of >10 G $\Omega$  were used. In the *I/V* study of the single channels, the cell resting potential was measured by the end of the

experiment by rupturing the patch and immediately recording the potential in current clamp mode.

In our loose-seal studies (Stühmer et al., 1983), the seal resistance was 20–40 M $\Omega$ . In both single-channel and loose-seal studies, suction was applied to the pipette for mechanical stimulation (Guharay & Sachs, 1984).

In the whole-cell experiments, we found that after mechanical stimulation the cells became sensitive to changes in perfusion conditions often causing loss of stable recordings, especially when the replacing solution was nonphysiological. Because of this high failure rate, we were often unable to compare recordings from the same cell in different solutions, and had to resort to population studies. The reason that mechanical stimulation caused cells to become sensitive to perfusion is not clear, although it is possible that strain may disrupt the cells' attachments to the substrate.

In the whole-cell experiments, we monitored the cell under a phase-contrast microscope (magnification 200 $\times$ ) during mechanical stimulation. Cell diameter was measured using a micropipette as a pointer. We moved the pipette from one side of the cell to the other by changing the voltage applied to the stimulating manipulator, and converted the voltage difference to the displacement. In some experiments, particularly when we measured the lateral strain, we videotaped the image of the cell using a CCD camera (GBC, CCD-500, USA) and a VCR (JVC, HR-S7000U, Japan). These images were digitized for off-line analysis using a frame grabber (Data Translation, Model-2861).

### SOLUTIONS (IN mM)

*Normal saline (NS)*: 150 NaCl, 5 KCl, 2 CaCl<sub>2</sub>, 1 MgCl<sub>2</sub>, 10 HEPES, pH 7.4 titrated with 1N NaOH, 329 mOsm; *High K<sup>+</sup> saline (HK)*: 5 NaCl, 150 KCl, 0.5 K-EGTA, 10 HEPES, pH 7.4 titrated with 1N KOH, 323 mOsm; *Na-isethionate*: 160 Na-isethionate, 10 HEPES, pH 7.4 titrated with 1N NaOH, 330 mOsm; *Mannitol solution*: 330 D-mannitol, 2 CaCl<sub>2</sub>, 336 mOsm. *Hypotonic mannitol solution*: 250 D-mannitol, 2 CaCl<sub>2</sub>, 256 mOsm. For perforated patches, the pipette was filled with HK containing 200  $\mu$ g/ml nystatin (nystatin first dissolved in DMSO at 20 mg/ml) or 100–200  $\mu$ g/ml amphotericin B and sonicated before filling the pipette, noted as *nystatin solution* and *amphotericin B solution* respectively. For loose-seal experiments, we used both NS and HK, with and without Ca<sup>2+</sup>, as the pipette solution. The bath solution was always NS unless otherwise specified. *Grammostola spatulata* venom was obtained from Spider Pharm, Seasterville, PA.

### DATA ACQUISITION AND PROCESSING

Analog signals (real-time or replayed tape recordings) were sampled through a computer interface BNC-2080 connected to an I/O board AT-MIO-16X using LabVIEW software (National Instruments, Austin, TX) into a computer (Gateway2000 Model 486DX2/50). LabVIEW was also used to generate command protocols for whole-cell voltage clamping, to drive the piezoelectrics for mechanical stimulation, and for preliminary data processing as well. AXUM (TriMetrix, Seattle, WA), SCIENTIST™ (Micromath, Salt Lake City, UT), IPROC (Axon), and other software were used for data processing and graphing. The sampling rate ranged from 500 Hz to 10 kHz depending on the speed and the time length of the event of interest, and was bandlimited at the Nyquist limit or lower. When plotting, the less important data were often decimated to simplify graphing while maintaining the visual effect. Unless otherwise specified, all the statistical results given are in the form of mean  $\pm$  SD.

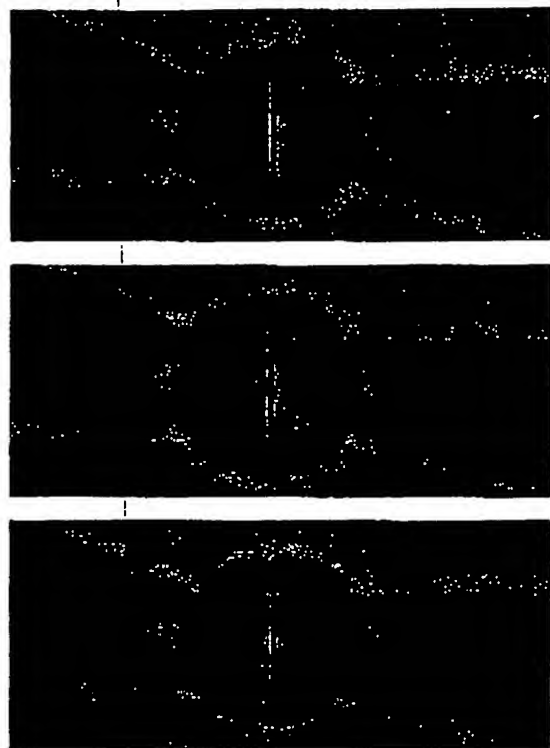


Fig. 1. Phase contrast photomicrographs of a cell and the stimulation (right) and recording (left) pipettes showing the relatively small change in shape associated with stimulation. Panels A and C were taken, respectively, before and after stimulation, and panel B was taken while the cell was pressed by the stimulation pipette. The diameter of the maximal cross-section of the cell in panel B is used as the scale bar, and is 16  $\mu\text{m}$ . The diameters of the cell in A and C are similar, 15  $\mu\text{m}$ , indicating good recovery. The downward displacement of the stimulation pipette was 3.8  $\mu\text{m}$ .

#### ABBREVIATIONS

MS (mechanosensitive), SAC (Stretch-Activated Channel), MSC (Whole-Cell Mechanosensitive Current)

#### Results

##### GENERAL DESCRIPTION OF THE CELL

The cells we studied had resting potentials of  $-69.9 \pm 3.6$  mV ( $n = 25$ , measured from single cells) at room temperature at  $22\text{--}24^\circ\text{C}$ . They could be electrically or mechanically stimulated to beat and produced action potentials. They displayed typical voltage-sensitive  $\text{Na}^+$ ,  $\text{Ca}^{2+}$ , and  $\text{K}^+$  currents when step-voltage clamped. The cells were generally spherical with a diameter of  $15.7 \pm 2.1$   $\mu\text{m}$  ( $n = 9$ ), and a capacitance of  $7.0 \pm 1.97$  pF ( $n = 25$ ). Figure 1 shows photomicrographs of a cell with and

without mechanical stimulation. When this cell was pressed against the coverslip by 3.8  $\mu\text{m}$ , the maximal diameter increased from 15.4  $\mu\text{m}$  to 16.1  $\mu\text{m}$ .

##### THE MSC IN NORMAL SALINE

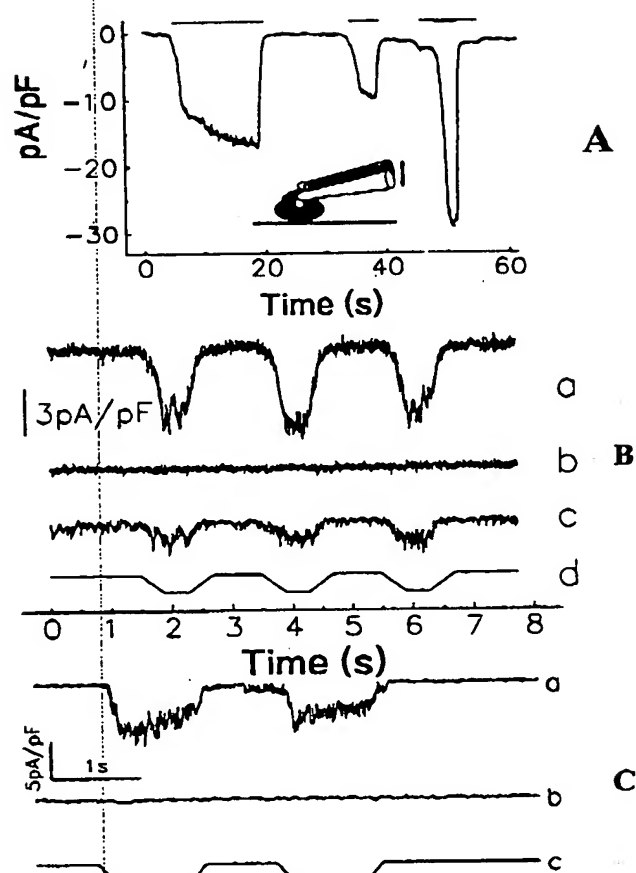
An example of whole-cell currents recorded with NS in the bath are shown in Fig. 2A. The MSC was inward at holding potential of  $-71$  mV, reversible, and its amplitude was monotonic with the displacement of the mechanical stimulation pipette. The currents were depressed by  $83 \pm 6\%$  ( $n = 4$ ) in 20  $\mu\text{M}$   $\text{Gd}^{3+}$ , unmeasurable in 30  $\mu\text{M}$   $\text{Gd}^{3+}$ , and displayed only partial recovery during washouts lasting 15–30 min ( $n = 3$ ). Higher concentrations of  $\text{Gd}^{3+}$  (100  $\mu\text{M}$ ) also blocked MSCs, but recovery during washout was small (Fig. 2B,  $n = 3$ ).

Spider venom from *Grammastola spatulata* that has been shown to block SAC activity in other cells (Chen et al., 1996; Niggel et al., 1996), also completely blocked the MSC (Fig. 2C,  $n = 4$ ) and SACs in cell attached patches (Hu, 1996). Washout was generally irreversible within 15–30 min, although the cells could still generate normal voltage dependent currents (Hu, 1996).

To measure the  $I/V$  curve of the MSC, we applied a ramp voltage in the presence and absence of mechanical stimulation (Fig. 3). These total whole-cell  $I/V$  curves are representative (Fig. 3A) and show the expected strong inward  $\text{K}^+$  rectification (Josephson & Sperelakis, 1990). In Fig. 3B, the difference current had a linear regression of  $I = 1.01 + 0.06V$ , indicating a reversal potential of  $-17$  mV and a conductance of 60 pS/pF. The mean overall reversal potential was  $-16.4 \pm 1.3$  mV ( $n = 5$ ), almost identical to the value of  $-15$  mV reported for guinea-pig ventricular cells (Sasaki et al., 1992). The conductance was modulated by the strain, but it was not possible to make quantitative comparisons between cells because of the lack of control of local strain. The maximal observed conductance in NS (but not necessarily saturating) was 600 pS/pF.

Since earlier experiments showed a wide range of responses to mechanical stimulation (Sasaki et al., 1992), it was important to test the reproducibility of our stimulation. For repeated stimuli applied to the same cell, the response was stable over time provided the stimulus was not repeated very often. The peak MSC varied by less than 10% over 2–4 seconds ( $n = 15$  stimuli applied to 4 cells, e.g. trace a of Fig. 2B), and less than 15% over 5–20 min ( $n = 3$ ). For the short term study, we applied sets of stimuli to each cell with patterns as shown in trace d of Fig. 2B. The peak displacements ranged from 1.7  $\mu\text{m}$  to 3.3  $\mu\text{m}$ , but were the same in each set. We averaged the 3 peak MS currents within each set, calculated the ratio of each current to the mean current, and pooled these ratios to characterize the stability as a standard deviation. For the long-term study (Fig. 4), we applied

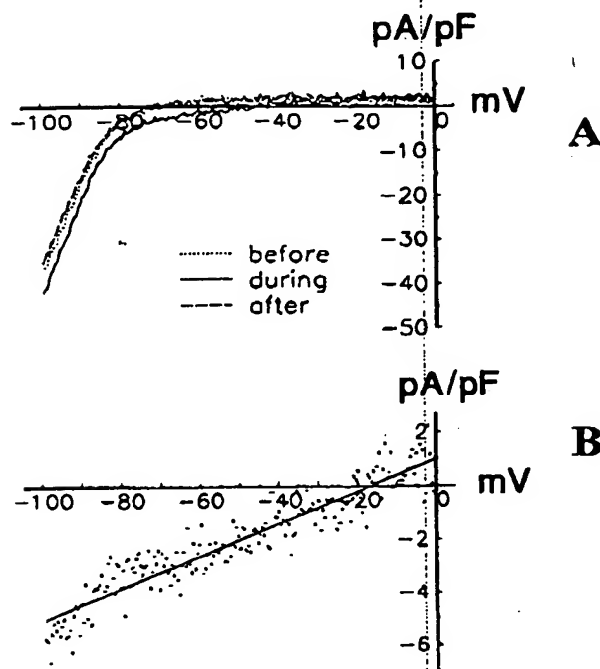




**Fig. 2.** MSCs in normal saline and blockage by  $Gd^{3+}$  and *Grammostola spanulata* venom. (A) Stimulus-response relationship and reversibility of MSCs. Inward currents are downward. The three horizontal bars from left to right represent stimuli (manually controlled) of  $-2.5 \mu m$ ,  $-1.5 \mu m$  and  $-3.5 \mu m$ , with the line thickness representing the magnitude of the stimuli. Cell clamped at the resting potential of  $-71 mV$ , capacitance  $4.5 pF$ . Bath solution: NS; pipette solution: nystatin. The MSC was substantially noisier than the resting current suggesting that the current arose from channels. (B) Block of MSCs by high levels of  $Gd^{3+}$  ( $100 \mu M$ ). Trace a: current before  $Gd^{3+}$ ; trace b: with  $Gd^{3+}$ ; trace c: washout; trace d: displacement of the stimulation pipette ( $1.7 \mu m$  peak). Cell capacitance  $9.1 pF$ , membrane potential  $-50 mV$ . (C) Block of MSCs by *Grammostola spanulata* spider venom at a dilution of 1:2,000. Trace a: control, the MSC in NS; trace b: response in the venom solution; trace c: displacement of the stimulation pipette,  $1.7 \mu m$  peak. Cell capacitance  $3.4 pF$ , membrane potential  $-45 mV$ .

the mechanical stimulus soon after the whole-cell condition was stable, and then again 10–15 min later. We calculated the ratio of the absolute difference current to the initial current, and averaged these to characterize the stability. Unfortunately, repeated stimulation did cause a loss in responsiveness for reasons unknown and this “use dependent” rundown prevented us from using extensive experimental protocols.

The same stimulus displacement produced different



**Fig. 3.** Measurement of the  $I/V$  curve of the MSC in normal saline. (A)  $I/V$  curves of the total whole-cell currents. The membrane potential was driven by a ramp voltage, and the currents were recorded before, during and after the mechanical stimulus (dotted, solid and dashed lines, respectively). The currents before and after stimulation were essentially identical. Mechanical stimulation generated increased inward current at negative potentials and outward current at positive potentials. The total currents (average of 3–5 responses) showed strong inward rectification. Bath: NS; pipette: amphotericin B. Cell capacitance  $4.8 pF$ , resting potential  $-70 mV$ . (B)  $I/V$  relationship of the MSC (dots) derived by subtraction of the  $I/V$  curves obtained in the presence and absence of stimulation shown in A. Linear regression of the data gives  $I = 1.0 + 0.06V$ , indicating a conductance of  $60 pS$  ( $0.06 nS$ ) and a reversal potential of  $-17 mV$ .

currents in different cells. For example, using four different cells, a displacement of  $1.7 \mu m$  produced a conductance of  $146 \pm 72 pS/pF$ . This variability was caused, at least in part, by the uncertainty of judging when the stimulation pipette touched the cell. Such variability discouraged us from attempting quantitative dose-response studies of the MSCs.

#### IONIC BASIS OF THE MSC

The reversal potential of the MSC,  $-16 mV$ , suggested that it might be carried by nonselective cation channels (Craeli et al., 1993; Ruknudin et al., 1993),  $Cl^-$  channels (Hagiwara et al., 1992; Zhang et al., 1993), or a mixture of channels. To examine these possibilities, we substituted  $Na^+$ ,  $K^+$ ,  $Ca^{2+}$ , and  $Cl^-$ .

If  $Cl^-$  were a major carrier of the MSC, then by

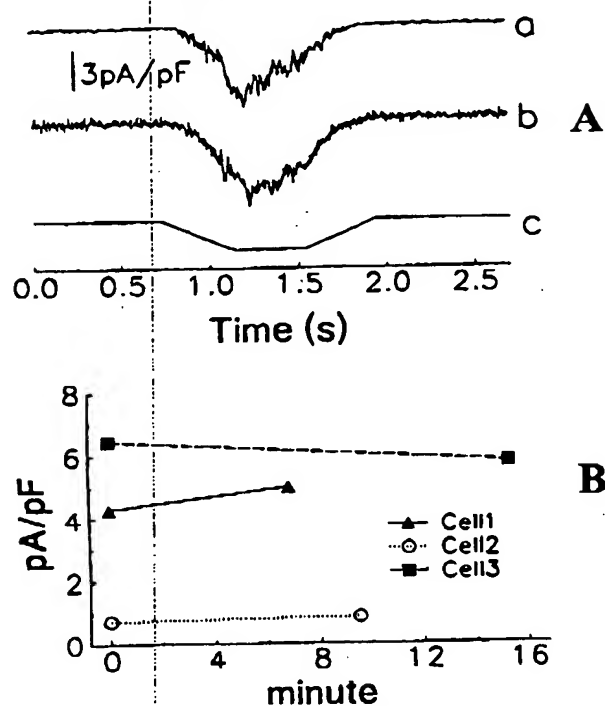


Fig. 4. The MSC of a cell is reproducible over time. (A) Currents recorded at different times from a single cell. Trace *a*: current seen when the whole-cell condition was initially formed; *b*: current 6'50" after trace *a* was recorded; *c*: peak displacement 3.3  $\mu\text{m}$  of the stimulation pipette. The response pattern of *b* was similar to that of *a*, indicating that the MSC was basically unchanged. Bath: NS; pipette: nystatin. Cell capacitance 9.1 pF, held at -50 mV. (B) Peak MSC measured at different time intervals from three different cells. The raw data for cell 1 are shown in A. Bath: NS; pipette: nystatin.

removing  $\text{Cl}^-$  from the bath there should be no significant outward current since there would be no  $\text{Cl}^-$  influx. However, with  $\text{Cl}^-$  replaced by isethionate we observed distinct outward MSCs, as well as inward MSCs, with conductances similar to those observed in normal  $\text{Cl}^-$ . The reversal potential was essentially unchanged at  $-14.0 \pm 3.3$  mV ( $n = 3$ ). These results suggest that  $\text{Cl}^-$  does not carry the MSC. Since  $\text{Na}^+$  was the only other external ion in significant concentration, it must have been the charge carrier for the inward current.

MSCs in HK were usually larger than those observed in NS (Fig. 5). For example, with a stimulus displacement of 1.7  $\mu\text{m}$ , the conductance was  $690 \pm 360$  pS/pF ( $n = 3$ ), compared to  $150 \pm 70$  pS/pF ( $n = 4$ ) observed in NS. The ranges do not overlap and a *t* test with unequal variances found the difference significant at 5.8%. In one experiment, the conductance of a cell was first measured in NS and then in HK, and for a 2.5  $\mu\text{m}$  displacement the conductance increased from 280 pS/pF to 1520 pS/pF. This is a ratio comparable to the population means above. These data suggest that the

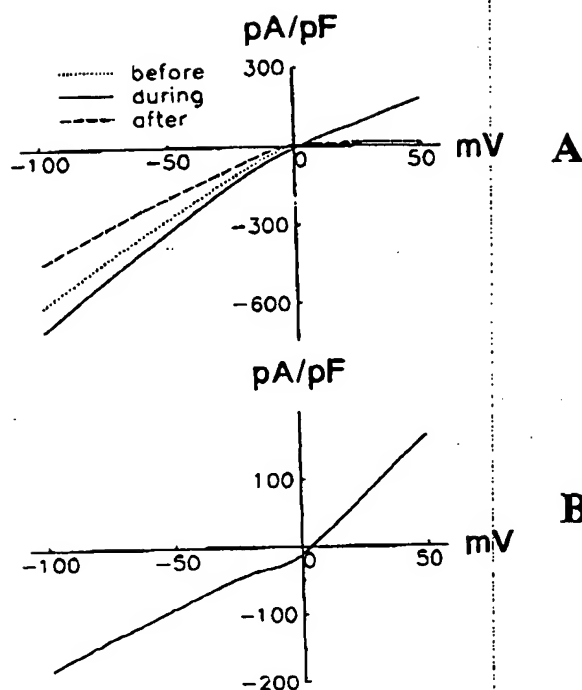


Fig. 5. The MSC in HK bath solution. (A) *I/V* curves of total currents before (dotted line), during (solid line) and after (dashed line) a mechanical stimulus. The curves before and after the stimulus showed strong inward rectification, which was greatly reduced in the curve during the stimulation. The current was larger with stimulation indicating that additional conductance was activated. (B) The *I/V* curve of the MSC obtained by subtracting the average of the currents before and after mechanical stimulation from the one during the stimulation. The net MSC was not inwardly rectifying.

MSC is more permeable to  $\text{K}^+$  than  $\text{Na}^+$ . The reversal potential in HK was  $0.7 \pm 1.9$  mV ( $n = 5$ ), as expected from the nearly symmetric solutions. Total whole-cell currents in the absence of mechanical stimulation showed strong inward rectification, while during stimulation, the rectification was reduced because of domination by the linear MSC.

#### MSC IS OBSERVED IN NOMINALLY $\text{Ca}^{2+}$ -FREE SOLUTIONS

Removing external  $\text{Ca}^{2+}$  ions did not significantly affect MSCs. For example, in Na-isethionate solution with no added  $\text{Ca}^{2+}$ , the evoked MSC was similar to that obtained in NS bath solution. Using HK as the bath solution, which was also nominally  $\text{Ca}^{2+}$  free, we observed even larger MSCs (Fig. 5). When we excluded  $\text{Ca}^{2+}$  from the NS we still observed MSCs similar to those in NS bath solution, with a mean conductance of  $130 \pm 50$  pS/pF ( $n = 4$ ) for a displacement of 1.7  $\mu\text{m}$ . These results sug-



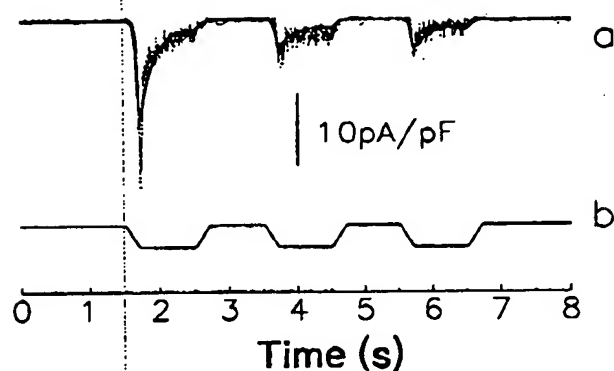


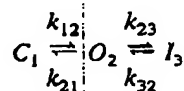
Fig. 6. Inactivation of the MSC. Trace a: recorded current (dots) with the model-simulated current (smooth trace) superimposed; trace b: displacement, 3.3  $\mu\text{m}$  peak; membrane potential -35 mV.

gest that extracellular  $\text{Ca}^{2+}$  is not needed to generate MSCs.

#### INACTIVATION OF THE MSC

With constant strain, the MSC rose monotonically to a steady state in most experiments. However, out of 84 cells stimulated under computer control, 15 showed inactivation (Fig. 6), and such inactivation was observed with both inward and outward MSCs. During inactivation, the current decayed with time while a constant stimulus was maintained, reaching a steady-state amplitude. When the stimulation was removed, the MSC recovered, usually within 15–20 sec. By examining the cells with direct imaging and video analysis, the inactivation did not appear to originate from the cell slipping from beneath the stimulation pipette. In contrast to the behavior of SACs in *Xenopus* oocytes (Hamill & McBride, 1992), inactivation properties were not strongly dependent upon the membrane potential.

To summarize the time response of the inactivation process, we fit the currents to a three-state linear model consisting of closed (C), open (O) and inactivated (I) states:



with  $k_{12} = k_{12}^0 \exp(\alpha_{12}d)$ , and  $k_{23} = k_{23}^0 \exp(\alpha_{23}d)$ , where  $d$  is the time-dependent displacement of the stimulation pipette (the directly recorded trapezoidal trace, e.g., Fig. 6b),  $\alpha_{ij}$ s are the sensitivity parameters and the  $k_{ij}^0$ s are the rates in the absence of stimulation. The rates  $k_{21}$  and  $k_{32}$  could be left independent of stimulation. The model was specified by the first order differential equations to allow the use of the trapezoidal driving function.

Using the familiar variables  $m$  for activation and  $h$  for inactivation, the current was,

$$I = I_{\text{peak}}mh - I_b, \quad (1)$$

where  $I_{\text{peak}}$  and  $I_b$  are peak and background currents respectively,

$$\frac{dm}{dt} = -m(k_{21} + k_{12}) + k_{12}, \quad (2)$$

and

$$\frac{dh}{dt} = -h(k_{23} + k_{32}) + k_{32}. \quad (3)$$

Using the program Scientist<sup>TM</sup>, we fit the data from ten cells exhibiting large currents and the results are shown in the Table (excluding the results from two cells whose values of  $k_{32}$  were outliers).

To simplify fitting  $k_{12}^0$  and  $k_{23}^0$  were fixed based on the results of previous trials. The means and standard deviations were calculated from the optimal parameters obtained from the different records, ignoring the covariance obtained from each individual fitting.

#### THE MSC IS DISTINCT FROM THE HYPOTONICALLY-INDUCED CURRENT

Because many papers on heart cells have reported a  $\text{Cl}^-$ -selective 'mechanically-induced current' following hypotonic stress (or inflation of the cell) (Tseng, 1992; Hagiwara et al., 1992; Zhang et al., 1993) and our MSCs were cation selective, we compared the result of hypotonic stress with that from direct mechanical strain (Fig. 7). The clearest demonstration of the differences came from using a bath solution almost free of ions (containing only 2 mM  $\text{CaCl}_2$ , as Zhang, Hall & Lieberman, 1994 have reported that  $\text{Ca}^{2+}$  was needed to observe the hypotonically-induced current). In this distinctly nonphysiological solution, the ionic strength of the bath was much smaller than that of the intracellular phase and the whole-cell current was dominated by efflux.  $\text{K}^+$  currents should have had a negative reversal potential, while  $\text{Cl}^-$  currents should have had a positive reversal potential.

With the low ionic strength bath solution, direct mechanical stimulation produced currents with a negative reversal potential ranging from -10 to -30 mV ( $n = 3$ ). One example is shown as trace a of Fig. 7. The current was primarily outward, and showed complete and rapid recovery upon removal of the stimulus. At more negative voltages there was a tiny inward current, which was likely carried by the 2 mM extracellular  $\text{Ca}^{2+}$ . Clearly, the current induced by direct mechanical stimulation is cation-selective.

Table. Parameters of the three-state MSC inactivation model

	$k_{21}$ (sec <sup>-1</sup> )	$k_{32}$ (sec <sup>-1</sup> )	$\alpha_{12}$ ( $\mu\text{M}^{-1}$ )	$\alpha_{23}$ ( $\mu\text{M}^{-1}$ )	$k_{12}^0$ (sec <sup>-1</sup> )	$k_{23}^0$ (sec <sup>-1</sup> )
Mean $\pm$ SD	$31 \pm 15$	$0.12 \pm 0.06$	$2.7 \pm 0.8$	$0.6 \pm 0.2$	0.1	0.5

Means calculated using 10 records from 8 cells.

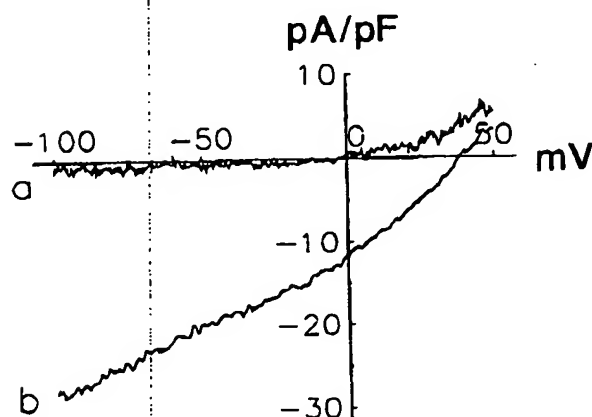


Fig. 7. The MSC is distinct from the hypotonically-induced current. Trace a: the net MSC in isotonic mannitol solution, obtained by subtracting the average of the currents before and after mechanical stimulation from the current during stimulation. The MSC is outward-going at positive potentials, indicating a  $\text{K}^+$  efflux. Trace b: the net hypotonically-induced current obtained in a similar way, by subtracting the current in the isotonic mannitol solution from that in the hypotonic mannitol solution. The current is primarily inward-going, indicating a  $\text{Cl}^-$  efflux.

Hypotonically-induced currents were generated by perfusing the bath with the same solution, but with lowered mannitol concentrations (hypotonic mannitol solution). A net hypotonically-induced current is shown as trace b of Fig. 7. In contrast to the mechanically induced currents, hypotonically induced currents were mainly inward-going with a reversal potential of  $+45 \pm 10$  mV ( $n = 4$ , corrected for junction potentials and interpolated to zero current when necessary). The hypotonically induced conductance recovered by 60–80% after returning to the normal osmolality solution.

From the composition of the intracellular and extracellular solutions, the only possible carriers for the hypotonically induced inward current were extracellular  $\text{Ca}^{2+}$  and intracellular  $\text{Cl}^-$ . The concentration of extracellular  $\text{Ca}^{2+}$  was too low to generate such a large current and the Nernst potential of  $\text{Ca}^{2+}$ ,  $\approx 125$  mV, is far more positive than the observed reversal potential. If the current were carried purely by  $\text{Cl}^-$ , the observed reversal potential of  $+45$  mV would predict an intracellular  $\text{Cl}^-$  concentration of 24 mM. This is 11 mM lower than the reported value of 35 mM obtained with an extracellular  $\text{Cl}^-$  concentration of 85 mM (Zhang et al., 1993), but is

reasonable given the low  $\text{Cl}^-$  bath solution. Regardless of any peculiarities induced by the nonphysiological solutions, it is clear from these experiments that hypotonic stress can induce currents of different ionic selectivity from those induced by direct mechanical stimulation.

Why should the results of direct strain and osmotically induced strain be so different when there is no reason to expect osmotic swelling not to activate MSCs? As opposed to direct mechanical strain in a patch or whole-cell recording, osmotic challenge dilutes the intracellular medium and stresses internal membranous organelles. These latter effects may lead to second messenger activation of  $\text{Cl}^-$  current. Some researchers have found that swelling-induced  $\text{Cl}^-$  currents are dependent upon intracellular  $\text{Ca}^{2+}$  (Zhang et al., 1994) or ATP (Oike, Droogmans & Nilius, 1994). Osmotic swelling probably does cause some activation of MSCs, but the net current is clearly dominated by the anionic  $\text{Cl}^-$  current. The disparity between the response to osmotic strain and direct mechanical strain has been noted previously (Sasaki et al., 1992; Ackerman et al., 1994).

#### SINGLE SAC STUDY

Can SACs account for the MSC? We performed cell-attached single-channel studies using NS in both the bath and the pipette. Out of 13 patches providing sufficient  $I/V$  data, we observed 5 patches containing a 90 pS SAC whose currents reversed at  $-70 \pm 5$  mV ( $n = 3$  cells), and 11 patches containing a 21 pS SAC whose currents reversed at  $-2 \pm 4$  mV ( $n = 6$  cells). Typical results are shown in Fig. 8. (The number of conductance and reversal potential measurements cited above are not equal since we did not obtain the resting membrane potential of all 13 cells.) Several patches exhibited activity of more than one channel, sometimes of both types. The 90 pS channel had a conductance and reversal potential similar to the 100 pS  $\text{K}^+$ -selective SAC found in tissue cultured chick heart cells (Ruknudin et al., 1993), but the 21 pS channel seemed quite distinct. This difference in channel populations may be due to a number of differences in the preparations including the difference in age of the embryos and the environment-attached vs. unattached, rounded vs. confluent, electrically uncoupled vs. coupled. The activity of both SACs in this preparation was completely blocked by  $30 \mu\text{M}$   $\text{Gd}^{3+}$  ( $n = 6$  for the 21 pS channel and  $n = 4$  for the 90 pS channel), and

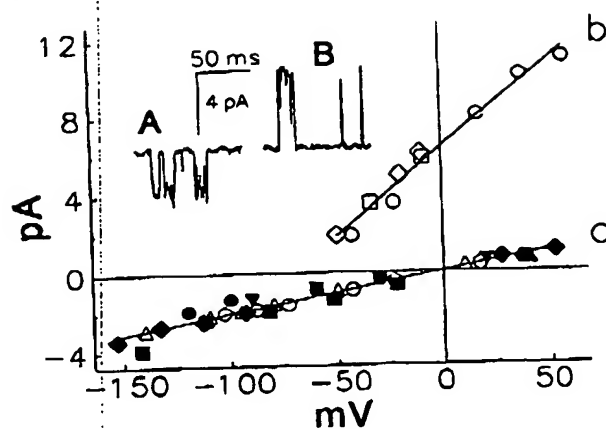


Fig. 8. Single-channel data and the  $I/V$  regression curves of the two observed types of SACs. Different symbols represent data from different patches. In one patch (circle), both types of SACs were present. Regression  $a$  gives a conductance  $\gamma = 21 \pm 0.9$  pS and a reversal potential  $V_r = -2.2 \pm 3.7$  mV ( $n = 6$  cells) regression  $b$  gives  $\gamma = 90 \pm 4.7$  pS and  $V_r = -70 \pm 5$  mV ( $n = 3$  cells). Bath and pipette: NS. Inset: representative currents of the 21 pS (A) and 90 pS (B) channels recorded with membrane potentials of  $-103$  mV and  $-20$  mV respectively.

1:1000 dilution of *Grammastola spatulata* spider venom ( $n = 3$  for both the 21 pS channel and the 90 pS channel). Since the reversal potential of the MSC fell between the reversal potentials of the two SACs, it appears that both are simultaneously activated in the whole-cell studies. The frequency of occurrence of the 21 pS channel was about three times that of the 90 pS channel.

The observation of MSCs and single SAC activity were highly correlated. In 7 out of 35 of the cell preparations we did not observe MSCs in any of the cells. Using three such preparations, we made 11 cell-attached patches and found no SAC activity. In contrast, using four preparations exhibiting MSCs, 16 out of 20 patches showed SAC activity. These results support the idea that MSCs are produced by SACs.

## Discussion

### PHYSIOLOGICAL CORRELATION OF MS CURRENTS

If SACs are active in these cells, they should be able to alter the action potentials. About  $1/3$  of quiescent cells could be mechanically stimulated to beat in NS bath solution at room temperature (21 out of 67 cells). However, in the presence of  $Gd^{3+}$  we observed no stimulated beating (0 out of 13), although there were spontaneously beating cells in the dishes. Consistent with these results, stretch has been shown to induce beating in the quiescent early embryonic chick heart in vivo (Rajala et al., 1977).

Because the traditional method of stimulating SACs

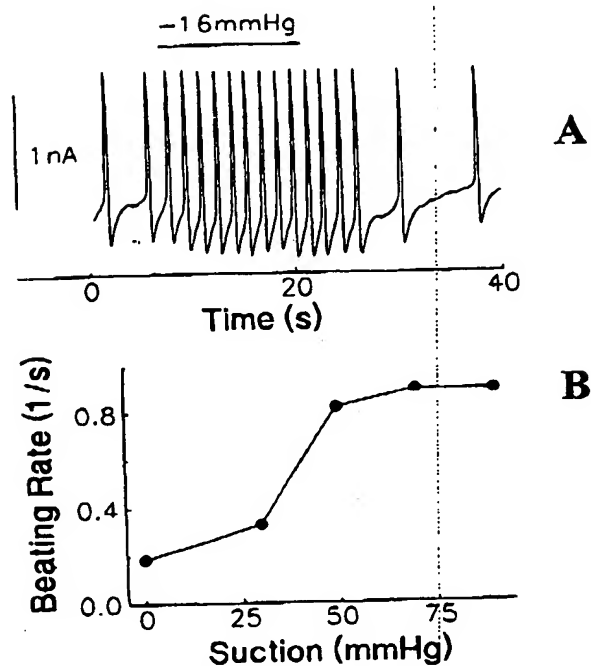


Fig. 9. Cell beating rate increased with suction in the loose-seal recording pipette (manual control of suction). (A) action current recording. (B) typical response of beating rate versus suction (different cell from panel A).

in tight-seal patch experiments is via pipette suction, we tested its effect on cell beating. To minimize changes in the cell structure associated with patching, we made loose seals (20–40 M $\Omega$ ) rather than tight seals. Applying suction to the recording pipette reversibly increased the cell beating rate (Fig. 9), though the sensitivity varied from cell to cell. We observed no significant differences when we used either NS or HK with or without  $Ca^{2+}$  in the pipette. These results suggest that it was not the specific ions but the currents injected into the cell that altered the cell beating rate.

### SMALL CURRENTS ARE REQUIRED TO ALTER BEATING RATES

To estimate how much current was needed to significantly alter the beating rate of a cell using a loose patch, we applied voltage to the pipette in voltage-clamp mode. The cell beating rate reversibly increased with positive pipette voltages. An increase of 5 mV elevated the beating rate by 15–50%. Assuming that the resistance of the membrane inside the pipette was  $\sim 10$  G $\Omega$  (the whole-cell resistance was  $\sim 1$  G $\Omega$ ), the injected current was  $< (5 \text{ mV}) / (10 \text{ G}\Omega) = 0.5 \text{ pA}$ . Thus, a current of  $\sim 0.5 \text{ pA}$  (equivalent to  $\sim 0.1 \text{ pA/pF}$ ) can significantly alter the cell beating rate. Given that the pacemaker potential has a

slope of  $-10$  mV/sec, the net current necessary to produce this slope in a  $5$  pF cell is  $I = 5 \text{ pF} \cdot 10 \text{ mV/sec} = 0.05 \text{ pA}$ . Thus,  $0.5 \text{ pA}$  is far in excess of that minimal required current.

To see what  $0.5 \text{ pA}$  means in terms of SAC activity, consider the following calculation. The cell has a resting potential of  $-70$  mV, close to the reversal potential of the  $90 \text{ pS}$  channel, so that when these channels open they will carry little current. For the  $21 \text{ pS}$  channel with a reversal potential of  $-0$  mV, if we assume that the area of the patch is  $\sim 20 \mu\text{m}^2$  (Sokabe, Sachs & Jing, 1991), the channel density is  $\sim 0.3/\mu\text{m}^2$  (Ruknudin et al., 1993), and let  $P_o$  be the probability of being open. Suction produces a current of

$$I_{MS} = 20(\mu\text{m}^2) \times 0.3(/\mu\text{m}^2) \times 21 \text{ (pS)} \\ \times 0.07 \text{ (V)} \times P_o = 8.8 P_o \text{ (pA).} \quad (4)$$

Thus,  $0.5 \text{ pA}$  requires a change of  $P_o$  of only  $\sim 6\%$ , a value readily consistent with SAC properties (Sachs, 1992).

#### COMPARING MSC AND VOLTAGE-SENSITIVE CURRENTS

The peak MSCs we observed ranged from  $60$ – $600 \text{ pS/pF}$ , with no attempt to saturate the system. To judge the significance of these currents relative to more familiar voltage-sensitive currents, we used standard step and ramp protocols. The peak  $\text{Na}^+$  and  $\text{Ca}^{2+}$  currents were  $\sim 500 \text{ pA/pF}$  and  $15 \text{ pA/pF}$  respectively, and the corresponding conductances were estimated as  $\sim 4,000 \text{ pS/pF}$  and  $150 \text{ pS/pF}$ . The inward rectifying  $\text{K}^+$  current was  $\sim 50 \text{ pA/pF}$  at  $-120$  mV membrane potential, indicating a conductance of  $\sim 1,500 \text{ pS/pF}$ . These currents are comparable to values reported by others in chick heart cells (Horres, Aiton & Lieberman, 1979; Clapham & Logothetis, 1988; Josephson & Sperelakis, 1992). Thus, the MSC conductance is smaller than the peak  $\text{Na}^+$  conductance but larger than the  $\text{Ca}^{2+}$  conductance, and comparable to the inward rectifying  $\text{K}^+$  (IRK) conductance, although it is much larger than IRK within the physiological potential range. The magnitude and reversal potential of the observed MSC current seem adequate to explain many of the observed effects of stretch on action potential properties in a variety of cardiac preparations (Sachs, 1994).

Although MSCs are somewhat labile, apparently varying with the preparation technique, they do not appear to be a selective property of damaged cells. Preparations that had MSCs had normal voltage-sensitive currents, however all preparations, including those without MSCs, exhibited voltage sensitive currents suggesting that they are more robust. This labile nature of mechanical responses has been seen before. In isolated heart cells, stretching was found to change the resting mem-

brane potential in some preparations but not in others (Lab, 1980; White et al., 1993). It is known that SAC responses are dependent upon stimulation history, probably as a result of alterations in the cytoskeleton (Hamill & McBride, Jr. 1992).

#### THE MSC IS NOT A LEAKAGE CURRENT

The current produced by mechanical deformation is not a leakage current, but is caused by specific ion channels. Fig. 2B and C illustrate that treatment with two very different reagents removes the MSCs. Also, some of our preparations had no MSCs while exhibiting normal voltage-gated currents. This conclusion is in agreement with the results of Sigurdson et al. (1992) that the mechanically-induced  $\text{Ca}^{2+}$  influx in heart cells was blocked by  $\text{Gd}^{3+}$  and the results of Morris and Horn (1991) that a variety of mechanical strains caused no change in the current of molluscan neurons.

#### INACTIVATION OF MECHANOSENSITIVE CURRENTS

Although we used a state model to describe the inactivation of the MSC, the actual origin of inactivation remains to be determined. It may result from different states of the channels (as we modeled it), relaxation of the cytoskeleton that alters the actual force applied to the channel (Pender & McCulloch, 1991; Sokabe et al., 1992), or inactivation of other conductances by second messengers (Wellner & Isenberg, 1995). Adaptation caused by a long lasting increase in  $\text{Ca}^{2+}/\text{K}^+$  conductance, as that observed by Wellner & Isenberg (1995), is unlikely since there was no outward current upon release of the stimulus.

Inactivation has been previously observed in single MS channels (Gustin et al., 1988; Stockbridge & French, 1988; Hamill & McBride, Jr. 1992; Bowman & Lohr, 1994; Chen, Guber & Plant, 1994). In *Xenopus* oocytes, inactivation was labile, only observed at negative membrane potentials (Hamill & McBride, Jr. 1992) and only when the gigaseal was formed using gentle suction. A different dynamic behavior, delayed activation, was observed in *Lymnaea*  $\text{K}^+$  selective SACs (Small & Morris, 1994). A delay of 1- to 4-sec was observed between the onset of the channel activity and the application of pressure jumps. Such delays were eliminated by cytochalasin D, or repeated mechanical stimuli suggesting involvement of the cytoskeleton. At present, we do not know why some cells inactivate and others do not, but macroscopic experiments have shown velocity sensitive effects on arrhythmia generation (Franz et al., 1992) but not on stretch induced potentials changes of the working myocardium (Stacy, Jr. et al., 1992). This result has been postulated to arise from a subpopulation of specialized cells.

## CONTRIBUTION OF BOTH SACs TO THE MSCs

If the MSC reported here was due to the activity of the two types of SACs observed in these cells, then it is possible to estimate the ratio of the probabilities of the channels being open. Since we found no consistent variation of the reversal potential with the amount of strain, it would appear that the channels are acted upon by proportional forces and the probabilities of being open are also in proportion. From the definition of the reversal potential of the MSC, the following equation holds,

$$(E_r - E_{90})g_{90}N_{90}(P_o)_{90} = (E_{21} - E_r)g_{21}N_{21}(P_o)_{21} \quad (5)$$

where,  $E_r$  is the reversal potential of the MSC,  $E_{90}$  and  $E_{21}$  are the reversal potentials of the 90 pS and the 21 pS SAC respectively,  $g_r$  are the conductance of the SACs,  $N_r$  the numbers of channels, and  $P_{or}$  the probabilities of the SACs being open. Using the observed  $N_{21}/N_{90} = 3$  as the occurrence ratio of the 21 pS channel over the 90 pS channel, we can get

$$\frac{(P_o)_{21}}{(P_o)_{90}} = 5.6 \quad (6)$$

This suggests that the 21 pS channel is open 5.6 times more often than the 90 pS channel. This is somewhat higher than the rough estimates of 1:1 we made from cell-attached patches, but more detailed studies are required to see whether this ratio is preserved in the patch. Given the large deformations involved in forming a patch (Milton & Caldwell, 1990) and the sensitivity of the kinetics to cytoskeletal alteration (Morris & Horn, 1991; Hamill & McBride, Jr. 1992; Small & Morris, 1994), such a ratio need not be preserved.

## ESTIMATING THE CORTICAL TENSION GENERATED BY THE MECHANICAL STIMULATION

The stresses produced by the stimulation are difficult to calculate in detail since both the constitutive properties of the structural elements and the detailed geometry of the strain are not known. However, if we use the common "liquid drop" model in which the cell is modeled as an elastic membrane covering a liquid core, we can make some estimates. Assuming that compression by the stimulation pipette transformed the spherical cell into an oblate of equivalent volume. The relative increase in area ( $A$ ) for such a process is

$$\frac{\Delta A}{A} = \frac{1}{2x} + \frac{x^2}{4R} \ln \frac{1+R}{1-R} - 1, \quad (7)$$

where  $R = \sqrt{1-x^2}$ ,  $x = b/r$ , and  $r$  is the radius of the

sphere and  $b$  is the semi minor-axis of the ellipsoid. The estimated area changes were <5%. Measurements of patch elasticity give values for the area elastic constant of the cell cortex in the range of 20–60 dyne/cm (Sokabe et al., 1991; Sigurdson & Sachs, 1994). These are probably upper limits since patches are normally under resting tension due to adhesion of the membrane to the walls of the pipette (Sokabe et al., 1991). For a change in area of 5%, these values would give a cortical mean tension of <1–3 dyne/cm. As shown by Sokabe et al. (1991), in patches the elasticity arises from stress in the cytoskeleton, not from the bilayer.

The above calculation assumes uniform deformation of an elastic membrane surrounding a liquid core. With an elastic core bound to the membrane, the stresses are bound to be different, but are difficult to estimate and it is unclear whether the true stresses are lower because of the sharing of elastic energy between the core and the cortex, or higher because of shear stresses near the stimulating pipette. The significance of local stresses was emphasized by Sigurdson et al. (1992) who showed that the  $Ca^{2+}$  influx arising from local mechanical stimulation occurs at the site of stimulation. To minimize the local strain, we used the side of the stimulation pipette rather than the tip to press against the cell.

Our results stand in sharp contrast to the negative results of Morris and Horn (1991) obtained on *Lymnaea* neurons, in which the inability to evoke significant MSCs were presented as evidence for the artifactual nature of single-channel MS activity and for the physiological irrelevance of SACs. Although it remains unclear under what conditions it is difficult to evoke MSCs, Morris and Horn's conclusion is clearly not general. MSCs evoked by direct mechanical stimulation have been recorded in several other preparations including vascular smooth muscle (Davis, Donovitz & Hood, 1992), guinea pig heart (Sasaki et al., 1992) and bladder smooth muscle (Wellner & Isenberg, 1994). Cloning of a SAC from *E. Coli* (Sukharev et al., 1994) should be convincing evidence for the non artifactual nature of SACs.

From this work paper, SACs would appear to be capable of physiologically significant activity in the heart. While the normal physiological function of the MSC is as yet unproved, we can speculate that it serves to adjust the pacemaker potential according to the degree of filling of the atria (accounting for the old observation by Bainbridge, 1915). In ventricular cells it may serve to improve the uniformity of contraction. Weaker cells, stretched during systole, could be encouraged to contract more strongly on subsequent beats by increasing  $Ca^{2+}$  entry through direct fluxes and  $Na^+/Ca^{2+}$  exchange.

We thank Drs. W. Sigurdson, C. Bowman, A. Auerbach and G.C.L. Bett for advice and criticism, and Ms. M. Teeling and R. Borschel for technical assistance. Supported by the American Heart Association-NY Affiliate, USARO and NIH (FS) and the Mark Diamond Research Fund of SUNY at Buffalo (HH).

Note: Some results have been published in abstract form (Hu & Sachs, 1994b; Hu & Sachs, 1994a; Hu & Sachs, 1995).

## References

- Ackerman, M.J., Wickman, K.D., Clapham, D.E. 1994. Hypotonicity activates a native chloride current in *Xenopus* oocytes. *J. Gen. Physiol.* 103:153-179
- Bainbridge, F.A. 1915. The influence of venous filling upon the rate of the heart. *J. Physiol.* 50:65-84
- Bowman, C.L., Lohr, J. 1994. Adaptation of mechanosensitive ion channels in C6 glioma cells. *Biophys. J.* 66:A169 (Abstr.)
- Bustamante, J.O., Ruknudin, A., Sachs, F. 1991. Stretch-activated channels in heart cells: Relevance to cardiac hypertrophy. *J. Cardiovasc. Pharmacol.* 17:S110-S113
- Chen, V., Guber, H.A., Palant, C.E. 1994. Mechanosensitive single channel calcium currents in rat mesangial cells. *Biochem. Biophys. Res. Comm.* 203:773-779
- Chen, Y., Simasko, S.M., Niggel, J., Sigurdson, W.J., Sachs, F. 1996.  $Ca^{2+}$  uptake in GH3 cells during hypotonic swelling: the sensory role of stretch-activated ion channels. *Am. J. Physiol.* 270:C1790-C1798
- Clapham, D.E., Logothetis, D.E. 1988. Delayed rectifier  $K^+$  current in embryonic chick heart ventricle. *Am. J. Physiol.* 254:H192-H197
- Craelius, W. 1993. Stretch-activation of rat cardiac myocytes. *Exp. Physiol.* 78:411-423
- Davis, M.J., Donovan, J.A., Hood, J.D. 1992. Stretch-activated single-channel and whole cell currents in vascular smooth muscle cells. *Am. J. Physiol.* 262:C1083-C1088
- Dean, J.W., Lub, M.J. 1989. Arrhythmia in heart failure: Role of mechanically induced changes in electrophysiology. *The Lancet* 1:1309-1312
- Franz, M.R., Burkhoff, D., Yeu, D.T., Sagawa, K. 1989. Mechanically induced action potential changes and arrhythmia in isolated and in situ canine hearts. *Cardiovas. Res.* 23:213-223
- Franz, M.R., Cima, R., Wang, D., Proffitt, D., Kurz, R. 1992. Electrophysiological effects of myocardial stretch and mechanical determinants of stretch-activated arrhythmias [published erratum appears in *Circ.* 86:1663 (1992)]. *Circ.* 86:968-978
- Guharay, F., Sachs, F. 1984. Stretch-activated single ion channel currents in tissue-cultured embryonic chick skeletal muscle. *J. Physiol.* 352:685-701
- Gustin, M.C., Zhou, X., Martinac, B., Kung, C. 1988. A mechanosensitive ion channel in the yeast plasma membrane. *Science* 242:762-766
- Hagiwara, N., Masuda, H., Shoda, M., Irisawa, H. 1992. Stretch-activated anion currents of rabbit cardiac myocytes. *J. Physiol.* 456:285-302
- Hamill, O.P., Marty, A., Neher, E., Sakmann, B., Sigworth, F.J. 1981. Improved patch-clamp techniques for high-resolution current recording from cells and cell-free membrane patches. *Pflügers Arch.* 391:85-100
- Hamill, O.P., McBride, D.W., Jr. 1992. Rapid adaptation of single mechanosensitive channels in *Xenopus* oocytes. *Proc. Natl. Acad. Sci. USA* 89:7462-7466
- Hansen, D.E., Craig, C.S., Hondeghem, L.M. 1990. Stretch-induced arrhythmias in the isolated canine ventricle. Evidence for the importance of mechanoelectrical feedback. *Circ.* 81:1094-1105
- Hansen, D.E., Borganelli, M., Stacy, G.P., Jr., Taylor, L.K. 1991. Dose-dependent inhibition of stretch-induced arrhythmias by gadolinium in isolated canine ventricles. Evidence for a unique mode of anti-arrhythmic action. *Circ. Res.* 69:820-831
- Horn, R., Marty, A. 1988. Muscarinic activation of ionic currents measured by a new whole-cell recording method. *J. Gen. Physiol.* 92:145-159
- Horres, C.R., Aiton, J.F., Lieberman, M. 1979. Potassium permeability of embryonic avian heart cells in tissue culture. *Am. J. Physiol.* 236(3):C163-C170
- Hu, H., Sachs, F. 1994a. Effects of mechanical stimulation on embryonic chick heart cells. *Biophys. J.* 66:A170
- Hu, H., Sachs, F. 1994b. Characterizing whole-cell mechanosensitive currents in chick heart. *The Physiologist* 37:49
- Hu, H., Sachs, F. 1995. Whole cell mechanosensitive currents in acutely isolated chick heart cells: correlation with mechanosensitive channels. *Biophys. J.* 68:A393
- Hu, H. 1996. Mechanically activated currents in chick heart cells. Thesis, SUNY Biophysical Sciences, Buffalo, NY
- Josephson, I.R., Sperelakis, N. 1990. Developmental increases in the inwardly-rectifying  $K^+$  current of embryonic chick ventricular myocytes. *Biochim. Biophys. Acta* 1052:123-127
- Josephson, I.R., Sperelakis, N. 1992. Kinetic and steady-state properties of  $Na^+$  channel and  $Ca^{2+}$  channel charge movements in ventricular myocytes of embryonic chick heart. *J. Gen. Physiol.* 100:195-216
- Kim, D. 1992. A mechanosensitive  $K^+$  channel in heart cells—activation by arachidonic acid. *J. Gen. Physiol.* 100:1021-1040
- Kim, D. 1993. Novel cation-selective mechanosensitive ion channel in the atrial cell membrane. *Circ. Res.* 72:225-231
- Kim, D., Fu, C. 1993. Activation of a nonselective cation channel by swelling in atrial cells. *J. Membrane Biol.* 135:27-37
- Kohl, P., Kamkin, A.G., Kiseleva, I.S., Streubel, T. 1992. Mechanosensitive cells in the atrium of frog heart. *Exp. Physiol.* 77:213-216
- Lab, M.J. 1980. Transient depolarization and action potential alterations following mechanical changes in isolated myocardium. *Cardiovas. Res.* 14:624-637
- Milton, R.L., Caldwell, J.H. 1990. How do patch clamp seals form? *Pflügers Arch.* 416:758-765
- Morris, C.E., Horn, R. 1991. Failure to elicit neuronal macroscopic mechanosensitive currents anticipated by single-channel studies. *Science* 251:1246-1249
- Naruse, K., Sokabe, M. 1993. Involvement of stretch activated (SA) ion channels in cardiovascular responses to mechanical stimuli. *Nippon. Rinsho.* 51:1891-1898
- Niggel, J., Hu, H., Sigurdson, W.J., Bowman, C., Sachs, F. 1996. *Grammostola spatulata* venom blocks mechanical transduction in GH3 neurons, *Xenopus* oocytes and chick heart cells. *Biophys. J.* 70:A347
- Oike, M., Droogmans, G., Nilius, B. 1994. The volume-activated chloride current in human endothelial cells depends on intracellular ATP. *Pflügers Arch.* 427:184-186
- Pender, N., McCulloch, C.A. 1991. Quantitation of actin polymerization in two human fibroblast sub-types responding to mechanical stretching. *J. Cell Sci.* 100:187-193
- Rajala, G.M., Kalbfleisch, J.H., Kaplan, S. 1976. Evidence that blood pressure controls heart rate in the chick embryo prior to neural control. *J. Embryol. Exp. Morphol.* 36:685-695
- Rajala, G.M., Pinter, M.J., Kaplan, S. 1977. Response of the quiescent heart tube to mechanical stretch in the intact chick embryo. *Dev. Biol.* 61:330-337
- Ruknudin, A., Sachs, F., Bustamante, J.O. 1993. Stretch-activated ion channels in tissue-cultured chick heart. *Am. J. Physiol.* 264:H960-H972
- Sachs, F. 1992. Stretch sensitive ion channels: an update. In: Sensory Transduction, D.P. Corey, and S.D. Roper, editors. pp. 241-260. Rockefeller Univ. Press, NY
- Sachs, F. 1994. Modeling mechanical-electrical transduction in the heart. In: Cell Mechanics and Cellular Engineering. V.C. Mow, F.

- Guliak, R. Tran-son-tray, R.M. Hochmuth, editors. pp. 308-328. Springer Verlag, New York
- Sada, H., Kojima, M., Sperelakis, N. 1988. Use of single heart cells from chick embryos for the  $\text{Na}^+$  current measurements. *Mol. Cell. Biochem.* 80:9-19
- Sasaki, N., Mitsuiye, T., Noma, A. 1992. Effects of mechanical stretch on membrane currents of single ventricular myocytes of guinea-pig heart. *Jpn. J. Physiol.* 42:957-970
- Sigurdson, W.J., Ruknudin, A., Sachs, F. 1992. Calcium imaging of mechanically induced fluxes in tissue-cultured chick heart: role of stretch-activated ion channels. *Am. J. Physiol.* 262:H1110-H1115
- Sigurdson, W.J., Sachs, F. 1994. Sarcolemmal mechanical properties in mouse myoblasts and muscle fibers. *Biophys. J.* 66:A171 (Abstr.)
- Small, D.L., Morris, C.E. 1994. Delayed activation of single mechanosensitive channels in *Lymnaea* neurons. *Am. J. Physiol.* 267:CS98-606
- Sokabe, M., Sachs, F., Jing, Z. 1991. Quantitative video microscopy of patch clamped membranes—stress, strain, capacitance and stretch channel activation. *Biophys. J.* 59:722-728
- Sokabe, M., Sigurdson, W.J., Sachs, F. 1992. Effects of excision and cytochalasin on the viscoelastic properties of patch clamped membranes in heart and skeletal muscle cells. *Biophys. J.* 61:A513 (Abstr.)
- Stacy, G.P., Jr., Jobe, R.L., Taylor, L.K., Hansen, D.E. 1992. Stretch-induced depolarizations as a trigger of arrhythmias in isolated canine left ventricles. *Am. J. Physiol.* 263:H613-H621
- Stockbridge, L.L., French, A.S. 1988. Stretch activated cation channels in human fibroblasts. *Biophys. J.* 54:187-190
- Stühmer, W., Roberts, W.M., Almers, W. 1983. The loose patch clamp. In: Single-Channel Recording, B. Sakmann, E. Neher, editors. pp. 123-132. Plenum Press, New York
- Sukharev, S.I., Blount, P., Martinac, B., Blattner, F.R., Kung, C. 1994. A large conductance mechanosensitive channel in *E. coli* encoded by *mscL* alone. *Nature* 368:265-268
- Tse, G.N. 1992. Cell swelling increases membrane conductance for canine cardiac cells: evidence for a volume-sensitive  $\text{Cl}^-$  channel. *Am. J. Physiol.* 262:C1056-1068
- Van Wagoner, D.R. 1993. Mechanosensitive gating of atrial ATP-sensitive potassium channels. *Circ. Res.* 72:973-983
- Wellner, M.C., Isenberg, G. 1994. Stretch effects on whole-cell currents of guinea-pig urinary bladder myocytes. *J. Physiol.* 480:439-448
- Wellner, M.C., Isenberg, G. 1995. cAMP accelerates the decay of stretch-activated inward currents in guinea-pig urinary bladder myocytes. *J. Physiol.* 482:141-156
- White, E., Le Guennec, J.Y., Nigretto, J.M., Gannier, F., Argibay, J.A., Garnier, D. 1993. The effects of increasing cell length on auxotonic contractions: membrane potential and intracellular calcium transients in single guinea-pig ventricular myocytes. *Exp. Physiol.* 78:65-78
- Yang, X.C. 1989. Characterization of stretch-activated ion channels in *Xenopus* oocytes. Ph. D. dissertation, Biophysical Sciences, SUNYAB
- Yang, X.C., Sachs, F. 1989. Block of stretch-activated ion channels in *Xenopus* oocytes by gadolinium and calcium ions. *Science* 243:1068-1071
- Yang, X.C., Sachs, F. 1990. Characterization of stretch-activated ion channels in *Xenopus* oocytes. *J. Physiol.* 431:103-122
- Zhang, J., Rasmusson, R.L., Hall, S.K., Lieberman, M. 1993. A chloride current associated with swelling of cultured chick heart cells. *J. Physiol.* 472:801-820
- Zhang, J., Hall, S.K., Lieberman, M. 1994. An early transient current activates the swelling-induced chloride conductance in cardiac myocytes. *Biophys. J.* 66:A442 (Abstr.)



## Topical Review

### Amiloride and Its Analogs as Tools in the Study of Ion Transport

Thomas R. Kleyman\* and Edward J. Cragoe, Jr.

Department of Medicine, Columbia University, New York, New York 10032, and Merck Sharp and Dohme Research Laboratories, West Point, Pennsylvania 19486

#### I. Introduction

The synthesis of amiloride and amiloride analogs was first described by Cragoe et al. in 1967 [21]. Amiloride was initially demonstrated to inhibit the  $\text{Na}^+$  channel present in urinary epithelia. Amiloride and its analogs were subsequently shown to inhibit other ion transport processes as well [3]. As more ion transport systems are studied, it becomes increasingly clear that amiloride analogs are "specific" inhibitors of relatively few ion transporters. They inhibit a large number of membrane transport processes and enzymes. They have also been shown to interact with specific drug and hormone receptors and to inhibit cellular metabolism and DNA, RNA, and protein synthesis. This review addresses the structure-activity relationships of amiloride and its analogs on the large number of ion transporters and other cellular processes that are inhibited by amiloride, and examines the use of these drugs as probes for the characterization of transport proteins.

#### II. Pharmacology of Inhibition of Ion Transporters, Enzymes, and Receptors by Amiloride and Amiloride Analogs

The structure of amiloride is shown in Fig. 1. Amiloride is pyrazinoylguanidine bearing amino groups on the 3- and 5-positions and a chloro group on the

6-position of the pyrazine ring. Approximately one thousand analogs have been synthesized [19], and representative members have been examined for their inhibitory activity on the  $\text{Na}^+$  channel,  $\text{Na}^+/\text{H}^+$  exchanger, and the  $\text{Na}^+/\text{Ca}^{2+}$  exchanger. Amiloride analogs that have been thoroughly studied are listed in Tables 1-7, along with their effects on inhibition of  $\text{Na}^+$  transport in these systems. This section reviews the structure-activity relationships for amiloride and its analogs on ion transport systems, enzymes, drug and hormone receptors, DNA, RNA, and protein synthesis, and cellular metabolism.

##### A. EPITHELIAL $\text{Na}^+$ CHANNEL

High resistance (or "tight") epithelia that transport  $\text{Na}^+$  have been found to possess  $\text{Na}^+$  channels which are functionally restricted to the apical plasma membrane.  $\text{Na}^+$  crosses the apical membrane by passive diffusion through this channel, and is actively extruded from the cell by a  $\text{Na}^+/\text{K}^+$ -ATPase present on the basolateral plasma membrane. The diuretic amiloride, at a concentration less than  $10^{-6}$  M, inhibits  $\text{Na}^+$  transport when added to the solution bathing the apical plasma membrane. The inhibition is rapidly reversed by removing amiloride from the apical solution. Addition of a low concentration of amiloride to the solution bathing the basolateral plasma membrane has no effect on  $\text{Na}^+$  transport [8, 72]. Subsequent observations of single-channel recording using the patch-clamp technique have shown that amiloride reduces the mean open time of the  $\text{Na}^+$  channel, but has no effect on single-channel conductance [36, 65].

A large number of amiloride analogs have been synthesized, and the effect of many of these analogs

**Key Words** amiloride · amiloride analogs · ion transport ·  $\text{Na}$  channel ·  $\text{Na}/\text{H}$  exchanger ·  $\text{Na}/\text{Ca}$  exchanger

\* Present address: Renal and Electrolyte Section, Department of Medicine, University of Pennsylvania, 3400 Spruce Street, Philadelphia, PA 19104.

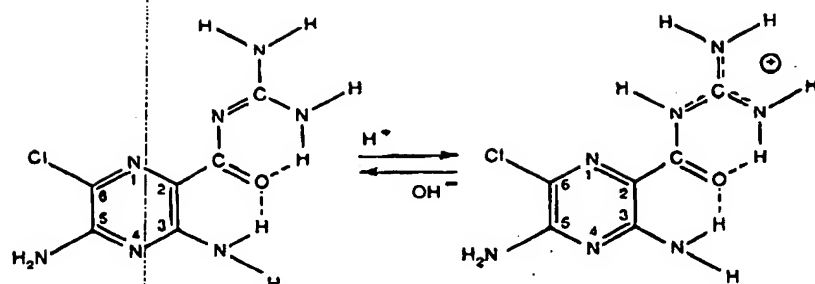
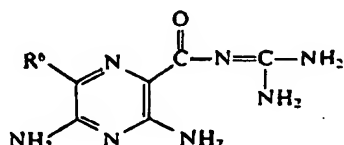


Fig. 1. Ground state structure of amiloride in the unprotonated and protonated form

Table 1.



No.	R <sup>o</sup>	IC <sub>50</sub> (μM) for amiloride and potency relative to amiloride		
		Na <sup>+</sup> channel <sup>a</sup>	Na <sup>+</sup> /H <sup>+</sup> antiporter <sup>b</sup>	Na <sup>+</sup> /Ca <sup>2+</sup> exchanger <sup>c</sup>
1	Cl— (Amiloride)	(0.34) 1 (0.35)* 1*	(83.8) 1	(1100) 1
2	H—	0.006	0.08	1
3	F—	0.085	0.12	0.1
4	Br—	1	1.9	1
5	I—	0.14	4.6	1

Evaluated by the method of (a) Cuthbert et al., *Br. J. Pharmacol.* 261:2839 (1978), or \*Verrey et al., *J. Cell Biol.* 104:1231 (1987). (b) Simchowicz et al., *Mol. Pharmacol.* 30:112 (1986). (c) Kaczorowski et al., *Biochemistry*, 24:1394 (1985).

on Na<sup>+</sup> transport across tight epithelia has been studied. The most thorough studies have involved use of frog skin or toad urinary bladder as model "tight" epithelia, monitoring transepithelial Na<sup>+</sup> transport electrically as short-circuit current (*I*<sub>sc</sub>) with tissue mounted in an Ussing chamber. The concentration of an amiloride analog required to achieve 50% inhibition of *I*<sub>sc</sub> (the IC<sub>50</sub>) was used as a measure of its apparent affinity for the Na<sup>+</sup> channel. This measurement is dependent on a number of variables including:

**a. Extracellular Na<sup>+</sup> Concentration.** Lowering the Na<sup>+</sup> concentration of the solution bathing the apical membrane of tight epithelia results in a decrease in Na<sup>+</sup> transport. In addition, as the Na<sup>+</sup> concentration is lowered, the IC<sub>50</sub> for inhibition of Na<sup>+</sup> transport by amiloride decreases [27].

**b. Extracellular pH.** Amiloride is a weak base (pK<sub>a</sub> = 8.7 in 30% ethanol, 8.8 in H<sub>2</sub>O) (see Table 8) and interacts only in its protonated form with the Na<sup>+</sup> channel to inhibit *I*<sub>sc</sub> [7, 23]. As the pH of a solution

increases, the fraction of amiloride in the protonated form will decrease.

**c. Intracellular Accumulation of Amiloride.** The unprotonated form of amiloride and many of its analogs are quite lipid soluble. They may bind to and easily cross cell membranes, accumulate within cells, and alter a number of cellular processes (see below).

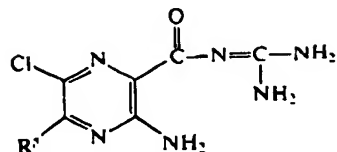
**d. Apical Plasma Membrane Potential.** The extent of inhibition of the channel by amiloride has been shown to be dependent on the apical plasma membrane potential. It is the charged form of amiloride that interacts with the channel in a manner sensitive to the membrane potential [36, 64].

#### 1. Structure-Activity Relationships for Amiloride and Its Analogs with the Na<sup>+</sup> Channel

The effects of modification of the structure of amiloride on the inhibition of the Na<sup>+</sup> channel are sum-

T.R. Kleyman and E.J. Cragoc, Jr.: Amiloride and Its Analogs

Table 2.








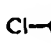
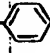
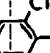
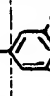
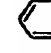
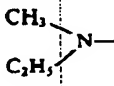
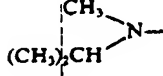
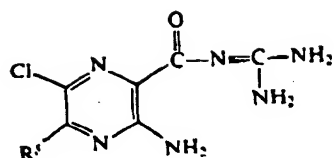
No.	R <sup>a</sup>	IC <sub>50</sub> (μM) for amiloride and potency relative to amiloride					
		Na <sup>+</sup> - channel <sup>b</sup>	Na <sup>+</sup> /H <sup>+</sup> antiporter				Na <sup>+</sup> /Ca <sup>2+</sup> - exchanger <sup>c</sup>
			b	c	d	e	
1	H <sub>2</sub> N—(amiloride)	(0.34) 1 (0.35)* 1*	(83.8)	(7) 1	(3) 1	(4) 1	(1100) 1
6	H—	<0.035*	0.5				1.5
7	C <sub>2</sub> H <sub>5</sub> NH—	0.0003	7.4	1.8		1.5	
8	CH <sub>3</sub> (CH <sub>2</sub> ) <sub>2</sub> NH—	0.0004		2.3		2	
9	 NH—	0.002	6.3				
10	CH <sub>2</sub> =CHCH <sub>2</sub> NH—	0.0001	7.4				
11	(CH <sub>3</sub> ) <sub>3</sub> CNH—	<0.035*	26				11
12	CH <sub>3</sub> (CH <sub>2</sub> ) <sub>3</sub> NH—		26				
13	 NH—		5.1				54
14	HOCH <sub>2</sub> (CHOH) <sub>4</sub> CH <sub>2</sub> NH—	<0.035*	13	0.7			<0.5
15	(CH <sub>3</sub> ) <sub>2</sub> N(CH <sub>2</sub> ) <sub>2</sub> NH—		0.6				
16	H <sub>2</sub> NCH <sub>2</sub> C(CH <sub>3</sub> ) <sub>2</sub> CH <sub>2</sub> NH—		4.1				
17	   H <sub>2</sub> N—C=N—		3.6	3.5			
18	 CH <sub>2</sub> NH—	<0.035*	6.6	3.5			45
19	 CH <sub>2</sub> NH—		9	1.4			50
20	 CH <sub>2</sub> NH—		10				55
21	CH <sub>3</sub> —  CH <sub>2</sub> NH—	<0.0035*	9.6	0.35	1.6		55
22	Cl—  CH <sub>2</sub> NH—						115
23	CH <sub>3</sub> —  CH <sub>2</sub> NH—		3.3				50
24	 NH—		22		20	67	
25	(CH <sub>3</sub> ) <sub>2</sub> N—	<0.035*	12	23	20	24	2
26		0.0005	133	35			
27		0.0005	349	35	50	13	

Table 2 continued next page

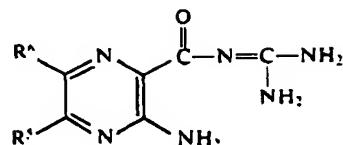
Table 2. (continued)



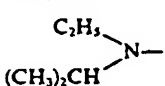


No.	R <sup>6</sup>	IC <sub>50</sub> (μM) for amiloride and potency relative to amiloride				
		Na <sup>+</sup> channel <sup>a</sup>	Na <sup>+</sup> /H <sup>+</sup> antiporter			Na <sup>+</sup> /Ca <sup>2+</sup> exchanger <sup>f</sup>
			b	c	d	e
28			123	7		13
29			349	14		
30			190			8.5
31		<0.035*	223	140		8.5
32			102			
33		<0.035*	524			11
34			226			55
35			29			75
36			61			75
37		<0.035*	125			60
38			13	0.4		
39			8.7	3.5		
40		<0.035*	62			0.7

Evaluated by the method of (a) Cuthbert et al., *Br. J. Pharmacol.* 261:2839 (1978), or \*Verrey et al., *J. Cell Biol.* 104:1231 (1987). (b) Simchowicz et al., *Mol. Pharmacol.* 30:112 (1986). (c) Vigne et al., *Mol. Pharmacol.* 25:131 (1985). (d) L'Allemain et al., *J. Biol. Chem.* 259:4313 (1984). (e) Zhuang et al., *Biochemistry* 23:4481 (1984). (f) Kaczorowski et al., *Biochemistry*, 24:1394 (1985).

Table 3.



No.	R <sup>4</sup>	R <sup>5</sup>	IC <sub>50</sub> (μM) for amiloride and potency relative to amiloride		
			Na <sup>+</sup> channel <sup>a</sup>	Na <sup>+</sup> /H <sup>+</sup> antiporter <sup>b</sup>	Na <sup>+</sup> /Ca <sup>2+</sup> exchanger <sup>c</sup>
1	Cl—	H <sub>2</sub> N—(amiloride)	(0.34) 1 (0.35)* 1*	(83.8)	(1100)
41	H—	H—	<0.035*	0.08	0.08
42	Cl— 	H—		21.2	
43	H—	(CH <sub>3</sub> ) <sub>2</sub> CNH—		1.7	
44	Br—	H—	0.4	1	0.15
45	Br—	 N—		566	
46	I—	(CH <sub>3</sub> ) <sub>2</sub> N—		68	
47	I—			313	1.2

Evaluated by the method of (a) Cuthbert et al., *Br. J. Pharmacol.* 261:2839 (1978), or \*Verrey et al., *J. Cell Biol.* 104:1231 (1987). (b) Simchowicz et al., *Mol. Pharmacol.* 30:112 (1986). (c) Kaczorowski et al., *Biochemistry*, 24:1394 (1985).

marized. These are grouped according to the structural changes at various sites in the molecule (see Tables 1–7).

**a. 2-Carbonylguanidino Substituents.** Substitution of hydrophobic groups on the terminal nitrogen atom of the guanidino moiety has produced a number of analogs with markedly enhanced IC<sub>50</sub> values [26]. Several of these analogs appear to have the highest affinity and specificity for the Na<sup>+</sup> channel. These include the benzyl (No. 54, benzamil) and substituted benzyl analogs (Nos. 55–66), phenyl (No. 76, phenamil), phenethyl (No. 71) and substituted phenyl (No. 77) and phenethyl (No. 72) analogs, as well as straight and branched chain alkyl groups (Nos. 48 and 49). This increase in the potency has been shown to be due to changes in both the on- and off- rate constants of these amiloride analogs [56].

The introduction of two hydrophobic groups on a single terminal guanidino nitrogen atom has not been studied extensively. Two alkyl substituents on a single terminal guanidino nitrogen atom (Nos. 78 and 79) increases activity. However, a methyl and a benzyl group (No. 80) located in this position decreases activity by an order of magnitude.

The carbonylguanidino moiety of amiloride is required for inhibition of the Na<sup>+</sup> channel. Replacement of the imidocarbonyl group of the guanidino moiety with C=S (No. 84) or deletion of the guanidino moiety and replacement with HO— (No. 85) results in a loss of activity. The insertion of a NH group between the carbonyl group and guanidino moiety of amiloride (No. 83) results in a 40% decrease in activity.

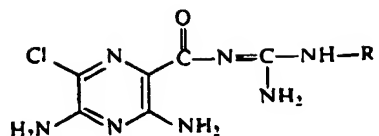
**b. 5-Position Substituents.** An unsubstituted 5-amino group is required for optimal inhibition of the Na<sup>+</sup> channel. Amiloride analogs bearing one or two substituents on the 5-amino nitrogen atom exhibit substantial loss in activity. This is true whether one or both substituents are alkyl (Nos. 7, 8, 11, 25–27, 31), substituted alkyl (Nos. 14, 40), cycloalkyl (Nos. 9, 33), or aralkyl (Nos. 18, 21, 37). Analogs where the amino group has been replaced with H— (No. 6), alkoxy (i.e., CH<sub>3</sub>O—, C<sub>2</sub>H<sub>5</sub>O—), HS—, CH<sub>3</sub>S—, HO—, or Cl— have a substantial loss of activity, as measured by saluretic and antika-liuretic activity in whole animal studies [19, 20].

**c. 6-Position Substituents.** Optimal activity is observed when the 6-position is occupied by a chloro

6

T.R. Kleyman and E.J. Cragoe, Jr.: Amiloride and Its Analogs

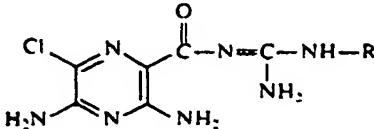
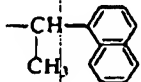
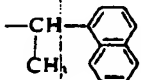
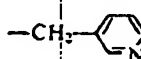
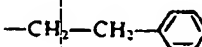
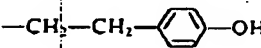
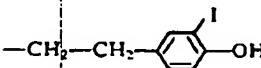
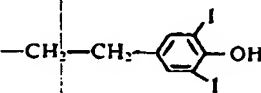
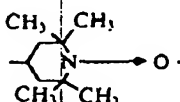

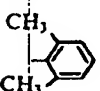
Table 4.



No.	-R	IC <sub>50</sub> (μM) for amiloride and potency relative to amiloride		
		Na <sup>+</sup> channel <sup>a</sup>	Na <sup>+</sup> /H <sup>+</sup> antiporter <sup>b</sup>	Na <sup>+</sup> /Ca <sup>2+</sup> exchanger <sup>c</sup>
1	-H (amiloride)	(0.34) 1 (0.35)* 1	(83.8) 1	(1100) 1
48	-C(CH <sub>3</sub> ) <sub>2</sub> CH <sub>2</sub> C(CH <sub>3</sub> ) <sub>3</sub>	13	<0.08	7.9
49	-(CH <sub>2</sub> ) <sub>11</sub> CH <sub>3</sub>	2*		9
50	-CH <sub>2</sub> CH <sub>2</sub> OH	3		<0.5
51	-CH <sub>2</sub> CF <sub>3</sub>	1		1
52	-(CH <sub>2</sub> ) <sub>3</sub> COOH	0.6*		0.5
53	-(CH <sub>2</sub> ) <sub>3</sub> COOC <sub>2</sub> H <sub>5</sub>	2*		<4
54	-CH <sub>2</sub> -	9	<0.08	11
55	-CH <sub>2</sub> -	10		11
56	-CH <sub>2</sub> -	13		55
57	-CH <sub>2</sub> -	9		15
58	-CH <sub>2</sub> -	2.5	<1	92
59	-CH <sub>2</sub> -	4		37
60	-CH <sub>2</sub> -	47*		75
61	-CH <sub>2</sub> -	13		16
62	-CH <sub>2</sub> -	4		110
63	-CH <sub>2</sub> -			42
64	-CH <sub>2</sub> -	10		8.5
65	-CH <sub>2</sub> -	7*		28
66	-CH-() <sub>2</sub>	18*		115
67	-CH <sub>2</sub> -	4		31



Table 4. (continued)

Table 4. (continued)				
No.	—R	IC <sub>50</sub> (μM) for amiloride and potency relative to amiloride		
		Na <sup>+</sup> channel <sup>a</sup>	Na <sup>+</sup> /H <sup>+</sup> antiporter <sup>b</sup>	Na <sup>+</sup> /Ca <sup>2+</sup> exchanger <sup>c</sup>
68	 R(+)			94
69	 S(-)			94
70		1.2		1
71		13	<0.008	12
72		18 <sup>a</sup>		1
73				16
74				6
75		1.6		
76		17	<0.008	5.5
77		23		7.3

Evaluated by the method of (a) Cuthbert et al., *Br. J. Pharmacol.* 261:2839 (1978), or \*Verrey et al., *J. Cell Biol.* 104:1231 (1987). (b) Simchowicz et al., *Mol. Pharmacol.* 30:112 (1986). (c) Kaczorowski et al., *Biochemistry*, 24:1394 (1985).

(No. 1), amiloride) or bromo (No. 4) group. The 6-iodo (No. 5), 6-fluoro (No. 3), and the 6-H compounds (No. 2) are 7-, 12-, and 170-fold less potent than amiloride, respectively. The decrease in the IC<sub>50</sub> is due to an increase in the off-rate constant [55]. Analogs with replacement of the halogen by CH<sub>3</sub>O—, C<sub>6</sub>H<sub>5</sub>S—, and CN— have significant loss of activity, as measured in whole animal studies [19, 20].

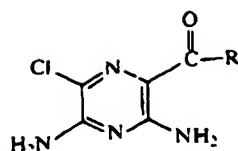
**d. Replacement of the Pyrazine Nucleus.** Replacement of the pyrazine ring with a hydrophobic moiety results in a loss of activity (Nos. 89 and 91).

**e. 3-Position Substituents.** The effect of substitutions at this site on inhibition of the Na<sup>+</sup> channel have received limited study. Replacement of the 3-amino group with H— results in substantial loss of activity [19, 20].

## 2. Specificity of Amiloride and Its Analogs for the Na<sup>+</sup> Channel

The Na<sup>+</sup> channel is the only ion transporter inhibited by amiloride with an IC<sub>50</sub> of less than 1 μM. In the presence of a physiologic Na<sup>+</sup> concentration, the IC<sub>50</sub> for inhibition of Na<sup>+</sup> transport is in the

Table 5.



No.	—R	IC <sub>50</sub> (μM) for amiloride and potency relative to amiloride		
		Na <sup>+</sup> channel <sup>a</sup>	Na <sup>+</sup> /H <sup>+</sup> antiporter <sup>b</sup>	Na <sup>+</sup> /Ca <sup>2+</sup> exchanger <sup>c</sup>
	—N=C—NH <sub>2</sub> (amiloride)	(0.34) 1		
1		(0.35)* 1*	(83.8) 1	(1100) 1
78	—N=C—N(C <sub>2</sub> H <sub>5</sub> ) <sub>2</sub>   NH <sub>2</sub>	3		<0.5
79	—N=C—N[(CH <sub>2</sub> ) <sub>3</sub> CH <sub>3</sub> ] <sub>2</sub>   NH <sub>2</sub>	3		3.3
80		0.1		7.3
81	—N=C—N=C—N(CH <sub>3</sub> ) <sub>2</sub>            NH <sub>2</sub> NHCH <sub>3</sub>	0.12		<0.08
82				2.2
83	—NHN=C—NH <sub>2</sub>   NH <sub>2</sub>	0.6	<0.08	<0.08
84	—NH—C—NH <sub>2</sub>    S	0.001	<0.08	
85	—OH	<0.035		<0.08

Evaluated by the method of (a) Cuthbert et al., *Br. J. Pharmacol.* 261:2839 (1978), or \*Verrey et al., *J. Cell Biol.* 104:1231 (1987). (b) Simchowicz et al., *Mol. Pharmacol.* 30:112 (1986). (c) Kaczorowski et al., *Biochemistry*, 24:1394 (1985).

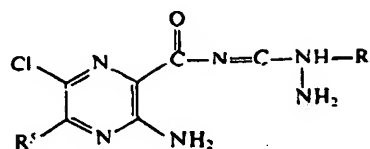
range of 0.1 to 0.5 μM. The IC<sub>50</sub> obtained from studies of different transport processes are difficult to compare, since the interaction of amiloride with the various Na<sup>+</sup> transporters may be effected by a number of variables including extracellular pH and [Na<sup>+</sup>], and the apical transmembrane potential. The IC<sub>50</sub> for Na<sup>+</sup>/H<sup>+</sup> exchange is as low as 3 μM when measured in the presence of a low external [Na<sup>+</sup>] [50] but as high as 1 mM in the presence of a high [Na<sup>+</sup>]. Amiloride is a weak inhibitor of the Na<sup>+</sup>/Ca<sup>2+</sup> exchanger, with an IC<sub>50</sub> of 1 mM.

The most specific inhibitors of the epithelial

Na<sup>+</sup> channel are amiloride analogs bearing hydrophobic substituents on the terminal nitrogen atom of the guanidino moiety. The benzyl and phenyl analogs have been most extensively studied. These analogs inhibit *I<sub>sc</sub>* with IC<sub>50</sub> of approximately 10 nM. This is more than three orders of magnitude lower than that reported for inhibition of Na<sup>+</sup>/H<sup>+</sup> and Na<sup>+</sup>/Ca<sup>2+</sup> exchangers, Na<sup>+</sup>/K<sup>+</sup>-ATPase, and Na<sup>+</sup>-glucose and Na<sup>+</sup>-alanine cotransporters (see below). The effect of these analogs on protein kinases has not been reported.

Several amiloride analogs have proved useful in

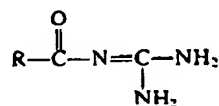
Table 6.



No.	R'	-R	IC <sub>50</sub> (μM) for amiloride and potency relative to amiloride		
			Na <sup>+</sup> channel <sup>a</sup>	Na <sup>+</sup> /H <sup>+</sup> antiporter <sup>b</sup>	Na <sup>+</sup> /Ca <sup>2+</sup> exchanger <sup>c</sup>
1	H <sub>2</sub> N—(amiloride)	—H	(0.34) 1 (0.35)* 1*	(83.8) 1	(1100) 1
86	CH <sub>3</sub> (CH <sub>2</sub> ) <sub>2</sub> CH <sub>3</sub> (CH <sub>2</sub> ) <sub>3</sub> \ N—	—CH <sub>2</sub> —			300
87		—CH <sub>2</sub> —	<0.035*		150

Evaluated by the method of (a) Cuthbert et al., *Br. J. Pharmacol.* 261:2839 (1978), or \*Verrey et al., *J. Cell Biol.* 104:1231 (1987). (b) Simchowicz et al., *Mol. Pharmacol.* 30:112 (1986). (c) Kaczorowski et al., *Biochemistry*, 24:1394 (1985).

Table 7.



No.	R—	IC <sub>50</sub> (μM) for amiloride and potency relative to amiloride		
		Na <sup>+</sup> channel <sup>a</sup>	Na <sup>+</sup> /H <sup>+</sup> antiporter <sup>b</sup>	Na <sup>+</sup> /Ca <sup>2+</sup> exchanger <sup>c</sup>
1	(amiloride)	(0.34) 1 (0.35)* 1*	(83.8) 1	(1100) 1
88			1	<0.1
89		<0.035*	1.2	11
90			11	<0.1
91		<0.035*	23	11

Evaluated by the method of (a) Cuthbert et al., *Br. J. Pharmacol.* 261:2839 (1978), or \*Verrey et al., *J. Cell Biol.* 104:1231 (1987). (b) Simchowicz et al., *Mol. Pharmacol.* 30:112 (1986). (c) Kaczorowski et al., *Biochemistry*, 24:1394 (1985).

Table 8.  $pK_a$  and lipophilicity data

Compound number	$pK_a^a$	Lipophilicity <sup>b</sup>	Compound number	$pK_a^a$	Lipophilicity <sup>b</sup>
		1			
1	8.7	5 <sup>c</sup>	49		99.4
2	9.2	1	50	8.5	2 <sup>c</sup>
3	8.9	7	54	8.1	56
4	8.6	8 <sup>c</sup>	56	7.4	98
5	8.8	10	59	7.63	>99.8
6	7.0	2 <sup>c</sup>	62	7.45	99
10	8.8	4 <sup>c</sup>	70	4.4	47
14	8.9	0.4	71	8.2	90
15	7.8	0.7	75	7.4	99
	9.2				
21	9.0	93	76	7.8	98.7
25	8.8	6	77	7.5	99.5
30	8.1	94	78	7.6	78
33	8.5	93	81	10.5	4
37	3.68	99.5	83	9.0	1 <sup>c</sup>
	8.30				
40	6.4	6			
	9.2				

<sup>a</sup> Determined as the half neutralization point in water containing 30% ethanol.

<sup>b</sup> Percent distributed in octanol or (c) chloroform when equilibrated between equal volumes of the solvent and pH 7.4 aqueous phosphate buffer (0.1 M).

biochemical characterization of the  $Na^+$  channel. Tritiated benzamil, phenamil, and 6-bromomethylamiloride (where the methyl group is located on the amide nitrogen atom) have been used to study binding of amiloride analogs to channel containing membranes [2, 25, 46, 71]. The binding of radiolabeled amiloride analogs has recently been used to follow the channel during solubilization and purification [2, 5]. Photoactive analogs of benzamil (6-bromobenzamil and the benzamil derivative No. 65) and 6-bromomethylamiloride have been used to identify components of the  $Na^+$  channel [6, 44, 46] (see section III.C). A spin-labeled analog (No. 75) has recently been used as a probe for the  $Na^+$  channel [18].

Finally, it has been observed that it is difficult to reverse the inhibition of  $Na^+$  transport due to phenamil by removing phenamil from the solution bathing the apical plasma membrane of frog skin or toad urinary bladder [34]. This may be due to hydrophobic interactions of the drug with the channel. Studies with [ $^3H$ ]phenamil show clearly that the drug is not binding covalently to the channel [2].

#### B. $Na^+/H^+$ ANTIporter

A plasma membrane transporter that exchanges  $Na^+$  for  $H^+$  in an electroneutral fashion has been described in cells and plasma membranes derived from a variety of species [74]. This exchanger appears to be involved in regulation of intracellular pH and may provide a major pathway for  $Na^+$  entry into specific cells. Amiloride inhibition of the  $Na^+/H^+$  exchanger was first described in 1976 [40], and has been used subsequently as an inhibitor not only of  $Na^+/H^+$  exchange, but of subsequent events that might be altered through regulation of this transporter. The effects of a large number of amiloride analogs on  $Na^+/H^+$  exchange have been studied in a number of different cell types including Chinese hamster lung fibroblasts [50], human fibroblasts [62], the epidermoid cell line A431 [86], chick skeletal muscle cells [82], human neutrophils [75], and the pig kidney epithelial cell line LLC-PK [35]. The inhibition of  $Na^+/H^+$  exchange by amiloride analogs has also been studied in rabbit renal microvillus membrane vesicles [51].

The methods used for measurement of  $\text{Na}^+/\text{H}^+$  exchange are numerous and are described in detail elsewhere [35, 50, 51, 62, 75, 82, 86]. A number of factors may influence the inhibition of transport by amiloride and its analogs, including:

*a. Extracellular pH.* Amiloride and its analogs inhibit the  $\text{Na}^+/\text{H}^+$  exchanger in the protonated form [50]. Therefore, the pH of the extracellular (or extravesicular) solution must be well below the  $\text{pK}_a$  of the amiloride analog (see Table 8).

*b. Collapse of pH Gradient.* Amiloride and a large number of its analogs (in particular, a number of analogs that have been shown to be potent inhibitors of  $\text{Na}^+/\text{H}^+$  exchange) bear hydrophobic substituents and are quite lipophilic, especially when the analogs are unprotonated. These amiloride analogs are permeable weak bases, and may accumulate in acidic compartments and collapse a pH gradient across plasma membranes, organelles, or membrane vesicles (see below). We<sup>1</sup> and others [31] have observed that amiloride and several of its analogs will collapse a pH gradient across membrane vesicles. This is dependent, at least in part, upon the hydrophobicity of the amiloride analog.

*c. Intracellular Accumulation of Amiloride.* Amiloride has been shown to accumulate within cells. This may potentially influence inhibition of  $\text{Na}^+/\text{H}^+$  exchange by a number of mechanisms, such as inhibition of intracellular proteins (such as protein kinases) which may be involved in the regulation of  $\text{Na}^+/\text{H}^+$  exchange [61, 70], or through increasing intracellular pH which may inactivate the  $\text{Na}^+/\text{H}^+$  exchanger [1]. The  $\text{Na}^+/\text{H}^+$  exchanger is regulated by intracellular pH. Lowering intracellular (or intravesicular) pH activates the exchanger by increasing its affinity for internal  $\text{H}^+$  without changing the  $K_m$  for external  $\text{Na}^+$  or  $K_i$  for amiloride [66, 67]. Among several cell lines that have been studied, either an increase in  $V_{\max}$  [12, 83] or no change in  $V_{\max}$  has been observed [66, 67] following a decrease in intracellular pH.

*d. Extracellular  $\text{Na}^+$  Concentration.* The extracellular (or extravesicular)  $\text{Na}^+$  concentration has been shown to effect the interaction of amiloride analogs with the  $\text{Na}^+/\text{H}^+$  exchanger. Increasing the extracellular (or extravesicular)  $\text{Na}^+$  concentration decreases the apparent affinity of amiloride analogs for the  $\text{Na}^+/\text{H}^+$  exchanger. In addition, amiloride increases the  $K_m$  for  $\text{Na}^+$  without changing the  $V_{\max}$ .

Amiloride analogs and  $\text{Na}^+$  share a common binding site on the  $\text{Na}^+/\text{H}^+$  exchanger [43]. In addition, amiloride has been shown to inhibit the  $\text{Na}^+/\text{H}^+$  exchanger by binding to a second site which is independent of the  $\text{Na}^+$  binding site [39].

*e. Extracellular anions.* Studies with brush border membrane vesicles derived from rabbit kidney cortex have demonstrated that the  $\text{IC}_{50}$  of amiloride for the  $\text{Na}^+/\text{H}^+$  exchanger is reduced in the presence of a gluconate containing buffer when compared with a chloride containing buffer [84].

### 1. Structure-Activity Relationships for Amiloride Analogs with the $\text{Na}^+/\text{H}^+$ Exchanger

A large number of amiloride analogs have been used to inhibit  $\text{Na}^+/\text{H}^+$  exchange in different cell types and in membrane vesicles by a variety of methods. A consensus on the structural modifications that enhance the affinity of amiloride analogs for the  $\text{Na}^+/\text{H}^+$  exchanger is apparent from these studies, although the absolute  $K_i$  varies, in part dependent upon the method used to study  $\text{Na}^+/\text{H}^+$  exchange. It is clear that the most potent and specific inhibitors of the  $\text{Na}^+/\text{H}^+$  exchanger are amiloride analogs with hydrophobic groups on the 5-amino nitrogen atom. A representative list of amiloride analogs that have been studied appears in Tables 1-7. General observations on the effect of these amiloride analogs on  $\text{Na}^+/\text{H}^+$  exchange are discussed in relation to changes at various sites on the pyrazine ring utilizing data obtained in studies of the human neutrophil  $\text{Na}^+/\text{H}^+$  exchanger [75]. The  $\text{IC}_{50}$  for inhibition of the exchanger by amiloride is  $84 \mu\text{M}$  in human neutrophils, and as low as 3 to  $7 \mu\text{M}$  in other tissues. This variation is likely due, in part, to differences in the concentration of  $\text{Na}^+$  used in the assay. The  $\text{IC}_{50}$  for inhibition of  $\text{Na}^+/\text{H}^+$  exchange, relative to the  $\text{IC}_{50}$  for inhibition by amiloride are, in general, similar among the various cells studied.

*a. 5-Position Substituents.* The most potent inhibitors of  $\text{Na}^+/\text{H}^+$  exchange are amiloride analogs in which the 5-amino nitrogen atom bears one or two substituents. Two substituents are generally superior to one and the substituents are generally hydrophobic in nature. However, some hydrophilic groups (e.g. polyhydroxyalkyl) and basic moieties capable of protonation at a second site in the molecule (e.g. aminoalkyl (No. 14), guanidino (No. 17) and guanidinoacylalkyl (No. 40)) confer considerable activity to the molecule. In several cell lines, the most potent compounds in this class exhibit  $\text{IC}_{50}$  values for inhibition of  $\text{Na}^+/\text{H}^+$  exchange below 100 nM.

<sup>1</sup> Kaczorowski, G., Garcia, M., Kleyman, T., and Cragoe, E.J., Jr. (unpublished observations).

The generalities summarized above are illustrated in Table 2. Among the more potent analogs which have received a considerable amount of study in a variety of tissues are the 5-(N-methyl-N-isopropyl) (No. 27), the 5-(N-methyl-N-isobutyl) (No. 30), the 5-(N-ethyl-N-isopropyl) (No. 31), the 5-(N,N-hexamethylene) (No. 33) and the 5-(N,N-dimethyl) (No. 25) analogs of amiloride which exhibit 10- to 500-fold greater potency than amiloride.

The 5-H analog of amiloride (No. 6) is only half as potent as amiloride itself, indicating that an unsubstituted 5-amino group does not confer much of an enhancing effect on the molecule.

**b. 6-Position Substituents.** The 6-Br (No. 4) and 6-I (No. 5) are, respectively, two- and fivefold more potent than amiloride, whereas the 6-H (No. 2) and 6-F (No. 3) analogs of amiloride are, respectively, 13- and eightfold less potent.

**c. 2-Carbonylguanidino Substituents.** The carbonylguanidino moiety is required for activity. When this group is replaced by the carbonylaminoguanidino (No. 83) or the carbonylthioureido (No. 84) group, activity is lost. Substitution on the terminal guanidino nitrogen atom with hydrophobic groups such as alkyl (No. 48), benzyl (No. 54), substituted benzyl (No. 58), phenethyl (No. 71) or phenyl (No. 76) decreases activity.

**d. 5- and 6-Position Substituents.** The 5-H, 6-H compound (No. 41) is a poor inhibitor of  $\text{Na}^+/\text{H}^+$  exchange, as is the 5- $\text{NH}_2$ , 6-H compound (No. 2). The 5-H, 6-*p*-chlorophenyl analog (No. 42) is 21-fold more potent than amiloride. The 5-(N,N-dimethyl)-6-I (No. 46) is approximately fivefold more potent than its 6-Cl counterpart (No. 25), just as 6-I amiloride (No. 5) is fivefold more potent than amiloride (No. 1).

**e. Replacement of the Pyrazine Ring.** Compounds have been synthesized with cyclic or heterocyclic groups in place of the substituted pyrazine ring. Several of these compounds are more potent than amiloride in inhibiting the  $\text{Na}^+/\text{H}^+$  exchanger. Replacement of the 3,5-diamino-6-chloropyrazinyl moiety by 2-anthraquinonyl (No. 90) or 1-(4-chlorophenyl)2-propenyl (No. 91) produced compounds 11- and 23-fold more active, respectively, than amiloride. Replacement by 2-(4-pyridyl) ethenyl (No. 88) or diphenylmethyl (No. 89) provided compounds as active as amiloride.

**f. 3-Position Substituents.** The effect on the  $\text{Na}^+/\text{H}^+$  exchanger of amiloride analogs with substitutions at this site has not been studied.

## 2. Specificity of Amiloride and Its Analogs for Inhibition of the $\text{Na}^+/\text{H}^+$ Exchanger

Amiloride analogs bearing hydrophobic substituents on the 5-amino group of the pyrazine ring have both the highest activity and specificity for the  $\text{Na}^+/\text{H}^+$  exchanger. When studied in the presence of a low  $[\text{Na}^+]$ ,  $\text{IC}_{50} < 100 \text{ nM}$  have been observed for a number of amiloride analogs. This is 100-fold less than the  $\text{IC}_{50}$  observed with these analogs for inhibition of the epithelial  $\text{Na}^+$  channel [26],  $\text{Na}^+/\text{Ca}^{2+}$  exchanger [41],  $\text{Na}^+/\text{K}^+$ -ATPase [86], and  $\text{Na}^+$ -D-glucose cotransporter [16].

The effect of amiloride analogs on protein kinases has not been extensively studied. Amiloride and 5-(N,N-dimethyl)amiloride are 9 and 100 times more potent, respectively, in inhibiting  $\text{Na}^+/\text{H}^+$  exchange than in inhibiting protein kinase C [9]. Amiloride has also been shown to inhibit a number of other kinases with  $\text{IC}_{50}$  similar to that reported for protein kinase C [29]. Amiloride inhibits adenylate cyclase with an  $\text{IC}_{50}$  similar to the  $\text{IC}_{50}$  for inhibition of  $\text{Na}^+/\text{H}^+$  exchange [58]. The effect of 5-amino substituted amiloride analogs on adenylate cyclase has not been examined.

## C. $\text{Na}^+/\text{Ca}^{2+}$ EXCHANGER

Changes in the intracellular  $[\text{Ca}^{2+}]$  have been shown to mediate a variety of cellular processes. The intracellular  $[\text{Ca}^{2+}]$  is tightly regulated in eukaryotic cells by a variety of mechanisms, including transport of  $\text{Ca}^{2+}$  across plasma membranes, transport across membranes surrounding intracellular organelles, and binding to negatively charged groups. The  $\text{Na}^+/\text{Ca}^{2+}$  exchanger is a major mechanism of transport of  $\text{Ca}^{2+}$  across plasma membranes [52] and has been described in a variety of cell types, including electrically excitable cells such as giant squid axon, cardiac muscle, skeletal muscle, and pituitary cells. The exchanger has also been found in both leaky and tight epithelia, and in erythrocytes.

The  $\text{Na}^+/\text{Ca}^{2+}$  exchanger is a reversible electrogenic transporter that exchanges 3  $\text{Na}^+$  ions for each  $\text{Ca}^{2+}$  ion. Amiloride is a poor inhibitor of the  $\text{Na}^+/\text{Ca}^{2+}$  exchanger, with an  $\text{IC}_{50}$  of approximately 1 mM [41]. It is a reversible inhibitor of the exchanger and the inhibition is competitive with respect to  $\text{Na}^+$ . Amiloride interacts with more than one  $\text{Na}^+$  binding site on the transporter [41]. Amiloride analogs have been shown to block  $\text{Na}^+/\text{Ca}^{2+}$  exchange in intact cardiac myocytes [11, 42]. The pharmacology of amiloride inhibition of the  $\text{Na}^+/\text{Ca}^{2+}$  exchanger has been studied by measuring the inhibition of  $\text{Na}^+$  or  $\text{Ca}^{2+}$  fluxes across membrane vesicles. As with other amiloride-sensitive trans-



porters, the  $IC_{50}$  is dependent on the extracellular (or extravesicular)  $Na^+$  concentration, and it is the protonated form of the drug which interacts with the exchanger [41, 73].

### 1. Structure-Function Relationships for Amiloride and Its Analogs with the $Na^+/Ca^{2+}$ Exchanger

**a. 2-Carbonylguanidino moiety.** The introduction of hydrophobic groups on the terminal guanidino nitrogen atom (Nos. 48 and 49) increases the activity over that of amiloride. A benzyl substituent (No. 54) increases activity by an order of magnitude. Appropriate substitution of the benzyl group further enhances activity. The 2'-Cl (No. 56), 2',4'-Cl<sub>2</sub> (No. 58), 3',4'-Cl<sub>2</sub> (No. 59), 2',6'-Cl<sub>2</sub> (No. 60), and the 2',4'-(CH<sub>3</sub>)<sub>2</sub> (No. 62) analogs are between 40- to 110-fold more active than amiloride. Addition of phenyl to the methylene portion of the benzyl group (No. 66) enhances the activity of benzamil (No. 54) by another order of magnitude. The 2-phenethyl compound (No. 71) is as potent as benzamil (No. 54). The phenyl (No. 76, phenamil) and 2,6-dimethylphenyl (No. 77) substituents are, respectively, 5- to 7- fold more active than amiloride. The introduction of two small alkyl groups (No. 78) on a terminal guanidino nitrogen atom decreases activity; however, two large alkyl groups (No. 79) slightly enhances activity.

The guanidino moiety is required for inhibition of the exchanger. Analogs with substitution of the guanidino moiety with an aminoguanidino group (No. 83) or deletion of the guanidino moiety and replacement with HO— (No. 85) are inactive.

**b. 5-Amino Substituents.** Amiloride analogs with hydrophobic substituents on the 5-amino moiety have enhanced activity against the  $Na^+/Ca^{2+}$  exchanger. The introduction of adamantyl (No. 13), benzyl (No. 18), substituted benzyl (Nos. 19–23), dialkyl (No. 34), or an alkyl and a substituted benzyl (No. 35–37) are between 50- to 115- fold more potent than amiloride.

**c. 6-Position Substituents.** Replacement of the 6-Cl group of amiloride by H (No. 2), Br (No. 4) or I (No. 5) does not alter activity. However, the 6-F (No. 3) compound is an order of magnitude less active.

**d. 5-Position and Terminal Guanidino Substituents.** Introduction of a substituted benzyl group on the terminal guanidino nitrogen atom and a substituted benzyl group (No. 87) or two alkyl groups (No. 86) on the 5-amino nitrogen atom produced compounds 150- to 300-fold more potent than amiloride. This

structural maneuver enhances activity against the  $Na^+/Ca^{2+}$  exchanger, but markedly diminishes activity against the  $Na^+$  channel.

**e. Replacement of the Pyrazine Ring.** As seen with the  $Na^+/H^+$  exchanger, the replacement of the 3,5-diamino-6-chloropyrazinyl moiety by certain other groups can be accomplished and still achieve enhancement of  $Na^+/Ca^{2+}$  exchange inhibitory activity over that observed with amiloride. The diphenylmethyl and 2-(4-chlorophenyl)propenyl substituted analogs (Nos. 89 and 91) are 11-fold more active than amiloride. The 2-(4-pyridyl)ethenyl (No. 88) and the 2-anthraquinolyl (No. 90) analogs are inactive against the  $Na^+/Ca^{2+}$  exchanger, but maintain or enhance activity against the  $Na^+/H^+$  exchanger.

**f. 5- and 6-Position Substituents.** Replacement of the 5- and 6-substituents of amiloride by H— (No. 41) results in a profound decrease in activity. Replacing the 6-Cl group of 5-(N-ethyl-N-isopropyl) amiloride (No. 31) by 6-I (No. 47) decreases activity.

**g. 3-Position substituents.** The effect of amiloride analogs with substitutions at this site on the  $Na^+/Ca^{2+}$  exchanger has not been studied.

### 2. Specificity of Amiloride Analogs for Inhibition of the $Na^+/Ca^{2+}$ Exchanger

Relatively high concentrations of amiloride are required to inhibit the  $Na^+/Ca^{2+}$  exchanger. Although proper substituents on either the 5-amino or the terminal guanidino nitrogen atoms increase the activity of these analogs by up to 100-fold, the  $IC_{50}$  is only in the range of 10  $\mu M$ . This is a considerably greater concentration than is required for inhibition of a number of other transporters, such as the epithelial  $Na^+$  channel and the  $Na^+/H^+$  exchanger. It is important to note that of the amiloride analogs examined, those active against the  $Na^+/Ca^{2+}$  exchanger are equal or more potent inhibitors of the  $Ca^{2+}$  channel (Nos. 1, 25, 30, 31, 54, 59, 76)<sup>2</sup> [11].

Amiloride analogs bearing substituents on both the 5-amino and terminal guanidino nitrogen atoms have increased activity for the exchanger, with  $IC_{50}$  of 3.5 to 7  $\mu M$ . These analogs do not inhibit the  $Na^+$  channel at this concentration and therefore do show some specificity for the  $Na^+/Ca^{2+}$  exchanger. However, the effects of these analogs on other transport

<sup>2</sup> Kaczorowski, G., and Garcia, M. (unpublished observations).

systems and on kinases has not been examined. Also these compounds are quite hydrophobic and are difficult to use at concentrations above 10  $\mu\text{M}$ .

#### D. $\text{Na}^+/\text{K}^+$ -ATPASE

The  $\text{Na}^+/\text{K}^+$ -ATPase is present in many eukaryotic cells, transporting  $\text{Na}^+$  out of and  $\text{K}^+$  into cells creating transcellular chemical gradients for both  $\text{Na}^+$  and  $\text{K}^+$ . The  $\text{Na}^+/\text{K}^+$ -ATPase is inhibited by cardiac glycosides and is also inhibited by amiloride. The inhibition of the  $\text{Na}^+/\text{K}^+$ -ATPase by amiloride has been studied by a number of investigators using intact cells, membrane vesicles, and partially purified pump [37, 69, 78, 86]. It is unclear if amiloride interacts with the pump by binding to a  $\text{Na}^+$  binding site, an ATP binding site, or by an alternative mechanism. It is also unclear if amiloride binds to an extracellular or intracellular site on the protein.

The pharmacology of amiloride inhibition of the pump has been characterized most extensively using partially purified pump from dog kidney. The  $\text{IC}_{50}$  for inhibition of ATPase activity by amiloride is greater than 3 mM. Appropriate substitution of the 5-amino moiety of amiloride decreases the  $\text{IC}_{50}$  to as low as 200  $\mu\text{M}$  [86]. 5-(N,N-Dimethyl)amiloride inhibits the pump with an  $\text{IC}_{50}$  of 3 mM, which is four orders of magnitude greater than the  $\text{IC}_{50}$  for inhibition of  $\text{Na}^+/\text{H}^+$  exchanger [86]. The effect of introduction of substituents on the terminal nitrogen atom of the guanidino moiety has not been studied except for benzamil, which has an  $\text{IC}_{50}$  less than 1 mM when studied in membrane vesicles from rabbit kidney [37].

#### E. $\text{Na}^+$ -COUPLED SOLUTE TRANSPORT

The transport of a number of solutes across the apical plasma membrane of epithelia has been shown to be tightly coupled to  $\text{Na}^+$ . The  $\text{Na}^+$ -D-glucose,  $\text{Na}^+$ -L-alanine, and  $\text{Na}^+$ - $\text{PO}_4^{3-}$  transporters are inhibited by amiloride at concentrations greater than 1 mM [16, 37]. The interaction of amiloride with the  $\text{Na}^+$ -D-glucose transporter has been studied in brush border membrane vesicles from rabbit kidney cortex and in LLC-PK1/CL4 cells, a cell line with transport characteristics resembling renal proximal tubular cells. The  $\text{IC}_{50}$  of amiloride is 2 mM [37]. The inhibition is binding to a  $\text{Na}^+$  binding site on the transporter [16, 37]. Amiloride is also a competitive inhibitor of  $\text{Na}^+$ -dependent [ $^3\text{H}$ ]phlorizin binding [37]. This transporter is inhibited by amiloride analogs bearing hydrophobic substituents on the 5-amino moiety (Nos. 30, 31) or on terminal nitrogen of the guanidino moiety (Nos. 59, 76) with  $\text{IC}_{50}$  be-

T.R. Kleyman and E.J. Cragoe, Jr.: Amiloride and Its Analogs

tween 0.1 and 0.3 mM [16], when assayed in the presence of a low concentration of  $\text{Na}^+$ .

$\text{Na}^+$ -dependent L-alanine and  $\text{PO}_4^{3-}$  transporters are inhibited by amiloride at concentrations greater than 1 mM. Introduction of hydrophobic groups on the 5-amino moiety or the terminal nitrogen atom of the guanidino moiety slightly decreases the  $\text{IC}_{50}$  [37].

#### F. OTHER ION TRANSPORTERS

*a. Voltage-Gated  $\text{Na}^+$  Channel.* A voltage-gated  $\text{Na}^+$ -selective ion channel is present in electrically excitable cells and is inhibited specifically by the toxins tetrodotoxin and saxitoxin in the nanomolar range. It has recently been shown that amiloride inhibits this channel in both synaptosomes and heart membrane vesicles, as measured by inhibition of veratridine-activated  $^{22}\text{Na}^+$  flux across membrane vesicles [80]. The  $\text{IC}_{50}$  for inhibition of the  $^{22}\text{Na}^+$  flux by amiloride is 600  $\mu\text{M}$ . Amiloride analogs bearing hydrophobic substituents on the 5-amino moiety or the terminal nitrogen of the guanidino moiety have lower  $\text{IC}_{50}$  (6  $\mu\text{M}$  for 5-(N-ethyl-N-isopropyl)amiloride (No. 31) and 37  $\mu\text{M}$  for benzamil (No. 54)). It is unknown if varying the  $\text{Na}^+$  concentration used in the assay affects the  $\text{IC}_{50}$ . Amiloride and analogs with hydrophobic substituents on the 5-amino moiety or on the terminal nitrogen atom of the guanidino moiety inhibit the binding of [ $^3\text{H}$ ]batrachotoxin-A 20- $\alpha$ -benzoate and [ $^3\text{H}$ ]tetracaine to the channel [80].

*b. Voltage-Gated  $\text{Ca}^{2+}$  Channel.* The voltage-gated  $\text{Ca}^{2+}$  channel in sarcolemma vesicles from pig heart is inhibited by amiloride with an  $\text{IC}_{50}$  of 90  $\mu\text{M}$ . Amiloride analogs bearing hydrophobic substituents on the 5-amino moiety or the terminal nitrogen of the guanidino moiety (Nos. 25, 30, 31, 54, 59, 76) are between five- to 75-fold more active than amiloride.<sup>3</sup> Amiloride analogs bind to a cation binding site in the pore of the  $\text{Ca}^{2+}$  channel and allosterically alter binding of dihydropyridines, aralkylamines and benzothiazepines [33]. Electrophysiologic studies with intact frog atrial myocytes have shown that the amiloride 3',4'-dichlorobenzamil (No. 59) inhibits the voltage-gated  $\text{Ca}^{2+}$  channel with an  $\text{IC}_{50}$  of 0.8  $\mu\text{M}$  and is a more potent inhibitor of the  $\text{Ca}^{2+}$  channel than of the  $\text{Na}^+/\text{Ca}^{2+}$  exchanger [11].

*c.  $\text{K}^+$  channel.* Electrophysiologic studies with intact frog atria myocytes suggest that 3',4'-dichloro-

<sup>3</sup> Kaczorowski, G., and Garcia, M. (unpublished observations).

T.R. Kleyman and E.J. Cragoe, Jr.: Amiloride and Its Analogs

15

benzamil (No. 59) inhibits the delayed rectifier  $K^+$  channel with 30 to 40% inhibition of the  $K^+$  current at a concentration of  $5 \mu M$  [11].

*d. Nicotinic Acetylcholine Receptor.* Amiloride has been observed to inhibit the nicotinic acetylcholine receptor isolated from *Torpedo*<sup>a</sup>. The  $IC_{50}$  is approximately  $100 \mu M$ .

## G. ENZYMES AND RECEPTORS

*a. Protein Kinases.* Phosphorylation of cellular proteins by protein kinases has been shown to be involved in the regulation of a variety of cellular processes including metabolism, transport, growth and differentiation. Amiloride has been shown to inhibit a number of protein kinases, including types I and II cAMP-dependent protein kinase [68], protein kinase C [9], and protein kinase activity associated with the insulin receptor, epidermal growth factor (EGF) receptor, and the platelet-derived growth factor receptor [29]. The  $IC_{50}$  for inhibition of EGF receptor protein kinase is  $350 \mu M$ . The inhibition is competitive with ATP, suggesting that amiloride binds to an ATP binding site on the enzyme. Amiloride is a noncompetitive inhibitor of substrate (histone) phosphorylation [29]. Both amiloride and 5-(N,N-dimethyl)amiloride inhibit purified protein kinase C with  $IC_{50}$  of approximately  $1 \text{ mM}$  [9]. Amiloride inhibits types I and II cAMP-dependent protein kinases with an  $IC_{50}$  of approximately  $1 \text{ mM}$  [68]. The interaction of other amiloride analogs with protein kinases has not been studied.

*b. Adenylate Cyclase.* Amiloride inhibits protein kinases through competition with ATP for an ATP binding site, and therefore might inhibit other ATP-dependent processes. Adenylate cyclase catalyzes the conversion of ATP to cAMP. The generation of cAMP in fish erythrocytes is inhibited by amiloride in a dose-dependent manner, with an  $IC_{50}$  of  $6 \mu M$  [58]. The effect of amiloride analogs in this system have not been examined.

*c. Monoamine Oxidase.* Amiloride is a comparative inhibitor of monoamine oxidase activity measured in rat brain homogenate [63].

*d. Acetylcholinesterase.* Amiloride is a noncompetitive inhibitor of acetylcholinesterase, with an  $IC_{50}$  in the range of 20 to  $60 \mu M$  [28].

*e. Urokinase-Type Plasminogen Activator.* Amiloride inhibits urokinase-type plasminogen activator

with an  $IC_{50}$  of  $7 \mu M$  [79]. Amiloride does not inhibit tissue-type plasminogen activator, plasma kallikrein, or thrombin.

*f. Renal Kinins.* Amiloride is a noncompetitive inhibitor of rat and human renal kallikrein, with an  $IC_{50}$  in the 85 to  $230 \mu M$  range [59].

*g. Muscarinic Acetylcholine Receptor.* Amiloride has been shown to inhibit the muscarinic acetylcholine receptor. Studies with rabbit pancreatic acini have shown that amiloride inhibits amylase secretion induced by carbachol with an  $IC_{50}$  of  $40 \mu M$ ,  $^{45}Ca^{2+}$  efflux induced by carbachol with an  $IC_{50}$  of  $80 \mu M$ , and is a competitive inhibitor of [ $^3H$ ]quinuclidinyl benzylate binding to the muscarinic acetylcholine receptor [49].

*h. Alpha and Beta Adrenergic Receptors.* Amiloride is a competitive inhibitor of [ $^3H$ ]prazosin binding to  $\alpha_1$  receptors in membrane vesicles from rat renal cortex or bovine carotid artery with an  $IC_{50}$  of 24 to  $33 \mu M$  [10, 38]. Amiloride is also a competitive inhibitor of [ $^3H$ ]rauwolfscine binding to  $\alpha_2$  receptors and [ $^{125}I$ ]iodocyanopindolol binding to beta adrenergic receptors in rat renal cortical membranes with  $IC_{50}$  of 14 and  $84 \mu M$ , respectively [38]. Both benzamil and 5-(N-ethyl-N-isopropyl)-amiloride are between two- to 25-fold more potent than amiloride in inhibiting specific ligand binding to  $\alpha_1$ ,  $\alpha_2$ , and beta adrenergic receptors. Amiloride blocks both veratridine and norepinephrine-stimulated smooth muscle contraction. The inhibition of smooth muscle contraction by amiloride may be due to inhibition of the  $\alpha_1$  adrenergic receptor or due to inhibition of a number of other cellular processes [10].

*i. Atrial Natriuretic Factor (ANF) Receptor.* ANF is a peptide hormone secreted by atrial myocytes and binds to specific cell surface receptors. Recent studies have shown that ANF binds to both low and high affinity receptors, and that amiloride ( $100 \mu M$ ) increases the number of high affinity sites in membranes obtained from adrenal zona glomerulosa [60]. This change in the number of binding sites is associated with a conformational change in the 15,000-Da receptor, as shown by a change in the elution profile on steric exclusion chromatography [60].

## H. OTHER CELLULAR EFFECTS

*a. DNA and RNA Synthesis.* Cells grown in the absence of growth factors may arrest in G0. Addition of serum or defined growth factors stimulates

<sup>a</sup> Karlin, A. (personal communication).

DNA, RNA, and protein synthesis. In intact cells, addition of amiloride inhibits the growth factor-induced DNA, RNA, and protein synthesis [48, 50]. The effect of amiloride on protein synthesis is a direct effect (*see below*). The effect of amiloride on DNA and RNA synthesis may be indirect. Lowering the extracellular  $\text{Na}^+$  concentration inhibits DNA and RNA synthesis, suggesting that entry of  $\text{Na}^+$  into cells may be a requirement for these events. Amiloride analogs inhibit DNA replication with  $\text{IC}_{50}$  similar to that observed for inhibition of  $\text{Na}^+/\text{H}^+$  exchanger [50], suggesting that amiloride inhibition of DNA synthesis is indirect, possibly through inhibition of  $\text{Na}^+/\text{H}^+$  exchange.

Amiloride also blocks RNA synthesis, as measured by incorporation of [ $^3\text{H}$ ]uridine into RNA. Following stimulation of cells with growth factors, two peaks of incorporation of [ $^3\text{H}$ ]uridine into RNA are observed. Amiloride abolishes the late peak of [ $^3\text{H}$ ]uridine incorporation, while only slightly decreasing the initial peak [48]. It is unknown if this is direct or an indirect effect of amiloride. The effect of amiloride analogs on RNA synthesis has not been examined.

**b. Protein Synthesis.** In both intact cells and cell free reticulocyte lysate, amiloride inhibits protein synthesis as measured by incorporation of radiolabeled amino acids into proteins [48, 54, 57, 86]. The  $\text{IC}_{50}$  for inhibition of protein synthesis in reticulocyte lysate is approximately 300 to 400  $\mu\text{M}$  [54, 57, 86]. Amiloride inhibits protein synthesis in intact cells with an  $\text{IC}_{50}$  between 100 and 400  $\mu\text{M}$ , and varies with the cell type studied. Fibroblasts (Swiss 3T3 cells ( $\text{IC}_{50} = 100 \mu\text{M}$ ) [57] are more sensitive than hepatocytes and A431 cells ( $\text{IC}_{50} = 400 \mu\text{M}$ ) [54, 57, 86]. Amiloride both lowers the initial rate of incorporation of [ $^3\text{S}$ ]methionine into proteins and the plateau levels of [ $^3\text{S}$ ]methionine labeled proteins [54]. The  $\text{IC}_{50}$  for inhibition of synthesis of albumin in hepatocytes is 30  $\mu\text{M}$ , and is 14-fold more sensitive to amiloride inhibition than is the rate of overall protein synthesis, suggesting that the  $\text{IC}_{50}$  for inhibition of synthesis of individual proteins may vary [54]. The effect of amiloride analogs on the inhibition of protein synthesis has been studied. In cell free systems, amiloride analogs bearing hydrophobic substituents on the 5-amino moiety showed little variation in their  $\text{IC}_{50}$  for inhibition of protein synthesis. However, when protein synthesis was studied in intact cells, the  $\text{IC}_{50}$  of these analogs varies over 25-fold. The rank order of inhibition of protein synthesis by these amiloride analogs correlated with the rank order of decreasing Rb content of cells, although the absolute  $\text{IC}_{50}$  was 5–7 times higher for inhibition of protein synthesis.

These data suggest that amiloride analogs may inhibit protein synthesis in intact cells indirectly through inhibition of ion transport or metabolism [86]. The mechanism by which amiloride directly inhibits protein syntheses in cell free systems is unclear. As protein synthesis requires ATP, amiloride inhibition may be occurring through competition with ATP and inhibition of ATP-dependent enzymes.

**c. Metabolism.** It has been recently demonstrated that amiloride analogs deplete intracellular levels of ATP [77, 86]. Addition of analogs with substituents on the 5-amino moiety (at concentrations  $>30 \mu\text{M}$ ) to A431 cells or to proximal tubular cells in suspension results in a fall in the intracellular levels of ATP, whereas addition of either amiloride or 5-(N,N-dimethyl)amiloride (A431 cells) at concentrations of 2 mM had no effect [86].

The depletion of intracellular ATP levels may be due in part to inhibition of oxidative phosphorylation. The consumption of  $\text{O}_2$  in renal proximal tubular cells is tightly coupled to the rate of ion transport. Addition of carbonyl cyanide *p*-trifluoromethoxyphenylhydrazone (FCCP) uncouples  $\text{O}_2$  consumption from ion transport. Amiloride analogs bearing hydrophobic substituents on the 5-amino moiety inhibit  $\text{O}_2$  consumption in FCCP-treated renal proximal tubular cells in suspension with  $\text{IC}_{50}$  of 250 to 500  $\mu\text{M}$ . The  $\text{IC}_{50}$  of amiloride is greater than 1 mM. These data suggest that amiloride analogs have a direct effect on oxidative phosphorylation, independent of their effects on ion transport [77].

### III. Use of Amiloride Analogs of Probes for Characterizing Transport Proteins

#### A. RADIOLABELED AMILORIDE ANALOGS

**a. Amiloride.** [ $^{14}\text{C}$ ]Amiloride has been synthesized with a specific activity of 54 mCi/mmol by the reaction of [ $^{14}\text{C}$ ]guanidine with methyl 3,5-diamino-6-chloropyrazinecarboxylate [21]. [ $^3\text{H}$ ]Amiloride has not been synthesized, as all of amiloride's protons are freely exchangeable.

**b. Amiloride Analogs Bearing Substituents on the 2-Carbonylguanidino Moiety.** A number of tritium-labeled amiloride analogs have been synthesized, including [ $^3\text{H}$ -phenyl]phenamil, [ $^3\text{H}$ -benzyl]benzamil [24], and [ $^3\text{H}$ -benzyl]6-bromobenzamil, with specific activities between 2 and 21 Ci/mmol. These analogs have been synthesized by the reaction of synthon I (*see* Fig. 2) 1-methyl-2-(3,5-diamino-6-

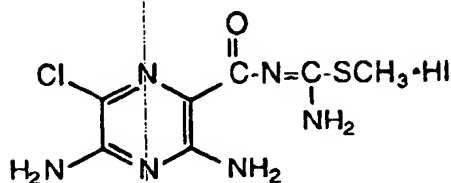


Fig. 2. Synthon for the synthesis of amiloride analogs bearing substituents on the terminal guanidino nitrogen atom

chloropyrazinoyl)pseudothiuronium iodide or the 6-Br synthon I with [ $^3\text{H}$ ]aniline or [ $^3\text{H}$ ]benzylamine [22]. [ $^3\text{H}$ -Methyl]-6-bromomethylamiloride has been synthesized by the reaction of bromoamiloride with [ $^3\text{H}$ ]  $\text{CH}_3\text{I}$  and has a specific activity of 1 Ci/mmol [53]. The methyl group is attached to the guanidino nitrogen atom adjacent to the carbonyl moiety.

Amiloride has been coupled to albumin via the N-hydroxysuccinimide ester of the amiloride analog bearing a 5-carboxypentyl group on the terminal guanidino nitrogen [45]. This was then radioiodinated by conventional techniques placing the  $^{125}\text{I}$  on albumin. A new amiloride analog bearing a 4'-hydroxyphenethyl moiety (No. 72) should prove useful in synthesis of radioiodinated amiloride analogs (No. 73 and 74).

*c. Amiloride Analogs Bearing Substituents on the 5-Amino Group.* Both 5-([N-ethyl-N- $^3\text{H}$ ]propyl)amiloride [81] and 5-([N-methyl-N- $^3\text{H}$ ]isobutyl)amiloride<sup>3</sup> have been synthesized with specific activities of 2 and 28 Ci/mmol, respectively.

*d. Amiloride Analogs Bearing Substituents on the 6-Position of the Pyrazine Ring.* A new method has recently been described for replacing an H- in the 6-position with  $^{125}\text{I}$  [15]. 6-Iodoamiloride and a number of 6-iodoamiloride analogs have been synthesized with this procedure.

## B. BINDING STUDIES USING RADIOLABELED AMILORIDE ANALOGS

A number of studies have been published recently using radiolabeled amiloride analogs to identify and characterize binding sites of amiloride analogs, with plasma membranes or microsomal membranes derived from cells known to have amiloride-sensitive transporters. Analogs bearing substituents on the 5-

amino group, including 5-(N-methyl-N- $^3\text{H}$ ]isobutyl)amiloride and 5-(N-ethyl-N- $^3\text{H}$ ]isopropyl)amiloride have been used to characterize binding to the putative  $\text{Na}^+/\text{H}^+$  exchanger [30, 81]. [ $^3\text{H}$ ]Benzamil, [ $^3\text{H}$ ]phenamil, and [ $^3\text{H}$ ]6-bromomethylamiloride have been used to characterize binding to epithelial  $\text{Na}^+$  channel [2, 5, 25, 46, 71].

## C. PHOTOAFFINITY LABELS

Three major photoactive groups have been used in the development of photoreactive amiloride analogs. These include arylhalides, arylazides, and aromatic ethers.

*a. Aryl Halides.* Photolysis of 6-bromo, 6-iodo, or 6-chloro analogs of amiloride can lead to the formation of a free radical, and subsequent covalent incorporation into adjacent proteins. This approach has been used to identify putative subunits of the epithelial  $\text{Na}^+$  channel, using [ $^3\text{H}$ ]6-bromobenzamil and [ $^3\text{H}$ ]6-bromomethylamiloride as photoactive amiloride analogs that bind to the  $\text{Na}^+$  channel with both high affinity and specificity [6, 46]. Amiloride and 6-bromobenzamil have a major absorption peak at 360 nm, and we have used this wavelength light to photoactive 6-bromobenzamil [46]. [ $^{14}\text{C}$ ]5-(N-ethyl-N-isopropyl)-6-bromoamiloride has been used as a photoaffinity label for the  $\text{Na}^+/\text{H}^+$  exchanger [32].

*b. Arylazides.* 4-Azidophenamil has been synthesized; however, conditions to demonstrate incorporation of this amiloride analog into the  $\text{Na}^+$  channel have not been defined.

*c. Aromatic Ethers.* Aromatic ethers have been shown to undergo photoactivation and photoincorporation into proteins by the mechanism of aromatic nucleophilic photosubstitution [17]. Photoactivation leads to formation of a reactive intermediate with a half life of less than one msec, at which time nucleophiles can bind covalently to the amiloride analog. If no incorporation occurs, the drug returns to the ground state.

Photoreactive amiloride analogs have been synthesized with a 2'-methoxy-5'-nitrobenzyl moiety located either on the terminal nitrogen atom of the guanidino moiety or on the 5-amino moiety (which also bears either a hydrogen or an ethyl group). These drugs undergo photoactivation with 313 nm wavelength light. The 2'-methoxy-5'-nitrobenzamil has been used to photolabel and identify putative components of the  $\text{Na}^+$  channel [44]. Anti-amiloride antibodies were used to detect the photolabel after

<sup>3</sup> 5-(N-methyl-N- $^3\text{H}$ -isobutyl)amiloride was prepared by New England Nuclear by the catalytic tritiation of 5-[N-methyl-N-(2-methylallyl)]amiloride.

photoincorporation into the channel. An amiloride analog with the photoactive group on the 5-amino moiety has been used to label the  $\text{Na}^+/\text{H}^+$  exchanger [85].

#### D. AFFINITY MATRICES

Amiloride has been coupled to support matrices through either the terminal nitrogen atom of the guanidino moiety or through the 5-amino group of the pyrazine ring. Three separate methods have been used to couple amiloride to a matrix through the guanidino moiety. One method has been used to couple through the 5-amino moiety.

The first method involves a reactive amiloride synthon, 1-methyl-2-(3,5-diamino-6-chloropyrazinoyl)pseudothiuronium iodide (see Fig. 2). The synthon reacts with primary or secondary amines to form the corresponding pyrazinoylguanidine. The synthon was allowed to react with aminohexylsepharose in the presence of a hindered base (triethylamine). The product was amiloride coupled to sepharose through a six-carbon spacer arm [47].

The second method involves the use of an amiloride analog bearing a 5'-carboxypentyl group on the terminal guanidino nitrogen atom. A mixed anhydride was synthesized using isobutyl chloroformate, which reacts with primary amines to form the corresponding amide. Amiloride was coupled to albumin using this procedure, and coupling to aminohexylsepharose by this method should be straightforward. The amiloride-albumin complex was subsequently coupled to sepharose and has been used to affinity purify anti-amiloride antibodies [45].

A third method involves the reaction of amiloride with cyanogen bromide-activated sepharose. The site on the amiloride which binds to the resin is unclear. Coupling may occur on the terminal nitrogen atom of the guanidino moiety. The amiloride sepharose resin was subsequently used as an affinity resin to purify the epithelial  $\text{Na}^+$  channel [5].

A method for coupling amiloride through the 5-amino group utilized an amiloride analog bearing an isothiocyanato group. 5-[N-(3-aminophenyl)] amiloride was converted to its corresponding isothiocyanate and then coupled to dextran [14].

#### E. ANTI-AMILORIDE ANTIBODIES

An amiloride analog bearing a 5-carboxypentyl group on the terminal nitrogen of the acylguanidino moiety of amiloride was coupled to albumin by generation of a mixed anhydride. Approximately 10 moles of amiloride were bound per mole of albumin. The amiloride-bovine serum albumin was used to

T.R. Kleyman and E.J. Cragoe, Jr.: Amiloride and Its Analogs

raise anti-amiloride antibodies in rabbits, which were subsequently affinity purified with an amiloride-rabbit serum albumin affinity column [45].

#### F. METHODOLOGIC PROBLEMS

*a. Solubility Characteristics.* Amiloride and many of its analogs are soluble in aqueous solutions at concentrations less than 1 to 10 mM. The solubility of the analogs usually decreases with addition of hydrophobic groups. Stock solutions of amiloride and many of the amiloride analogs may be made in DMSO at concentrations of 1 M. We generally make stock solutions of amiloride analogs at a concentration of 10 mM in DMSO and store the solutions at  $-20^\circ\text{C}$  protected from light.

*b.  $pK_a$ .* The guanidino moiety of amiloride is protonated at physiologic pH, and it is this positively charged species that appears to be required for inhibition of ion transport. The  $pK_a$  of amiloride is 8.7 in 30% ethanol of 8.8 in water. The  $pK_a$  tends to decrease with substitution of electron-withdrawing groups on the terminal nitrogen of the guanidino moiety. Table 8 lists of  $pK_a$ 's of amiloride and several amiloride analogs.

*c. Lipid Solubility.* Both amiloride and amiloride analogs bearing hydrophobic substituents on the 5-amino and acylguanidino moieties of amiloride are hydrophobic when uncharged, and dissolve easily in organic solvents, such as octanol. The protonated (i.e., charged) species are more soluble in aqueous solutions, and have varying solubility in octanol. The lipophilicity of amiloride and its analogs has been determined by measuring the distribution between a buffered aqueous phase and octanol or chloroform. The results for several amiloride analogs are listed in Table 8.

*d. Intracellular Accumulation.* Several studies have shown that amiloride accumulates within cells. Amiloride and its analogs may diffuse across membranes in the unprotonated or protonated form, or may be transported across. Amiloride uptake into hepatocytes was shown to be dependent on the extracellular  $\text{Na}^+$  concentration and on temperature [54]. The  $t_{1/2}$  for cellular uptake was 5 to 10 min. These data suggest that amiloride uptake in hepatocytes was due, in part, to transport across the plasma membrane. The intracellular concentration of amiloride was 10-fold greater than the extracellular concentration, assuming that cellular amiloride was free in solution and not bound to lipid or compartmentalized. Amiloride was also shown to accumulate within frog skin epithelial cells [13] and



within A431 cells [29] at intracellular concentrations greater than the extracellular concentration. Amiloride has been shown to diffuse across red blood cell and neutrophil plasma membranes with a permeability coefficient of approximately  $10^{-7}$  cm  $\cdot$  sec $^{-1}$  [4, 76]. The uptake of amiloride was shown to be temperature dependent and independent of the extracellular  $[Na^+]$ . In neutrophils 75% of the intracellular amiloride was considered to be in the lysosomal compartment [76]. In other cell types, the extent to which intracellular amiloride localized to intracellular compartments or is bound to membranes is uncertain.

*e. Absorption Characteristics.* The absorption characteristics of amiloride and a number of its analogs have been studied. In general, three major absorption peaks have been observed at approximately 360 to 370 nm, 265 to 290 nm, and 215 to 235 nm. The absorption peaks are broad and appear to vary slightly among the different analogs and with the solvent system used. The extinction coefficients at these wavelengths are in the range of 10,000 M $^{-1}$  cm $^{-1}$  to 25,000 M $^{-1}$  cm $^{-1}$ .

*f. Fluorescence Characteristics.* Amiloride and its analogs are aromatic compounds and are highly fluorescent. Amiloride has excitation maxima at 286 and 360 nm, and an emission maximum at 410 to 414 nm. Both the fluorescence and absorption properties of the analogs may interfere with techniques that utilize fluorescent probes to measure intracellular pH and intracellular  $Ca^{2+}$ . Amiloride may quench the fluorescence of both acridine orange and carboxyfluorescein, probes that have been used to measure intravesicular and intracellular pH. The absorption peak of amiloride at 360 nm may interfere with the absorption of quin 2 (excitation at 342 nm) and fura 2 (excitation at 340 and 380 nm), probes that have been used to measure intracellular calcium ions.

#### IV. Summary

Amiloride inhibits most plasma membrane  $Na^+$  transport systems. We have reviewed the pharmacology of inhibition of these transporters by amiloride and its analogs. Thorough studies of the  $Na^+$  channel, the  $Na^+/H^+$  exchanger, and the  $Na^+/Ca^{2+}$  exchanger, clearly show that appropriate modification of the structure of amiloride will generate analogs with increased affinity and specificity for a particular transport system. Introduction of hydrophobic substituents on the terminal nitrogen of the guanidino moiety enhances activity against the  $Na^+$

channel; whereas addition of hydrophobic (or hydrophilic) groups on the 5-amino moiety enhances activity against the  $Na^+/H^+$  exchanger. Activity against the  $Na^+/Ca^{2+}$  exchanger and  $Ca^{2+}$  channel is increased with hydrophobic substituents at either of these sites. Appropriate modification of amiloride has produced analogs that are several hundred-fold more active than amiloride against specific transporters. The availability of radioactive and photoactive amiloride analogs, anti-amiloride antibodies, and analogs coupled to support matrices should prove useful in future studies of amiloride-sensitive transport systems.

The use of amiloride and its analogs in the study of ion transport requires a knowledge of the pharmacology of inhibition of transport proteins, as well as effects on enzymes, receptors, and other cellular processes, such as DNA, RNA, and protein synthesis, and cellular metabolism. One must consider whether the effects seen on various cellular processes are direct or due to a cascade of events triggered by an effect on an ion transport system.

The authors are grateful to Drs. G. Kaczorowski, L. Simchowicz, and D. Warnock for reviewing the manuscript, and to Drs. G. Fanelli, G. Kaczorowski, A. Karlin, and L. Simchowicz for providing unpublished data on inhibition of  $Na^+$  transport systems by amiloride analogs. We are also grateful to Drs. A. Pellanda, I. Borghini, P. Dome, P. Kaelin, and S. Schorderet for testing several of the amiloride analogs. This work was supported by grant AM34742 from the United States Public Health Service. T.R.K. is a recipient of a Clinician-Scientist Award from the American Heart Association.

#### References

1. Aronson, P.S., Nee, J., Shum, M.A. 1982. *Nature (London)* 299:161-163
2. Barby, P., Chassande, O., Vigne, P., Frelin, C., Ellory, C., Cragoe, E.J., Jr., Lazdunski, M. 1987. *Proc. Natl. Acad. Sci. USA* 84:4836-4840
3. Benos, D.J. 1982. *Am. J. Physiol.* 242:C131-C145
4. Benos, D.J., Reyes, J., Shoemaker, D.G. 1983. *Biochim. Biophys. Acta* 734:99-104
5. Benos, D.J., Saccomani, G., Brenner, B.M., Sariban-Sohraby, S. 1986. *Proc. Natl. Acad. Sci. USA* 83:8525-8529
6. Benos, D.J., Saccomani, G., Sariban-Sohraby, S. 1987. *J. Biol. Chem.* 262:10613-10618
7. Benos, D.J., Simon, S.A., Mandel, L.J., Cala, P.M. 1976. *J. Gen. Physiol.* 68:43-63
8. Bently, P.J. 1968. *J. Physiol. (London)* 195:317-330
9. Besterman, J.M., May, W.S., Jr., Le Vine, H., III, Cragoe, E.J., Jr., Cuatrecasas, P. 1985. *J. Biol. Chem.* 260:1155-1159
10. Bhalla, R.C., Sharma, R.V. 1986. *J. Cardiovasc. Pharmacol.* 8:927-932
11. Bielefeld, D.R., Hadley, R.W., Vassilev, P.M., Hume, J.R. 1986. *Circ. Res.* 59:381-389
12. Bierman, A.J., Tertoolen, L.G.J., Laat, S.W. de, Mooleenaar, W.H. 1987. *J. Biol. Chem.* 262:9621-9628



13. Briggman, J.V., Graves, J.S., Spicer, S.S., Cragoe, E.J., Jr. 1983. *Histochem. J.* 15:239-255
14. Cassel, D., Cragoe, E.J., Jr., Rotman, M. 1987. *J. Biol. Chem.* 262:4587-4591
15. Cassel, D., Rotman, M., Cragoe, E.J., Jr., Igarashi, P. 1988. *Anal. Biochem.* 170:63-67
16. Cook, J.S., Shaffer, C., Cragoe, E.J., Jr. 1987. *Am. J. Physiol.* 253:C199-C204
17. Cornelisse, J., Havinga, E. 1975. *Chem. Rev.* 75:353-388
18. Costa, C.J., Kirschner, L.B., Cragoe, E.J., Jr. 1984. *J. Membrane Biol.* 82:49-57
19. Cragoe, E.J., Jr. 1979. In: *Amiloride and Epithelial Sodium Transport*. A.W. Cuthbert, G.M. Fanelli, and A. Scriabine, editors. pp. 1-20. Urban & Schwarzenberg, Baltimore-Munich
20. Cragoe, E.J., Jr. 1983. In: *Diuretics: Chemistry, Pharmacology, and Medicine*. E.J. Cragoe, Jr., editor. pp. 303-343. John Wiley & Sons, New York
21. Cragoe, E.J., Jr., Woltersdorf, O.W., Jr., Bicking, J.B., Kwong, S.F., Jones, J.H. 1967. *J. Med. Chem.* 10:66-75
22. Cragoe, E.J., Jr., Woltersdorf, O.W., Jr., Solms, S.J. de 1981. U.S. Patent 4,246,406.
23. Cuthbert, A.W. 1976. *Mol. Pharmacol.* 12:945-957
24. Cuthbert, A.W., Edwardson, J.M. 1979. *J. Pharm. Pharmacol.* 31:382-386
25. Cuthbert, A.W., Edwardson, J.M. 1981. *Biochem. Pharmacol.* 30:1175-1183
26. Cuthbert, A.W., Fanelli, G.M. 1978. *Br. J. Pharmacol.* 63:139-149
27. Cuthbert, A.W., Shum, W.K. 1974. *Naunyn-Schmiedeberg's Arch. Pharmacol.* 281:261-269
28. Dannenbaum, D., Rosenheck, K. 1986. *Biophys. J.* 49:A370 (abstr.)
29. Davis, R.J., Czech, M.P. 1985. *J. Biol. Chem.* 260:2543-2551
30. Dixon, S.J., Cohen, S., Cragoe, E.J., Jr., Grinstein, S. 1986. *J. Gen. Physiol.* 88:19a (abstr.)
31. Dubinsky, W.P., Frizzell, R.A. 1983. *Am. J. Physiol.* 245:C157-C159
32. Friedrich, T., Sablotni, J., Burckhardt, G. 1986. *J. Membrane Biol.* 94:253-266
33. Garcia, M.L., King, V.F., Cragoe, E.J., Jr., Kaczorowski, G.J. 1987. *Biophys. J.* 51:428a (abstr.)
34. Garvin, J.L., Simon, S.A., Cragoe, E.J., Jr., Mandel, L.J. 1985. *J. Membrane Biol.* 87:45-54
35. Haggerty, J.G., Cragoe, E.J., Jr., Slayman, C.W., Adelberg, E.A. 1985. *Biochem. Biophys. Res. Commun.* 127:759-767
36. Hamilton, K.L., Eaton, D.C. 1985. *Am. J. Physiol.* 245:C200-C207
37. Harris, R.C., Lufburrow, R.A., III, Cragoe, E.J., Jr., Seifter, J.L. 1985. *Kidney Int.* 27:310 (abstr.)
38. Howard, M.J., Mullen, M.D., Insel, P.A. 1987. *Am. J. Physiol.* 253:F21-F25
39. Ives, H.E., Yee, V.J., Warnock, D.G. 1983. *J. Biol. Chem.* 258:9710-9716
40. Johnson, J.D., Epel, D., Paul, M. 1976. *Nature (London)* 262:661-664
41. Kaczorowski, G.J., Barrows, G.J., Dethmers, J.K., Trumble, M.J. 1985. *Biochemistry* 24:1394-1403
42. Kim, B., Smith, T.W. 1986. *Mol. Pharmacol.* 30:164-170
43. Kinsella, J.L., Aronson, P.S. 1981. *Am. J. Physiol.* 241:F374-F379
44. Kleyman, T., Crudo, J., Cragoe, E., Jr., Al-Awqati, Q., Rossier, B., Kraehenbuhl, J.-P. 1987. *Experientia* 43:688 (abstr.)
45. Kleyman, T.R., Rajagopalan, R., Cragoe, E.J., Jr., Erlanger, B.F., Al-Awqati, Q. 1986. *Am. J. Physiol.* 250:C165-C170
46. Kleyman, T.R., Yulo, T.R., Ashbaugh, C., Landry, D., Cragoe, E., Jr., Karlin, A., Al-Awqati, Q. 1986. *J. Biol. Chem.* 261:2839-2943
47. Kleyman, T., Yulo, T., Cragoe, E.J., Jr., Al-Awqati, Q. 1986. *Kidney Int.* 29:400 (abstr.)
48. Koch, K.S., Leffert, H.L. 1979. *Cell* 18:153-163
49. Kuijpers, G.A.J., DePont, J., Nooy, I., van, Fleuren-Jakobs, A., Bonting, S., Rodrigues de Miranda, J. 1984. *Biochim. Biophys. Acta* 804:237-244
50. L'Allemain, G., Franchi, A., Cragoe, E., Jr., Pouyssegur, J. 1984. *J. Biol. Chem.* 259:4313-4319
51. LaBelle, E.F., Woodward, P.L., Cragoe, E.J., Jr. 1984. *Biochim. Biophys. Acta* 778:129-138
52. Langer, G.A. 1982. *Annu. Rev. Physiol.* 44:435-449
53. Lazorick, K., Miller, C., Sariban-Sohraby, S., Benos, D. 1985. *J. Membrane Biol.* 86:69-77
54. Leffert, H.L., Koch, K.S., Fehlmann, M., Heiser, W., Lad, P.J., Skelly, H. 1982. *Biochem. Biophys. Res. Commun.* 108:738-745
55. Li, J.H.-Y., Cragoe, E.J., Jr., Lindemann, B. 1985. *J. Membrane Biol.* 83:45-56
56. Li, J.H.-Y., Cragoe, E.J., Lindemann, B. 1987. *J. Membrane Biol.* 95:171-185
57. Lubin, M., Cahn, F., Coutermarsh, B.A. 1982. *J. Cell. Physiol.* 113:247-251
58. Mahe, Y., Garcia-Romeu, F., Montais, R. 1985. *Eur. J. Pharmacol.* 116:199-206
59. Margolius, H.S., Chao, J. 1980. *J. Clin. Invest.* 65:1343-1350
60. Meloche, S., Ong, H., De Lean, A. 1987. *J. Biol. Chem.* 262:10252-10258
61. Moolenaar, W.H., Tertoolen, L.G.V., Laat, S.W. de 1984. *Nature (London)* 312:371-374
62. O'Donnell, M.E., Cragoe, E., Jr., Villereal, M.L. 1983. *J. Pharmacol. Exp. Ther.* 226:368-372
63. Palaty, V. 1985. *Can. J. Physiol. Pharmacol.* 63:1586-1589
64. Palmer, L.G. 1984. *J. Membrane Biol.* 80:153-165
65. Palmer, L.G., Frindt, G. 1986. *Proc. Natl. Acad. Sci. USA* 83:2767-2770
66. Paris, S., Pouyssegur, J. 1984. *J. Biol. Chem.* 259:10989-10994
67. Pouyssegur, J., Chambard, J.C., Franchi, A., Paris, S., Obberghen-Schilling, E. van 1982. *Proc. Natl. Acad. Sci. USA* 79:3935-3939
68. Ralph, R.K., Smart, J., Wojcik, S.M., McQuillan, J. 1982. *Biochem. Biophys. Res. Commun.* 104:1054-1059
69. Renner, E.L., Lake, J.R., Cragoe, E.J., Jr., Scharschmidt, B.F. 1986. *J. Cell Biol.* 103:457a (abstr.)
70. Reuss, L., Petersen, K.U. 1985. *J. Gen. Physiol.* 85:409-429
71. Sariban-Sohraby, S., Benos, D.J. 1986. *Biochemistry* 25:4639-4646
72. Sariban-Sohraby, S., Benos, D.J. 1986. *Am. J. Physiol.* 250:C175-C190
73. Schellenberg, G.D., Anderson, L., Cragoe, E.J., Jr., Swanson, P.D. 1985. *Mol. Pharmacol.* 27:537-543
74. Seifter, J.L., Aronson, P.S. 1986. *J. Clin. Invest.* 78:859-864
75. Simchowicz, L., Cragoe, E.J., Jr. 1986. *Mol. Pharmacol.* 30:112-120
76. Simchowicz, L., Woltersdorf, O.W., Jr., Cragoe, E.J., Jr. 1987. *J. Biol. Chem.* 262:15875-15975
77. Soltoff, S.P., Cragoe, E.J., Jr., Mandel, L.J. 1986. *Am. J. Physiol.* 250:C744-C749

78. Soltoff, S.P., Mandell, L.J. 1983. *Science* 220:957-958
79. Vassalli, J.-D., Belin, D. 1987. *FEBS Lett.* 214:187-191
80. Velly, J., Grima, M., Decker, N., Cragoe, E.J., Jr., Schwartz, J. 1988. *Eur. J. Physiol.* 149:97-105
81. Vigne, P., Frelin, C., Audinot, M., Borsotto, M., Cragoe, E.J., Jr., Lazdunski, M. 1984. *EMBO J.* 3:2647-2651
82. Vigne, P., Frelin, C., Cragoe, E.J., Jr., Lazdunski, M. 1984. *Mol. Pharmacol.* 25:131-136
83. Vigne, P., Frelin, C., Lazdunski, M. 1985. *J. Biol. Chem.* 260:8008-8013
84. Yang, W.C., Lowe, A., Warnock, D.G. 1987. *Kidney Int.* 31:443 (abstr.)
85. Warnock, D., Kleyman, T., Cragoe, E.J., Jr. 1988. *FASEB J.* 2:A753 (abstr.)
86. Zhuang, Y., Cragoe, E.J., Jr., Shaikewitz, T., Glaser, L., Cassel, D. 1984. *Biochemistry* 23:4481-4488

Received 4 January 1988; revised 31 March 1988

## [42] Cation Transport Probes: The Amiloride Series

By THOMAS R. KLEYMAN and EDWARD J. CRAGOE, JR.

### Introduction

Amiloride and a large number of amiloride analogs were synthesized in the mid-1960s while in search of diuretic agents which possessed both natriuretic as well as antikaluretic properties.<sup>1,2</sup> Amiloride inhibits the  $\text{Na}^+$  channel present in urinary epithelia, and both the natriuresis and antika-liuresis observed clinically are a direct result of inhibition of the  $\text{Na}^+$  channel.<sup>3</sup> Amiloride and its analogs have been subsequently shown to inhibit a variety of other ion transporters and enzymes, to interact with specific drug or hormone receptors, and to inhibit DNA, RNA, and protein synthesis<sup>4,5</sup> (Table I).

Amiloride is a pyrazinoylguanidine bearing amino groups in the 3- and 5-positions and a chloro group in the 6-position of the pyrazine ring (Table II). Over 1000 analogs have been synthesized.<sup>1</sup> This chapter reviews the use of amiloride analogs as probes for the characterization of ion transport proteins.

### Ion Transport Systems

Amiloride and a large number of amiloride analogs have been used as reversible inhibitors of ion transport.<sup>4,5</sup> Amiloride analogs have a guanidino moiety, and its protonated form is required for inhibition of ion transport.<sup>6-8</sup> The  $\text{pK}_a$  of amiloride is 8.8 in  $\text{H}_2\text{O}$  (8.7 in 30% ethanol) and decreases with substitution of electron-withdrawing groups on the terminal nitrogen of the guanidino moiety.<sup>4</sup> The concentrations of amiloride required to achieve half-maximal inhibition ( $\text{IC}_{50}$ ) of the epithelial  $\text{Na}^+$  channel,  $\text{Na}^+/\text{H}^+$  exchanger,  $\text{Na}^+/\text{Ca}^{2+}$  exchanger,  $\text{Na}^+, \text{K}^+$ -ATPase, volt-

<sup>1</sup> E. J. Cragoe, Jr., in "Diuretics" (E. J. Cragoe, Jr., ed.), p. 303. Wiley, New York, 1983.

<sup>2</sup> E. J. Cragoe, Jr., O. W. Woltersdorf, Jr., J. B. Bicking, S. F. Kwong, and J. H. Jones, *J. Med. Chem.* 10, 66 (1967).

<sup>3</sup> T. R. Kleyman and E. J. Cragoe, Jr., *Semin. Nephrol.* 8, 242 (1988).

<sup>4</sup> T. R. Kleyman and E. J. Cragoe, Jr., *J. Membr. Biol.* 105, 1 (1988).

<sup>5</sup> D. J. Benos, *Am. J. Physiol.* 242, C131 (1982).

<sup>6</sup> D. J. Benos, S. A. Simon, L. J. Mandel, and P. M. Cala, *J. Gen. Physiol.* 68, 43 (1976).

<sup>7</sup> G. L'Allemain, A. Franchi, E. Cragoe, Jr., and J. Pouyssegur, *J. Biol. Chem.* 259, 4313 (1984).

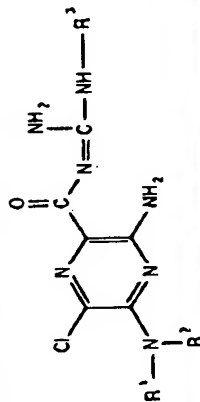
<sup>8</sup> G. J. Kaczorowski, F. Barros, J. K. Dethmers, and M. J. Trumble, *Biochemistry* 24, 1394 (1985).

TABLE I  
ION TRANSPORTERS, ENZYMES, AND DRUG AND HORMONE RECEPTORS THAT ARE INHIBITED OR INTERACT WITH AMILORIDE OR AMILORIDE ANALOGS

Ion transporters	Enzymes	Drug and hormone receptors
Epithelial Na <sup>+</sup> channel	Protein kinases	$\alpha_1$ -Adrenergic receptor
Na <sup>+</sup> /H <sup>+</sup> exchanger	Type I cAMP-dependent protein kinase	$\alpha_2$ -Adrenergic receptor
Na <sup>+</sup> /Ca <sup>2+</sup> exchanger	Type II cAMP-dependent protein kinase	$\beta$ -Adrenergic receptor
Na <sup>+</sup> , K <sup>+</sup> -ATPase	Epidermal growth factor receptor protein kinase	Atrial natriuretic receptor
Na <sup>+</sup> -D-glucose cotransporter	Platelet-derived growth factor receptor protein kinase	Guanine nucleotide regulatory proteins
Na <sup>+</sup> -L-alanine cotransporter	Insulin receptor protein kinase	Muscarinic acetylcholine receptor
Na <sup>+</sup> -PO <sub>4</sub> <sup>3-</sup> -cotransporter	Protein kinase C	Nicotinic acetylcholine receptor
Voltage-gated Na <sup>+</sup> channel	Acetylcholinesterase	
Voltage-gated Ca <sup>2+</sup> channel	Adenylate cyclase	
Delayed rectifier K <sup>+</sup> channel	DNA topoisomerase II	
Nicotinic acetylcholine receptor	Monoamine oxidase	
	Renal kallikrein	
	Urokinase-type plasminogen activator	

TABLE II

CONCENTRATIONS OF AMILORIDE REQUIRED TO ACHIEVE HALF-MAXIMAL INHIBITION ( $IC_{50}$ ) OF THE EPIHELIAL  $Na^+$  CHANNEL,  $Na^+/H^+$  EXCHANGER,  $Na^+/Ca^{2+}$  EXCHANGER,  $Na^+$ ,  $K^+$ -ATPASE, VOLTAGE-GATED  $Na^+$  CHANNEL, AND VOLTAGE-GATED  $Ca^{2+}$  CHANNEL (L TYPE)<sup>a</sup>



$IC_{50}$  ( $\mu M$ ) for Amiloride and Potency Relative to Amiloride

Amiloride Analog	R <sup>1</sup>	R <sup>2</sup>	R <sup>3</sup>	Epithelial $Na^+$ Channel (0.35)	$Na^+/H^+$ Exchanger (84)	$Na^+/Ca^{2+}$ Exchanger (1100)	$Na^+/K^+$ -ATPase (4000)	Voltage-gated $Na^+$ Channel (600)	Voltage-gated $Ca^{2+}$ Channel (90)
Amiloride	H—	H—	H—	1	1	1	1	1	1
Phenamil	H—	H—		17	<0.01	5			10
Benzamil	H—	H—		9	<0.08	11	5	16	14
3',4'-Dichlorobenzamil	H—	H—		4		37			25
5-(N,N-Dimethyl)amiloride	CH <sub>3</sub> —	CH <sub>3</sub> —	H—	<0.04	12	2	1.4	100	5
5-(N-Ethyl-N-isopropyl)amiloride	C <sub>2</sub> H <sub>5</sub> —	(CH <sub>3</sub> ) <sub>2</sub> CH—	H—	<0.04	220	8	14		56
5-(N-Methyl-N-isobutyl)amiloride	CH <sub>3</sub> —	(CH <sub>3</sub> ) <sub>2</sub> CHCH <sub>2</sub> —	H—		190	8			75

<sup>a</sup> Amiloride analogs that have been commonly used are included in this table along with their potency, relative to amiloride, in inhibiting the ion transporters listed.<sup>4,8,17,19,20,25,29,33</sup> To determine the  $IC_{50}$  of a specific amiloride analog for a transport protein listed above, divide the  $IC_{50}$  for amiloride by the relative potency of the amiloride analog. The  $IC_{50}$  values for the voltage-gated  $Ca^{2+}$  channel (L type) were derived from binding experiments.

age-gated  $\text{Na}^+$  channel, and voltage-gated  $\text{Ca}^{2+}$  channel (L-type) are listed in Table II. Amiloride analogs that have been commonly used are included in this table, along with their potency, relative to amiloride, in inhibiting the ion transporters listed.

#### *Factors that Influence the $\text{IC}_{50}$ of Amiloride and Its Analogs*

The  $\text{IC}_{50}$  values of amiloride and amiloride analogs are not absolute, but vary depending on assay conditions. A decrease in the extracellular (or extravascular)  $\text{Na}^+$  concentration results in a decrease in the  $\text{IC}_{50}$  for the  $\text{Na}^+$  channel,  $\text{Na}^+/\text{H}^+$  exchanger, and  $\text{Na}^+/\text{Ca}^{2+}$  exchanger.<sup>4,8-10</sup>

Amiloride and a large number of its analogs (in particular, a number of analogs that have been shown to be potent inhibitors of  $\text{Na}^+/\text{H}^+$  exchange) bear hydrophobic substituents and are permeable weak bases. These amiloride analogs may collapse pH gradients across membranes and decrease the driving force for  $\text{Na}^+/\text{H}^+$  exchange.<sup>11,12</sup> Amiloride has also been shown to accumulate within cells and may indirectly effect ion transport through inhibition of intracellular enzymes (such as protein kinases and adenylate cyclase) which may be involved in the regulation of ion transport proteins (see Enzymes, Receptors, and Cellular Metabolism, below).

The extent of inhibition of the sodium channel by amiloride has been shown to be dependent on the apical plasma membrane potential. Amiloride interacts with the channel in a manner that is sensitive to the membrane potential.<sup>13,14</sup>

#### *Epithelial $\text{Na}^+$ Channel*

Sodium ion channels are present on the apical plasma membrane of high-resistance (or "tight") epithelia that transport  $\text{Na}^+$ .<sup>15,16</sup> This channel is the only ion transporter inhibited by amiloride with an  $\text{IC}_{50}$  of less than  $1 \mu\text{M}$ .<sup>4</sup> In the presence of a physiologic  $\text{Na}^+$  concentration, the  $\text{IC}_{50}$  for inhibition of  $\text{Na}^+$  transport is in the range of 0.1 to  $0.5 \mu\text{M}$ .<sup>4,16</sup> The most specific inhibitors of the epithelial  $\text{Na}^+$  channel are amiloride analogs bearing hydrophobic substituents on the terminal nitrogen atom of the

<sup>9</sup> A. W. Cuthbert and W. K. Shum, *Naunyn-Schmiedeberg's Arch. Pharmacol.* 281, 261 (1974).

<sup>10</sup> J. L. Kinsella and P. S. Aronson, *Am. J. Physiol.* 241, F374 (1981).

<sup>11</sup> G. Kaczorowski, M. Garcia, T. Kleyman, and E. J. Cragoe, Jr., unpublished observations.

<sup>12</sup> W. P. Dubinsky and R. A. Frizzel, *Am. J. Physiol.* 245, C157 (1983).

<sup>13</sup> L. G. Palmer, *J. Membr. Biol.* 80, 153 (1984).

<sup>14</sup> K. L. Hamilton and D. C. Eaton, *Am. J. Physiol.* 245, C200 (1985).

<sup>15</sup> P. J. Bently, *J. Physiol. (London)* 195, 317 (1986).

<sup>16</sup> S. Sariban-Sohraby and D. J. Benos, *Am. J. Physiol.* 250, C175 (1986).

guanidino moiety, such as the benzyl (benzamil) and phenyl (phenamil) analogs. These analogs inhibit  $\text{Na}^+$  transport with  $\text{IC}_{50}$  values of approximately 10 nM.<sup>4,17</sup> This is more than three orders of magnitude lower than that reported for inhibition of  $\text{Na}^+/\text{H}^+$  and  $\text{Na}^+/\text{Ca}^{2+}$  exchangers,  $\text{Na}^+/\text{K}^+$ -ATPase, and  $\text{Na}^+$ -glucose and  $\text{Na}^+$ -alanine cotransporters<sup>4,7,8</sup> (see the next three sections).

### $\text{Na}^+/\text{H}^+$ Exchanger

A plasma membrane transporter that exchanges  $\text{Na}^+$  for  $\text{H}^+$  in an electroneutral fashion has been described in a variety of cells<sup>18</sup> and is involved in regulation of intracellular pH. Amiloride and its analogs have been used as inhibitors of both  $\text{Na}^+/\text{H}^+$  exchange and subsequent events that might be altered through regulation of this transporter.<sup>7,18</sup>

The  $\text{IC}_{50}$  for inhibition of the exchanger by amiloride is 84  $\mu\text{M}$  in human neutrophils,<sup>19</sup> and as low as 3 to 7  $\mu\text{M}$  in other cells.<sup>4,7,20</sup> This variation is likely to be due, in part, to differences in the concentration of  $\text{Na}^+$  used to assay  $\text{Na}^+/\text{H}^+$  exchange. A recent study also suggests that the  $\text{Na}^+/\text{H}^+$  exchanger present on the basolateral plasma membrane of epithelia is more sensitive to 5-(*N*-ethyl-*N*-isopropyl)amiloride than is the  $\text{Na}^+/\text{H}^+$  exchanger present on the apical plasma membrane.<sup>20a</sup> Amiloride analogs bearing hydrophobic substituents on the 5-amino group located on the pyrazine ring have both the highest activity and specificity for the  $\text{Na}^+/\text{H}^+$  exchanger. Several analogs with hydrophilic substituents in this position are potent inhibitors of the exchanger.<sup>4,19</sup> When studied in the presence of a low  $[\text{Na}^+]$ ,  $\text{IC}_{50}$  values less than 100 nM have been observed for a number of amiloride analogs.<sup>4,7,20</sup> This is 100-fold less than the  $\text{IC}_{50}$  observed with these analogs for inhibition of the epithelial  $\text{Na}^+$  channel,<sup>4,17</sup>  $\text{Na}^+/\text{Ca}^{2+}$  exchanger,<sup>8</sup>  $\text{Na}^+/\text{K}^+$ -ATPase,<sup>20</sup> and  $\text{Na}^+$ -D-glucose,  $\text{Na}^+$ -L-alanine, and  $\text{Na}^+$ - $\text{PO}_4^{3-}$  cotransporters.<sup>21</sup>

Amiloride and 5-(*N,N*-dimethyl)amiloride are 9 and 100 times more potent, respectively, in inhibiting  $\text{Na}^+/\text{H}^+$  exchange than in inhibiting protein kinase C.<sup>22</sup> Amiloride inhibits a number of other kinases with  $\text{IC}_{50}$

<sup>17</sup> A. W. Cuthbert and G. M. Fanelli, *Br. J. Pharmacol.* 63, 139 (1978).

<sup>18</sup> J. L. Seifter and P. S. Aronson, *J. Clin. Invest.* 78, 859 (1986).

<sup>19</sup> L. Simchowicz and E. J. Cragoe, Jr., *Mol. Pharmacol.* 30, 112 (1986).

<sup>20</sup> Y. Zhuang, E. J. Cragoe, Jr., T. Shaikewitz, L. Glaser, and D. Cassel, *Biochemistry* 23, 4481 (1984).

<sup>20a</sup> J. G. Haggerty, N. Argarwal, R. F. Reilly, E. A. Adelberg, and C. W. Slayman, *Proc. Natl. Acad. Sci. U.S.A.* 85, 6797 (1988).

<sup>21</sup> R. C. Harris, R. A. Lufburrow III, E. J. Cragoe, Jr., and J. L. Seifter, *Kidney Int.* 27, 310 (abstr.) (1985).

<sup>22</sup> J. M. Besterman, W. S. May, Jr., H. Le Vine III, E. J. Cragoe, Jr., and P. Cuatrecasas, *J. Biol. Chem.* 260, 1155 (1985).



values similar to that reported for protein kinase C.<sup>23</sup> Amiloride inhibits adenylate cyclase with an  $IC_{50}$  similar to the  $IC_{50}$  for inhibition of  $Na^+/H^+$  exchange.<sup>24</sup>

### *$Na^+/Ca^{2+}$ Exchanger*

The  $Na^+/Ca^{2+}$  exchanger is a reversible electrogenic transporter and is inhibited by amiloride with an  $IC_{50}$  of approximately 1 mM.<sup>8</sup> Although proper substituents on either (or both) the 5-amino or the terminal guanidino nitrogen atoms increase the activity of these analogs by up to 100-fold, the  $IC_{50}$  is only in the range of 10  $\mu M$ .<sup>4,8</sup> With the exception of analogs with substituents at both sites, this is a considerably greater concentration than is required for inhibition of the epithelial  $Na^+$  channel and the  $Na^+/H^+$  exchanger. Of the amiloride analogs examined, those active against the  $Na^+/Ca^{2+}$  exchanger are equal or more potent inhibitors of the  $Ca^{2+}$  channel<sup>25</sup> (see Table II).

### *$Na^+,K^+$ -ATPase*

The inhibition of the  $Na^+,K^+$ -ATPase by amiloride has been studied in intact cells, membrane vesicles, and with partially purified  $Na^+,K^+$ -ATPase.<sup>20,21,26,27</sup> The  $IC_{50}$  for inhibition of ATPase activity by amiloride is greater than 3 mM. Appropriate substitution of the 5-amino moiety of amiloride decreases the  $IC_{50}$  to as low as 200  $\mu M$ .<sup>20</sup> 5-(*N,N*-Dimethyl)amiloride inhibits the  $Na^+,K^+$ -ATPase with an  $IC_{50}$  of 3 mM, which is four orders of magnitude greater than the  $IC_{50}$  for inhibition of  $Na^+/H^+$  exchanger.<sup>20</sup> The effect of introduction of substituents on the terminal nitrogen atom of the guanidino moiety has not been studied except for benzamil, which has an  $IC_{50}$  of less than 1 mM.

### *$Na^+$ -Coupled Solute Transport*

The transport of a number of solutes across the apical plasma membrane of epithelia is tightly coupled to  $Na^+$ . The  $Na^+$ -D-glucose,  $Na^+$ -L-alanine, and  $Na^+$ - $PO_4^{3-}$  transporters are inhibited by amiloride at concentrations greater than 1 mM.<sup>21,28</sup> Benzamil and 5-(*N,N*-dimethyl)

<sup>23</sup> R. J. Davis and M. P. Czech, *J. Biol. Chem.* 260, 2543 (1985).

<sup>24</sup> Y. Mahe, F. Garcia-Romeu, and R. Montais, *Eur. J. Pharmacol.* 116, 199 (1985).

<sup>25</sup> G. Kaczorowski, personal communication (1988).

<sup>26</sup> S. P. Soltoff and L. J. Mandell, *Science* 220, 957 (1983).

<sup>27</sup> E. L. Renner, J. R. Lake, E. J. Cragoe, Jr., and B. F. Scharschmidt, *J. Hepatol.* 6, 1193 (1986).

<sup>28</sup> J. S. Cook, C. Shaffer, and E. J. Cragoe, Jr., *Am. J. Physiol.* 253, C199 (1987).

amiloride inhibit the  $\text{Na}^+$ -D-glucose transporter in rabbit kidney brush border membranes with an  $\text{IC}_{50}$  between 0.5 and 1 mM. The  $\text{IC}_{50}$  of amiloride is approximately 2 mM.<sup>21</sup> The  $\text{Na}^+$ -coupled glucose transporter in LLC-PK<sub>1</sub> cells is inhibited by amiloride analogs bearing hydrophobic substituents on the 5-amino moiety or on terminal nitrogen of the guanidino moiety with  $\text{IC}_{50}$  values (measured using a low  $[\text{Na}^+]$ ) between 0.1 and 0.3 mM.<sup>28</sup>

$\text{Na}^+$ -dependent L-alanine and  $\text{PO}_4^{3-}$  transporters are inhibited by amiloride at concentrations greater than 1 mM. Introduction of hydrophobic groups on the 5-amino moiety or the terminal nitrogen atom of the guanidino moiety decreases the  $\text{IC}_{50}$ .<sup>21</sup>

### *Voltage-Gated $\text{Na}^+$ /Channel*

A voltage-gated  $\text{Na}^+$ -selective ion channel is present in electrically excitable cells. Amiloride inhibits this channel in both synaptosomes and heart membrane vesicles with an  $\text{IC}_{50}$  of 600  $\mu\text{M}$ .<sup>29</sup> Amiloride analogs bearing hydrophobic substituents on the 5-amino moiety or the terminal nitrogen of the guanidino moiety have lower  $\text{IC}_{50}$  values [6  $\mu\text{M}$  for 5-(N-ethyl-N-isopropyl)amiloride and 37  $\mu\text{M}$  for benzamil]. Amiloride and analogs with hydrophobic substituents on the 5-amino moiety and terminal nitrogen atom of the guanidino moiety inhibit [ $^3\text{H}$ ]batrachotoxin-A 20- $\alpha$ -benzoate and [ $^3\text{H}$ ]tetracaine binding to the channel.

### *Voltage-Gated $\text{Ca}^{2+}$ Channels*

Amiloride and 3',4'-dichlorobenzamil inhibit L-type, N-type, and T-type voltage-gated  $\text{Ca}^{2+}$  channels.<sup>25,30-34</sup> Amiloride binds to the L-type  $\text{Ca}^{2+}$  channel with an  $\text{IC}_{50}$  of 90  $\mu\text{M}$ . Amiloride analogs bearing hydrophobic substituents on the 5-amino moiety or the terminal nitrogen of the guanidino moiety have  $\text{IC}_{50}$  values 5- to 75-fold lower than amiloride<sup>25,33</sup> (Table II). Amiloride analogs bind to a cation-binding site in the pore of the  $\text{Ca}^{2+}$  channel and allosterically alter binding of dihydropyridines, aralkylamines, and benzothiazepines.<sup>33</sup>

<sup>29</sup> J. Velly, M. Grima, N. Decker, E. J. Cragoe, Jr., and J. Schwartz, *Eur. J. Physiol.* **149**, 97 (1988).

<sup>30</sup> C.-M. Tang, F. Presser, and M. Morad, *Science* **240**, 213 (1988).

<sup>31</sup> G. Suarez-Kurtz and G. Kaczorowski, *J. Pharmacol. Exp. Ther.* **247**, 248 (1988).

<sup>32</sup> P. Feigenbaum, M. L. Garcia, and G. Kaczorowski, *Biochem. Biophys. Res. Commun.* **154**, 298 (1988).

<sup>33</sup> M. L. Garcia, V. F. King, J. L. Shevell, R. S. Slaughter, G. Suarez-Kurtz, R. J. Winquist, and G. J. Kaczorowski, *J. Biol. Chem.* **265**, 3763 (1990).

<sup>34</sup> D. R. Bielefeld, R. W. Hadley, P. M. Vassilev, and J. R. Hume, *Circ. Res.* **59**, 381 (1986).

### *K<sup>+</sup> Channel*

3',4'-Dichlorobenzamil inhibits the delayed rectifier K<sup>+</sup> channel in intact frog atrial myocytes with 30 to 40% inhibition of the K<sup>+</sup> current at a concentration of 5  $\mu$ M.<sup>34</sup>

### *Nicotine Acetylcholine Receptor*

Amiloride inhibits the nicotinic acetylcholine receptor isolate from *Torpedo*. The IC<sub>50</sub> is approximately 100  $\mu$ M.<sup>35</sup>

## Enzymes, Receptors, and Cellular Metabolism

### *Protein Kinases*

Amiloride inhibits a number of protein kinases, including type I and type II cAMP-dependent protein kinases,<sup>36</sup> protein kinase C,<sup>22</sup> and protein kinase activity associated with the insulin receptor, epidermal growth factor (EGF) receptor, and the platelet-derived growth factor receptor.<sup>23</sup> The IC<sub>50</sub> for inhibition of EGF receptor protein kinase is 350  $\mu$ M. Amiloride inhibits types I and II cAMP-dependent protein kinases with an IC<sub>50</sub> of approximately 1 mM.<sup>36</sup> Both amiloride and 5-(*N,N*-dimethyl)amiloride inhibit purified protein kinase C with an IC<sub>50</sub> of approximately 1 mM.<sup>22</sup> The inhibition of protein kinase activity associated with the EGF receptor is competitive with ATP, suggesting that amiloride binds to an ATP-binding site. Amiloride is a noncompetitive inhibitor of substrate (histone) phosphorylation.<sup>23</sup>

### *Adenylate Cyclase*

The generation of cAMP in fish erythrocytes is inhibited by amiloride in a dose-dependent manner, with an IC<sub>50</sub> of 6  $\mu$ M.<sup>24</sup> The effect of amiloride analogs in this system have not been examined.

### *$\alpha$ - and $\beta$ -Adrenergic Receptors*

Amiloride is a competitive inhibitor of [<sup>3</sup>H]prazosin binding to  $\alpha_1$  receptors in membrane vesicles from rat renal cortex or bovine carotid artery with an IC<sub>50</sub> of 24 to 33  $\mu$ M.<sup>37,38</sup> Amiloride is also a competitive

<sup>35</sup> A. Karlin, personal communication (1986).

<sup>36</sup> R. K. Ralph, J. Smart, S. M. Wojcik, and J. McQuillan, *Biochem. Biophys. Res. Commun.* 104, 1054 (1982).

<sup>37</sup> M. J. Howard, M. D. Mullen, and P. A. Insel, *Am. J. Physiol.* 253, F21 (1987).

<sup>38</sup> R. C. Bhalla and R. V. Sharma, *J. Cardiovasc. Pharmacol.* 8, 927 (1986).

inhibitor of [ $^3\text{H}$ ]rauwolscine binding to  $\alpha_2$  receptors and [ $^{125}\text{I}$ ]iodocyano-pindolol binding to  $\beta$ -adrenergic receptors in rat renal cortical membranes with  $\text{IC}_{50}$  values of 14 and 84  $\mu\text{M}$ , respectively.<sup>37</sup> Both benzamil and 5-(*N*-ethyl-*N*-isopropyl)amiloride are between 2- to 25-fold more potent than amiloride in inhibiting specific ligand binding to  $\alpha_1$ -,  $\alpha_2$ -, and  $\beta$ -adrenergic receptors.

#### *Atrial Natriuretic Factor (ANF) Receptor*

ANF is a peptide hormone secreted by atrial myocytes and which binds to specific cell surface receptors. Recent studies have shown that ANF binds to both low- and high-affinity receptors, and that amiloride (100  $\mu\text{M}$ ) increases the number of high-affinity sites in membranes obtained from adrenal zona glomerulosa.<sup>39</sup> This change in the number of binding sites is associated with a conformational change in the 150,000-Da receptor.

#### *Guanine Nucleotide Regulatory Proteins*

Pertussis toxin catalyzed ADP ribosylation of the guanine nucleotide regulatory proteins  $\text{G}_o$  and  $\text{G}_i$  and is inhibited by  $10^{-4}$  *M* amiloride. Amiloride did not inhibit cholera toxin-catalyzed ADP ribosylation of  $\text{G}_o$ .<sup>40</sup>

#### *Muscarinic Acetylcholine Receptor*

Amiloride inhibits amylase secretion induced by carbachol with an  $\text{IC}_{50}$  of 40  $\mu\text{M}$ ,<sup>45</sup>  $\text{Ca}^{2+}$  efflux induced by carbachol with an  $\text{IC}_{50}$  of 80  $\mu\text{M}$ , and is a competitive inhibitor of [ $^3\text{H}$ ]quinuclidinyl benzylate binding to the muscarinic acetylcholine receptor.<sup>41</sup>

#### *Inhibition of Cellular Metabolism*

Several amiloride analogs with substituents on the 5-amino moiety (at concentrations  $> 30$   $\mu\text{M}$ ) deplete intracellular levels of ATP,<sup>20,42</sup> whereas amiloride and 5-(*N,N*-dimethyl)amiloride at concentrations of 2 *mM* had no effect.<sup>20</sup> The depletion of intracellular ATP levels may be due in part to inhibition of oxidative phosphorylation. Amiloride analogs bearing hydrophobic substituents on the 5-amino moiety inhibit  $\text{O}_2$  consumption in

<sup>39</sup> S. Meloche, H. Ong, and A. De Léan, *J. Biol. Chem.* 262, 10252 (1987).

<sup>40</sup> M. B. Anand-Srivastava, *J. Biol. Chem.* 264, 9491 (1989).

<sup>41</sup> G. A. J. Kuipers, J. DePont, I. van Nooy, A. Fleuren-Jakobs, S. Bonting, and J. Rodrigues de Miranda, *Biochim. Biophys. Acta* 804, 237 (1984).

<sup>42</sup> S. P. Soltoff, E. J. Cragoe, Jr., and L. J. Mandel, *Am. J. Physiol.* 250, C744 (1986).

carbonyl cyanide *p*-(trifluoro methoxy)-phenylhydrazone (FCCP)-treated renal proximal tubular cells in suspension with  $IC_{50}$  values of 250 to 500  $\mu M$ . The  $IC_{50}$  for amiloride is greater than 1 mM.

### *Others*

Amiloride is a noncompetitive inhibitor of acetylcholinesterase, with an  $IC_{50}$  in the range of 20 to 60  $\mu M$ ,<sup>43</sup> and is a noncompetitive inhibitor of rat and human renal kallekrein with an  $IC_{50}$  in the 85 to 230  $\mu M$  range.<sup>44</sup> Amiloride is a competitive inhibitor of monoamine oxidase activity measure in rat brain homogenate.<sup>45</sup> Amiloride inhibits urokinase-type plasminogen activator with an  $IC_{50}$  7  $\mu M$ .<sup>46</sup> Amiloride does not inhibit tissue-type plasminogen activator.

## DNA, RNA, and Protein Synthesis

### *DNA and RNA Synthesis*

Amiloride inhibits growth factor-induced DNA, RNA, and protein synthesis.<sup>7,47</sup> The effect of amiloride on DNA and RNA synthesis may be indirect. Lowering the extracellular  $Na^+$  concentration inhibits DNA and RNA synthesis, suggesting that entry of  $Na^+$  into cells may be a requirement for these events. In addition, amiloride analogs inhibit DNA replication with  $IC_{50}$  values similar to that observed for inhibition of  $Na^+/H^+$  exchange.<sup>7</sup> Amiloride may also have a direct inhibitory effect on DNA and RNA synthesis. Amiloride and several of its analogs have been shown to intercalate into DNA and to inhibit DNA topoisomerase II.<sup>48</sup>

### *Protein Synthesis*

Amiloride inhibits protein synthesis, as measured by incorporation of radiolabeled amino acids into proteins in both intact cells and cell-free reticulocyte lysate<sup>20,47,49,50</sup> with an  $IC_{50}$  between 100 and 400  $\mu M$ . The  $IC_{50}$  varies with the cell type studied. The  $IC_{50}$  for inhibition of synthesis of individual proteins may also vary.<sup>49</sup> Amiloride lowers both the initial rate

<sup>43</sup> D. Dannenbaum and K. Rosenheck, *Biophys. J.* **49**, 370a (abstr.) (1986).

<sup>44</sup> H. S. Margolius and J. Chao, *J. Clin. Invest.* **65**, 1343 (1980).

<sup>45</sup> V. Palaty, *Can. J. Physiol. Pharmacol.* **63**, 1586 (1985).

<sup>46</sup> J.-D. Vassalli and D. Belin, *FEBS Lett.* **214**, 187 (1987).

<sup>47</sup> K. S. Koch and H. L. Leffert, *Cell (Cambridge, Mass.)* **18**, 153 (1979).

<sup>48</sup> J. M. Besterman, L. P. Elwell, E. J. Cragoe, Jr., C. W. Andrews, and M. Cory, *J. Biol. Chem.* **265**, 2324 (1989).

<sup>49</sup> H. L. Leffert, K. S. Koch, M. Fehlmann, W. Heiser, P. J. Lad, and H. Skelly, *Biochem. Biophys. Res. Commun.* **108**, 738 (1982).

<sup>50</sup> M. Lubin, F. Cahn, and B. A. Countermarsh, *J. Cell. Physiol.* **113**, 247 (1982).

of incorporation of [ $^{35}\text{S}$ ]methionine as well as plateau levels of [ $^{35}\text{S}$ ]methionine-labeled proteins.<sup>49</sup> In cell-free systems, amiloride analogs bearing hydrophobic substituents on the 5-amino moiety have similar  $\text{IC}_{50}$  values for inhibition of protein synthesis. However, in intact cells the  $\text{IC}_{50}$  of these analogs varies over 25-fold, suggesting that amiloride analogs may inhibit protein synthesis in intact cells indirectly through inhibition of ion transport.<sup>20</sup> The mechanism by which amiloride directly inhibits protein synthesis in cell-free systems is unclear.

### Amiloride and Amiloride Analogs as Probes for Characterizing Transport Proteins

#### *Solubility Characteristics*

Amiloride and many of its analogs are soluble in aqueous solutions at concentrations less than 1 to 10 mM. Stock solutions of most amiloride analogs may be made in dimethyl sulfoxide (DMSO) at concentrations of 1 M. We generally store stock solutions at  $10^{-2}$  M protected from light at  $-20^{\circ}$ .

#### *Absorption and Fluorescence Characteristics*

Three major absorption peaks have been observed for amiloride and several analogs at approximately 360 to 370 nm, 265 to 290 nm, and 215 to 235 nm. Extinction coefficients at these wavelengths are in the range of 10,000 to 25,000  $\text{M}^{-1} \text{cm}^{-1}$ . The absorption peaks are broad and vary slightly among the different analogs and with the solvent system used. Amiloride analogs are highly fluorescent aromatic compounds. Amiloride has excitation maxima at 286 and 360 nm, and an emission maximum at 410 to 415 nm.<sup>23</sup> The fluorescence and absorption properties of the analogs may interfere with techniques which utilize fluorescent probes to measure intracellular pH and intracellular  $\text{Ca}^{2+}$ . Amiloride may quench the fluorescence of both acridine orange and carboxyfluorescein, probes which have been used to measure intravesicular and intracellular pH. The absorption peak of amiloride at 360 nm may interfere with the absorption of quin2 (excitation at 342 nm) and Fura-2 (excitation at 340 and 380 nm), probes which have been used to measure intracellular calcium ions.

#### *Intracellular Accumulation*

Several studies have shown that amiloride accumulates within cells. Amiloride and its analogs may diffuse or be transported across membranes. Amiloride has been shown to be transported across the plasma membrane

of hepatocytes and reach an intracellular concentration 10-fold greater than the extracellular concentration,<sup>49</sup> assuming that cellular amiloride was free in solution and not bound to lipid or compartmentalized. Amiloride accumulates within frog skin epithelial cells<sup>51</sup> and within A431 cells<sup>23</sup> at intracellular concentrations greater than the extracellular concentration. Amiloride diffuses across red blood cell and neutrophil plasma membranes with a permeability coefficient of approximately  $10^{-7}$  cm·sec<sup>-1</sup>.<sup>52,53</sup> In neutrophils 75% of the intracellular amiloride was considered to be in the lysosomal compartment.<sup>53</sup> In other cell types, the extent to which intracellular amiloride is compartmentalized is uncertain.

### *Radiolabeled Amiloride Analogs*

[<sup>14</sup>C]Amiloride has been synthesized with a specific activity of 54 mCi/mmol by the reaction of [<sup>14</sup>C]guanidine with methyl 3,5-diamino-6-chloropyrazinecarboxylate.<sup>2</sup> This procedure has been used to synthesize other [<sup>14</sup>C]-labeled analogs.

A number of tritium-labeled amiloride analogs have been synthesized, including [phenyl-<sup>3</sup>H]phenamil, [benzyl-<sup>3</sup>H]benzamil,<sup>54</sup> and [benzyl-<sup>3</sup>H]-6-bromobenzamil, with specific activities between 2 and 21 Ci/mmol. These analogs have been synthesized by the reaction of 1-methyl-2-(3,5-diamino-6-chloropyrazinoyl) pseudothiourium iodide or its 6-Br analog with [<sup>3</sup>H]aniline or [<sup>3</sup>H]benzylamine.<sup>4,55</sup> 6-[methyl-<sup>3</sup>H]Bromomethylamiloride has been synthesized by the reaction of bromoamiloride with [<sup>3</sup>H]CH<sub>3</sub>I with a specific activity of 1 Ci/mmol.<sup>56</sup> The methyl group is attached to the guanidino nitrogen atom adjacent to the carbonyl moiety. Both 5-([N-ethyl-N-<sup>3</sup>H]propyl)amiloride and 5-([N-methyl-N-<sup>3</sup>H]isobutyl)amiloride have been synthesized with specific activities of 2 and 28 Ci/mmol, respectively.<sup>57,58</sup>

6-[<sup>125</sup>I]Iodoamiloride and a number of 6-[<sup>125</sup>I]iodoamiloride analogs have been synthesized by reacting 6-H amiloride analogs with <sup>125</sup>ICl.<sup>59</sup> A

<sup>51</sup> J. V. Briggman, J. S. Graves, S. S. Spicer, and E. J. Cragoe, Jr., *Histochem. J.* **15**, 239 (1983).

<sup>52</sup> D. J. Benos, J. Reyes, and D. G. Shoemaker, *Biochim. Biophys. Acta* **734**, 99 (1983).

<sup>53</sup> L. Simchowitz, O. W. Woltersdorf, Jr., and E. J. Cragoe, Jr., *J. Biol. Chem.* **262**, 15875 (1987).

<sup>54</sup> A. W. Cuthbert and J. M. Edwardson, *J. Pharm. Pharmacol.* **31**, 382 (1979).

<sup>55</sup> E. J. Cragoe, Jr., O. W. Woltersdorf, Jr., and S. J. deSolms, U.S. patent 4,246,406 (1981).

<sup>56</sup> K. Lazorick, C. Miller, S. Sariban-Sohraby, and D. Benos, *J. Membr. Biol.* **86**, 69 (1985).

<sup>57</sup> P. Vigne, C. Frelin, M. Audinot, M. Borsotto, E. J. Cragoe, Jr., and M. Lazdunski, *EMBO J.* **3**, 2647 (1984).

<sup>58</sup> 5-(N-Methyl-N-<sup>3</sup>H-isobutyl)amiloride was prepared by New England Nuclear by the catalytic tritiation of 5-[N-methyl-N-(2-methylallyl)amiloride.

<sup>59</sup> D. Cassel, M. Rotman, E. J. Cragoe, Jr., and P. Igarashi, *Anal. Biochem.* **170**, 63 (1988).



new amiloride analog bearing a 4'-hydroxyphenethyl moiety may also prove useful in synthesis of radioiodinated amiloride analogs.<sup>4</sup>

### *Binding Assays Using Radiolabeled Amiloride Analogs*

Several recent studies have used radiolabeled amiloride analogs to identify and characterize binding sites of amiloride analogs in plasma membranes or microsomal membranes derived from cells known to have amiloride-sensitive transporters. Analogs bearing substituents on the 5-amino group, including 5-([N-methyl-N-<sup>3</sup>H]isobutyl)amiloride and 5-([N-ethyl-N-<sup>3</sup>H]propyl)amiloride have been used to characterize binding to the putative Na<sup>+</sup>/H<sup>+</sup> exchanger.<sup>54,60</sup> [<sup>3</sup>H]Benzamil, [<sup>3</sup>H]phenamil, and 6-[<sup>3</sup>H]bromomethylamiloride have been used to characterize binding to the epithelial Na<sup>+</sup> channel and to follow the channel during solubilization and purification.<sup>61-66</sup> Methods for assaying the binding of amiloride analogs to membranes and to detergent-solubilized proteins are outlined below.

**Equilibrium Dialysis.** Binding of [<sup>3</sup>H]benzamil to the epithelial Na<sup>+</sup> channel in renal cortical microsomal membranes is measured by equilibrium dialysis with  $M_r$  12,000–14,000  $M_r$  cutoff dialysis tubing. Membrane vesicles (approximately 250  $\mu$ g of protein) in a phosphate buffer and [<sup>3</sup>H]benzamil are placed in dialysis tubing, which is then placed in a test tube with 7.5 ml of buffer containing the same concentration of [<sup>3</sup>H]benzamil. The tubes are stirred on a flat-bed rotary mixer for 16 hr at 4 °C, by which time equilibrium is achieved. Aliquots are removed from the dialysis bag and dialysed and counted. Protein determinations on aliquots from the dialysis bag are performed. Nonspecific binding is determined in parallel experiments in which 1  $\mu$ M unlabeled benzamil is added to the microsomes and dialysate.

**Filtration Assay.** Measurement of the binding of [<sup>3</sup>H]benzamil to membrane vesicles may also be performed using filtration to separate bound from free drug. Glass fiber filters have been used to bind the

<sup>60</sup> S. J. Dixon, S. Cohen, E. J. Cragoe, Jr., and S. Grinstein, *J. Gen. Physiol.* **88**, 19a (abstr.) (1986).

<sup>61</sup> T. R. Kleyman, T. Yulo, C. Ashbaugh, D. Landry, E. Cragoe, Jr., A. Karlin, and Q. Al-Awqati, *J. Biol. Chem.* **261**, 2839 (1986).

<sup>62</sup> A. W. Cuthbert and J. M. Edwardson, *Biochem. Pharmacol.* **30**, 1175 (1981).

<sup>63</sup> T. Kleyman, T. Yulo, E. J. Cragoe, Jr., and Q. Al-Awqati, *Kidney Int.* **29**, 400 (abstr.) (1986).

<sup>64</sup> P. Barby, O. Chassande, P. Vigne, C. Frelin, C. Ellory, E. J. Cragoe, Jr., and M. Lazdunski, *Proc. Natl. Acad. Sci. U.S.A.* **84**, 4836 (1987).

<sup>65</sup> S. Sariban-Sohraby and D. J. Benos, *Biochemistry* **25**, 4639 (1986).

<sup>66</sup> D. J. Benos, G. Saccomani, B. M. Brenner, and S. Sariban-Sohraby, *Proc. Natl. Acad. Sci. U.S.A.* **83**, 8525 (1986).

vesicles, with minimal nonspecific trapping of the drug on the filter paper. Nitrocellulose and cellulose acetate filter paper should not be used, as there is considerable nonspecific trapping of the radiolabeled amiloride analog on the filter.

**Rapid Gel Filtration Assay.** The binding of [ $^3\text{H}$ ]benzamil to the putative  $\text{Na}^+$  channel using detergent-solubilized membrane proteins is measured by a rapid gel filtration assay. Sephadex G-25 (fine grade) is swollen with water and washed with buffer used for solubilization (200 mM sucrose, 1 mM EGTA, and 10 mM Tris-Cl, pH 8.0, with the addition of protease inhibitors). A saturating concentration of [ $^3\text{H}$ ]benzamil (final concentration = 50 nM) is added to solubilized proteins (total volume = 200  $\mu\text{l}$ ) and incubated on ice for > 10 min, by which time equilibrium has been achieved. The mixture is placed over a 1.5-ml column in a 3-ml plastic syringe (using Whatman grade 1 filter paper for support) which is suspended in a plastic test tube, and then spun at 500 g for 30 sec (the speed and duration of the spin must be optimized). The eluate is weighed to determine the total volume and aliquots are removed for counting and for protein determination. In parallel assays, 5  $\mu\text{M}$  benzamil is added to the incubation mixture to determine nonspecific binding (see also Refs. 64 and 65).

### Photoaffinity Labels

Two major photoreactive groups, arylhalides and aromatic ethers, have been used in the development of photoactive amiloride analogs. Photolysis of 6-bromo, 6-iodo, or 6-chloro analogs of amiloride can lead to the formation of a free radical, and subsequent covalent incorporation into adjacent proteins. This approach has been used to identify putative subunits of the epithelial  $\text{Na}^+$  channel, using 6- $^3\text{H}$ ]bromobenzamil and 6- $^3\text{H}$ ]bromomethylamiloride as photoreactive amiloride analogs that bind to the  $\text{Na}^+$  channel with both high affinity and specificity.<sup>61,67</sup> Amiloride and 6-bromobenzamil have a major absorption peak at 360 nm, and we have used this wavelength of light to photoactivate 6-bromobenzamil.<sup>61</sup> 5-(*N*-Ethyl-*N*-isopropyl)-6- $^{14}\text{C}$ ]bromoamiloride has been used to label the  $\text{Na}^+/\text{H}^+$  exchanger.<sup>68</sup>

Aromatic ethers have been shown to undergo photoactivation and photoincorporation into proteins by the mechanism of aromatic nucleophilic photosubstitution.<sup>69</sup> Photoreactive amiloride analogs have been syn-

<sup>67</sup> D. J. Benos, G. Saccomani, and S. Sariban-Sohraby, *J. Biol. Chem.* 262, 10613 (1987).

<sup>68</sup> T. Friedrich, J. Sablotni, and G. Burckhardt, *J. Membr. Biol.* 94, 253 (1986).

<sup>69</sup> J. Cornelisse and E. Havinga, *Chem. Rev.* 75, 353 (1975).

thesized with a 2'-methoxy-5'-nitrobenzyl moiety located either on the terminal nitrogen atom of the guanidino moiety or on the 5-amino moiety (which also bears an ethyl group). These drugs undergo photoactivation with 313-nm wavelength light. 2'-Methoxy-5'-nitrobenzamil has been used to photolabel and identify the amiloride-binding subunit of the epithelial  $\text{Na}^+$  channel.<sup>70</sup> An analog with the photoreactive group on the 5-amino moiety has been used to label the  $\text{Na}^+/\text{H}^+$  exchanger.<sup>71</sup> Anti-amiloride antibodies were used to detect these photolabels after photoincorporation into the channel or exchanger.<sup>70-72</sup> Radioactive counterparts of these analogs have recently been synthesized.<sup>59,73</sup>

*Methods for Photoaffinity Labeling the Binding Sites of Amiloride Analogs.* Sodium ion channel-containing microsomes (150  $\mu\text{g}/\text{ml}$ ) are preequilibrated for 1 hr in a phosphate buffer containing protease inhibitors and 20 nM 6-[ $^3\text{H}$ ]bromobenzamil (the concentration of the photolabel will depend on the affinity of the amiloride analog for the particular transporter) and then gassed for 5 min with  $\text{N}_2$ . The vesicles are photolyzed with a 50-W high-pressure mercury arc lamp with 300–400 band pass and  $>345$  long pass filters. The solution is constantly stirred, cooled in a water jacket to  $4^\circ$ , and the surface gassed with  $\text{N}_2$ . The vesicles are initially photolyzed for varying times to determine the optimal duration of photolysis by measuring photoincorporation of tritium into trichloroacetic acid-precipitable protein. To identify labeled proteins following photolysis, the microsomes are collected by centrifugation and then analyzed by SDS-PAGE and autofluorography. Photolabeling with 2'-methoxy-5'-nitrobenzamil is performed under similar conditions using a 313-nm narrow band pass filter.

### Affinity Matrices

Amiloride has been coupled to support matrices through either the terminal nitrogen atom of the guanidino moiety or through the 5-amino group of the pyrazine ring. Three separate methods have been used to couple amiloride to a matrix through the guanidino moiety. One method has been used to couple through the 5-amino moiety.

Amiloride has been coupled directly to cyanogen bromide-activated Sepharose.<sup>66</sup> Alternatively, a reactive amiloride precursor, 1-methyl-2-

<sup>70</sup> T. R. Kleyman, E. J. Cragoe, Jr., and J. P. Kraehenbuhl, *J. Biol. Chem.* **264**, 11995 (1989).

<sup>71</sup> D. Warnock, T. Kleyman, and E. J. Cragoe, Jr., *FASEB J.* **2**, A753 (abstr.) (1988).

<sup>72</sup> T. R. Kleyman, R. Rajagopalan, E. J. Cragoe, Jr., B. F. Erlanger, and Q. Al-Awqati, *Am. J. Physiol.* **250**, C165 (1986).

<sup>73</sup> T. R. Kleyman, unpublished observations.

(3,5-diamino-6-chloropyrazinoyl) pseudothiourium iodide,<sup>4,55</sup> was allowed to react with aminohexyl-Sepharose in the presence of a hindered base (triethylamine). The product was amiloride coupled to Sepharose through a six-carbon spacer arm.<sup>63</sup> A mixed anhydride of an amiloride analog bearing a 5'-carboxypentyl group on the terminal guanidino nitrogen atom was synthesized using isobutyl chloroformate, and then coupled to albumin. Coupling to aminohexyl-Sepharose by this method should be straightforward. The amiloride-albumin complex was subsequently coupled to Sepharose, and has been used to affinity purify anti-amiloride antibodies.<sup>72</sup> An amiloride analog bearing a 5-[N-(3-isothiocyanatophenyl)] moiety has been coupled directly to dextran and aminohexyl-Sepharose.<sup>74,75</sup>

### *Anti-Amiloride Antibodies*

An amiloride analog bearing a 5-carboxypentyl group on the terminal nitrogen of the acylguanidino moiety of amiloride was coupled to albumin by generation of a mixed anhydride. Approximately 10 mol of amiloride was bound/mol of albumin. The amiloride-bovine serum albumin was used to raise anti-amiloride antibodies in rabbits, which were subsequently affinity purified with an amiloride-rabbit serum albumin affinity column.<sup>72</sup> Utilizing amiloride coupled to albumin as an immunogen and rabbit anti-amiloride antibodies in the screening assay, monoclonal anti-idiotypic antibodies that recognize the epithelial Na<sup>+</sup> channel have recently been raised.<sup>76</sup> 5-[N-(3-Isothiocyanatophenyl)]amiloride has been coupled to albumin and used to raise anti-amiloride antibodies.<sup>75</sup> Antibodies raised against amiloride coupled to albumin through the acylguanidino group or the 5-amino group (using 5-[N-(3-isothiocyanatophenyl)]amiloride) recognize distinct epitopes on amiloride.<sup>75</sup>

### *Summary*

The use of amiloride and its analogs in the study of ion transport requires a knowledge of the pharmacology of inhibition of transport proteins, and of effects on enzymes, receptors, and other cellular processes, such as DNA, RNA, and protein synthesis, and cellular metabolism. We have reviewed the pharmacology of inhibition of these processes by ami-

<sup>74</sup> D. Cassel, E. J. Cragoe, Jr., and M. Rotman, *J. Biol. Chem.* 262, 4587 (1987).

<sup>75</sup> T. R. Kleyman, J. P. Kraehenbuhl, B. C. Rossier, E. J. Cragoe, Jr., and D. G. Warnock, *Am. J. Physiol.* 257, C1135 (1989).

<sup>76</sup> T. R. Kleyman, B. Rossier, B. F. Erlanger, and J. P. Kraehenbuhl, *Kidney Int.* 35, 160 (abstr.) (1989).

loride and its analogs, as well as the use of amiloride analogs as potential probes for the characterization of ion transport systems.

### Acknowledgments

The authors are grateful to Drs. A. George and G. Kaczorowski for reviewing the manuscript, and to Drs. G. Fanelli, G. Kaczorowski, A. Karlin, and L. Simchowicz for providing unpublished data on inhibition of  $\text{Na}^+$  transport systems by amiloride analogs. This work was supported by the Zyma Foundation and by Grant AM34742 from the United States Public Health Service. T.R.K. is a recipient of Clinician-Scientist Award from the American Heart Association.

## [43] Photoaffinity-Labeling Analogs of Phlorizin and Phloretin: Synthesis and Effects on Cell Membranes

By DONALD F. DIEDRICH

### Introduction<sup>1</sup>

The inhibitory effects of the glucoside phlorizin (I, Fig. 1) and its aglycone, phloretin (IA, Fig. 1), on the sugar transport systems in a variety of cell types have been examined by many workers. The  $\text{Na}^+$ -coupled, D-glucose cotransporter in renal and intestinal brush border epithelial membranes is especially sensitive to phlorizin at low micromolar levels while phloretin is almost inactive. This vulnerability to the glycoside distinguishes the brush border system from the  $\text{Na}^+$ -independent, equilibrating sugar transporter in the basolateral membrane of these cells; the latter resembles the erythrocyte transporter in being inhibited at low micromolar levels of phloretin (by a strictly competitive mechanism), but not the glucoside, which is at least 100 times less potent. This is somewhat puzzling since one intuitively might think that phlorizin's glucosidic moiety should compete for the sugar-binding site on both transporters. Yet, even though the receptor site of the equilibrating system possesses a high-affinity inhibitory site for phloretin, the  $\beta$ -glucosidic group of phlorizin either prevents the binding or negates the inhibitory effect of the aglycone moiety. Con-

Abbreviations include *p*-AmBPht and *p*-AzBPht (*p*-aminobenzyl phloretin and *p*-azidobenzylphloretin, respectively), *p*-AmBPhtz and *p*-AzBPhtz (*p*-aminobenzylphlorizin and *p*-azidobenzylphlorizin, respectively); TLC, thin-layer chromatography; BBMVs, brush border membrane vesicles; SDS-PAGE, sodium dodecyl sulfate-polyacrylamide gel electrophoresis.

# Review

## Apoptosis, Oncosis, and Necrosis

### An Overview of Cell Death

Guido Majno and Isabelle Joris

*From the Department of Pathology, University of Massachusetts Medical School, Worcester, Massachusetts*

*The historical development of the cell death concept is reviewed, with special attention to the origin of the terms necrosis, coagulation necrosis, autolysis, physiological cell death, programmed cell death, chromatolysis (the first name of apoptosis in 1914), karyorrhexis, karyolysis, and cell suicide, of which there are three forms: by lysosomes, by free radicals, and by a genetic mechanism (apoptosis). Some of the typical features of apoptosis are discussed, such as budding (as opposed to blebbing and zellösung) and the inflammatory response. For cell death not by apoptosis the most satisfactory term is accidental cell death. Necrosis is commonly used but it is not appropriate, because it does not indicate a form of cell death but refers to changes secondary to cell death by any mechanism, including apoptosis. Abundant data are available on one form of accidental cell death, namely ischemic cell death, which can be considered an entity of its own, caused by failure of the ionic pumps of the plasma membrane. Because ischemic cell death (in known models) is accompanied by swelling, the name oncosis is proposed for this condition. The term oncosis (derived from *ónkos*, meaning swelling) was proposed in 1910 by von Recklinghausen precisely to mean cell death with swelling. Oncosis leads to necrosis with karyolysis and stands in contrast to apoptosis, which leads to necrosis with karyorrhexis and cell shrinkage. (*Am J Pathol* 1995, 146:3-15)*

Knowledge in the field of cell death has greatly increased during the past 20 years or so. In the course

of this rapid advance, new concepts, such as apoptosis, appeared on the scene, and ancient terms such as necrosis came to be used in a new context. Inevitably, some conceptual and semantic strains developed; a recent reviewer saw fit to conclude that "there is no field of basic cell biology and cell pathology that is more confusing and more unintelligible than is the area of *apoptosis versus necrosis*."<sup>1</sup> The purpose of this paper is to offer a critical and, we hope, constructive overview of the terms and concepts related to cell death.

It will be useful to begin by tracing the main steps that led us to where we now stand.

#### Development of the Cell Death Concept

The fact that cells can perish is discussed in Lecture XV of Virchow's *Cellular Pathology* among "passive processes and degenerations."<sup>2</sup> Understandably, no microscopic description of cell death is included, as histological stains were not used in 1858. Thus, topics related to cell death are treated in this lecture at a gross level, under names such as degeneration, softening, necrosis, and mortification, which was synonymous with gangrene. For our present purposes it is relevant to note that Virchow uses necrosis to mean an advanced stage of tissue breakdown, similar to what we would now call gangrene: "In necrosis we

Supported in part by National Institutes of Health Grant DK 32520 (IJ).

Accepted for publication August 10, 1994.

Address reprint requests to Dr. Guido Majno, Department of Pathology, University of Massachusetts Medical Center, 55 Lake Avenue North, Worcester, MA 01655-0125.

We dedicate this paper to the memory of Dr. Marcel Beaulieu, pioneer in the study of cell death, eminent clinician, and founder of the first Institute of Cellular Pathology, who passed away in Paris on March 28, 1994.

conceive the mortified [gangrenous] part to be preserved more or less in its external form" (p. 358). This had been the traditional usage of the term necrosis, not only in the textbook of Virchow's teacher Rokitan-sky<sup>3</sup> but also, as *nécrosis*, in ancient Greek texts at least since Galen.<sup>4</sup>

Virchow's Lecture XV also creates a special category of regressive processes under the name necrobiosis, a term he borrowed from a contemporary author, K. H. Schultz. Included among the necrobiotic processes, for example, were the "softenings." Necrobiosis is thus defined, perhaps, to fit the model of brain softening: "The part vanishes, so that we can no longer perceive it in its previous form. We have no necrosed fragment at the end of the process." A footnote extends the definition (emphasis original): "Necrobiosis is death brought on by (altered) life - a spontaneous wearing out of living parts - the destruction and annihilation consequent upon life - natural as opposed to violent death (mortification)." The use of necrobiosis throughout Virchow's book and later indicates that this term was sometimes meant to imply also "slow death" or "death of tissues within the living body." Needless to say, necrobiosis was a vague and ambiguous term. After a long career it is finally disappearing. Another term from Virchow's Lecture XV that needs rethinking is degeneration. Virchow's "fatty degeneration" still clings on<sup>5</sup>; it should be banished, because cells can die but certainly cannot degenerate into something else. In our opinion, there are few defensible uses of this term in general pathology; we can think of two: for the breakdown of axons, as in Wallerian degeneration, and for the breakdown of cartilage matrix in degenerative osteoarthritis.

The next step, around 1877, was the identification of coagulation necrosis by Carl Weigert and Julius Cohnheim. Today this term evokes a rather obvious and noncontroversial lesion, mainly the white infarct, but this was not true in the beginning, when it applied to a condition that in our view has virtually nothing to do with coagulation necrosis.

When Carl Weigert (1845-1904) was training under Virchow, diphtheria was a common cause of death, as the vaccine was not available before 1880. Diphtheria causes necrosis of the tracheobronchial epithelium, which becomes impregnated with fibrin and leukocytes and tends to slough off as a leathery, whitish pseudomembrane (*diphthéra* is Greek for tanned hide). Weigert, who was especially interested in fibrin (witness the fibrin stain of his name), became impressed by this combination of epithelial necrosis and fibrin.<sup>6-9</sup> He held the current view that dead leukocytes cause fibrinogen to coagulate and proposed that the same mechanism that produced the diph-

theritic pseudomembrane was at work also in producing what we now call white infarcts. He even referred to the typical wedge-shaped white infarcts as fibrin wedges (*Fibrinkeile*).<sup>9</sup> Julius Cohnheim, another disciple of Virchow, accepted this view and introduced, in the 1877 edition of his textbook, the term coagulation necrosis.<sup>10</sup> Soon the fibrin component was found to be unrelated to the coagulation of the tissue<sup>11</sup>; today Weigert's concept survives only in what we call fibrinous necrosis. However, an important byproduct of Weigert's studies was the observation that necrotic cells lose their nuclei.<sup>6</sup>

The role of protein denaturation in the genesis of coagulation necrosis was vaguely hinted in Cohnheim's textbook<sup>10</sup>; it could not escape the pathologists' attention that necrotic tissue looked like "coagulated albumen."<sup>12</sup> Interestingly, the notion that protein denaturation may participate in cell death was first proposed in 1886 by a botanist, G. Berthold.<sup>13,14</sup> This is just one of the many contributions made by plant pathology to animal pathology, the latest one being the tetrazolium method for detecting dead tissue on gross specimens, originally used by botanists for identifying nonviable seeds (reviewed in reference 15).

Weigert's notion of coagulation necrosis had the virtue of triggering, after 1880, many experimental studies on cell death,<sup>16</sup> produced by ligating the renal artery, by maintaining tissue fragments septicly or aseptically *in vitro*,<sup>11</sup> or by introducing them into the peritoneal cavity of experimental animals.<sup>17</sup> Much of the present terminology of cell death, besides coagulation necrosis, stems from that era. Autolysis was proposed in 1900, although the concept was known earlier.<sup>13,16,18</sup> Pyknosis was in use around 1890.<sup>19</sup> Karyolysis and karyorrhexis were proposed in 1879<sup>20</sup> by Edwin Klebs of Klebsiella fame (he spelled his Karyorrhexis right, but the erroneous Karyorrhexis appeared in the title of an 80-page paper in 1890<sup>19</sup> and has lasted ever since). Chromatin margination (Randstellung) was described in 1890.<sup>17</sup> Some terms born in those days changed meaning, such as chromatolysis (1885),<sup>21</sup> and others disappeared, such as plasmarhexis,<sup>20</sup> chromatopyknosis, and deconstitution.<sup>22</sup>

Spontaneous cell death as a physiological event was discussed almost as soon as stains became available. It was born with a bang in 1885 in a paper<sup>21</sup> by the same Walther Flemming who created the terms chromatin and mitosis.<sup>23</sup> Flemming studied ovarian follicles in mammals and noticed that the epithelial lining of regressing follicles was littered with cells the nuclei of which were breaking up (Figure 1).<sup>21</sup> His careful *camera lucida* drawings illustrate the half-



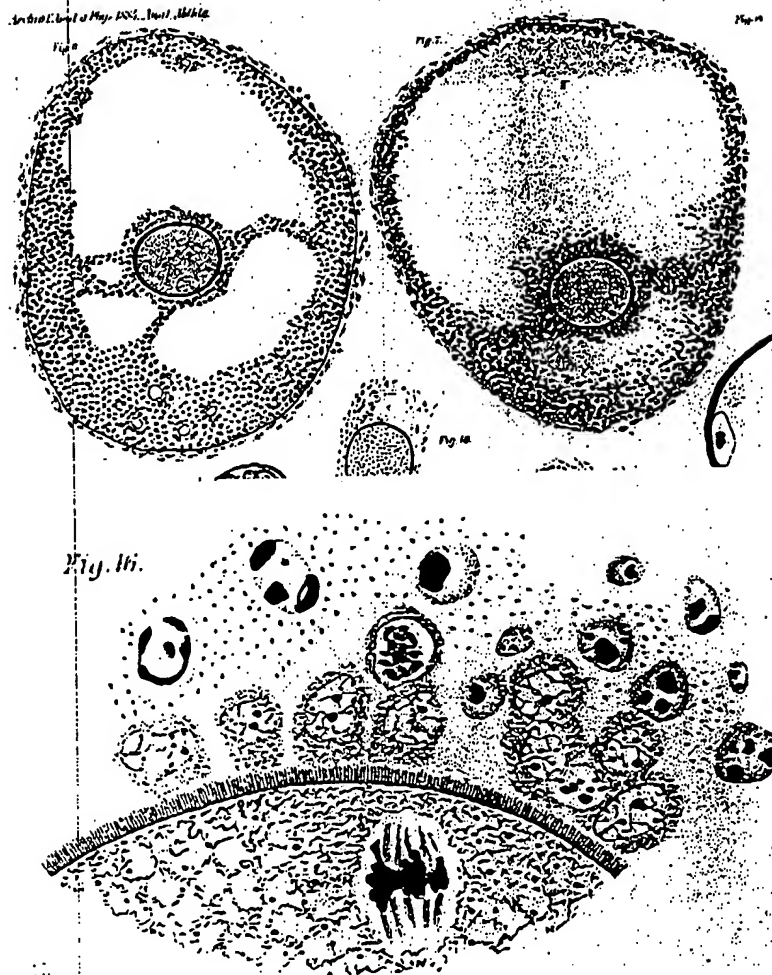


Figure 1. Apoptosis as observed in 1885 by Flemming,<sup>21</sup> who called it chromatolysis. Top left: Normal rabbit ovarian follicle near maturity, 1 mm in diameter. Numerous epithelial mitoses. Top right: Early stage of involution in a nearby follicle. Many epithelial cells are in various stages of death by chromatolysis; some are shed into the lumen. Bottom: detail of the same involuting follicle. Most epithelial cells in contact with the ovum are normal (one is in mitosis); those further removed are undergoing chromatolysis. Note the half-moons of chromatin typical of apoptosis. (Osmium fixation; safranin and gentian violet staining. Camera lucida drawings.)

moons of pyknotic chromatin typical of apoptosis (Figure 1) as well as apoptotic bodies loose in the cavity of the follicle. Flemming gave a name to the process, chromatolysis, referring to the fact that the broken up nucleus ultimately disappears. A few months later the same observations were published by a German medical student, Franz Nissen,<sup>24</sup> who observed chromatolysis also in lactating mammary glands (Figure 2).

Chromatolysis and nuclear pathology became a fashionable topic<sup>25,19</sup>; beautiful examples of what we would label apoptosis were seen in breast cancers by Ströbe,<sup>26</sup> and by 1914 enough data were available for a German anatomist, Ludwig Gräper, to publish a paper entitled (in translation) "A new point of view regarding the elimination of cells."<sup>27</sup> Gräper's premise is that some mechanism must exist to counterbalance mitosis, especially in epithelia, and concludes that Flemming's chromatolysis is the answer: "Chroma-

tolysis must exist in all organs in which cells must be eliminated" (p. 377). The debris, he writes, are taken up by neighboring epithelial cells, but sometimes they are so abundant that they are eliminated into an organ's lumen, as is the case for "uterine milk" (both features are typical of what we now call apoptosis). Gräper also experiments on the yolk sac, which, he argues, must shrink progressively; its cells do not shrink, so the sac as a whole could only become smaller by one of two mechanisms: 1) by developing folds or 2) by eliminating cells, which Gräper recognizes as the right answer (Figure 3). Gräper concludes that the "physiologische Zellelimination" occurs by chromatolysis during the shrinkage of organs, as well as normally in certain glands. In essence, "a sister cell [Schwesterzelle] engulfs a neighboring cell that breaks down" (p. 391). An interesting side issue comes up as Gräper points out that the persistent descriptions of so-called amitosis (nuclear division

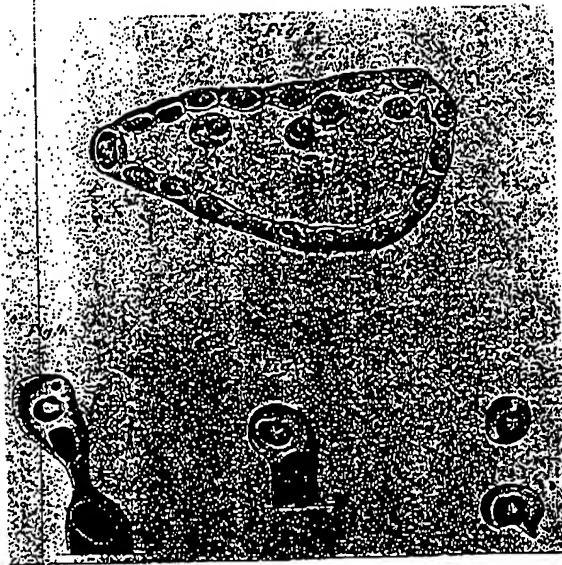


Figure 2. Apoptosis as seen in 1886 by a German medical student, Franz Nissen, in the lactating mammary gland.<sup>24</sup> Nissen became aware of Flemming's study,<sup>21</sup> after having completed his own, and concluded that the name chromatolysis was very suitable also to his own findings.

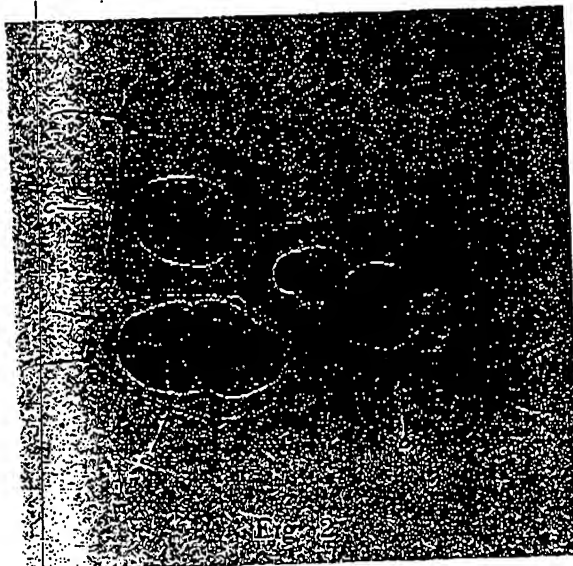


Figure 3. Apoptosis illustrated in 1914 by L. Gräper as chromatolysis.<sup>27</sup> Wall of the yolk sac in the course of involution, in a 20-cm embryo of *Acanthias*, a creature that we have been unable to identify. An epithelial cell has taken up the fragmented nucleus of a neighboring cell that died during the involution process.

without mitosis) were due to the erroneous interpretation of cells that had taken up nuclear material from a nearby cell that died by chromatolysis.

This milestone paper made no significant impact. Perhaps it was overlooked because it appeared at the outset of World War I in a German journal on cellular

investigation that many pathologists might have missed. The term chromatolysis was adopted by neuropathologists to mean something entirely different, namely the apparent breakdown of Nissl substance after transection of the axon. However, the original concept of chromatolysis did survive among embryologists, who understood its importance as a morphogenetic mechanism. This line of studies was summarized in a masterly paper by Glücksmann in 1950.<sup>28</sup> Here is his description of physiological cell death in the embryo.

"The initial stage, chromatopycnosis, consists ... in the appearance of a single chromatic mass sitting as a cap on the vacuole formed by the non-chromatic material.... Both the nucleus and the cytoplasm ... shrink by the loss of fluid.... The granule loses its affinity for nuclear stains, becomes Feulgen-negative, breaks up and disappears: this is chromatolysis.... The degenerating cell may be phagocytosed by a neighbour." It is further specified that "the nucleus may break up into several pycnotic granules," and that "mitochondria rarely show changes" such as are found in cells exposed to injurious agents.

All this is, of course, another fine description of apoptosis. Glücksmann realized that he was describing a special form of cell death, but his studies were limited to cell death in embryonic tissues. Thus it was natural for him to assume that this particular form of cell death was characteristic of vertebrate ontogenesis and therefore different from, rather than applicable to, cell death in adult tissues. Gräper had gone farther.

Oddly enough, the role of protein denaturation in cell death was not confirmed until 1960, by studies of optical density, light diffraction, and autofluorescence of dying and dead tissues.<sup>29</sup> These studies were carried out by the old method of implanting fragments of rat liver into the peritoneum of other rats. The following appear to be the basic rules of ischemic cell death for the liver; variations should be expected for other cell types:

- 1) Cell death and necrosis are very different entities. Ischemic cell death, defined functionally by the point of no return, occurs long before necrosis and is not detectable histologically (for rat liver the point of no return is known to occur at approximately to 2 to 2.5 hours); indeed, it is useful to point out that the difference between cell death and necrosis, biologically a key issue, has been completely overlooked in recent literature.<sup>2</sup>

- 2) Ischemic liver cells swell for 6 to 7 hours, then lose water and shrink (Figure 4). Early in the swelling process they die. We can now add that the swelling process is understood as a result of ion pump failure

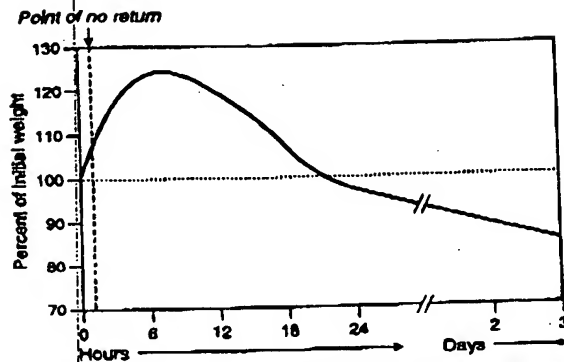


Figure 4. Curve obtained by weighing fragments of rat liver after they had been left in the peritoneal cavity of other rats for 0 to 72 hours. It shows that ischemic liver cells swell before they die, continue to swell thereafter, then shrink. The approximate time of cell death is indicated as the point of no return. Data from Majno et al.<sup>39</sup>

by lack of ATP and that the swelling is accompanied by intense blebbing (to be discussed further).

3) The dying and dead cell's proteins face two possible fates: hydrolysis and/or denaturation.

4) Protein denaturation begins while the cell is still alive, being detectable at 30 minutes. Today we can interpret this finding by assuming that the ubiquitin system, which targets denatured cells for hydrolysis by an energy-requiring system,<sup>30,31</sup> is overwhelmed and can no longer function for lack of ATP. The denaturation process is still going on after 12 days.

5) During ischemic cell death and the subsequent coagulation necrosis, large amounts of calcium are taken up by the affected cells.<sup>32</sup>

The concept of cell suicide surfaced for the first time after the lysosomes were discovered in the late 1950s. De Duve proposed that cells might be killed from within, by an explosion of their lysosomes acting as "suicide bags" (summarized in reference 15). The idea was soon discredited, but we now know that it is probably true in special circumstances, namely in the crystal diseases, in which leukocytes phagocytize crystals that break open the lysosomes (summarized in reference 15).

Free radical pathology appeared in the 1960s, and it led to the identification of another mechanism of cell suicide, especially in liver cells as a result of certain intoxications,<sup>33</sup> namely, the intracellular release of free radicals, which can damage cellular organelles (summarized in reference 15). This line of research helped lead to the proposal of a final common pathway for cell death from different causes, i.e., a rise in intracellular calcium.<sup>34,35</sup>

Then came apoptosis, the third and perhaps the ultimate form of cell suicide, purposeful suicide, and one of the most exciting developments in modern bi-

ology. The critical experiment (published in 1971) was extraordinarily simple; Kerr<sup>36</sup> induced liver atrophy in the rat by tying off a large branch of the portal vein. He noticed a discrete drop-off of cells by a sequence of changes that he called at first shrinkage necrosis and a year later apoptosis.<sup>37</sup> The next critical step came independently from the study of irradiated lymphoid tissues. It was known from histological studies that the nuclei of irradiated lymphocytes break down.<sup>38</sup> In 1976<sup>39</sup> and 1981<sup>40,41</sup> three groups examined electrophoretically the chromatin of irradiated tissues and found that it broke down into fragments that produced a typical, ladder-like pattern, suggesting that the fragments were multiples of nucleosomes.<sup>41</sup> Then Wyllie et al.<sup>42</sup> in 1984 linked the ladder pattern with the phenomenon of apoptosis and thereby added a specific biochemical marker to the distinctive morphological changes of apoptotic cells. This discovery led to an enormous increase in papers on apoptosis, with the latest developments in this field concerning the genes involved in cell suicide and the possibility of using apoptosis as an approach to tumor diagnosis and therapy.<sup>43-47</sup>

In retrospect, it is mind-boggling that earlier pathologists (ourselves included) paid so little attention to the mechanism of organ shrinkage during atrophy, even after it had been carefully described. Perhaps it appeared too simple and self-evident, or as dull as autolysis *in vivo*.<sup>48</sup> It is a fair guess that today the mechanism of atrophy would have a low priority in competing for grant support.

We will now examine more closely the two best known modalities of cell demise: cell death by suicide (apoptosis) and cell death by murder (accidental cell death).

### Cell Death by Suicide: Apoptosis

As mentioned earlier, cells can commit suicide by at least three mechanisms, but apoptosis stands out as a form of intentional suicide based on a genetic mechanism. For our purposes it will suffice to list the key features of apoptosis, as many comprehensive reviews are available.<sup>49-52</sup>

1) Apoptosis is a form of cell death characterized by morphological as well as biochemical criteria and can be considered as a counterpart of mitosis, as Gräper had proposed.

2) Morphologically the cell shrinks and becomes denser, as implied in the original name shrinkage necrosis.<sup>36</sup> The chromatin becomes pyknotic and packed into smooth masses applied against the nuclear membrane (margination of chromatin; Figure

5), creating curved profiles that have inspired descriptive terms for over a century, such as half-moon-, horse-shoe-, sickle-,<sup>19</sup> lancet-, and ship-like (navicular<sup>30</sup>). The nucleus may also break up (karyorhexis), and the cell emits processes (the budding phenomenon) that often contain pyknotic nuclear fragments. These processes tend to break off and become apoptotic bodies, which may be phagocytized by macrophages or neighboring cells or remain free; however, the cell may also shrink into a dense, rounded mass, as a single apoptotic body.

3) There is little or no swelling of mitochondria or other organelles.

4) Biochemically, the DNA is broken down into segments that are multiples of approximately 185 bp, due to specific cleavage between nucleosomes.

5) The process is under genetic control<sup>46,47</sup> and can be initiated by an internal clock, or by extracellular agents such as hormones, cytokines, killer cells, and a variety of chemical, physical, and viral agents.

6) Apoptosis can run its course very fast, even in minutes (34 minutes from the onset of budding to complete breakup in the movie by Bessis to be discussed below). For this reason apoptosis is remarkably unobtrusive in tissue sections.<sup>53</sup> In routine sections the best cytological marker of apoptosis is karyorhexis, especially in an isolated cell. Fortunately,

a recent technical advance makes the identification of apoptosis a matter of simple histochemistry, a method that takes advantage of the fact that the DNA breaking points (nicks) expose molecular endings that are chemically specific.<sup>54</sup>

7) The rapidly developing tale of apoptosis warns us that generalizations are dangerous because, first, cell suicide does not always take the form of apoptosis; second, cell murder by cytotoxic lymphocytes leads to apoptosis; third, there seem to be several varieties of apoptosis<sup>55</sup> and fourth, different cell types may follow different rules.<sup>2</sup>

The only flaw that we find in the name of apoptosis is that it includes both cell death (presumably represented by cell shrinkage and pyknosis) and necrosis (the secondary breakup into a cluster of apoptotic bodies). This has created some confusion: how can apoptosis be opposed to necrosis, as many authors do, if apoptosis produces classic images of necrosis? The remedy may be simple enough: the second phase of apoptosis should be called *apoptotic necrosis*, as opposed to ischemic, toxic, or massive necrosis (see below). Examples of apoptotic necrosis are the sunburn cells of the epidermis and the Councilman bodies of the liver.<sup>53</sup>

We might add that the Greek name apoptosis is most felicitous, suggesting as it does the discrete image of leaves dropping off here and there from a tree (*apó*, meaning from and *ptósis*, meaning a fall) as opposed to the massive cell death of an infarct. We will only note that the pronunciation *apo'tosis* (skipping the second *p*)<sup>37</sup> is not confirmed by the Greek scholars whom we have consulted. A recent letter to *Nature*<sup>56</sup> makes the same point: nobody says *helico'ters*.

### The Shrinkage and Condensation of Apoptotic Cells

It is interesting to compare these two features of apoptosis with the shrinkage and condensation that occur after ischemic cell death as a result of protein denaturation<sup>23</sup> (Figure 4). To this day, the shrinkage and condensation of the apoptotic cell are not explained.<sup>46</sup> Could they be rooted in the same mechanisms that operate in ischemic cell death? The increased density, visible on light and electron micrographs, could reflect the accumulation of denatured proteins, perhaps by failure of the ubiquitin system. Protein denaturation has been linked to increased intracellular calcium,<sup>34,35</sup> and in some forms



Figure 5. The two main regulators of cell populations, mitosis (bottom left) and apoptosis (top right). In the apoptotic cell, the nucleus is fragmented (karyorhexis) and the chromatin is pyknotic. One of the nuclear fragments contains a characteristic half-moon of condensed chromatin. (Electron micrograph from a rat prostate 2 days after castration. Bar = 2  $\mu$ ).

of apoptosis calcium does increase.<sup>46,56</sup> Because denatured proteins are autofluorescent, their presence in apoptotic cells should be fairly easy to test, and we are presently attempting to do so.

### The Budding Phenomenon

In their agony, cells dying by apoptosis emit a number of pseudopodia, a process that Kerr has aptly described as budding.<sup>50</sup> The emission of cellular processes, obvious on electron micrographs of apoptotic cells,<sup>50</sup> becomes dramatic when witnessed by time-lapse cinematography of isolated cells. We can say this because apoptosis was filmed accidentally in the 1950s, during a study of cell death,<sup>58-60</sup> well before apoptosis was recognized as a special entity. A French hematologist, the late Marcel Bessis, examined by time-lapse cinematography the modes of cell death of human leukocytes maintained between slide and coverslip (Figure 6). One of the sequences shows a leukocyte emitting pseudopodia (budding) and finally breaking up with almost explosive suddenness. Bessis described this cellular behavior as "cell death by fragmentation."<sup>60</sup> A study frame by frame even shows two half-moons of chromatin in an apoptotic body (Figure 6). The sequence was seen by Dr. Kerr who agreed that it appears to represent apoptosis (JFR/Kerr, personal communication, 1994).

The pathogenesis of the budding phenomenon is not understood; perhaps it is related to the final breakup of the cell. It is milder in the stiff keratinocytes,<sup>53</sup> perhaps explaining why apoptosis of keratinocytes can produce the relatively large, rounded intraepithelial bodies called sunburn cells.<sup>53</sup> The buds may contain any type of organelles, including nuclear fragments, and do not swell; they should not be confused with blebs. Blebs are typical of ischemic cell death. They are blister-like, fluid-filled structures, typically devoid of organelles, that arise from the cell membrane and are apt to swell and burst, and some may pinch off and float away. Some blebs are reversible. The mechanism of blebbing appears to depend on a disconnection between the cell membrane and the underlying cytoskeleton (reviewed in reference 15).

Students of apoptosis sometimes refer to the dying cell as performing zeiosis.<sup>52,53</sup> The term zeiosis (from the Greek *zéō*, meaning I boil) was created by Costero and Pomerat in 1951<sup>61</sup> to describe a bubbling process observed in living cultured fragments of nervous tissue. The bubbling occurred along dendrites and was not studied in detail, but it seems to

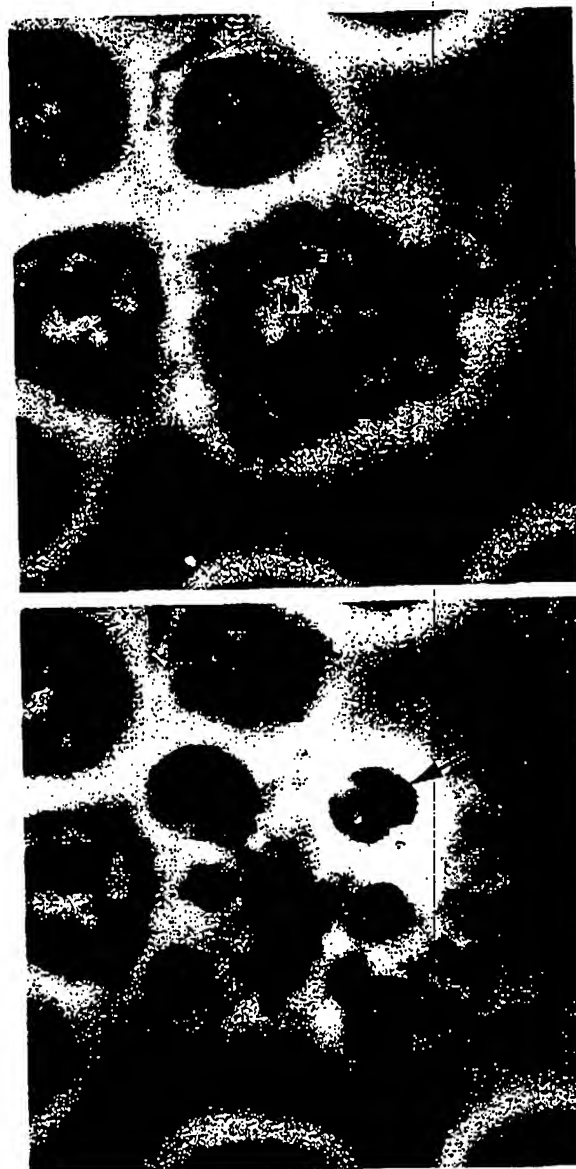


Figure 6. The first known cinematographic recording of apoptosis. Two frames from a 1955 time-lapse movie by Marcel Bessis, showing a leukocyte in vitro said to be dying "by fragmentation."<sup>52-54</sup> Top: A leukocyte (probably a monocyte, M) just before its demise. Bottom: The same leukocyte 33 minutes later, after an episode of budding (not shown). It has suddenly broken up into apoptotic bodies, two of which contain clumps of dense chromatin (arrow), most likely the typical half-moons of apoptosis. (Reproduction authorized for Dr. M. Bessis by Dr. J. L. Bluet.)

have represented blebbing. To our knowledge, blebbing has never been seen in electron micrographs of apoptotic cells. Therefore, in the context of apoptosis, it is best to use the term budding instead of zeiosis.

## Apoptosis and Karyorrhexis

Karyorrhexis, which used to be a descriptive term of little relevance, has gained new status since it turned out to be a feature of apoptosis. It is true that karyorrhexis, when observed in isolated cells, suggests apoptosis. However, it is certainly not pathognomonic of apoptosis. Its originator, Klebs, saw it in a variety of dying (and infected) tissues.<sup>20</sup> Neurons can show karyorrhexis as a result of ischemia<sup>62</sup> and hyperoxia.<sup>63</sup> Karyorrhexis occurring in tumors might be taken as a manifestation of programmed cell death and, therefore, as a good prognostic sign, in opposition to the number of mitoses (and to the extent of massive necrosis).<sup>64</sup> However, the literature in this regard is somewhat confusing. Some authors interpret karyorrhexis in malignant tumors in the same way as massive necrosis, that is, as a bad sign. Because many mitoses are also an indication of poor prognosis, karyorrhexis and mitosis have been lumped together as a mitosis-karyorrhexis index, used to mean "number of nuclei showing either mitosis or karyorrhexis per high power field."<sup>65</sup> When this is done, frequent karyorrhexis correlates with poor prognosis, at least for neuroblastoma. Is this a misunderstanding, or are we dealing with a form of karyorrhexis that does not represent apoptosis? This puzzling issue should be easily settled by using the specific histochemical stain,<sup>54</sup> rather than karyorrhexis, for diagnosing apoptosis.

## Apoptosis and Inflammation

It is usually stated that apoptosis does not induce an inflammatory response, whereas ischemic cell death does. This needs to be qualified. Once the macrophages have made contact with their apoptotic target, they stick to it by means of vitronectin receptors,<sup>66</sup> but how do they find their target in the first place? They must have been somehow attracted to it, albeit over a short distance, and this sequence is certainly typical of inflammation.

It is true that apoptotic cells do not seem to attract neutrophils or lymphocytes. This could reflect a qualitative difference of apoptotic cell death, but it could also mean that cells dying singly (as apoptotic cells usually do) release such small quantities of chemoattractants that not all the molecular species reach the vascular endothelium in effective concentrations (the endothelial cells are responsible for initiating the sequence of leukocyte emigration; reviewed in reference 15).

When apoptosis occurs on a large scale, as in certain phases of embryonic development, hordes of

phagocytes appear on the scene. Saunders and collaborators<sup>67</sup> have beautifully illustrated this phenomenon in situations that they refer to as cataclysmic necrosis, such as the death of cells in the interdigital zones<sup>67-69</sup> (Figure 7). In these situations the entire mass of dead apoptotic cells is replaced by a crowd of mononuclear phagocytes; as matter of fact, the best method for demonstrating this cataclysmic event is to stain the tissue *in vivo* with Nile red, a lysosomotropic dye (reviewed in Reference 15). The dye reveals not the dead cells but the lysosomes of phagocytes in which their debris are packed. The phagocytes are so numerous that, once stained, the clusters can be seen with the naked eye (Figure 7). Microscopically the image is undoubtedly suggestive of inflammation, but the nature of the phagocytic cells is not certain. They are probably not derived from the blood because circulating monocytes are not present<sup>70</sup> at the stages under consideration. They are either tissue macrophages or parenchymal cells ("Schwesterzellen"<sup>27</sup>) that became phagocytic. This raises the interesting possibility that phagocytosis by nonprofessional phagocytic cells would be a useful adaptation to programmed cell death in the embryo, when a clean-up operation is required but a full-blown inflammatory response is not yet available.

One inflammatory feature of apoptosis does seem unusual, namely, the fact that the cell debris (apoptotic bodies) are often phagocytized by neighboring cells such as epithelial cells, which are not professional phagocytes. This does appear to be cellular cannibalism, but is it specific to apoptosis, or does it represent a general tendency of cells to devour their

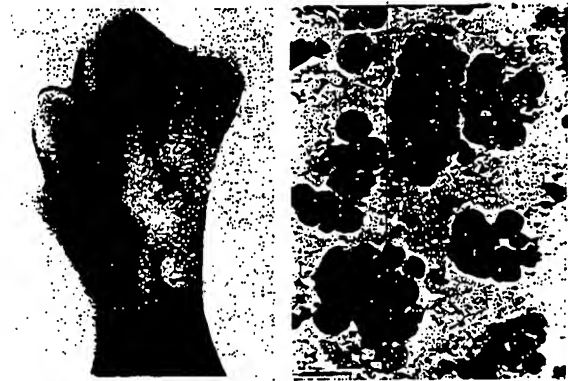


Figure 7. Left: A classic picture of programmed cell death in the leg bud of a chick embryo, stained *in vivo* with Nile red (which becomes concentrated in phagosomes). The dark interdigital zones represent myriads of red-stained macrophages scavenging the debris of cells that died on schedule. Right: A squash preparation of a 4-day chick embryo, stained with Nile red, showing phagocytes loaded with debris of dead cells. Bar = 10  $\mu$ . (From Saunders and Fallon<sup>66</sup> with permission).



disabled neighbors, however they may have died? More data are needed.

### *Apoptosis and Programmed Cell Death*

A misunderstanding has arisen here, due to the fact that two different programs are involved in apoptosis: 1) a program to carry out suicide and 2) another program to trigger the suicidal program.

The phenomenon properly called programmed cell death received its name before apoptosis<sup>67,71</sup>; it referred to situations in which cells are programmed to die at a fixed time. Such is the death on schedule of certain clusters of cells in the embryo.<sup>31</sup> For example, in the chick embryonic plate, a group of cells has to die at a precise time to help create the outline of a wing, much as a sculptor hammers off chips of marble to produce a statue. These doomed cells die on schedule even if they are transplanted elsewhere in the embryo.<sup>67</sup> This form of cell death is programmed in the sense that a genetic clock selects a given time for the death of certain cells. When the time has come, a different program must dictate to these cells how to engineer suicide (eg, apoptosis). In most cases the morphology of this death on schedule turns out to be apoptosis, but in other cases it is not, most notably in spermatocytes and spermatids in the course of normal spermatogenesis,<sup>72</sup> in the massive programmed cell death that occurs during the development of the nervous system,<sup>73</sup> or in the massive death of whole organs during the metamorphosis of certain insects.<sup>44</sup> In other words, there are many situations in which programmed cell death occurs by a morphological and biochemical mechanism that is not apoptosis. There is room here for additional discoveries.

In recent years there has been an unfortunate tendency to use programmed cell death and apoptosis interchangeably, because in both cases genetic programs are involved. This is confusing.<sup>74,75</sup> The genetic program of programmed cell death is a clock specifying the time for suicide, whereas the genetic program of apoptosis specifies the weapons (the means) to produce instant suicide.

We therefore recommend that the name programmed cell death continue to be used, as originally proposed, for death on schedule and not as a synonym of apoptosis.

### *Cell Death Not by Apoptosis: Accidental Cell Death*

The discovery, and naming, of apoptosis oblige us to find suitable names for the types of cell death that

occur by other modalities. This brings out the problem that the major sore spot in the nomenclature of cell death is precisely the lack of a suitable name for cell death that occurs not by apoptosis but by some external agent. Intuitively, the concept seems simple, as we are referring to cell death by accidental causes, such as heat, which would produce the cellular equivalent of murder. Indeed death by murder has been suggested, half in jest,<sup>76</sup> but it is quite misleading, as cell murder by killer cells, as we have seen, produces apoptosis.<sup>52</sup> Accidental cell death was proposed by Bessis,<sup>69</sup> and it is certainly the best available term, although it is not perfect because accidental causes, such as mild heat or toxic agents, can also induce apoptosis. Necrosis is the term currently used for nonapoptotic, accidental cell death.<sup>77</sup> We find it utterly confusing, because necrosis should not be used to define a mode of death, as we will now explain.

### *What is Necrosis?*

The starting point for answering this question should be that, once again, cell death and necrosis are two very different things. Cell death is a process that leads to the point of no return, which, for liver cells submitted to total ischemia, lies, as stated above, at approximately 150 minutes,<sup>15,32</sup> at which time scarcely any changes can be seen in histological sections. Necrosis is full-blown only after 12 to 24 hours. In other words, cells die long before any necrotic changes can be seen by light microscopy. To say cell death by necrosis implies that the cell dies when it becomes necrotic, which is patently untrue. It is rather like saying that clinical death occurs by postmortem autolysis. Furthermore, necrosis has been used for a very long time (approximately 2000 years) to mean drastic tissue changes visible to the naked eye and therefore occurring well after cell death. It is important, both conceptually and didactically, to preserve this usage.

Necrosis is signaled by irreversible changes in the nucleus (karyolysis, pyknosis, and karyorrhexis) and in the cytoplasm (condensation and intense eosinophilia, loss of structure, and fragmentation). We can safely assume that these are the features of a cell's cadaver, whatever the mechanism of the cell's death, be it ischemia, heat, toxins, mechanical trauma, or even apoptosis. The most common microscopic settings of necrosis are 1), cells that died singly displaying the morphological changes of apoptosis, for which we have suggested the term apoptotic necrosis, and 2), groups of cells that died of ischemia, which we can call ischemic necrosis or massive necrosis when the mechanism is not known.



But what was there before ischemic necrosis? Obviously, ischemic cell death. This is the only variety of cell death (other than apoptosis) that has been studied in detail. The data at hand are enough to offer a coherent picture of cell death by ischemia, outlining an entity that can be set up as a counterpart to apoptosis. Because entities need a name, we propose oncosis.

### Apoptosis versus oncosis

Ischemic cell death is characterized by swelling; thus it should be defined by a name that refers to swelling. There is such a name in the literature, namely, oncosis (from *ónkos*, meaning swelling). This term was coined by von Recklinghausen<sup>78</sup> almost 100 years ago, precisely with the meaning of cell death with swelling. In a monograph on rickets and osteomalacia, published posthumously in 1910, von Recklinghausen described death with swelling primarily in bone cells. It is an obvious but little known fact that osteocytes often die with enlargement of their lacunae and sometimes also of their canaliculi. Pathologists with expertise in bone diseases are familiar with such images, especially in bone tissue that dies by slow ischemia, eg, in the stumps of a fracture (even Virchow illustrates this phenomenon, without giving it a name, in Figure 129 of his *Cellular Pathology*<sup>2</sup>). Von Recklinghausen's color illustrations of oncotic osteocytes are striking (Figure 8). It is certainly a tour de force for the swelling osteocyte to enlarge its stony lacuna. Von Recklinghausen was probably correct in assuming that this process required an enzymatic effect, which he called trypsis. (Note that Von Recklinghausen included in oncosis also the mode of death of the so-

called hypertrophic cells of the growth cartilage. There is no doubt that these cells swell and become hydropic before they die. However, their mode of death, in our view, is still a mystery. Their swelling is probably quite unrelated to hypertrophy, as both Virchow<sup>2</sup> and von Recklinghausen<sup>78</sup> observed. Their mode of death is certainly programmed, which fits with apoptosis, but the swelling does not. Perhaps we are dealing here with yet another form of cell death.)

After von Recklinghausen the term oncosis continued to be used by European pathologists working on bone tissue. We propose that it be given a more general mission, as a counterpart, to apoptosis. It is concise and descriptive. By its reference to swelling it is particularly well suited to contrast with shrinkage necrosis, and it allows necrosis to cover, as it always did, those changes that occur after cell death. In today's medical jargon, the root onco- is not limited to the swelling of tumors (for example, oncotic pressure). Our proposal is summarized in Figure 9. It will be noticed in this figure that necrosis can occur after

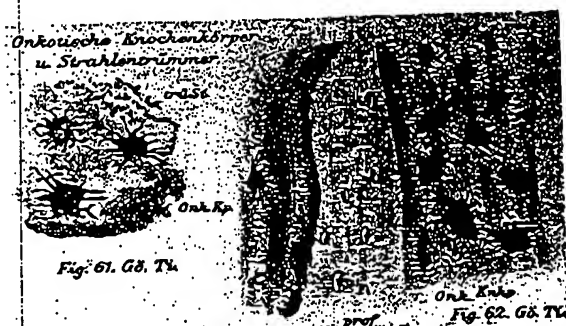


Figure 8. Oncosis in osteocytes as illustrated by von Recklinghausen in 1910. (reference 78 Tal. XXI). From the tibia of a 30-month-old girl with osteoporotic osteomalacia (rickets). prof, bone lamellae with normal osteocytes; Onk.Kp. swollen, dying, or dead osteocytes in enlarged lacunae; tr.St., cross sections of dilated bone canaliculi. (Sections of undecalcified bone stained with ibionine; dilated canaliculi and some lacunae appear black because they are filled with air injected into the bone (reference 78 p 135), a method not known in our day. Original drawing watercolored.)

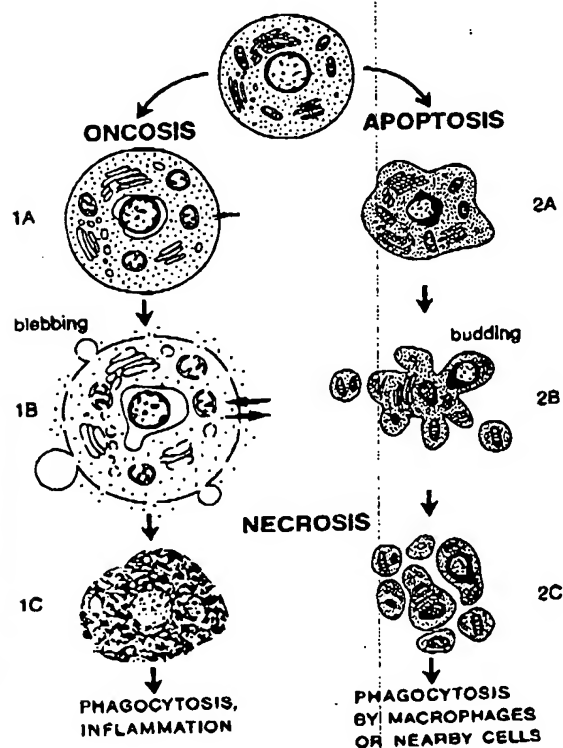


Figure 9. Two pathways of cell death leading to necrosis. At the top is shown a normal cell. 1A Swelling. 1B: Vacuolization, blebbing, and increased permeability. 1C: Necrotic changes, ie, coagulation, shrinkage, and karyolysis. 2A: Shrinkage and pyknotosis. 2B: Budding and karyorrhexis. 2C: Necrotic changes, ie, breakup into a cluster of apoptotic bodies (2C adapted from Weldon et al<sup>23</sup>).

both forms of cell death. A fine example of post-apoptotic necrosis is the cataclysmic necrosis in embryo tissues described by Saunders and Fallon.<sup>66</sup> Kerr and Harmon<sup>50</sup> have also pointed out that apoptotic cell bodies can incur extracellular breakdown and referred to this post-apoptotic change as secondary necrosis, thereby concurring with our view that necrosis can occur also after apoptosis.

In summary, we can define oncosis as follows: 1), oncosis is a form of cell death accompanied by cellular swelling, organelle swelling, blebbing, and increased membrane permeability; 2), its mechanism is based on failure of the ionic pumps of the plasma membrane; 3), it is caused, typically, by ischemia and possibly by toxic agents that interfere with ATP generation or increase the permeability of the plasma membrane; 4), it evolves within 24 hours to typical necrosis; 5), it is usually accompanied by karyolysis; 6), it can be diagnosed by tests of permeability on whole cells, either in suspension (by dye exclusion tests) or by electron microscopy (using a colloidal marker)<sup>79</sup>; 7), the DNA breaks down in a nonspecific fashion<sup>42</sup>; and 8), the cellular changes (increased permeability of the plasma membrane, cell swelling, organelle swelling and vacuolization, and simultaneous protein denaturation and hydrolysis) can only be hinted at by ordinary histological techniques.

Many experiments have shown that blebbing, described above, begins during the early stages of ischemic damage and is initially reversible. Large blebs may burst, and it has been suggested that this may be the final blow to a dying cell (reviewed in reference 15).

Why karyolysis should follow oncosis is not known. As regards the mechanism of karyolysis, a huge literature appeared early in the 1900s, when autolysis was a fashionable research topic (reviewed in references 13, 16, and 48). The basic problem was already identified by Weigert: has the chromatin leaked out, or has it lost its stainability? From the studies of Trump et al<sup>80</sup> it appears that both mechanisms can operate.

In closing, we would like to point out two facts. First, oncosis and apoptosis are merely two forms of cell death, among many others that remain to be described. Consider, for example, that form of cell death that makes histopathology possible, namely death by fixation. Histological fixatives are designed to produce the perfect crime, death without visible traces. What shall we call it? Second, in these days of molecular pathology, it is well to remember that the marvelous story of apoptosis was initiated by a very simple, almost elementary morphological observa-

tion, accessible to the microscopes of our great-grandfathers.

### Acknowledgments

We are indebted to Paula A. Dadian for secretarial and bibliographic help, to Christine L. Dunshee for photographic help, including prints from the Bessis movie, to Jean M. Underwood for electron microscopic preparations, to Mrs. Anne B. Greene for Figure 9, to Beth H. Maynard Mellor for Figure 4, and to Richard Wolfe, Curator of Rare Books at the Countway Library of Harvard Medical School, for help in obtaining and photographing precious old books.

### References

- Farber E: Ideas in pathology: programmed cell death: necrosis versus apoptosis. *Mod Pathol* 1994, 7:605-609
- Virchow R: Cellular Pathology as Based upon Physiological and Pathological Histology, ed 2. Translated from German by B Chance, 1859. Reproduced by Dover Publications, New York, 1971, pp 356-382
- Rokitansky C: Handbuch der allgemeinen pathologischen Anatomie. Vienna, Braumüller & Seidel, 1846
- Liddell HG, Scott R: A Greek-English Lexicon. Oxford, The Clarendon Press, 1968
- Saibara T, Himeno H, Ueda H, Onishi S, Yamamoto Y, Enzan H, Hara H, Takehara Y, Utsumi K: Acute hepatic failure with swollen mitochondria and microvesicular fatty degeneration of hepatocytes triggered by free radical initiator. *Lab Invest* 1994, 70:517-524
- Weigert C: Über Croup und Diphtheritis. Ein experimenteller und anatomischer Beitrag zur Pathologie der spezifischen Entzündungsformen. *Virchows Arch Pathol Anat* 1877-1878, 72:461-501
- Weigert C: Über Croup und Diphtheritis. II. Theil. Beobachtungen beim Menschen. *Virchows Arch Pathol Anat* 1878, 72:218-257
- Weigert C: Kritische und ergänzende Bemerkungen zur Lehre von der Coagulationsnekrose mit besonderer Berücksichtigung der Hyalinbildung und der Umprägung geronnener Massen. *D Med Wochenschrift* (XI) 1885, 45:780-782
- Weigert C: Über die pathologischen Gerinnungsvorgänge. *Virchows Arch Pathol Anat* 1880, 79:87-123
- Cohnheim J: Lectures on General Pathology: The Pathology of Nutrition, sect II, ed 2. Translated from German by AB McKee. Reproduced by The New Sydenham Society, London 1889
- Kraus F: Über die in abgestorbenen Geweben spontan eintretenden Veränderungen. *Arch Exp Pathol Pharmacol* 1887, 22:174-200
- Schmaus H, Albrecht E: Zur Frage der Coagulationsnekrose. *D Med Wochenschrift* 1899, 6:89-114

14 Majno and Joris  
*AJP January 1995, Vol. 146, No. 1*

13. Cameron GR: Pathology of the Cell. Springfield, Charles C. Thomas, 1951
14. Berthold G: Studien über Protoplasmamechanik. Leipzig, Verlag Arthur Felix, 1886
15. Majno G, Joris I: Cells, Tissues and Disease: Principles of General Pathology. Boston, Blackwell Science, Inc., (in press)
16. Wells GH: Chemical Pathology: Being a Discussion of General Pathology from the Standpoint of the Chemical Processes Involved. Philadelphia, WB Saunders Co 1925
17. Arnheim G: Coagulationsnekrose und Kernschwund. Virchows Arch Pathol Anat 1890, 120:367-383
18. Jacoby M: Über die fermentative Eiweisspaltung und Ammoniakbildung in der Leber. Hoppe-Seyler's Z Physiol Chem 1900, 30:149-159
19. Schmaus H, Albrecht E: Über Karyorrhexis. Virchows Arch Pathol Anat 1894, 138:1-80
20. Klebs E: Die Allgemeine Pathologie. Zweiter Theil. Störungen des Baues und der Zusammensetzung. Jena, Verlag Gustav Fischer, 1889
21. Flemming W: Über die Bildung von Richtungsfiguren in Säugethiereiern beim Untergang Graaf'scher Follikel. Arch Anat EntwGesch 1885, 221-244
22. Piltzner W: Zur pathologischen Anatomie des Zellkerns. Virchows Arch Pathol Anat 1886, 103:275-300
23. Waldeyer W: Über Karyokinese. Arch Physiol 1887, 1-28
24. Nissen F: Über das Verhalten der Kerne in den Milchdrüsenzellen bei der Absonderung. Arch Mikroskop Anat 1886, 26:337-342
25. Ruge G: Vorgänge am Eitollikel der Wirbelthiere. Morphol Jahrbuch 1889, 15:491-554
26. Ströbe H: Zur Kenntnis verschiedener cellularer Vorgänge und Erscheinungen in Geschwülsten. Beitr Pathol Anat 1892, 11:1-38
27. Gräper L: Eine neue Anschauung über physiologische Zellausschaltung. Arch Zellforsch 1914, 12:373-394
28. Glücksmann A: Cell deaths in normal vertebrate ontogeny. Biol Rev Camb Philos Soc 1951, 26:59-86
29. Majno G, La Gattuta M, Thompson TE: Cellular death and necrosis: chemical, physical and morphologic changes in rat liver. Virchows Arch Pathol Anat 1960, 333:421-465
30. Rechsteiner M: Ubiquitin. New York, Plenum Publishing, 1988
31. Ciechanover A, Schwartz AL: The ubiquitin-mediated proteolytic pathway: mechanisms of the recognition of the proteolytic substrate and involvement in the degradation of native cellular proteins. FASEB 1994, 8:182-191
32. Majno G: Death of liver tissue: a review of cell death, necrosis, and autolysis. The Liver, vol. 2. Edited by CH Rouiller. New York, Academic Press, 1964, pp 267-313
33. Farber E, Fisher MM: Toxic Injury of the Liver, part A. New York, Marcel Dekker, 1979
34. Farber JL: Biology of disease: membrane injury and calcium homeostasis in the pathogenesis of coagulative necrosis. Lab Invest 1982, 47:114-123
35. Farber JL: Calcium and the mechanisms of liver necrosis. Progress in Liver Diseases. Edited by H. Poppe, and F. Schaffner. New York, Grune & Stratton, 1982, pp 347-360
36. Kerr JFR: Shrinkage necrosis: a distinct mode of cellular death. J Pathol 1971, 105:13-20
37. Kerr JFR, Wyllie AH, Currie AR: Apoptosis: a basic biological phenomenon with wide-ranging implications in tissue kinetics. Br J Cancer 1972, 26:239-257
38. Spear FG, Glücksmann A: The effect of gamma radiation on cells *in vivo*: single exposures of the normal tadpole at room temperature. Br J Radiol 1938, 11:533-553
39. Skalka M, Matyášová J, Čejková M: DNA in chromatin of irradiated lymphoid tissues degrades *in vivo* into regular fragments. FEBS Lett 1976, 72:271-274
40. Yamada T, Ohyama H, Kinjo Y, Watanabe M: Evidence for the internucleosomal breakage of chromatin in rat thymocytes irradiated *in vitro*. Radiat Res 1981, 85:544-553
41. Zhivotovsky BD, Zvonareva NB, Hanson KP: Characteristics of rat thymus chromatin degradation products after whole-body X-irradiation. Int J Radiat Biol 1981, 39:437-440
42. Wyllie AH, Morris RG, Smith AL, Dunlop D: Chromatin cleavage in apoptosis: association with condensed chromatin morphology and dependence on macromolecular synthesis. J Pathol 1984, 142:67-77
43. Thompson HJ, Strange R, Schedin PJ: Apoptosis in the genesis and prevention of cancer. Cancer Epidemiol Biomarkers Prev 1992, 1:597-602
44. Schwartz LM, Osborne BA: Programmed cell death, apoptosis and killer genes. Immunol Today 1993, 14:583-590
45. Raff MC: Cell death genes: *Drosophila* enters the field. Science 1994, 264:668-683
46. Kerr JFR, Winterford CM, Harmon BV: Apoptosis: its significance in cancer and cancer therapy. Cancer 1994, 73:2013-2026
47. Wyllie AH: Death gets a brake. Nature 1994, 369:272-273
48. Bradley HC: Autolysis and atrophy. Physiol Rev 1922, 2:415-439
49. Bowen ID, Bowen SM: Programmed Cell Death in Tumors and Tissues. London, Chapman and Hall, 1990
50. Kerr JFR, Harmon BV: Definition and incidence of apoptosis: an historical perspective. Apoptosis: The Molecular Basis of Cell Death. Edited by LD Tomei and FO Cope. New York, Cold Spring Harbor Laboratory Press, 1991, pp 5-29
51. Tomei LD, Cope FO (Eds): Apoptosis: The Molecular Basis of Cell Death, vol 2. New York, Cold Spring Harbor Laboratory Press, 1994
52. Razvi ES, Welsh RM: Apoptosis in viral infections. Adv Virus Res 1995, 49:1-60
53. Weedon D, Searle J, Kerr JFR: Apoptosis: its nature and implications for dermatopathology. Am J Dermatopathol 1979, 1:133-144

54. Gavrieli Y, Sherman Y, Ben-Sasson SA: Identification of programmed cell death *in situ* via specific labeling of nuclear DNA fragmentation. *J Cell Biol* 1992, 119: 493-501
55. Martin SJ: Apoptosis: suicide, execution or murder? *Trends Cell Biol* 1993, 3:141-144
56. Funder J: Apoptosis: Two p or not two p? *Nature* 1994, 371:98 (Letter)
57. Duke RC, Witter RZ, Nash PB, Ding-E Young J, Ojcius DM: Cytolysis mediated by ionophores and pore-forming agents: role of intracellular calcium in apoptosis. *FASEB J* 1994, 8:237-246
58. Bessis MC: Mort d'une cellule: analyse d'un film en contraste de phase. *Semaine Hôpitaux* 1955, 60:21-32
59. Bessis MC: Death of a Cell, 16-mm film. New York, Swift Motion Picture Laboratories, 1958
60. Bessis M: Studies on cell agony and death: an attempt at classification. *Ciba Foundation Symposium on Cellular Injury*. Edited by AVS de Reuck and J Knight. London, J&A Churchill, 1964, pp 287-328
61. Costero I, Pomerat CM: Cultivation of neurons from the adult human cerebral and cerebellar cortex. *Am J Anat* 1951, 89:405-468
62. Squier M, Keeling JW: The incidence of prenatal brain injury. *Neuropathol Appl Neurobiol* 1991, 17:29-38
63. Andab-Barnada M, Moossy J, Nemoto EM, Lin MR: Hyperoxia produces neuronal necrosis in the rat. *J Neuropathol Exp Neurol* 1986, 45:233-246
64. Arends MJ, McGregor AH, Wyllie AH: Apoptosis is inversely related to necrosis and determines net growth in tumors bearing constitutively expressed *myc*, *ras*, and *HPV* oncogenes. *Am J Pathol* 1944, 144:1045-1057
65. Joshi V, Chatten J, Sather HN, Shimada H: Evaluation of the Shimada classification in advanced neuroblastoma with a special reference to the mitosis-karyorrhexis index: a report from the children's cancer study group. *Mod Pathol* 1991, 4:139-147
66. Savill J, Dransfield I, Hogg N, Haslett C: Vitronectin receptor-mediated phagocytosis of cells undergoing apoptosis. *Nature* 1990, 343:170-173
67. Saunders JW, Fallon JF: Cell death in morphogenesis. *Major Problems in Developmental Biology*. New York, Academic Press, 1967, pp 289-314
68. Saunders JA, Gasseling MT, Saunders LC: Cellular death in morphogenesis of the avian wing. *Dev Biol* 1962, 5:147-178
69. Saunders JW: Death in embryonic systems. *Science* 1966, 154:604-612
70. Romanoff A: The hematopoietic, vascular, and lymphatic systems. *The Avian Embryo*. New York, Macmillan, 1960, pp 571-678
71. Lockshin RA, Williams CM: Programmed cell death. II. Endocrine potentiation of the breakdown of the inter-segmental muscles of silkworms. *J Insect Physiol* 1964, 10:643-649
72. Allan DJ, Harmon BV, Kerr JFR: Cell death in spermatogenesis. *Perspectives on Mammalian Cell Death*. Edited by CS Potten. New York, Oxford University Press, 1987, pp 229-258
73. Server AC, Mobley WC: Neuronal cell death and the role of apoptosis. *Apoptosis: The Molecular Basis of Cell Death*. Edited by LD Tomei and FO Cope. New York, Cold Spring Harbor Laboratory Press, 1991, pp 263-278
74. Lockshin RA, Zakeri Z: Programmed cell death and apoptosis. *Apoptosis: The Molecular Basis of Cell Death*. Edited by LD Tomei and FO Cope. New York, Cold Spring Harbor Laboratory Press, 1991, pp 47-60
75. Bowen ID: Apoptosis or programmed cell death? *Cell Biol Int* 1993, 17:365-380
76. Budtz PE: Epidermal homeostasis: a new model that includes apoptosis. *Apoptosis: The Molecular Basis of Cell Death*, vol 2. Edited by LD Tomei and FO Cope. New York, Cold Spring Harbor Laboratory Press, 1994, pp 165-183
77. Wyllie AH, Kerr JFR, Currie AR: Cell death: the significance of apoptosis. *Int Rev Cytol* 1980, 68:251-306
78. Recklinghausen F von: Untersuchungen über Rachitis und Osteomalacie. Jena, Verlag Gustav Fischer, 1910
79. Hoffstein S, Gennaro DE, Fox AC, Hirsch J, Streuli F, Weissmann G: Colloidal lanthanum as a marker for impaired plasma membrane permeability in ischemic dog myocardium. *Am J Pathol* 1975, 79:207-218
80. Trump BF, Goldblatt PJ, Stowell RE: Studies of mouse liver necrosis *in vitro*. *Lab Invest* 1965, 14:1969-1999

## Stretch-activated whole cell currents in adult rat cardiac myocytes

TAO ZENG, GLENNA C. L. BETT, AND FREDERICK SACHS

*Department of Physiology and Biophysics, State University of New York, Buffalo, New York 14214*

**Zeng, Tao, Glenna C. L. Bett, and Frederick Sachs.** Stretch-activated whole cell currents in adult rat cardiac myocytes. *Am. J. Physiol. Heart Circ. Physiol.* 278: H548–H557, 2000.—Mechanoelectric transduction can initiate cardiac arrhythmias. To examine the origins of this effect at the cellular level, we made whole cell voltage-clamp recordings from acutely isolated rat ventricular myocytes under controlled strain. Longitudinal stretch elicited noninactivating inward cationic currents that increased the action potential duration. These stretch-activated currents could be blocked by 100  $\mu\text{M}$   $\text{Gd}^{3+}$  but not by octanol. The current-voltage relationship was nearly linear, with a reversal potential of approximately  $-6$  mV in normal Tyrode solution. Current density varied with sarcomere length (SL) according to  $I$  (pA/pF) =  $8.3 - 5.0\text{SL}$  ( $\mu\text{m}$ ). Repeated attempts to record single channel currents from stretch-activated ion channels failed, in accord with the absence of such data from the literature. The inability to record single channel currents may be a result of channels being located on internal membranes such as the T tubules or, possibly, inactivation of the channels by the mechanics of patch formation.

ion channel; patch clamp; mechanical stress; simulation; sarcomere

MECHANICAL STRESS changes the electrophysiological properties of the heart, a phenomenon known as mechanoelectric feedback (25). Stretching intact hearts or excised muscle can raise the beat rate (2, 3), cause diastolic depolarization (30), change the action potential configuration (7, 24), and induce arrhythmias (17). Stretch-activated channels (SACs), considered to be the origin of mechanoelectric transduction (21, 37, 53), are found in many cardiomyocytes, including those from molluscan ventricle (40), chick embryo ventricle (20, 33), rat atrium (22, 50) and ventricle (8), rabbit sinoatrium and atrium (12), guinea pig ventricle (6, 39), and pig atrium (19). Most of the above recordings were made with the cell-attached single-channel patch-clamp technique, in which the open probability ( $P_o$ ) of the channels increased with negative pressure applied to the patch pipette. None of the above data were obtained from adult ventricular cells, and there are almost no data on whole cell responses of cardiocytes to stretch under voltage clamp.

The costs of publication of this article were defrayed in part by the payment of page charges. The article must therefore be hereby marked "advertisement" in accordance with 18 U.S.C. Section 1734 solely to indicate this fact.

To record whole cell mechanosensitive currents under stretch, the cells must not only be voltage clamped but also stretched without damage. Stretching intact, isolated cells without damage has proven to be extremely difficult (5, 11), and only one paper has shown whole cell currents (39). In some experiments hydrostatic or osmotic pressure was used as a mechanical stimulus to inflate the cells, but it is unlikely that these stimuli are equivalent to axial stretch (20). Hagiwara et al. (12) evoked mechanosensitive  $\text{Cl}^-$  currents by inflating the cells through the clamping pipette, whereas Sorota (44) and Tseng (47) found an increase of  $\text{Cl}^-$  permeability in response to hypotonic swelling. Attempting to evoke axial strain, Sasaki et al. (39) attached cells to a coverslip or to a fire-polished glass tool and pulled on the other end with another glass tool or suction pipette. Currents were recorded with a separate pipette and had a reversal potential of  $-15$  mV in physiological saline. Hu and Sachs (20) recorded currents in chick heart cells through a perforated patch and stimulated them by compressing the rounded cells with a second pipette. In agreement with the results of Sasaki et al. (39), Hu and Sachs found a mechanosensitive cation current reversing at  $-16$  mV. In none of these papers was strain under reliable control.

In this paper, we present evidence of a gadolinium-sensitive whole cell stretch-activated current ( $I_{\text{stretch}}$ ) in adult rat ventricular cells under controlled strain. The cells were pulled with a pair of concentric pipettes as described by Palmer et al. (29). The axial strain was measured from calibrated displacements of the ends of the cell and from Fourier transforms of the sarcomere spacing. These measurements formed the basis for quantifying the relationship between strain and current.

### METHODS

**Cell preparation.** Ventricular myocytes were enzymatically isolated by retrograde perfusion of the heart (28, 49). Briefly, Sprague-Dawley (2–3 mo old) rats were injected with heparin (2,000 U/kg) and then Nembutal (60 mg/kg). When the rat was anesthetized, the heart was quickly excised, cannulated through the aorta in cold Tyrode buffer, and then mounted on a dual-channel tube Langendorff perfusion apparatus. Perfusion of the heart proceeded at  $37^\circ\text{C}$  for 10 min in Tyrode solution, 4.5 min in  $\text{Ca}^{2+}$ -free Tyrode solution, 30 min in the enzyme solution, and 5 min in low- $\text{Ca}^{2+}$  Tyrode solution. All perfusion solutions were equilibrated with 100% oxygen. The enzyme solution was limited to 60 ml and allowed to recirculate. After perfusion, the ventricle was cut off and minced. Cells were dispersed from the tissue by agitation, filtered into Tyrode solution through a 200- $\mu\text{m}$ -mesh net, and stored at

4°C until use. All experiments were done within 1–20 h after isolation.

**Dye loading.** Isolated cells were loaded for 30 min at room temperature in normal Tyrode solution containing 2  $\mu$ M fluo 3-AM (Molecular Probes) and 0.2% Pluronic-127 (Molecular Probes) (41). Cells were then rinsed three times in saline and left for 20 min to further hydrolyze the ester form of the dye.

**Cell stretch and patch clamp.** Isolated rod-shaped ventricular cells with clear sarcomeres were held by two concentric glass pipettes (29), with the inner pipette serving as a stop to prevent the cell from being sucked up the outer pipette. The outer pipette was pulled from a glass capillary (ID 1.0 mm, OD 1.5 mm; Drummond Scientific) with an inner tip diameter of  $\sim 15$   $\mu$ m. The inner pipette was made from a glass capillary (ID 0.5 mm, OD 1.0 mm; Dagan) with an outer tip diameter of  $\sim 12$   $\mu$ m. The inner pipette was inserted into the outer pipette by a manipulator, leaving a gap of  $\sim 8$   $\mu$ m to the tip of the outer pipette. The tip of the outside pipette was then cut by fusion of the tip to the filament of a microforge as described by Hilgemann (18). The cut end was lightly fire-polished so that the tips of the inside and outside pipettes were forged together and formed a cup to hold the cell.

To make the cells adhere to the glass, we tried a host of different agents. These included Cel-Tak (Collaborative Biomedical Products), a glue based on barnacle adhesive proteins, as suggested by Palmer et al. (29). This did not provide sufficient adhesion for prolonged pulling. Strong suction itself caused fatal cell contraction, probably via SACs. We tried many different adhesives, including covalent and noncovalent bonding agents such as poly-L-lysine. We tried adhesives activated by ultraviolet light (Master Bond), epoxies, cyanoacrylates ("crazy glue"), silicones (e.g., Kwik-sil, World Precision Instruments), charged silanes such as 3-aminopropyltriethoxysilane, and covalent silanes such as isocyanates. We tried covalently attaching wheat germ agglutinin to the glass with a silane linkage, but that, too, was unreliable. The problems varied from adhesives not sticking well to the glass or to the cells or damaging the cells to the adhesives not catalyzing under water or catalyzing too fast. We had hoped to find a volume-filling adhesive to take up the space between the pipettes and the cell, but as yet we have not been successful. Our best adhesive to date has been a dense layer of positive charge linked covalently to the glass. We first treated the concentric pipettes with a silane (I7840, United Chemical Technologies) that left the glass coated with isocyanate groups. The silane was prepared as a final concentration of 2% in 95% ethanol. Pipettes were immersed in the solution for 5 min and then cured 24 h at room temperature. Shortly before each experiment, the coating was reacted with an amino dendrimer (PAMAM dendrimer generation 4, Aldrich Chemical) by dipping the tip of pipettes in a 10% solution in methyl alcohol for 5 min.

To attach cells to the pipettes, two or three drops of the cell suspension were transferred to a custom-designed chamber with a bottom made from a coverslip. After 5 min most cells settled down, and the bath solution was then changed to a low- $\text{Ca}^{2+}$  or  $\text{Ca}^{2+}$ -free relaxing solution so that suction would not cause extensive contraction. The selected cell was first drawn into one concentric pipette by gentle suction, with the intercalated disk region firmly contacting the inner pipette. The cell was then lifted  $\sim 50$   $\mu$ m above the bottom of the dish. The second concentric pipette was then moved close to the free end of the cell, and it was gently drawn in as for the first pipette. The pipette positions were adjusted so that the cell was relaxed and aligned axially with the two pipettes. We waited 10 min to allow the dendrimer to bond to the membrane. The cell was then patched with a third pipette. Despite

our efforts to get the best adhesion possible, and even with small strains, it was usually not possible to stretch a cell more than four or five times before it pulled loose from one of the pipettes. Consequently, many of the results are presented as statistical averages across cells.

The patch pipette and one of the concentric pipettes were mounted on PCS-800 piezoelectric manipulators (Burleigh Instruments), and the other concentric pipette was attached to a second manipulator (MP-300, Sutter Instruments). During the experiment, the cell was stretched axially by sending an electrical command to the PCS-800 manipulator at one end of the cell. To reduce local strain in the region of the patch pipette, this command was scaled and sent to the PCS-800 manipulator controlling the patch pipette, so that it moved sideways in proportion to the local strain.

**Data recording and analysis.** Standard whole cell recording methods (14) were used to clamp the membrane voltage and record currents. The fire-polished patch pipette had a tip ID of 1–2  $\mu$ m, with a resistance of 0.5–2.0 M $\Omega$  when the pipette was filled with high- $\text{K}^{+}$  pipette solution. The seal resistance was usually  $> 2.0$  G $\Omega$ . Cell capacitance was derived by fitting the transient currents generated by a voltage pulse after the whole cell configuration was formed (26).

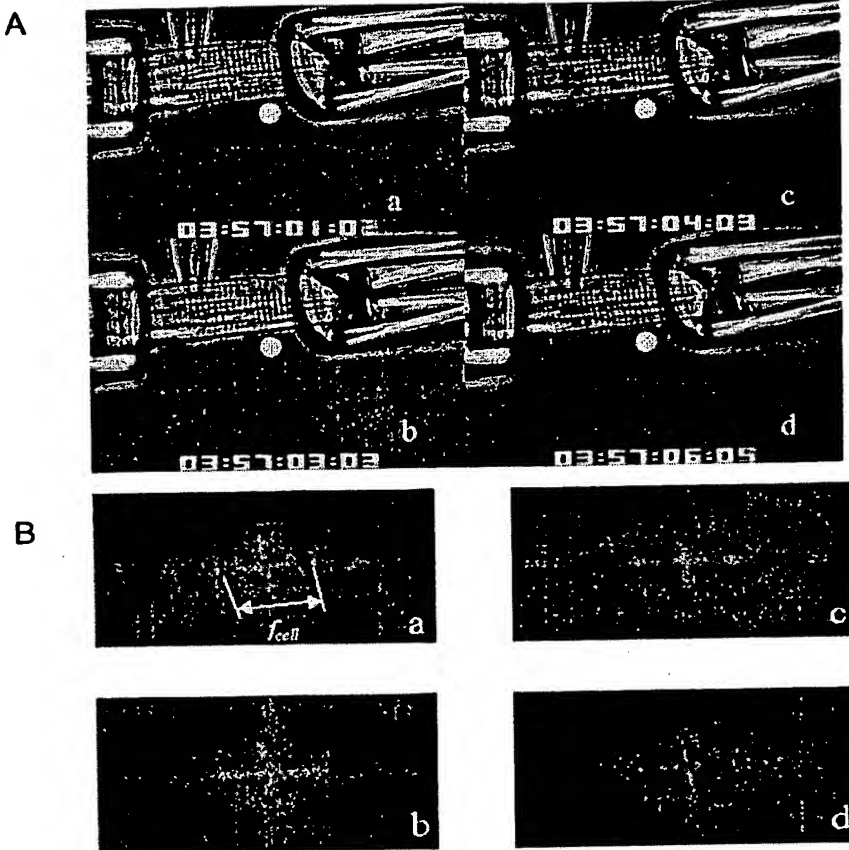
Voltage and current signals from the patch-clamp amplifier (Axopatch-1B, Axon Instruments) and movement commands of the stretching pipette were filtered at 2.5 kHz and then digitized by a data acquisition board (AT-MIO-16E-2, National Instruments) in a personal computer (XPS H266, Dell). This data acquisition board was the control unit for all of the experiments, generating voltage, stretching, and synchronization command potentials. The board was controlled by custom software (T. Zeng, unpublished) that was programmed in LabVIEW (National Instruments). A charge-coupled device camera (KP-M2U, Hitachi) was attached to the microscope (DIAPHOT 200 with  $\times 40$  oil-immersion objective and water-immersion condenser, Nikon) to monitor the cells. During cell stretching, a digital signal from the data acquisition board triggered a frame-grabber board (IMAQ PCI-1408, National Instruments) to sample the images of cells at specific times (Fig. 1A). Continuous real-time video images were also logged onto S-VHS tape for archival storage. To change the bath solutions around the cell, a pulse was sent from the board to control the valves of a perfusion system (PS-8, ALA Scientific Instruments), whose output was held in a fourth manipulator.

Once the patch was broken by the zap pulse from the amplifier, we waited 5–10 min to reach a steady state. A small stretch was then given to test whether the cell was still firmly held by the concentric pipettes. Data were recorded by applying larger stretches until the cell came loose or contracted. The stretch-activated current was measured as the differential before and after stretching. We have attempted  $\sim 100$  cells, but only 15–20 were held sufficiently firmly and remained relaxed while being patched.

Sarcomere length (SL) was determined from the cell images using a two-dimensional (2-D) Fourier transform operating off-line (Fig. 1B). A region of interest (256  $\times$  128 pixels with 256 gray levels) was transformed into the 2-D power spectrum and the spatial frequency peak ( $f_{\text{cell}}$ ) corresponding to the SL was located by software. SL was computed by the equation  $\text{SL} = l_{\text{cal}} \times f_{\text{cal}}/f_{\text{cell}}$ , where  $l_{\text{cal}}$  is a calibration distance (5  $\mu$ m) obtained from the image of a stage micrometer and  $f_{\text{cal}}$  is its corresponding maximum spatial frequency. The analysis software was also written in LabVIEW. The mean SL of our cells in resting condition was  $1.77 \pm 0.08$   $\mu$ m ( $n = 18$ ) when held by the pipettes. Statistical significance was calculated using Student's *t*-test.



Fig. 1. Cell stretching and measurement of sarcomere length (SL). A: cell was attached to 2 concentric pipettes (left and right) and voltage-clamped by a third (middle). Right concentric pipette moved right to stretch cell, and patch pipette moved with local strain to reduce stress around tip. Images were sampled by a frame grabber at specific times. White dot indicates a fiducial fixed point. B: diffraction patterns of cell in A. Spatial frequency ( $f_{\text{cell}}$ ) corresponds to SL. Actual SLs in a-d are 1.78, 1.84, 1.84, and 1.78  $\mu\text{m}$ , respectively, obtained by comparison with a calibrated stage micrometer.



**Solutions.** The Tyrode solution contained (mM) 137 NaCl, 5.4 KCl, 0.5  $\text{MgCl}_2$ , 1.8  $\text{CaCl}_2$ , 10 HEPES, and 5.0 glucose, pH 7.4 with NaOH. The  $\text{Ca}^{2+}$ -free solution was Tyrode solution without added  $\text{Ca}^{2+}$ . For the low- $\text{Ca}^{2+}$  Tyrode solution we reduced  $\text{Ca}^{2+}$  in Tyrode solution from 1.8 to 0.2 mM. Tris-Tyrode solution was Tyrode solution with  $\text{Na}^+$  replaced by  $\text{Tris}^+$ . The enzyme solution was 60 ml of  $\text{Ca}^{2+}$ -free Tyrode plus 30 mg of collagenase A (Boehringer Mannheim) and 6 mg Protease XIV (Sigma). The pipette solution was (mM) 130 KCl, 10 NaCl, 5  $\text{MgCl}_2$ , 11 EGTA, 1  $\text{CaCl}_2$ , and 10 HEPES, pH 7.4 with KOH. In some experiments,  $\text{Cl}^-$  was replaced by  $\text{F}^-$  as indicated.

**Mathematical modeling.**  $I_{\text{stretch}}$  was modeled using a simple linear nonspecific current with two components, the  $\text{Na}^+$ -carrying element and the  $\text{K}^+$ -carrying element

$$I_{\text{stretch}} = \gamma_{\text{stretch,Na}}(8.3 - 5.0\text{SL})(E_m - E_{\text{Na}}) + \gamma_{\text{stretch,K}}(8.3 - 5.0\text{SL})(E_m - E_{\text{K}})$$

where  $E_{\text{Na}}$  and  $E_{\text{K}}$  are the reversal potentials for sodium and potassium respectively,  $E_m$  is the membrane potential, and  $\gamma_{\text{stretch,Na}}$  and  $\gamma_{\text{stretch,K}}$  are the whole cell conductances of the stretch current to potassium and sodium ions, respectively. The components were kept separate to ease calculation of ion concentration changes within the cell as well as the electrogenic effect of the current.

$I_{\text{stretch}}$  was incorporated into a model based on the Oxsoft Heart Model (Biologic) of the isolated rat ventricular cell, which was modified to include a parameter for EGTA. The on and off rates for  $\text{Ca}^{2+}$  binding to EGTA were  $10^{6.3} \text{ M}^{-1} \text{ s}^{-1}$  and

$0.4 \text{ s}^{-1}$ , respectively (48). Oxsoft Heart is a mathematical representation of the heart based on experimental electrophysiological data from a variety of sources. It simulates the behavior of transmembrane currents, exchangers, and transporters, the sarcoplasmic reticulum, the intracellular buffers, and the movement of intracellular and extracellular ion concentrations.

## RESULTS

**Stretch increases action potential duration and depolarizes resting potential.** In normal- $\text{Ca}^{2+}$  solution, heart cells are apt to contract when touched by a glass pipette, particularly when subjected to suction. We presume that this represents action of SACs. To check the effect of stretch on cell excitability, we recorded the membrane potential while stretching the cell. In current-clamp mode, pulses of 1 ms and 2 nA repeated every 5 s could elicit action potentials. After the action potential was stable, we pulled on one of the concentric pipettes to stretch the cell. The displacement was  $\sim 5 \mu\text{m}$  and lasted 20 s. The pipette was then returned to its original position. Figure 2 shows action potentials recorded during stretching.

Compared with the control value of  $621 \pm 12 \text{ ms}$  ( $n = 5$ ), action potential duration (APD) at 90% repolarization ( $\text{APD}_{90}$ ) increased to  $764 \pm 50 \text{ ms}$  ( $n = 4$ ,  $P < 0.01$ ) with stretching. On return to the resting length, there



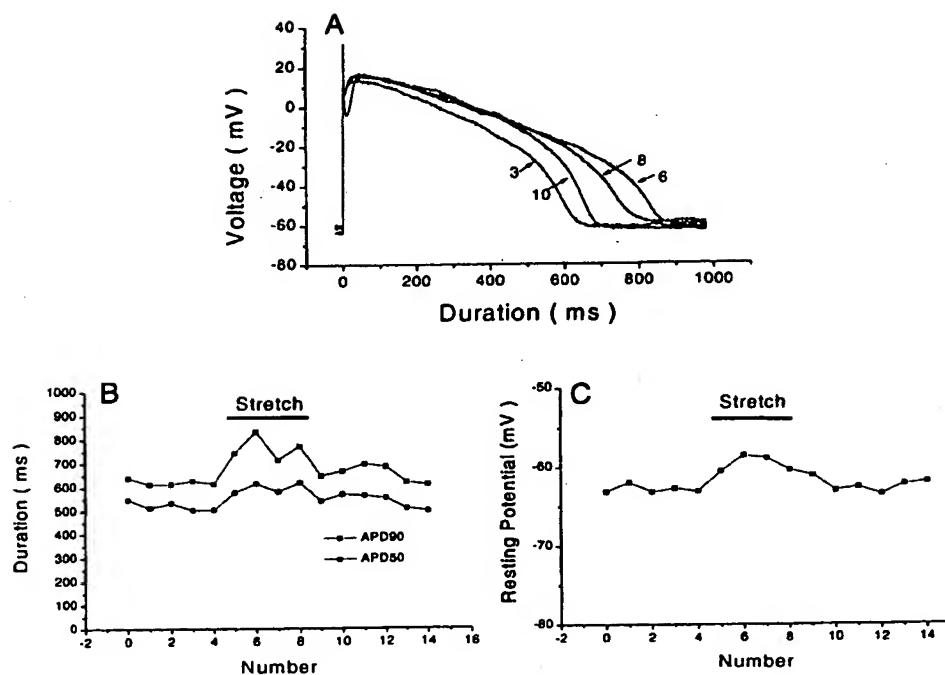


Fig. 2. Longitudinal stretch increased action potential duration (APD) and depolarized the cell. Action potentials were recorded in current-clamp mode with 1 ms, 2 nA stimulation at 0.2 Hz. A: action potentials (nos. refer to ordinal location of stimulus: 3, before stretch; 6 and 8, during stretch; 10, after stretch). B: APD at both 90% and 50% repolarization (APD<sub>90</sub> and APD<sub>50</sub>) increased during stretching (5–8) and returned close to control duration after strain was released (9–14). C: resting potential was depolarized during stretching. Cell was in low-calcium (0.2 mM) Tyrode solution.

was no significant difference in APD<sub>90</sub> ( $653 \pm 35$  ms,  $n = 5$ , at  $P = 0.1$  level). Stretching had a similar effect on APD<sub>50</sub>, causing it to increase from  $516 \pm 19$  ms ( $n = 5$ ) to  $597 \pm 22$  ms ( $n = 4$ ,  $P < 0.01$ ). Stretch also caused depolarization of the resting potential. During our small stretches, the cell depolarized to  $-59.7 \pm 1.2$  mV ( $n = 4$ ,  $P < 0.01$ ) from the control level of  $-62.4 \pm 1.1$  mV ( $n = 9$ ). The effects of stretch on the action potential and the resting potential are consistent with the activation of inward currents.

**Longitudinal stretch-activated inward currents.** When the membrane potential was held at  $-100$  mV in Tyrode solution, stretching the cell elicited an inward current (Fig. 3). This current activated without visible delay after initiation of stretch and was maintained during stretch. After release, the current returned to its prestretch level. While the cell remained attached, repeated stretching gave nearly the same response. For example, in one of our more extensive experiments ( $n = 4$ ), the mean current was  $1.03 \pm 0.18$  pA/pF at  $-100$  mV. Currents elicited in  $\text{Ca}^{2+}$ -free or low- $\text{Ca}^{2+}$  (0.2 mM) solutions were similar to those obtained in normal Tyrode solution. Because the cells were much more likely to contract after being attached to the pulling pipettes in normal- $\text{Ca}^{2+}$  solution than in low- $\text{Ca}^{2+}$  solutions, we usually conducted experiments in  $\text{Ca}^{2+}$ -free or low- $\text{Ca}^{2+}$  Tyrode solution.

The stretch-induced current was not an artifact of membrane breakage, because cells loaded with fluo 3 in normal- $\text{Ca}^{2+}$  medium did not show significant leakage of  $\text{Ca}^{2+}$  while being stretched ( $n = 3$ , Fig. 4). The strain-induced currents did not seem to originate in the vicinity of the patch pipette because even small, deliberate movements of the pipette evoked no measurable current.

Because  $\text{Gd}^{3+}$  is a blocker of many SACs (15, 57), we examined its effect on the whole cell currents. In one cell,  $40 \mu\text{M}$   $\text{Gd}^{3+}$  blocked inward currents by 60%. In another cell,  $100 \mu\text{M}$   $\text{Gd}^{3+}$  reduced the current by 90% (Fig. 5). The block by  $\text{Gd}^{3+}$  was partly reversible after 5 min of washout.

Octanol, a gap junction blocker (45), did not have any significant effect on the mechanosensitive current (Fig. 6). The mean current was  $93 \pm 29$  pA in control and  $79 \pm 10$  pA in  $100 \mu\text{M}$  octanol. The difference was not significant ( $P = 0.05$ ,  $n = 4$ ).

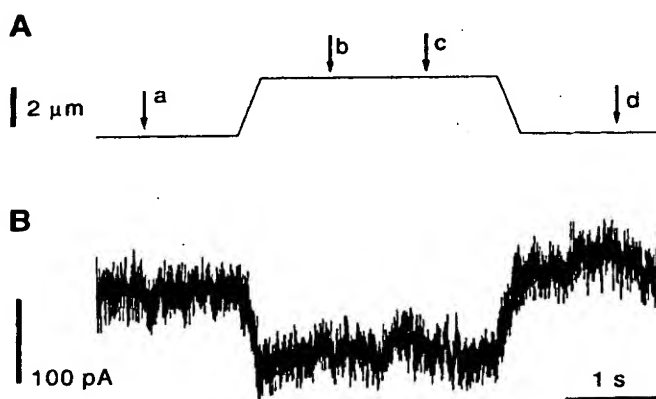


Fig. 3. Stretch-induced inward current of a rat ventricular cell. A: trapezoidal stimulus pulse that drove piezomanipulator. Stretching paradigm was trapezoidal to reduce parasitic mechanical oscillation. a–d, time at which images were taken corresponding to Fig. 1. B: whole cell inward current that started without obvious delay and was sustained during stretch; cell membrane potential was held at  $-100$  mV. Bath contained normal Tyrode solution; cell capacitance was 87 pF.

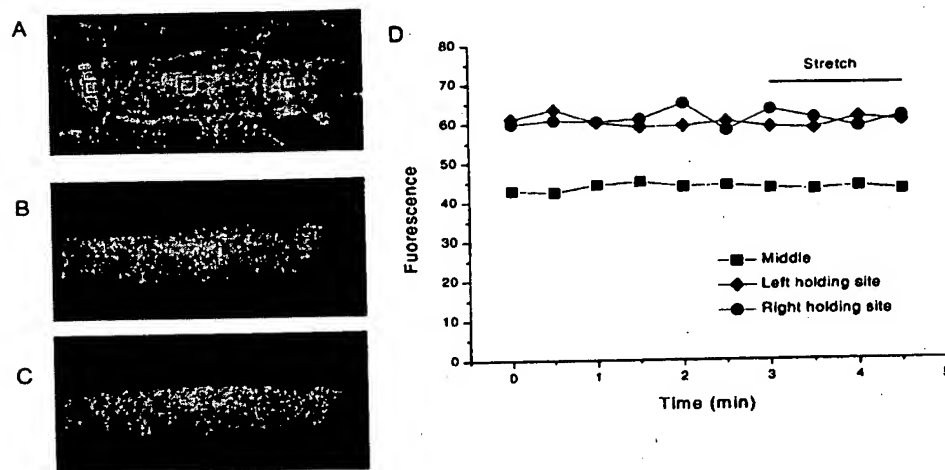


Fig. 4. Fluo 3  $\text{Ca}^{2+}$  images did not show local leakage during stretch in normal Tyrode solution. A: SIT camera image of a fluo 3-labeled cell being held by pipettes. A small amount of transmitted light was added to epi-illumination to provide contrast that makes pipettes visible. Small squares indicate areas of interest used to measure fluo 3 signals over time. B: fluorescence images of cell before stretch (transmitted illumination removed). C: fluorescence image during stretch (as in B). D: fluo 3 brightness signals (arbitrary units) from small regions of interest marked in A. White is value 0, and black is value 255. Stretch was applied at 3 min. Cell was loaded with 2  $\mu\text{M}$  fluo 3 for 30 min in normal Tyrode solution. Difference in absolute intensities between ends and middle may reflect compression of cell by pipettes forcing more of the cell to be in the effective focal volume.

$I_{\text{stretch}}$  has a reversal potential of  $-6$  mV. We examined the voltage dependence of the currents in Tyrode solution by applying test pulses between  $-120$  and  $+20$  mV from a holding potential of  $-100$  mV. Because stretching the same cell more than four times without losing the attachment was very difficult, we collected the data from four different cells and normalized the currents by the cell capacitance. The cells were stretched  $5$   $\mu\text{m}$ , equivalent to  $\sim 3\%$  strain. All currents were calculated as the mean current between the rising and falling phases. The mean current-voltage ( $I$ - $V$ ) curve

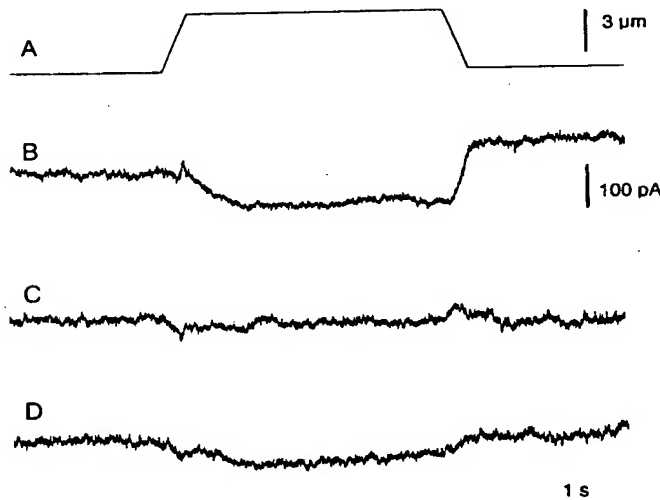


Fig. 5. Stretch-activated inward current blocked by  $100$   $\mu\text{M}$   $\text{Gd}^{3+}$ . A: stretching protocol. B: control. C: with  $\text{Gd}^{3+}$ . D: partial recovery after  $5$  min of washing. Cell was in normal Tyrode solution at a holding potential of  $-100$  mV.

(Fig. 7) showed an essentially linear relationship with a reversal potential of  $-6$  mV.

$I_{\text{stretch}}$  increase with SL. By programming the voltage sent to the piezomanipulators, we could apply different global strains to the cell. Video images of cells before and after stretching were grabbed into the computer, and mean SL was computed from the power spectrum of the images. Figure 8 shows that in the narrow range of strain available, the change in mechanosensitive current was approximately linear with both SL and strain. Both SL and SL strain were fit to the current by linear regression. At  $-100$  mV, the former follows the relationship  $I$  (pA/pF) =  $8.3 - 5.0\text{SL}$  ( $\mu\text{m}$ ), and the latter follows  $I$  (pA/pF) =  $-0.30\text{SL}\%$ . The first equation

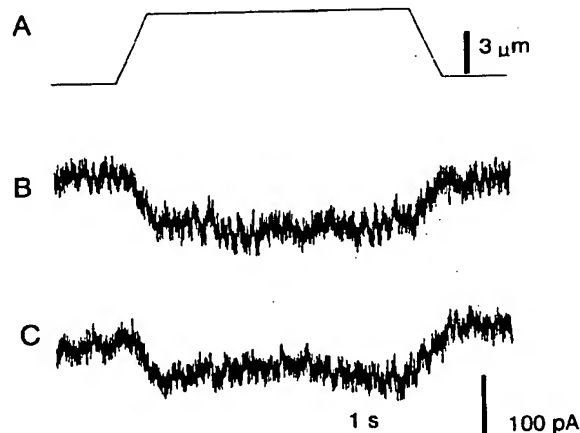


Fig. 6. Octanol does not significantly affect currents. A: stretching protocol. B: control. C: with  $100$   $\mu\text{M}$  octanol in bath. Cell was in normal Tyrode solution at a holding potential of  $-100$  mV.

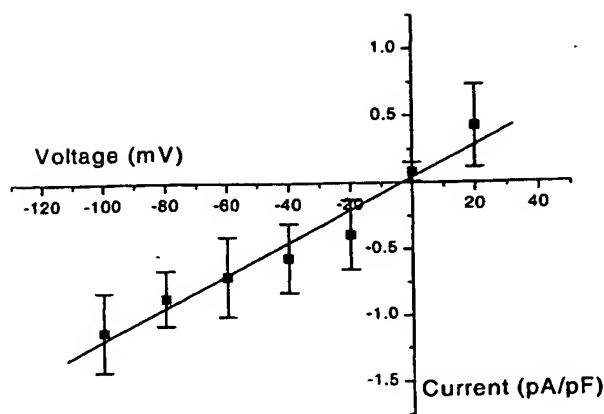


Fig. 7. Current-voltage ( $I$ - $V$ ) relationship, normalized to cell capacitance, is nearly linear, with a reversal potential of  $-6$  mV in Tyrode solution. Cells were stretched by  $5\text{ }\mu\text{m}$ , equivalent to  $\sim 3\%$  strain; mean resting SL was  $1.79 \pm 0.02\text{ }\mu\text{m}$  ( $n = 4$ ). Line, linear fit of experimental data by  $I$  (pA/pF) =  $0.012V$  (mV) +  $0.07$ .

predicts that SAC currents will persist to  $1.66\text{ }\mu\text{m}$ . The 95% confidence limits, however, include zero current at longer SLs, and we do not trust the precision of this prediction. There are probably small-scale nonuniformities in SL that do not show up in our first-order analysis of the diffraction pattern. The sample size and the optical resolution in three dimensions limit the effective resolution of the SL. The net result of these systematic and random errors is scatter in the data. In Fig. 8B, the large fraction of data points outside the 95% confidence intervals suggests some significant nonrandom errors such as a nonuniform SL distribution.

$\text{Na}^+$  is the main carrier of mechanically sensitive currents at resting potential. Because  $I_{\text{stretch}}$  was inward at  $-100$  mV, that current must be carried by an influx of cations, an efflux of anions, or a mixture of the two. Replacing  $\text{Cl}^-$  in the pipette solution with  $\text{F}^-$  produced similar currents ( $n = 5$ , see Fig. 9 for example), suggesting that the current was carried by cations rather than anions (13).

To examine the components of the cation influx, we superfused the cells with Tris-Tyrode solution in which  $\text{Na}^+$  was replaced by Tris $^+$ . The heart cells were not

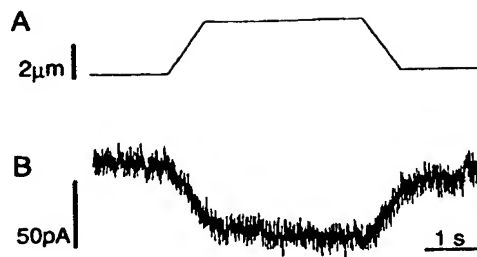


Fig. 9. Replacing  $\text{Cl}^-$  in pipette solution with  $\text{F}^-$  produced a typical inward current, suggesting that stretch-activated current is not a  $\text{Cl}^-$  efflux. A: stretching protocol. B: stretch-activated current. Cell capacitance was  $72\text{ pF}$ ; holding potential was  $-100$  mV. Cell was in normal Tyrode solution.

stable for long in this nonphysiological Tris-Tyrode solution, so perfusion was started only 3 s before stretching and was shut down 1 s after the cell was restored to its original position. Figure 10 indicates that inward currents were largely reduced in the presence of Tris-Tyrode solution ( $n = 2$ ), suggesting that  $\text{Na}^+$  is the main carrier of the currents at resting potential.

Stretch-activated ion channels are thought to be responsible for the mechanically sensitive current, so we looked for single channel currents in cell-attached patches. Much to our dismay, we recorded no single channel activity. Dozens of patches were tried using three different setups and the assistance of two additional independent and experienced investigators. In no case were we able to observe stretch-activated single channel currents. Despite its negative character, this result correlates with the absence of publications on SACs in adult mammalian ventricular myocytes.

**Modeling  $I_{\text{stretch}}$ .** The experimentally obtained  $I$ - $V$  curve for  $I_{\text{stretch}}$  was well fit by a straight line representing the equation

$$I_{\text{stretch}} = \gamma_{\text{stretch,Na}}(8.3 - 5.0\text{SL})(E_m - E_{\text{Na}}) + \gamma_{\text{stretch,K}}(8.3 - 5.0\text{SL})(E_m - E_K)$$

where  $\gamma_{\text{stretch,K}} = 0.9\text{ nS}$  and  $\gamma_{\text{stretch,Na}} = 1.17\text{ nS}$ , given the model rat's nominal whole capacitance of  $200\text{ pF}$  (see Fig. 7). These values were used with the equation

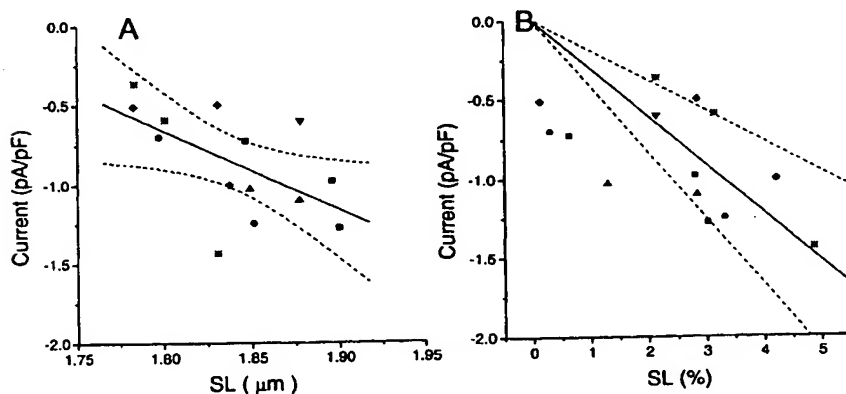


Fig. 8. Relationship between SL and mechanically activated current at a holding potential of  $-100$  mV. A: linear regression of SL ( $\mu\text{m}$ ) vs. current density (pA/pF) by equation  $Y = aX + b$  gives relationship  $I = 8.3 - 5.0\text{SL}$ . B: linear regression of strain, SL% (% change of SL) vs. current density (pA/pF) by equation  $Y = aX$  gives relationship  $I = -0.30\text{SL}\%$ . Solid line, mean regression; dashed lines, 95% confidence limits calculated in Origin 5.0. Confidence limits are based on Gaussian distributions of errors. Data were collected from 6 different cells labeled by different symbols.

above to test the effect of  $I_{\text{stretch}}$  on the rat action potential and compare it with the experimentally obtained results.

Because of the experimental complexities of keeping the cell attached to the pipettes and in whole cell voltage clamp while applying strain to the cell, the experimental stimulation frequency used was only 0.2 Hz. Decreasing the stimulation frequency of isolated rat ventricular cells increases the APD and increases calcium loading of the SR (27). However, this has little effect on the APD in the presence of 10 mM EGTA. The result of stimulating an action potential at 0.2 Hz in the absence and presence of  $I_{\text{stretch}}$  (based on SL of 1.89  $\mu\text{m}$ ), with an extracellular calcium concentration of 0.2 mM and 10 mM intracellular EGTA, is shown in Fig. 11.

The duration of the modeled cell action potential is shorter than that observed experimentally, but this is easily explained by the difference in temperatures: the nominal temperature of the model cell is 37°C, whereas the experiments were performed at room temperature. Kiyosue et al. (23) demonstrated that a decrease in temperature of 9° resulted in an increase in guinea pig APD from 146 to 314 ms. The difference between the model and experimental temperatures in our data is 17°C.

Activation of  $I_{\text{stretch}}$  depolarized the resting membrane of the cell and lengthened the action potential throughout its duration (i.e., at both APD<sub>50</sub> and APD<sub>90</sub>). A small stretch-activated current with the  $I$ - $V$  relation-

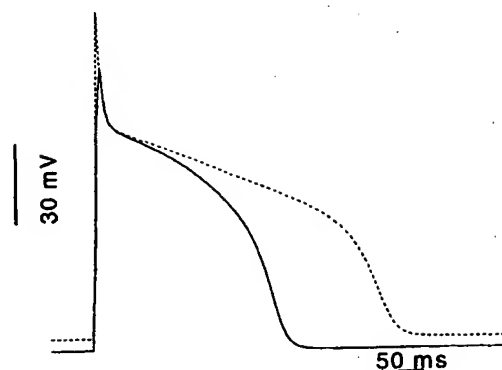


Fig. 11. Simulated rat ventricular action potentials at 0.2-Hz stimulation frequency with 10 mM EGTA inside cell and 0.2 mM  $\text{Ca}^{2+}$  extracellular solution. Solid line, control; dashed line, stretch. Resting potential is elevated and action potential is prolonged with stretch-activated current.

ship shown in Fig. 7 could be responsible for the experimentally observed effects on the action potential.

## DISCUSSION

This is the first study of stretch-activated whole cell currents in mammalian cardiocytes under controlled strain. We were able to show that in rat ventricular cells stretch activated a gadolinium-sensitive, noninactivating, inward current. Our data are similar to those published for other heart cells (20, 39) and smooth muscle cells (9, 52).

SACs in heart cells have been reported to be nonselective cation channels (8, 33) or  $\text{Cl}^-$  channels (12). In our experiments,  $I_{\text{stretch}}$  was not significantly different when the pipette solution contained  $\text{Cl}^-$  or  $\text{F}^-$ , suggesting that these currents are carried by cations. Further experiments are needed to define the selectivity more precisely. Removing external  $\text{Ca}^{2+}$  did not significantly affect the current, suggesting that  $\text{Ca}^{2+}$  does not act as a significant charge carrier or a second messenger, although  $\text{Ca}^{2+}$  is probably a permeant ion. Replacing  $\text{Na}^+$  with  $\text{Tris}^+$  reduced the current, although the blockage was not complete.  $I_{\text{stretch}}$  in rat heart cells appears to be cation selective, with  $\text{Na}^+$  acting as the major permeant ion at resting potential. Wellner and Isenberg (52) reported that in guinea pig smooth muscle cells, stretch increased a voltage-activated potassium current and reduced a calcium current. In heart cells, however, there is no evidence to suggest that stretching has any effect on voltage-sensitive channels (20, 39). Because of the experimental difficulty with our preparation, we did not directly check the effect of stretching on voltage-sensitive currents. However, we did observe that changing the membrane potential to -40 mV and removing  $\text{Ca}^{2+}$  from the bath solution produced little difference in the time course of the mechanically activated currents. Thus it is unlikely that voltage-dependent  $\text{K}^+$ ,  $\text{Na}^+$ , or  $\text{Ca}^{2+}$  channels are responsible for the mechanosensitive currents we observed.

Heart cells shorten >10% during contraction, but they are not readily stretched. In our system, 2–5%

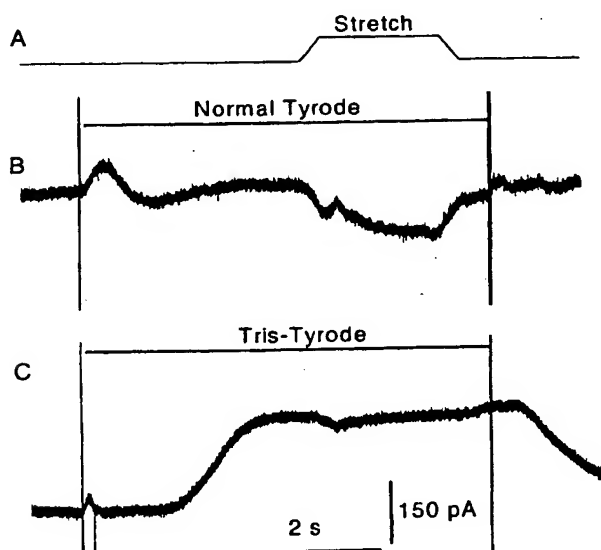


Fig. 10. Stretch-activated current was reduced when extracellular  $\text{Na}^+$  was replaced by  $\text{Tris}^+$ . A: stretching protocol. B: stretch-induced currents in normal Tyrode solution. Bath contained Tyrode, as did perfusate. Beginning of superfusion flow produced a transient upward-going current caused by changes in liquid junction potential. C: currents with cell superfused with Tris-Tyrode solution ( $\text{Na}^+$  replaced by  $\text{Tris}^+$ ). Stretch-induced current is greatly reduced, suggesting that most of it is carried by  $\text{Na}^+$ . Exposure of cell to Tris-saline produced a large outward background current. Cell membrane was held at -100 mV, and  $\text{Ca}^{2+}$  concentration was 0.2 mM in bath solution.

strain was possible. In some experiments, we moved the stretching pipette 10% of the cell length, but the attached cells would either contract immediately or slip out of the holding micropipette. In the latter case, the cells usually contracted into a ball in a few seconds. With a resting SL of 1.77  $\mu\text{m}$ , our results showed that <5% strain was sufficient to evoke stretch-sensitive currents. Comparing the passive elastic properties from detergent-skinned isolated cells and intact cardiac tissue, Brady (4) suggested that intracellular structures may contribute measurably to total cardiac passive elasticity at SL < 2.2  $\mu\text{m}$ , whereas extracellular elements form the major limitation at more extended lengths. Furthermore, he suggested that these intracellular structures were probably related to the cytoskeleton rather than membrane elements (5). Our data are consistent with a model in which stress in the membrane is coupled through the intracellular cytoskeleton to the channels.

How much current is contributed by SACs at "resting" SLs is difficult to determine and could only be measured with a specific inhibitor, which  $\text{Gd}^{3+}$  is not. Our definition of a mechanically sensitive current is one that changed with stretch of the cell, so that it is only a differential measurement. In Fig. 8 we plotted current versus SL during stretch and versus SL as strain. Taken literally, Fig. 8A suggests that at SL = 1.75  $\mu\text{m}$  there would be  $\sim 1$  pA/pF of inward current from SACs. This plot is of necessity made from differential data arising from different cells, and without allowance for a variation in SL throughout the cell (only the 1st-order diffraction line was used to define SL) we cannot place much confidence in the amplitude of the resting current. Furthermore, the resting current in isolated cells is unlikely to be the same as in cells in situ, where the normal extracellular contacts are in place.

We made multiple attempts to record stretch-activated ion channels from tight seal patches on the rat ventricular cells, but we never recorded single channel activity. Reviewing the literature, we found that all the reports of single channel stretch-activated activity in heart cells were obtained from neonatal (8, 20, 22), atrial (19, 50), or cultured (33, 38) cells. There are no data on freshly isolated ventricular cells. There appear to be three possible explanations for this absence of single channel data.

First, the channel density may be low, so the chance of catching one channel in a pipette is small. Is this reasonable? Our maximal currents were  $\sim 1$  pA/pF at  $-100$  mV. This current corresponds to a product of the unitary current and the probability ( $P_o$ ) of being open. If the single channel conductance had a typical value of  $\sim 25$  pS, the single channel current would be  $\sim 2.5$  pA/channel at  $-100$  mV. There is 1 pF of capacitance for every 100  $\mu\text{m}^2$  of membrane, so we would expect that the minimal density (if  $P_o = 1$ ) is 1 channel/40  $\mu\text{m}^2$ . Because cell-attached patches have areas of 10–30  $\mu\text{m}^2$  (34, 43), we might expect to see a channel in every other patch.  $P_o$  is probably  $\ll 1$  in the whole cell experiments because the strains were small and there was no hint of saturation in the plot of current versus SL. Conse-

quently, there should have been a higher density of channels, and we should have seen them in most patches. SACs typically occur with a density of  $\sim 1$ –3/patch. It does not seem likely, therefore, that the absence of single channel activity came from a low channel density.

A second possibility is that SACs are not in the surface plasmalemma but are located in the T system and hence invisible to plasmalemmal patching but not to whole cell stretching. An intracellular location for the channels, although an experimental nightmare, has conceptual appeal because strain may be better sensed in the contractile cell interior than in the convoluted plasma membrane. This interior membrane explanation would fit with the sensitivity of the cells to suction applied to the pulling pipettes and with fluorescent imaging showing  $\text{Gd}^{3+}$ -sensitive  $\text{Ca}^{2+}$  waves induced at the site of mechanical deformation (W. J. Sigurdson and F. Sachs, unpublished observation).

The third possibility is that formation of the patch disrupts channel activity in these cells. Patch formation is a major perturbation of the mechanical properties of the membrane and cortical cytoskeleton (1, 16, 36, 42, 43, 51). It is possible that some important structure in the adult ventricular cortex is disrupted under stress.

Physiologically, the effect of stretch is most likely expressed through changes in the action potential, although it also will affect the filling of  $\text{Ca}^{2+}$  stores. In many recordings of action potentials from intact tissue under stretch, the duration of the plateau is reduced and the tail of repolarization (phase 3) increases, leading to a crossover, or apparent reversal potential of the mechanosensitive current, at about  $-20$  mV (35, 58). In intact rabbit heart, a long static stretch created by inflating a balloon in the left ventricle extended the APD. The peak amplitude of the stretch-activated depolarization from rest and repolarization from the plateau exhibited a linear relationship to voltage and volume change (58). In single guinea pig cardiac myocytes, a 3% strain did not affect the resting potential but did decrease the APD (10, 54).

The rat ventricular action potential is significantly different from that of the rabbit and guinea pig, because it lacks the prolonged plateau and, during the contraction cycle, has a much greater reliance on calcium released from the SR rather than plasmalemmal calcium entry (46). As a test of whether the observed currents could account for the effects of stretch on the action potential, we simulated the rat action potential using the HEART program from Oxsoft. We introduced a stretch-activated current,  $I_{\text{stretch}}$ , that was permeable to potassium and sodium ions and closely fit the experimental  $I$ - $V$  curve.

The addition of this simple current could account for the depolarization of the resting potential and the observed changes in APD. At the negative potentials of the rat plateau, the reversal potential of the stretch current near 0 mV caused a net inward current and therefore prolonged and depolarized the action potential throughout its course. In cells with a high plateau

and a lower reversal potential of  $I_{\text{stretch}}$  (approximately  $-20$  mV), such as those of guinea pig and rabbit, there is a shortening of the plateau but prolongation of  $\text{APD}_{90}$  and a crossover potential during phase 3. White et al. (54) observed a stretch-induced reduction in APD in guinea pig, possibly reflecting the differences in the two preparations.

Although stretching single cells would appear to be the most reductionist level for studying the effects of stretch on whole cells, there is a fundamental problem of interpretation that is not readily resolved: What are we pulling on? The response of cells to mechanical deformation depends, in general, on which chemical groups are being distorted. For instance, in a study of cultured vascular smooth muscle cells subjected to periodic strain, Wilson and Kaczmarek (55) found that production and secretion of platelet-derived growth factor and DNA depended on the chemical composition of the substrate. Collagen, fibronectin, and vitronectin were effective, but little response was observed on elastin or laminin. Similarly, if the cells were cultured on pronectin or laminin, cyclic strain caused differential expression of mitogen-activated protein and amino terminal kinase (32). In fibroblasts, mechanically induced increases in cell  $\text{Ca}^{2+}$  occurred when  $\alpha_2$ - or  $\beta_1$ -integrin subunits were stressed but not the transferin receptor (31). L-type  $\text{Ca}^{2+}$ -channel currents can be activated or inhibited by different ligands for the integrins (56). These kinds of data warn against extrapolating from isolated cells to cells in their normal environment. Aside from the technical difficulties of stretching isolated cells, it is important to get data from cells in their native mechanical environment. Only with that data in hand can we properly extend the studies on isolated cells to discover which ligands produce the responses observed in vivo.

The authors thank Dr. Wade J. Sigurdson for assistance in experimental setup, Dr. Stephen Besch for assistance in adhesive testing, and Mary Teeling for technical support.

This work was supported by grants from the National Institutes of Health and the United States Army Research Office to F. Sachs.

Address for reprint requests and other correspondence: F. Sachs, Dept. of Physiology and Biophysics, SUNY, Buffalo, NY 14214 (E-mail: sachs@buffalo.edu).

Received 5 January 1999; accepted in final form 5 August 1999.

## REFERENCES

1. Akinlaja, J., and F. Sachs. The breakdown of cell membranes by electrical and mechanical stress. *Biophys. J.* 75: 247–254, 1998.
2. Bainbridge, F.A. The influence of venous filling upon the rate of the heart. *J. Physiol. (Lond.)* 50: 65–84, 1915.
3. Blinks, J. R. Positive chronotropic effect of increasing right atrial pressure in the isolated mammalian heart. *Am. J. Physiol.* 186: 299–303, 1956.
4. Brady, A. J. Length dependence of passive stiffness in single cardiac myocytes. *Am. J. Physiol. Heart Circ. Physiol.* 260: H1062–H1071, 1991.
5. Brady, A. J. Mechanical properties of isolated cardiac myocytes. *Physiol. Rev.* 71: 413–428, 1991.
6. Bustamante, J. O., A. Ruknudin, and F. Sachs. Stretch-activated channels in heart cells: relevance to cardiac hypertrophy. *J. Cardiovasc. Pharmacol.* 17, Suppl. 2: S110–S113, 1991.
7. Calkins, H., J. H. Levine, and D. A. Kass. Electrophysiological effect of varied rate and extent of acute in vivo left ventricular load increase. *Cardiovasc. Res.* 25: 637–644, 1991.
8. Craeliuss, W. Stretch-activation of rat cardiac myocytes. *Exp. Physiol.* 78: 411–423, 1993.
9. Davis, M. J., J. A. Donovitz, and J. D. Hood. Stretch-activated single-channel and whole cell currents in vascular smooth muscle cells. *Am. J. Physiol. Cell Physiol.* 262: C1083–C1088, 1992.
10. Gannier, F., J. C. Beranengo, V. Jacquemond, and D. Garnier. Measurements of sarcomere dynamics simultaneously with auxotonic force in isolated cardiac cells. *IEEE Trans. Biomed. Eng.* 40: 1226–1232, 1993.
11. Garnier, D. Attachment procedures for mechanical manipulation of isolated cardiac myocytes: a challenge. *Cardiovasc. Res.* 28: 1758–1764, 1994.
12. Hagiwara, N., H. Masuda, M. Shoda, and H. Irisawa. Stretch-activated anion currents of rabbit cardiac myocytes. *J. Physiol. (Lond.)* 456: 285–302, 1992.
13. Halm, D. R., and R. A. Frizzell. Anion permeation in an apical membrane chloride channel of a secretory epithelial cell. *J. Gen. Physiol.* 99: 339–366, 1992.
14. Hamill, O. P., A. Marty, E. Neher, P. Sakmann, and F. J. Sigworth. Improved patch-clamp techniques for high-resolution current recording from cells and cell-free membrane patches. *Eur. J. Physiol.* 2: 85–100, 1981.
15. Hamill, O. P., and D. W. McBride, Jr. The pharmacology of mechanogated membrane ion channels. *Pharmacol. Rev.* 48: 231–252, 1996.
16. Hamill, O. P., and D. W. McBride, Jr. Rapid adaptation of single mechanosensitive channels in *Xenopus* oocytes. *Proc. Natl. Acad. Sci. USA* 89: 7462–7466, 1992.
17. Hansen, D. E., C. S. Craig, and L. M. Hondeghem. Stretch-induced arrhythmias in the isolated canine ventricle. Evidence for the importance of mechanoelectrical feedback. *Circulation* 81: 1094–1105, 1990.
18. Hilgemann, D. W. The giant membrane patch. In: *Single-Channel Recording*, edited by B. Sakmann and E. Neher. New York: Plenum, 1995, p. 307–328.
19. Hoyer, J., A. Distler, W. Haase, and H. Gogelein.  $\text{Ca}^{2+}$  influx through stretch-activated cation channels activates maxi  $\text{K}^{+}$  channels in porcine endocardial endothelium. *Proc. Natl. Acad. Sci. USA* 91: 2367–2371, 1994.
20. Hu, H., and F. Sachs. Mechanically activated currents in chick heart cells. *J. Membr. Biol.* 154: 205–216, 1996.
21. Hu, H., and F. Sachs. Stretch-activated ion channels in the heart. *Cell Mol. Cardiol.* 29: 1511–1523, 1997.
22. Kim, D. Novel cation-selective mechanosensitive ion channel in the atrial cell membrane. *Circ. Res.* 72: 225–231, 1993.
23. Kiyosue, T., M. Arita, H. Muramatsu, A. J. Spindler, and D. Noble. Ionic mechanisms of action potential prolongation at low temperature in guinea-pig ventricular myocytes. *J. Physiol. (Lond.)* 468: 85–106, 1993.
24. Lab, M. J. Mechanically dependent changes in action potentials recorded from the intact frog ventricle. *Circ. Res.* 42: 519–528, 1978.
25. Lab, M. J. Mechanoelectric feedback (transduction) in heart: concepts and implications. *Cardiovasc. Res.* 32: 3–14, 1996.
26. Lindau, M., and E. Neher. Patch-clamp techniques for time-resolved capacitance measurements in single cells. *Pflügers Arch.* 411: 137–146, 1988.
27. Mitchell, M. R., Powell, T., Terrar, D. A., and Twist, V. W. Characteristics of the second inward current in cells isolated from rat ventricular muscle. *Proc. R. Soc. Lond. B. Biol. Sci.* 219, 447–469, 1983.
28. Mitra, R., and M. Morad. A uniform enzymatic method for dissociation of myocytes from hearts and stomachs of vertebrates. *Am. J. Physiol. Heart Circ. Physiol.* 249: H1056–H1060, 1985.
29. Palmer, R. E., A. J. Brady, and K. P. Roos. Mechanical measurements from isolated cardiac myocytes using a pipette attachment system. *Am. J. Physiol. Cell Physiol.* 270: C697–C704, 1996.

30. Penefsky, Z. A., and B. F. Hoffman. Effects of stretch on mechanical and electrical properties of cardiac muscle. *Am. J. Physiol.* 204: 433–438, 1963.
31. Pommerenke, H., E. Schreiber, F. Durr, B. Nebe, C. Hahnel, W. Moller, and J. Rychly. Stimulation of integrin receptors using a magnetic drag force device induces an intracellular free calcium response. *Eur. J. Cell Biol.* 70: 157–164, 1996.
32. Reusch, H. P., G. Chan, H. E. Ives, and R. A. Nemenoff. Activation of JNK/SAPK and ERK by mechanical strain in vascular smooth muscle cells depends on extracellular matrix composition. *Biochem. Biophys. Res. Commun.* 237: 239–244, 1997.
33. Ruknudin, A., F. Sachs, and J. O. Bustamante. Stretch-activated ion channels in tissue-cultured chick heart. *Am. J. Physiol. Heart Circ. Physiol.* 264: H960–H972, 1993.
34. Ruknudin, A., M. J. Song, and F. Sachs. The ultrastructure of patch-clamped membranes: a study using high voltage electron microscopy. *J. Cell Biol.* 112: 125–134, 1991.
35. Sachs, F. Modeling mechanical-electrical transduction in the heart. In: *Cell Mechanics and Cellular Engineering*, edited by V. C. Mow, F. Guliak, R. Tran-Son-Tray, and R. M. Hochmuth. New York: Springer, 1994, p. 308–328.
36. Sachs, F., and C. Morris. Mechanosensitive ion channels in non-specialized cells. In: *Reviews of Physiology and Biochemistry and Pharmacology*, edited by M. P. Blaustein, R. Greger, H. Grunicke, R. Jahn, L. M. Mendell, A. Miyajima, D. Pette, G. Schultz, and M. Schweiger. Berlin: Springer, 1998, p. 1–78.
37. Sadoshima, J., and S. Izumo. The cellular and molecular response of cardiac myocytes to mechanical stress. *Annu. Rev. Physiol.* 59: 551–571, 1997.
38. Sadoshima, J., L. Jahn, T. Takahashi, T. J. Kulik, and S. Izumo. Molecular characterization of the stretch-induced adaptation of cultured cardiac cells. An in vitro model of load-induced cardiac hypertrophy. *J. Biol. Chem.* 267: 10551–10560, 1992.
39. Sasaki, N., T. Mitsuiye, and A. Noma. Effects of mechanical stretch on membrane currents of single ventricular myocytes of guinea-pig heart. *Jpn. J. Physiol.* 42: 957–970, 1992.
40. Sigurdson, W. J., E. Bedard, and C. E. Morris. Stretch-activated K<sup>+</sup> channels in molluscan neurons (Abstract). *Biophys. J.* 51: 50a, 1987.
41. Sigurdson, W. J., A. Ruknudin, and F. Sachs. Calcium imaging of mechanically induced fluxes in tissue-cultured chick heart: role of stretch-activated ion channels. *Am. J. Physiol. Heart Circ. Physiol.* 262: H1110–H1115, 1992.
42. Small, D. L., and C. E. Morris. Delayed activation of single mechanosensitive channels in *Lymnaea* neurons. *Am. J. Physiol. Cell Physiol.* 267: C598–C606, 1994.
43. Sokabe, M., F. Sachs, and Z. Jing. Quantitative video microscopy of patch clamped membranes—stress, strain, capacitance and stretch channel activation. *Biophys. J.* 59: 722–728, 1991.
44. Sorota, S. Swelling-induced chloride-sensitive current in canine atrial cells revealed by whole-cell patch-clamp method. *Circ. Res.* 70: 679–687, 1992.
45. Spray, D. C., and M. V. Bennett. Physiology and pharmacology of gap junctions. *Annu. Rev. Physiol.* 47: 281–303, 1985.
46. Terracciano, C. M., and K. T. MacLeod. Measurements of Ca<sup>2+</sup> entry and sarcoplasmic reticulum Ca<sup>2+</sup> content during the cardiac cycle in guinea pig and rat ventricular myocytes. *Biophys. J.* 72: 1319–1326, 1997.
47. Tseng, G. N. Cell swelling increases membrane conductance for canine cardiac cells: evidence for a volume-sensitive Cl<sup>−</sup> channel. *Am. J. Physiol. Cell Physiol.* 262: C1056–C1068, 1992.
48. Tsien, R. Y. New calcium indicators and buffers with high selectivity against magnesium and protons: design, synthesis, and properties of prototype structures. *Biochemistry* 19: 2396–2404, 1980.
49. Tytgat, J. How to isolate cardiac myocytes. *Cardiovasc. Res.* 28: 280–283, 1994.
50. Van Wagoner, D. R. Mechanosensitive gating of atrial ATP-sensitive potassium channels. *Circ. Res.* 72: 973–983, 1993.
51. Wan, X., P. Juranka, and C. E. Morris. Activation of mechanosensitive currents in traumatized membrane. *Am. J. Physiol. Cell Physiol.* 276: C318–C327, 1999.
52. Wellner, M. C., and G. Isenberg. Stretch effects on whole-cell currents of guinea-pig urinary bladder myocytes. *J. Physiol. (Lond.)* 480: 439–448, 1994.
53. White, E. Length-dependent mechanisms in single cardiac cells. *Exp. Physiol.* 81: 885–897, 1996.
54. White, E., J. Y. Le Guennec, J. M. Nigretto, F. Gannier, J. A. Argibay, and D. Garnier. The effects of increasing cell length on auxotonic contractions: membrane potential and intracellular calcium transients in single guinea-pig ventricular myocytes. *Exp. Physiol.* 78: 65–78, 1993.
55. Wilson, G. F., and L. K. Kaczmarek. Mode-switching of a voltage-gated cation channel is mediated by a protein kinase A-regulated tyrosine phosphatase. *Nature* 366: 433–438, 1993.
56. Wu, X., J. E. Mogford, S. H. Platts, G. E. Davis, G. A. Meininger, and M. J. Davis. Modulation of calcium current in arteriolar smooth muscle by alpha(v)beta(3) and alpha(5)beta(1) integrin. *J. Cell Biol.* 143: 241–252, 1998.
57. Yang, X. C., and F. Sachs. Block of stretch-activated ion channels in *Xenopus* oocytes by gadolinium and calcium ions. *Science* 243: 1068–1071, 1989.
58. Zabel, M., B. S. Koller, F. Sachs, and M. R. Franz. Stretch-induced changes in the isolated heart: importance of the timing of stretch and implications for stretch-activated ion channels. *Cardiovasc. Res.* 32: 120–130, 1996.